Targeting the X for chromosome-wide gene regulation

by

Emily L. Petty

A dissertation submitted in partial fulfillment
of the requirements for the degree of
Doctor of Philosophy
(Molecular, Cellular, and Developmental Biology)
University of Michigan
2011

Doctoral Committee:

Assistant Professor Györgyi Csankovszki
Professor Kenneth M. Cadigan
Professor Steven E. Clark
Assistant Professor Yali Dou

© Emily L. Petty
2011

This work is dedicated

to my family- Mom, Dad, Eric, Kenny, Gabe, and Celia,

to my best friends- Aimee and Evita

to the memory of Genevieve Orstadius and Cindy Kessel

and to my future husband, Joe.

Acknowledgments

I would first like to thank my mentor Gyorgyi for all of her training and support. I have had many experiments fail during my time in this lab and Gyorgyi has always been encouraging and patient when I struggled with new techniques. I have been lucky to be in a lab where I have had the opportunity to not only attend but also present at scientific meetings. The regular journal clubs and lab meetings have also been extremely helpful in developing my presentation skills. I also really appreciated being able to pop into Gyoryi's office every so often with questions and data (usually both at the same time). I hope that hasn't been too disruptive! Most importantly, the scientific training I have received by being in the Csankovszki lab has been tremendous. I will leave the lab carrying with me a great scientific tool set.

Next, I would like to thank all of the members of their lab for their help over the years. I would like to specifically thank Dr. Tim Blauwkamp, for teaching me the ins and outs of qPCR. To the undergraduates I have had the privilege to work with, Alysse Cohen, Emily Laughlin, and Stephanie Campbell, thank you for all of your help. Some of my favorite experiences overall from graduate school have come out of working with Alysse, Emily, and Stephanie.

Thank you to all of the friends I have made over the course of my time here, especially Karishma and Yana. Yana and I actually met as roommates during our PIBS interview and it was such a relief to see a friendly face in that

first week here. Karishma and I started out as bench-mates but quickly became very good friends. I am so thankful that I've been able to work with such a wonderful person and consider myself blessed to have you as one of my friends.

Finally, thank you to my friends and family for all of their love and support. To my parents, thank you for always supporting me in my education and thank you for letting me crash back at home these last several months as I've been working toward this goal of graduating. To my friends, thank you for all of the fun and laughter and thank you for being so understanding every time I've told you, "No, I can't go, I have this experiment…,". And Joe, you have been the best surprise. Your love, support, and encouragement have helped me to get back on track when I have been exasperated with my experiments or life in general. I always know that if I call you crying I will hang up laughing. Thank you.

Table of Contents

List of Figures

List of Tables

CHAPTER 1

Introduction

How do gene regulatory machineries find their targets?

In 1944, Avery, MacLeod, and McCarty elegantly demonstrated that DNA is the genetic, or transforming, material. However, simply the presence of the information encoded by the DNA molecule is not enough, it has to be read and transmitted to the cell. So is access to DNA and the vital information it contains a free-for-all in the cell? This could result in a situation similar to trying to operate a computer with all of its programs running at once- slow to respond to a specific command, impossible to accomplish necessary tasks, and unable to communicate to the network. This is easily avoided by only running the programs required for the basic operation of the computer then selecting to run specialized programs as they are needed. Mechanisms have evolved to make sure that only the programs required by the cell at any given time are “running” at once and it has been proposed that at the foundation of these mechanisms is gating access to the sequence information of DNA.

An ancient mechanism to control access to genetic information is through organization of the DNA molecule. In *E. coli*, the single plasmid chromosome is

coiled up in a DNA-protein complex called the nucleoid. The genes that are expressed tend to be found at the outer loops of the nucleoid, while non-expressed genes are found in the interior of the structure [1]. In Archaea, ancestors of eukaryotic histones help to organize the genome by forming small nucleosome-like structures that wrap 60bp of DNA. Archaeal histones function in gene expression, suggesting that histone involvement in regulating gene expression is indeed an ancient function [1-3].

Eukaryotes utilize both the ancient strategies of DNA supercoiling and wrapping around histones to organize their genomes. Organization by these and other methods is essential not only to allow massive eukaryotic genomes to simply fit inside the cell, but also in gene regulation as in bacterial and Archaeal organisms. In eukaryotes, the DNA-protein structure is called chromatin, and this structure can be organized in different ways. Differences in chromatin organization were first observed by electron microscopy studies in the 1960's that revealed the nucleus contains darker staining areas that appeared more condensed (referred to as coiled bodies in [4]) and lighter staining areas that appeared less condensed [5]. These ultrastructural studies also revealed that chromatin organization within the nucleus differed between cell types [4]. In 1976, Weintraub and Groudine demonstrated that treatment of red blood cell nuclei with DNase I preferentially digests the active globin genes. Similar treatment of nuclei from other cell types that do not express globin genes did not result in digestion, leading the authors to propose that the chromatin structure of active genes allows access by DNase I, but not the structure of inactive genes.

The hypothesis that chromatin organization restricts access to the genome has been gaining more and more support in recent years (as reviewed in [6-8]) . Chromatin-gated access to DNA may help to explain how transcription factors with short, degenerate binding sites, ultimately bind and function at only a subset of potential sites [9-12]. Just this week, the Biggin and Stamatoyanopolous labs published an interesting localization survey of 21 developmentally important transcription factors and DNase I sensitive sites in *Drosophila* embryos [13]. The authors report that DNase I sensitivity is a better predictor of *in vivo* factor binding than the *in vitro* affinity of the factor for the target DNA sequence for all of the studied proteins. In other words, a transcription factor is more likely to bind a low-affinity sequence in an open chromatin region than a high-affinity site in chromatin that is not sensitive to DNase digestion *in vivo.* Also, changes in DNase sensitivity and transcription factor binding profiles at different developmental stages strongly correlate. Current evidence also supports that DNase sensitivity is upstream of transcription factor binding. Only the glucocorticoid receptor (GR) binding sites that are DNase accessible become bound by GR upon induction [11]. Also, expression of a pharynx-specific transcription factor in an intestinal cell in *C. elegans* is not sufficient for binding, suggesting that potential binding sites are inaccessible in the wrong cell type[14].

To get a better understanding of just how chromatin assists in regulatory factor binding, we utilize the model of chromosome-wide regulation of the X chromosome that occurs in *C. elegans* dosage compensation. This system allows us to more easily detect chromatin requirements for targeting a gene

regulatory complex as this happens on the scale of an entire chromosome, which is approximately 1/6 of the genome in *C. elegans*, versus a subset of genes scattered throughout the genome. In the following I will first describe dosage compensation biology in the three most heavily studied model organisms. Next, I will describe the biology of a histone variant called H2A.Z that we found to be important for targeting of the regulatory complex in *C. elegans* dosage compensation. Finally, I will discuss H3K4 methylation, a chromatin modification we studied in the context of dosage compensation complex targeting.

X-chromosome-wide gene regulation by dosage compensation

Many organisms utilize a chromosome-based mechanism to determine sex. Such mechanisms may rely on the expression of a sex chromosome-linked gene such as SRY, a Y-linked gene which triggers male development [15]). Sex determination may also rely on a chromosome counting mechanism whereby the cell can molecularly “sense” the number of X chromosomes to trigger female development in the presence of two copies of X and male when only one copy is present [16, 17].

Regardless of the precise mechanism of chromosome-based sex determination, a problem arises in organisms that utilize this strategy: The resulting sex chromosome aneuploidy in one of the sexes can lead to lethal gene expression imbalance of that chromosome. In general, chromosomal aneuploidy is not tolerated [18, 19]. Studies suggest that differences in chromosome copy number result in improper expression levels for genes on that chromosome [20,

21]. To further complicate matters, there is growing evidence that an imbalance in sex chromosome dose compared to autosomes can throw-off gene expression within a cell [22-25]. In other words, the gene expression problem arising from chromosome-based sex determination is two-fold. First, there is the imbalance between the sexes that needs to be corrected, and second there is an internal imbalance between the sex chromosome and autosomes that likely needs to be corrected.

The mechanisms organisms use to correct imbalances in sex-chromosome expression are collectively referred to as dosage compensation. Mechanisms of dosage compensation have been studied most heavily in mammals, the fruit fly *Drosophila melanogaster*, and the roundworm *Caenorhabditis elegans*. As with sex-determination, the precise dosage compensation strategies utilized in these organisms vary greatly. However, all three species utilize a specialized molecular machinery to regulate gene expression on the targeted chromosome(s). A crucial step in DC in mammals, flies, and worms is the chromosome-specific recruitment of the dosage compensation machinery to the proper chromosome(s). In the following, I will briefly describe the dosage compensation strategies in mammals, *D. melanogaster*, and *C. elegans*.

Mammalian X inactivation

The dosage compensation mechanism employed in mammals is the transcriptional inactivation of one of the two X chromosomes in females or X chromosome inactivation (XCI) to balance transcription from the single X in males [26]. In males, the X:A expression ratio is balanced by a two-fold upregulation of the male X upon differentiation [25], however the molecular mechanism governing upregulation in males is unknown. The process of X inactivation is more fully understood and is governed, in large part, by information contained on the X chromosome itself called the X inactivation center (XIC) [27](figure in barakat, gribnau review 2009). The driving force behind X inactivation is expression of the long, non-coding RNA Xist (*X i*nactivation *s*pecific *t*ranscript) which is encoded within the XIC [28, 29]. At the blastocyst stage of female mammalian development, repression of *Xist* keeps both X chromosomes active in the cells of the pluripotent inner cell mass. *Xist* expression is repressed by several mechanisms. The transcription of the non-coding RNA gene *Tsix* in the antisense direction directly competes with transcription at the *Xist* promoter. Also, binding of key pluripotency factors (Rex1, Klf4, and c-Myc) to the first intron of *Xist* contributes to repression [30-32]. Upon differentiation, *Xist* becomes expressed from both X chromosomes but more RNA will accumulate on one X and spread in *cis* to mark that X for inactivation in what is currently understood to be a stochastic process [33]. Accumulation of Xist on the inactive X (Xi) results in immediate recruitment of the Polycomb Repressor Complex 2 (PRC2) followed by PRC1 [34-36]. PRC2 is a histone 3

lysine 27 (H3K27) methyltransferase complex and its activity results in an accumulation of H3K27me3 on Xi. PRC1 then binds H3K27me3 and it contains an E3 ubiquitin ligase that ubiquitylates C-terminal lysine residues of H2A and the H2A variant H2A.Z [37, 38]. The accumulation of PRC2 and PRC1 on Xi is transient but H3K27me3 and H2A/H2A.Z-Ub enrichment are persistent [39].

Both H3K27me3 and H2A-Ub are marks of gene repression. Other repressive chromatin marks accumulate on the Xi such as H3K20me1 and H3K9me2/3 and Xi is correspondingly depleted of chromatin marks associated with gene activation such as H3K4 methylation and H4K16 acetylation [40-43]. One chromatin signature that is uniformly enriched on Xi is the histone variant macroH2A. The large C-terminal macro domain of macroH2A can prevent transcription *in vitro* [44] and is strongly associated with inactive genes in vivo [45-47]. However, enrichment of macroH2A is not required for the maintenance of XCI [48] so the role of this variant in XCI is unclear.

Traditionally, heterochromatin marks are thought to present a physical block or challenge to the transcription machinery either by burying required binding sites for basal transcription factors or by physically impeding the procession of the elongating RNA Polymerase II (RNAPol II) [49]. These general concepts may indeed contribute to gene silencing on Xi. Fluorescence *in situ* hybridization (FISH) studies have revealed that silenced loci are found within a tightly packed, central region of the Xi that colocalizes with H3K27me3 enrichment, while genes that escape inactivation are generally found on the periphery of the Xi [50]. By electron microscopy, the Xi regions positive for

H3K27me3 form dense, fibrous domains that has a unique ultrastructure compared to both constitutive heterochromatin and euchromatin [51]. Finally, the Xi is usually found in close association with the nuclear periphery in interphase suggesting that XCI results in the formation of a discrete, repressive chromatin compartment and this specific organization may contribute to stable gene silencing [50].

Hyperactivation of the male X in *Drosophila*

Drosophila dosage compensation, in my opinion, is the most straight-forward mechanism of the three dosage compensation strategies that have been heavily studied. By hyperactivating the single male X chromosome two-fold, *Drosophila* has addressed both the problem of correcting X chromosome dose between the sexes *and* correcting the X:A imbalance resulting from having only one X. Transcriptional hyperactivation is achieved by the activity of the male-specific lethal or MSL complex [52]. The complex is comprised of the proteins MSL1, MSL2, MSL3, MLE1, MOF (for males absent on the first) and the functionally redundant non-coding RNAs rox1 and rox2. Male-specific expression of MSL2 triggers the loading of the MSL complex onto the X chromosome [53, 54]. MSL1 interacts with MSL2 directly through its coiled-coil domain near the N-terminus [55] and serves as a scaffold for direct binding of MSL3 and MOF at the C-terminal PEHE domain [56, 57]. MLE interacts with the complex by binding MSL3 and its RNA binding domain functions to incorporate the non-coding rox RNAs [58].

The key enzymatic component of the MSL complex is MOF, a MYST-family acetyltransferase [59]. MOF is an H4K16 acetyltransferase but *in vitro* studies have shown that both substrate specificity and full enzymatic activity of MOF require interaction with MSL1 and MSL3 [56]. Msl2-driven loading of the MSL1-MOF-MSL3 H4K16 acetyltransferase complex onto the male X results in an enrichment of H4K16ac [60, 61]. High-resolution mapping of H4K16ac and MSL complex localization by ChIP-chip confirmed observations made by IF analysis that H4K16ac correlates directly with MSL binding and importantly, loss of MSL binding by mutation of one of the components leads to loss of H4K16ac [62].

High resolution analysis of MSL binding also revealed an interesting pattern of localization within genes. Unlike many other factors that exert control over gene expression through localization at the promoter, both the MSL complex and H4K16ac accumulate at the 3' end of expressed genes on the X chromosome [62, 63]. There is a direct correlation between MSL binding of genes and increased expression [64], so it was hypothesized that the 3' accumulation of the MSL complex was directly linked to its function in promoting gene expression. The pattern of MSL and H4K16ac 3' accumulation is similar to the pattern observed for H3K36 methylation that occurs concurrent with polymerase progression through the gene body. Interestingly, the MSL component MSL3 contains a domain that has been shown to recognize H3K36 methylation called the MRG domain. Loss of MSL3 from the complex, interestingly, results in reduced 3' accumulation of the MSL complex [62, 65].

The resulting model is that the MSL complex can recognize actively transcribed genes via MSL3 binding to H3K36me3 [62].

So how does accumulation of MSL complex activity at the latter half of a gene contribute to increased gene expression? Biophysical studies support the notion that nucleosomes present a physical challenge for a processing polymerase [66, 67]. The energy required for polymerase to move through nucleosomes is predicted to be reduced when H4K16 is acetylated [68, 69]. This led to the hypothesis that MSL increases gene expression by increasing the elongation rate of polymerase by reducing the energy required to move through nucleosomes within expressed genes. Experimental evidence in support of this hypothesis has just been published by the Kuroda lab. Larschan and colleagues utilized a technique called global run-on sequencing (GRO-seq) [70], where the origins of run-on sequences are used to map polymerase distribution across the whole of a gene. They compared sequence origin distribution by metagene analysis of autosomal and X-linked genes in male SL2 culture cells. To do this, the authors created a composite autosomal or X gene and graphed average counts of sequence origins along the legth of the composite gene. They report a higher number of sequences originating near the 3' ends of the average X-linked gene than the average autosomal gene, suggesting that polymerase occupancy is higher in this region on X-linked genes than autosomal genes. Importantly, this directly corresponds to H4K16ac enrichment and is dependent on the MSL complex. These exciting new data provide the first experimental evidence that *Drosophila* dosage compensation increases gene expression by directly

increasing transcription rates at the step of polymerase elongation. The increase in elongation occurs downstream (temporally and spatially) of any gene-specific regulation that is likely occurring at the promoter, so this elegant mechanism also explains how one dosage compensation strategy can regulate a diverse group of genes expressed at such a dynamic range.

The recognition of H3K36 methylation by MSL3 explains how the complex can recognize expressed genes on the male X chromosome, but how does the complex restrict its localization to the male X chromosome? Early analysis of MSL complex binding in different msl mutant animals revealed that MSL1 and MSL2 could bind to a limited number of sites on X in the absence of any of the other MSL components [53, 55]. These sites of MSL1-MSL2 minimal complex binding were called chromatin entry sites (CES) [71]. It was proposed that these sites might function as the primary sites of MSL complex recognition and binding followed by local spreading to sites with lower affinity for the complex. Additionally, the two *roX* loci function as chromatin entry sites. *roX* transcription is required for proper MSL loading, and an attractive hypothesis is that these non-coding RNAs serve a similar function as Xist RNA in mammalian X inactivation, as drivers of dosage compensation chromosome specificity [72].

It has since been understood that sites with affinity for the minimal MSL1-MSL2 complex or sites with highest affinity for the whole complex (identified in a study that used a ChIP-chip protocol with minimal cross-linking) are enriched with a GA-dinucleotide repeat and have low levels of nucleosome occupancy [73, 74]. In other words, these sites have a characteristic sequence and chromatin

makeup. The regions on X with highest affinity for the MSL complex are on average 800 bases long and are most often found proximal to genes (within 3kb) or within introns. Most of the binding within genes, particularly the 3' enrichment pattern described above is contingent on assembly of the whole complex [73]. Proximity of the GA repeat element to a gene can increase the expression of a reporter, identifying these sequences as MSL response elements (MREs). *In vivo* proximity of genes to regions containing the MRE sequence also positively correlates with the effect dosage compensation has on the transcription of that gene.

In summary, the male specific production of MSL2 triggers the loading of a complex that directly increases transcription elongation in a two-step process. The first step involves the binding of at least a minimal MSL1-MSL-2 complex to regions of the X containing an MRE sequence with low nucleosome occupancy. This includes binding to the *roX* loci, which is crucial for the assembly of the whole complex. High levels of recruitment to sites dispersed along the X may create a local enrichment of this complex within the X chromosome territory, promoting local dissemination to active genes as identified by H3K36 methylation binding by MSL3. MOF activity (assisted by MSL1 and MSL3) results in an accumulation of H4K16 acetylation within the gene body of MSL-bound genes, directly impacting the rate of transcription elongation and increasing gene expression.

Two-fold repression of both X chromosomes in *C. elegans*

Dosage compensation in the nematode *C. elegans* is achieved by yet another mechanism. Instead of inactivating one X chromosome in the hermaphrodite or increasing expression from the single X in males, *C. elegans* achieves dosage compensation by reducing expression from the two hermaphrodite X chromosomes by half [75-77]. Although this has yet to be absolutely confirmed by allelic analysis of X-linked gene expression, there is evidence to support this mechanism. Firstly, the dosage compensation complex (described below) localizes to both X chromosomes suggesting that both chromosomes are being regulated. Second, there is no evidence of X-linked mosaicism in worms as there is in mammalian females, arguing against single X inactivation [78]. Relatedly, X-linked mutations are not characteristically dominant with variable penetrance and expressivity, as would be expected if one of the hermaphrodite X chromosomes was silenced in each cell. As yet there is no evidence that the male X is upregulated as has been reported in mammals [25], so it is unclear how the X:A imbalance is addressed in *C. elegans*.

The multi-subunit DCC is responsible for dosage compensation function in hermaphrodites [79-81]. Many of the genes encoding complex members were originally identified in forward genetic screens for mutations causing hermaphrodite-specific lethality or in screens for rescue of males killed by ectopic dosage compensation [77, 82-85]. The DCC can be broken into two sub-complexes- a regulatory subcomplex made up primarily of the *s*ex *d*etermination and *d*osage *c*ompensation (*sdc*) genes and an enzymatic condensin complex

[22]. The regulatory portion of the complex is made up of SDC-2, SDC-3, SDC-1, DPY-21, and DPY-30. With the exception of DPY-30, these proteins are largely novel with various conserved domains. The components of the enzymatic condensin portion of the DCC are all homologous to condensin subunits found in all eukaryotes [79].

SDC-2 is the only DCC protein that is expressed solely in the hermaphrodite zygote- all other DCC proteins are maternally loaded into the oocyte [80, 86, 87]. The expression of SCD-2 triggers loading of the complex onto the X chromosomes [81]. Therefore, SDC-2 provides both sex and X-chromosome specificity in dosage compensation. It is a very large protein (344 kDa) with only a predicted phosphorylation site and scattered N-coil domains. The only isolated allele of *sdc-2* that has been characterized, *y74,* is a 4.8kb deletion at the very 5' end of the gene (including 2.1kb of potential upstream regulatory sequence) and is likely a null [87]. Additionally, there has been no structure-function work reported for SDC-2. Perhaps the size of the gene and protein has impeded these kinds of analyses. Nevertheless, the fact that SDC-2 can bind the X in the absence of other complex members and is required to facilitate wild-type levels of DCC binding of the rest of the complex to the X suggest that this protein can both bind chromatin or DNA and directly interact with other DCC proteins.

If SDC-2 is present, SDC-3 can also bind the X in the absence of other complex members and it too participates in the recruitment of the full complex [81]. This function depends on the integrity of SDC-3's zinc fingers, so perhaps

SDC-3 also interacts directly with DNA [88]. DPY-30 is another component of the regulatory subcomplex that is required for the normal DCC binding on X [89]. *sdc*-2 and *sdc*-3 mutations result in failure of the complex to localize to the X and eventually all nuclear DCC signal is lost in the course of development. However, in *dpy-30* animals unbound DCC signal persists into adulthood. This suggests that DPY-30 may have a unique function in regulating DCC localization (discussed further below and in Chapter 5). Although DPY-30 was first characterized as a dosage compensation component in *C. elegans,* homologs in yeast, *Drosophila*, and mammals are all components of H3K4 methyltransferase complexes. One interesting possibility is that the unique function of DPY-30 in dosage compensation may be linked to an evolutionarily conserved role in H3K4 methylation.

Finally, two other regulatory subunits, SDC-1 and DPY-21, are required for dosage compensation but do not ablate DCC binding to the X [90]. SDC-1 contains two C2H2 zinc fingers at its N-terminus, indicating a function in DNA binding [91]. DPY-21 has a proline rich N-terminus, which has been postulated to serve as a docking site for other proteins. As yet it is unclear whether these conserved domains contribute to *sdc-1* and *dpy-21* dosage compensation function.

The other half of the complex forms a *bona fide* condensin complex [79]. Condensins have been heavily studied in the context of mitotic and meiotic chromosome restructuring and segregation. Whether the activity of condensins is actually in condensing chromosomes is a matter of some controversy, but

evidence suggests that condensin complexes contribute to the organization of rigid chromosome structures so that they can withstand the pulling forces of microtubules during anaphase of mitosis and meiosis (reviewed in [92, 93]). There is only one condensin complex in yeast (Condensin I) but most eukaryotes have a second condensin (Condensin II) and the two complexes have unique functions in mitosis and meiosis. All condensins contain two SMC (structural maintainence of chromosomes) subunits with two terminal domains that come together to form an ATP binding domain upon folding of the protein at the hinge domain. In addition to the SMCs, there are three regulatory CAP subunits (chromosome associated polypeptide). The makeup of the CAP subunits differs between Condensin I-type and Condensin II-type complexes, so this may be how the specific functions of each Condensin is determined.

The dosage compensation specific condensin is a modified Condensin I complex called Condensin I^{DC} and only differs from the *C. elegans* mitotic/meiotic Condensin I (Condensin I^{M}) by one subunit [94]. The dosage compensation specific subunit is the SMC-4 homolog DPY-27. The other SMC protein is MIX-1 and the three CAP subunits in Condensin I^{DC} are DPY-26, DPY-28, and CAPG-1. The genes encoding DPY-26, -27, and -28, were identified in forward genetic screens for dosage compensation defective mutations [82, 95], but MIX-1 and CAPG-1 were identified more recently by biochemical approaches [94, 96]. The fact that dosage compensation in *C. elegans* involves the enrichment of a condensin complex on the X chromosomes has led to the hypothesis that changes in higher-order chromatin structure exerted by condensin are

responsible for the two-fold repression in gene expression [78, 93]. Although the biochemical function of Condensin I^{DC} has not been characterized, a mutation affecting the ATPase domains of either DPY-27 or MIX-1 disrupts dosage compensation, supporting the hypothesis that the enzymatic function of Condensin I^{DC} is required for dosage compensation in *C. elegans* [96, 97].

Much like MSL binding to high affinity or chromatin entry sites, it has been observed that the *C. elegans* DCC binds to different classes of sites on the X chromosomes. By observing DCC binding to pieces of the X chromosome detached from the rest of the chromosome either in the form of a free duplication or translocation, it was found that not all regions recruit the DCC independently of the X [98]. Sites that have the intrinsic capability to recruit the DCC have been termed *rex* sites for *r*ecruitment *e*lement on *X*. All other sites that bind DCC without recruitment ability have been named *dox* sites for *d*ependent *o*n *X* [99]. High resolution mapping of DCC binding by ChIP-chip also revealed that there is unequal binding of the complex along the X chromosome [76, 100]. Ercan and colleagues identified about 50 sites with exceptionally high levels of binding that they termed DCC Foci and it was hypothesized that these sites also represented sites of DCC recruitment, similar to the data for MSL binding in *Drosophila*. It was subsequently found, however, that DCC Foci do not necessarily have the ability to recruit DCC in single copy chromosomal deletion and translocation strains [94]. Sites with significantly higher levels of DCC binding only in the context of the X chromosome have been termed way-stations. The combined accumulation or stability of DCC binding on the X at *rex* sites and way-stations may aid in

chromosome-wide DCC dispersal. Also, this demonstrates that DCC binding on the X does not simply fall into two categories. Rather, like in *Drosophila* dosage compensation, there are multiple classes of DCC binding sites on X either with varying affinity for complex binding or relying on slightly different binding mechanisms.

Motif searches have been performed using both *rex* sites and Foci identified by the Meyer and Lieb groups [76, 100]. Similar motifs were identified. One version of this motif identified by the Meyer lab was called MEX for motif enriched on X, but, in spite of the name, it is only mildly enriched on the X chromosomes. Still, functional assays have shown that repeats of this motif in multicopy extrachromosomal arrays can recruit the DCC *in vivo* [76]. This has lead to the proposition that clustering of the motifs on the X perhaps contributes to DCC targeting and indeed the motif does appear to be more clustered on X than on autosomes. However, there are *rex* sites that do not contain this motif and there are occurrences of the motif on the X chromosome that are not bound by the DCC [76, 100]. It is likely that it is the combination of MEX sequences and some aspect of chromatin organization that results in successful targeting. This would be similar to the mechanism of MSL targeting in *Drosophila* where MSL high affinity binding occurs in regions that a) contain the GA dinucleotide repeats and b) are free of nucleosomes.

A significant subset of DCC binding is actually at the promoter region of expressed genes. This localization is dynamic as changes in the gene expression profile at different developmental stages correlates with changes in

DCC localization [101, 102]. Also, the DCC can spread from *rex* sites to the promoters of active autosomal genes on X:A translocation chromosomes, suggesting that promoter localization is dependent on gene activity rather than sequence [101]. Curiously, DCC binding to the promoter of a gene is not predictive of that gene being regulated by dosage compensation [76]. Microarray analysis of gene expression profiles in male and hermaphrodite embryos was performed to first identify X-linked genes with equal expression levels between the sexes. Genes with two-fold higher levels of expression in wildtype hermaphrodites are classified as not subject to dosage compensation. Jans and colleagues then looked at expression changes in dosage compensation mutants. An expression increase of a gene that is normally expressed equally in sexes was identified as a compensated gene. By these standards the genes that were identified as not compensated (~300) and the genes identified as compensated (~300) were equally likely to have DCC-bound promoters. This is in striking contrast to the direct correlation between MSL binding and regulation observed in *Drosophila* dosage compensation [73, 74]. The authors concluded that the lack of correlation between promoter binding and regulation suggests that the DCC does not exert its effects on gene expression locally. They propose that DCC binding may alter the three dimensional structure of the X chromosomes to regulate gene expression at a distance.

In the future, it will be interesting to look at changes in gene expression upon loss of dosage compensation using a more sensitive method of detection than microarray analysis. Before regulation at the promoter can be completely

ruled out, I think it will also be important to look at changes in expression either at very specific developmental timepoints or in a homogenous population of cells instead of using mixed populations of embryos at different developmental stages. Unfortunately, there is not a robust *C. elegans* cell culture system yet. Still, with developmental differences and reduced sensitivity potentially confounding these results, I am not convinced that we will not eventually understand that *C. elegans* dosage compensation involves direct regulation of gene expression to some extent.

Currently, there are significant gaps in our understanding of the *C. elegans* dosage compensation mechanism. The separation between DCC binding and regulation of gene expression creates one such gap in our understanding of how the DCC mechanistically represses expression levels on the X. The particular goal of my thesis, however, is to address the gap in our understanding of how the initial targeting of the DCC to the X chromosomes is achieved. In this work I have addressed the requirements within Condensin I^{DC} for X chromosome localization. I have also contributed to our understanding of the similar Condensin I complex in mitosis and meiosis. I have provided the first evidence that chromatin, specifically the histone variant H2A.Z/HTZ-1 contributes to DCC targeting in a way that was not appreciated or addressed before. Finally, I have demonstrated that the DCC regulatory subunit, DPY-30, functions in dosage compensation in a manner that is completely independent of its role in H3K4 methyltransferase complexes.

The histone variant H2A.Z has diverse functions in eukaryotic genomes

My work has identified the H2A histone variant H2A.Z (HTZ-1 in *C. elegans*) as an important player in DCC targeting as described in Chapter 3. However, this enigmatic histone variant has an interesting history of being functionally tied to a diverse range of activities in different organisms. To provide a foundation for understanding how this protein can function in different, even opposing functions I will first describe the physical characteristics of H2A.Z. I will then describe the currently understood functions of H2A.Z in transcription regulation as this is the most heavily studied aspect of H2A.Z biology. Finally, I will describe H2A.Z function in setting up chromatin boundaries as this relates directly to my work on H2A.Z in *C. elegans* dosage compensation.

The physical properties of H2A.Z

H2A.Z is essential in all eukaryotes studied except *S. cerevisiae*, with mutants of many organisms dying early in development. H2A.Z is also remarkably conserved among eukaryotes with ~90% amino acid sequence identity [103]. In comparison, the sequence identity between H2A.Z and H2A within the same organism is closer to 60% on average [104]. The essential functions of H2A.Z likely map to its unique regions when compared to canonical H2A. I will discuss the unique physical characteristics of H2A.Z below.

The crystal structure of the H2A.Z nucleosome was published in 2000 by the Tremethick and Luger groups and overall showed a similar structure to the canonical nucleosome [105]. There were a few noteworthy differences that are

nicely summarized by Thakar (2009) shown in Figure 1.X [106]. Within the structured histone fold domain, Loop 1 shows a significant difference by crystallography. This region is the only point of contact between the two H2A.Z or H2A molecules in the nucleosome and it was predicted that the conformation of the interaction domain of H2A.Z (which is more extensive) and H2A are sterically incompatible, making an H2A/H2A.Z, or heterotypic, nucleosome unlikely. The authors predicted that unique L1 loop structure, which is also observed in the H2A variant macroH2A, could serve as an internal mechanism to ensure nucleosomes contain only one type of H2A at once (homotypic). They go on to point out that the only histones with variants, H2A and H3, are the only histones in the nucleosome with interactions between the two copies, suggesting that this concept might apply to all histone variants. This prediction has not been met, however. It has been observed that H2A/H2A.Z heterotypic nucleosomes can certainly form *in vitro* [107] and the Henikoff lab has recently published a method to comparatively map heterotypic and homotypic nucleosome patterns *in vivo* [108]. The authors report that the *Drosophila* version of H2A.Z, H2Av, is found in heterotypic nucleosomes ubiquitously in the genome.

The H2A.Z/H2A.Z interaction surface may be more extensive and stable, but what about the interaction surface between the H2A.Z/H2B dimer and the H3/H4 tetramer? This interaction surface is termed the docking domain and is actually predicted to be *less* stable in the H2A.Z-containing nucleosome [105]. A single amino acid substitution in H2A.Z's docking domain disrupts three hydrogen bonds that normally form between H2A and H3. Also, the H2A.Z/H2B

dimer has an extended acidic patch compared to the H2A/H2B dimer that is predicted to change the interaction surface between it and the H4 N-terminal tail of a neighboring nucleosome. In domain swapping experiments the C-terminal region containing the docking domain from H2A in an H2Av construct was not able to rescue an H2Av null mutant in *Drosophila* and is also essential for H2A.Z function in *Xenopus*, so this unique region is vital for the biological function of H2A.Z [109, 110].

Many groups have sought to understand how the unique structural features of the H2A.Z nucleosome contribute to different functional outcomes. One feature that has been tested extensively is the stability of H2A.Z nucleosomes, and the results are conflicting. Initially, it was reported that H2A.Z-H2B dimers were more stable as it eluted from chromatin (isolated from Chicken erythrocytes) on a hydroxyapatite column at higher salt concentrations than H2A [111]. However, H2A.Z was later reported to be *less* stable by salt stability assays on nucleosome core particles (NPCs) assembled *in vitro* and isolated chromatin fibers in yeast [112, 113]. In 2006, Thambirajah and colleagues re-visited the question of H2A.Z stability using native chromatin again from chicken erythrocytes [114]. The authors utilized decreasing pH, sucrose sedimentation, and salt treatment and determined that native H2A.Z nucleosomes are slightly more stable than H2A nucleosomes. Treating the cells with a histone deacetylase (HDAC) inhibitor prior to chromatin isolation decreased the stability of H2A.Z nucleosomes. This indicates that increased histone acetylation disrupts H2A.Z-conferred stability. Although the authors specifically detected acetylated

H2A.Z in these samples, hyperacetylation of histones H3 and H4 may also contribute to this result as the HDAC inhibitor is non-specific. Finally, salt solubility at low concentration is considered a general characteristic of “open chromatin”. Low-salt soluble regions have been mapped in mammalian and drosophila genomes by the Henikoff lab [115]. Interestingly, homotypic H2A.Z nucleosomes (or H2Av in *Drosophila*) map to regions with low-salt solublity particularly at expressed genes, which might suggest that H2A.Z contributes to a less stable nucleosome *in vivo* [108]. However, the authors offer a different interpretation. They suggest that it is the slight stabilization that allows H2A.Z to preferentially accumulate over H2A in regions with high nucleosome turnover. The increased stability may allow for faster re-assembly of nucleosomes in regions where nucleosomes are constantly being assembled and disassembled to accommodate PolII passage. A complete understanding of how H2A.Z affects the stability of the nucleosome has yet to emerge, but for now it seems that in the context of native chromatin, H2A.Z may have a more stabilizing effect.

One property of the H2A.Z nucleosome that has been less controversial is its differential mobility compared to H2A. Nucleosome sliding can be an active process requiring nucleosome remodeling enzymes, but nuclesomes do have a limited capability to move on their own particularly at higher temperatures. Flaus et al. demonstrated that H2A.Z nucleosomes have increased thermal mobility compared to H2A nucleosomes [116]. Relatedly, the spacing or phasing of H2A.Z nucleosomes is slightly different than observed for H2A on both nucleosome fibers *in vitro* and chromatin *in vivo*. Reconstituted nucleosomes

position themselves on DNA very differently depending on whether they contain H2A or H2A.Z, suggesting that H2A.Z has the inherent ability to alter nucleosome position [106, 117, 118]. Homotypic H2Av nucleosomes within expressed genes in *Drosophila* tend to be uniquely shifted, which may reflect enhanced movement of the nucleosome in response to PolII elongation [108]. Also, recent evidence suggests that increased thermal mobility of H2A.Z nucleosomes serves an important function in plants as a mechanism to change gene expression in response to temperature stress. At high temperatures, H2A.Z is lost from promoters in *Arabidopsis*, allowing for the transcriptional changes required by plant cells to survive fluctuations in temperature [119]. The unique docking domain of H2A.Z as described above may confer enhanced mobility, as mutations in canonical histones that map to this interaction surface lead to increases in thermal mobility to a similar level as H2A.Z [116].

Another property of H2A.Z that has been addressed experimentally is the effect it has on higher-order chromatin organization. The Tremethick lab utilized salt sedimentation analysis of *in vitro* assembled nucleosome fibers to determine the extent of organization H2A.Z nucleosomes undergo on their own [118]. Upon increasing concentrations of Mg^{2+} in solution, individual nucleosome fibers will both fold upon themselves and oligomerize with other fibers, which can be observed by changes in ultracentrifuge sedimentation velocity. The authors observed that individual H2A.Z fibers formed a compact structure (about as compact as the 30nm fiber) more readily than H2A fibers, however further compaction by fiber oligomerization was impeded by H2A.Z. In a later study the

same group found that H2A.Z interacts with heterochromatin protein 1 (HP1) *in vivo* by reciprocal immunoprecipitation analysis [120]. The authors utilized the same *in vitro* nucleosome reconstitution system to test whether HP1 can directly interact with an H2A.Z nucleosome fiber and found that HP1 had a much higher affinity for the H2A.Z fiber, particularly in its intrafiber folded conformation. I mentioned previously that the H2A.Z acidic patch was predicted to be an important interaction surface for the H4 N-terminal tail of the neighboring nucleosome [105]. The Tremethick group demonstrated that the increased fiber folding and increased HP1 binding requires both the extended acidic patch of H2A.Z and the N-terminal tail of H4, consistent with that structural prediction. While it is true that reconstituted nucleosome fibers do not completely recapitulate the natural chromatin environment, these studies provide clear evidence that H2A.Z certainly *can* alter the properties of chromatin folding. It has been observed that H2A.Z and HP1 coloclalize at pericentric heterochromatin. Additionally, H2A.Z nucleosome fibers are refractory to linker histone binding [106]. So perhaps the compaction of H2A.Z fibers does not allow the linker histones proper access or the kind of ion-dependent *in vitro* folding of H2A.Z is maintained by HP1 in place of linker histones *in vivo.*

Changes in higher order chromosome organization brought about by H2A.Z *in vivo* are not completely understood. Although the lion's share of H2A.Z research has focused on its role in transcription, loss of H2A.Z is known to affect genome stability via chromosome loss and chromatin bridging [121, 122], both of which can occur as a result of disruptions in higher order chromatin organization.

So, formation of higher-order chromosome structures by H2A.Z likely contributes to its overall essential function in many eukaryotes.

As mentioned above, H2A.Z is subject to post-translational modifications. These modifications are similar to those observed for canonical H2A. The N-terminus of H2A.Z contains 5 lysine residues that are readily acetylated and non-acetylatable mutants in both *S. cerevisiae* and *S. pombe* cannot rescue *htz1Δ* mutants [123, 124]. Although it was originally observed in yeast that acetylation of one lysine (K14) predominates, recent studies indicate that acetylation of any one of the 5 residues is sufficient for function. Furthermore, there is no evidence that H2A.Z is differentially acetylated [124]. Acetylation of N-terminal lysines is a conserved characteristic; indeed we have observed N-terminal acetylation of *C. elegans* HTZ-1 by mass spectrometry (Figure 1.6).

H2A.Z is also subject to ubiquitylation at the C-terminus in mammals. Ubiquitylation occurs preferentially at lysine 121 by PRC1, the same complex responsible for H2A ubiquitylation [125]. Although it was originaly observed that H2A.Z was depleted on Xi [126], the H2A.Z antibodies used in these analyses are blocked by ubiquitylation. When an antibody raised against the N-terminal region of H2A.Z was used instead, Sarcinella and colleagues found that there is indeed a population of H2A.Z on the inactive X, although it is still found at lower levels than the rest of the genome. They concluded that the H2A.Z population on Xi is mono-ubiquitylated by PRC1 as is H2A and this may contribute to the formation of facultative heterochromatin and gene silencing during XCI. Mono-

ubiquitylation of H2A.Z has not yet been observed in other organisms, but it is not unlikely as the C-terminal lysine residues are conserved.

A final factor that contributes to the properties of an H2A.Z nucleosome is the makeup of the other histones and *their* post-translational modifications. There is a positive correlation between H2A.Z occupancy and H4K16ac and H3K4me3, two modifications that are associated with active or open chromatin. In yeast, H4K16ac is required for deposition of H2A.Z specifically in telomere-proximal chromatin and a subunit of the complex that is responsible for deposition of H2A.Z recognizes acetylated H3 and H4 N-terminal tails [127]. H3K4me3 is found enriched at active promoters as is H2A.Z and may even overlap within the same nucleosomes [128]. However, whether H3K4 methylation precedes H2A.Z deposition or vice-versa may differ from gene to gene. In an *in vitro* hematapoesis culture system it has been observed that hematopoetic stem cells have a set of genes containing both H3K4me3 and H3K27me3. These have been named bivalent genes as these two marks are associated with opposing effects on transcription. Upon differentiation, bivalent genes undergo either stable silencing or activation. The activated genes will lose H3K27me3, become further enriched with H3K4me3 and will then accumulate H2A.Z at the promoter [129]. However, at certain inducible genes in yeast, H2A.Z serves as a marker of transcriptional memory and is found at the promoter in the absence of transcription [130, 131]. Upon induction, these genes accumulate H3K4me3 [130]. Regardless of the order, the combination of both H2A.Z and H3K4me3 strongly correlate with active gene expression.

H2A.Z-containing nucleosomes can also contain H3.3, a variant of canonical histone H3. This interesting combination is found at the most labile nucleosomes *in vivo*. The sliding capability of H2A.Z nucleosomes is not affected by H3.3 incorporation *in vitro* and, interestingly, this group did not observe any significant change in salt-dependent stability of H2A.Z/H3.3 double variant nucleosome fibers [106]. Nonetheless, H2A.Z and H3.3 map to the same nucleosomes that correspond to both the “Nucleosome Depleted Regions” (NDRs) over the transcription start sites of genes, DNaseI hypersensitive sites, and low-salt soluble fractions [132]. Curiously, human H3.3 only differs from canonical H3 by 5 amino acids (as reviewed by Szenker [133]). None of these changes fall within predicted H2A.Z/H3.3 interaction surfaces, so it remains unclear whether the instability of these nucleosomes is a result of the unstable nature of these nucleosomes (although *in vitro* data so far does not support this), or whether the formation of the double variant nucleosome is a consequence of the high level of turnover brought about by other mechanisms.

Biological Function of H2A.Z

Although I have already touched on the proposed functions of H2A.Z in discussion of its structure and properties, I will explore this topic in more detail here. I will first describe the current understanding of H2A.Z in transcription followed by a description of the proposed boundary functions of H2A.Z in yeast, *Arabidopsis*, and mammals. Finally, I will describe the data available on H2A.Z function in *C. elegans*.

I should preface this discussion on the proposed role of H2A.Z functions with a warning that much of the data on this topic is highly correlative, rather than mechanistic. At the end of a brief comment in Nature Genetics Steve Henikoff concluded, “This reminds us how little we understand the process that makes DNA accessible for gene expression and regulation and suggests we might better focus our attention on connecting marks to mechanisms,” [132]. This is indeed an important challenge for all of chromatin research, and H2A.Z is no exception.

When H2A.Z variants were initially described, the localization of *Tetrahymena* H2A.Z (Hv1) in the transcriptionally active macronucleus [134] and the observation that H2A.Z fractionates with active chromatin upon salt treatment [111] suggested a positive function in transcription. Subsequently, genetic analyses in *S. cerevisiae* (again, the only eukaryote in which H2A.Z is not essential under normal growth conditions) pointed toward a role of H2A.Z in the positive regulation of gene expression [134]. *HTZ1* in budding yeast interacts with the SWI/SNF nucleosome remodeling complex to promote gene expression [135]. As H2A.Z nucleosomes have the propensity to slide as discussed above, there may be cooperation between SWI/SNF-dependent nucleosome sliding and H2A.Z sliding that provides the movement necessary for access to DNA by the basal transcription factors or movement of the elongation complex. Additionally, *HTZ1* is required for the proper activation of some nutrient and heat-shock inducible genes, and cell cycle regulated genes in yeast [113, 135-138]. ChIP-

qPCR analysis at such loci determined that Htz1p is normally found at these promoters supporting a direct role for *HTZ1* in regulating expression.

In an effort to get a better understanding of a general mechanism for H2A.Z in gene expression, a number of labs published genome-wide localization data for the budding yeast Htz1p [113, 117, 131, 139, 140]. All studies reported an enrichment of Htz1p at budding yeast promoters. Approximately 63% of all yeast genes harbor Htz1p in a particular pattern around the TSS. There is no strict correlation with Htz1p and activity, however, as Htz1p is observed at both active and inactive genes. Additionally, genes with highest expression rates were originally reported to be depleted for Htz1p, but this conclusion may have more to do with the overall paucity or instability of nucleosomes on such genes. Transcription start sites are often sites of high accessibility by nucleases and restriction enzymes and the low levels of nucleosome occupancy as measured by histone H3 occupancy. (These sites were originally referred to as Nucleosome Free Regions but this has since been updated to Nucleosome-Depleted Regions (NDRs) as more sensitive detection techniques have shown that nucleosomes are present at low levels.) Interestingly, the enrichment of Htz1p is in the two nucleosomes surrounding the NDR in budding yeast with perhaps the strongest enrichment in the +1 and +2 nucleosomes immediately downstream of the transcription start site (TSS) [131, 140]. Htz1p nucleosomes at promoters also have a more organized spacing compared to promoters without Htz1p (Yuan et al 2005 and Guillemette 2005) [131, 141]. The nucleosome organization was determined to be a direct result of Htz1p incorporation as *htz1Δ* mutants lose

organized spacing at individually tested promoters [131]. What is not lost in *htz1Δ* cells, however, is the NDR. This led to the hypothesis that sequence information at these loci determine the organization of chromatin surrounding it. The minimal sequence sufficient for NDR establishment has been identified in budding yeast and this sequence is sufficient to specify Htz1p occupancy in the surrounding nucleosomes [142].

In spite of the strong occurrence of Htz1 at promoters in yeast, microarray analysis of global gene expression changes in *htz1Δ* mutants showed only modest changes in expression for ~300 genes [143]. 200 genes are significantly downregulated and around 100 were significantly upregulated in *htz1Δ* cells collected during log phase growth in nutrient rich media. It is likely that constitutively expressed genes have multiple mechanisms driving expression such that loss of only *htz1* is not enough to significantly compromise transcription. Also, Htz1p is found at the promoters of many inducible genes that are not active under the conditions examined. The Brickner lab has published several studies on the effects of Htz1p in expression of inducible genes and found that loss of Htz1p can affect the rate at which these genes can be turned on, but expression eventually arrives at observed wildtype levels [130, 144]. Therefore, it is also possible that Htz1p positively affects the rate of transcription initiation, which would be undetectable by microarray analysis at a single, late time point.

High resolution mapping of H2A.Z in other eukaryotes has yielded similar results. The Zhao lab has published an extensive characterization of the

chromatin landscape of human T-cells, including the localization pattern of H2A.Z [128]. In this cell type, H2A.Z was found to be enriched at promoters, but in a slightly different manner than was observed in yeast. The accumulation of H2A.Z is not restricted to the two nucleosomes immediately surrounding the TSS, but rather is found several nucleosomes out on either side of the TSS. In particular, H2A.Z accumulates just downstream of the TSS and these nucleosomes are highly ordered compared to H2A nucleosomes. In T-cells there is also a strong correlation between H2A.Z at the promoter and gene activity. Barski and colleagues also noticed the high level of H2A.Z found coincident with H3K4 methylation potentially within the same nucleosome, suggesting that these two chromatin signatures may function together [128]. H2A.Z is also associated with at least a subset of inducible genes. In 2008, John et al. observed changes in chromatin structure as a result of activated glucocorticoid hormone signaling, and the changes they report were not restricted to the promoter region of responsive genes [11]. Indeed the authors mapped H2A.Z to glucocorticoid receptor (GR) binding sites at highly variable distances from the promoter regions of responsive genes. What remains to be tested extensively is how loss of H2A.Z affects gene expression both globally and in response to specific stimuli such as glucocorticoid signaling in mammals.

One such study has been conducted by Hardy and colleagues [145]. The authors studied the genome-wide localization of H2A.Z by ChIP-chip in human U2OS cells (an osteosarcoma cell line) compared to RNA Pol II and observed a high occurrence of both at promoters. However, transcriptional activity is not

necessary for H2A.Z to localize to promoters as it is found with both paused/stalled polymerase populations and elongating populations. In fact, their evidence suggests that H2A.Z may be important for recruitment of polymerase itself as they observed H2A.Z enrichment at an inducible promoter upon induction prior to RNA Pol II. In the absence of H2A.Z, RNA Pol II was not efficiently recruited, supporting a role for H2A.Z in recruitment of the transcription machinery itself. This is consistent with reports in yeast that Htz1p assists in RNA Pol II and cofactor recruitment [136, 137, 146].

In summary, H2A.Z is found at the promoters of both active and inactive but inducible promoters in a conserved manner. This conservation of proximity to the TSS observed in the species studied suggests that direct regulation of transcription onset by H2A.Z may be conserved. H2A.Z incorporation can precede RNA Pol II loading and loss of the variant prevents full RNA Pol II recruitment in yeast and mammals. Additionally, the observation that H2A.Z is found at key transcription factor binding sites such as GR, suggests that H2A.Z may function in gene-specific regulation of expression in addition playing a more general role in recruitment of the transcription machinery.

H2A.Z boundary function

Publications on the genome-wide localization of H2A.Z in all species studied thus far have focused almost exclusively on dissecting the pattern of H2A.Z at the 5' end of genes. However, H2A.Z is more broadly localized in these organisms. In budding yeast, Htz1p is found in wide domains of euchromatic

regions that neighbor silenced telomeres and mating loci [131]. In the recent study of *Drosophila* H2Av homotypic and heterotypic nucleosomes, it was found that both types of nucleosomes are essentially ubiquitous [108]. In mammals, H2A.Z is found in pericentric heterochromatin, the facultative heterochromatin of Xi, at insulator elements, and most sites of DNase I Hypersensitivity (DHS sites) both in and outside of promoter regions [125, 147, 148].

Of particular interest to my work is the observation that H2A.Z is associated with boundary elements and function. In 2000 it was reported that *htz1* function is required for silencing at the mating type HMR locus and at telomeres in budding yeast [149]. In Meneghini's microarray analysis in 2003, a significant portion of the *htz1* regulated genes mapped to within 35kb of telomeres [143]. Finally, high-resolution mapping of Htz1p by Guillemette et al. (2005) demonstrated that Htz1p deposition in chromatin adjacent to telomeres and the mating loci was much broader than the pattern observed at the 5' end of genes [131]. It was hypothesized that these broad Htz1p domains function to protect genes neighboring heterochromatin from being silenced. Upon testing of this hypothesis, it was found that Sir2p, the enzymatic component of the budding yeast silencing machinery, ectopically localizes to subtelomeric genes in the *htz1Δ* strain [131, 143]. Additionally, loss of Sir2p suppressed expression changes observed in *htz1Δ* mutants in subtelomeric genes. It was later found that H3K4 methylation also functions in blocking the spread of heterochromatin. Loss of the enzyme required for H3K4 methylation, Set1, also results in local Sir2p spreading [150]. Upon loss of both *htz1* and *set1*, Sir2p spreading is greatly

enhanced suggesting that Htz1p and H3K4me3 both function to block ectopic heterochromatinization by Sir2p genome-wide [151].

There is evidence that boundary function of H2A.Z is conserved. Acetylated H2A.Z is found at the insulator region of the chicken beta-globin locus [152] . The enrichment of H2A.Zac is independent of nearby expression events and changes in H2A.Z occupancy that accompany expression of nearby genes. Additionally, histone acetylation is limited to H2A.Z at the insulator. This is in contrast to the general accumulation of acetylation on H2A.Z, H3, and H4 that occurs at the 5' regions of nearby genes as they are expressed. The authors concluded that the function of H2A.Zac at the insulator is unrelated to the insulator activity of CTCF, as it is removed from any CTCF binding sites, and instead proposed that it serves to block the spread of heterochromatin through the beta-globin locus. This remains to be tested, but could be done by depletion of H2A.Z in erythrocytes by RNAi or introduction of a non-acetylatable form to observe whether these changes affect chromatin boundaries at this locus.

The Henikoff group has been directly addressing the potential function of H2A.Z as a block to silencing mechanisms by assessing the relationship between the variant and DNA methylation [153]. DNA methylation is an important mechanism in the stable silencing of genes and involves covalently modifying a cytosine base to 5-methylcytosine. The original study directly comparing the patterns of H2A.Z and DNA methylation were conducted in root tissue of *Arabidopsis*. The authors reported a near complete anti-correlation between H2A.Z and DNA methylation. Also, global increases or decreases in the levels of

either H2A.Z or DNA methylation had an opposite effect on the other mark in a direct manner. That is, in plants with reduced H2A.Z, DNA methylation expanded into regions once occupied by H2A.Z and vice versa [153]. This mutual antagonism is conserved in mammals and may be functionally linked to expression changes that occur during cancer progression [154].

Although the data on the transcriptional and boundary functions of H2A.Z suggest that H2A.Z is primarily associated with euchromatin, I will briefly outline data on the functions of H2A.Z in the formation of heterochromatin. In mammals, H2A.Z has been shown to colocalize with HP1 at pericentric heterochromatin and HP1 can directly bind H2A.Z nucleosome fibers *in vivo* and *in vitro* [120, 148]. By high resolution microscopy, it was also observed that H2A.Z/H3K4me2 containing nucleosomes alternate with H2A/H3K9me3 nucleosomes in within pericentric heterochromatin [147]. Shorter stretches of H2A.Z/H3K4me2 nucleosomes are interspersed between large H2A/CENP-A in centric heterochromatin in extended chromatin fibers. In 3-D, the interspersed H2A.Z/H3K4me2 domains of pericentric heterochromatin cluster together in a manner that results in polarization of the centromere (with an H2A.Z pericentric region to one side and H2A pericentric chromatin to the other) and clustering of the H2A.Z nucleosomes within centric heterochromatin may push CENP-A to the outer surface where it can function in kintetochore association. So, H2A.Z is likely to contribute to structure of the centromere and this may explain the genome instability phenotypes observed in many H2A.Z organisms. Similarly, H2Av in *Drosophila* is found at centric heterochromatin [155]. *H2Av* mutations

lead to reduced H3K9 methylation and reduced HP1 binding to chromatin, suggesting that heterochromatin formation is impaired.

The various functional contributions of H2A.Z to seemingly opposing activities may be partially explained by differential regulation of H2A.Z deposition and post-translational modification. The function of H2A.Z in both transcription regulation at the promoter and as a boundary element likely involves acetylation at the N-terminus. In support of this, acetylation is required for normal incorporation of H2A.Z into subtelomeric regions in yeast [122, 127, 156]. Also, the rapid silencing of genes in M phase involves global de-acetylation of H2A.Z in human bladder cancer cells [157]. Non-acetylated H2A.Z nucleosomes then become repositioned such that the +1 nucleosome resides at the TSS and the nucleosome depleted region shrinks considerably. Furthermore, heterochromatin-associated H2A.Z is not acetylated, supporting acetylation as a euchromatin-specifying modification of H2A.Z.

Finally, the incorporation of H2A.Z into euchromatic versus heterochromatic regions may rely on different mechanisms. In yeast, the complex that exchanges H2A/H2B dimers for Htz1p dimers is the Swr1 remodeling complex [158, 159]. Homologous complexes are found in *Drosophila,* mammals, and *C. elegans* suggesting that mechanisms of H2A.Z deposition are generally conserved [160, 161]. It was recently described in *Drosophila* that deposition of H2Av in heterochromatin involves a specific recruitment factor. Incorporation of H2Av into heterochromatin requires the remodeling and spacing factor RSF, which is a heterodimer of Rsf-1 and ISWI [161]. RSF specifically recruits the

H2Av replacement machinery (Tip60) as part of the heterochromatin assembly process and loss of RSF results in loss of H2Av and disrupted heterochromatin formation. It will be interesting to see whether RSF-dependent incorporation of H2A.Z into heterochromatin is a conserved mechanism. This could be tested directly in mammals by RSF RNAi followed by observations of H2A.Z at pericentric and centric heterochromatin.

Function of *C. elegans* H2A.Z/HTZ-1

Prior to my work on the role of HTZ-1 in dosage compensation was published there were only two studies describing HTZ-1 function and organization in *C. elegans* in the literature. The first was a study from the Mango lab which identified *htz-1* as a gene required for expression of the pharynx-specific transcription factor *pha-4* [160]. They found that *htz-1* was required for the timely activation of *pha-4* during development. They also proposed that *htz-1* activation is direct by observing binding of fluorescently tagged HTZ-1 to a fluorescently labeled reporter construct *in vivo.*

The second paper published described the results from genome-wide mapping of HTZ-1 localization in developing *C. elegans* embryos [162]. HTZ-1 in *C. elegans* is also localized strongly to the 5' regions of 23% of genes, although due to trans-splicing mechanisms TSSs have not been mapped so translation start site is used as a proxy. *C. elegans* contains operons and interestingly, HTZ-1 can be found at the start of *internally* coded genes, not just the first gene in the operon. This is found in 37% of all operons and suggests that some internal

operon genes may be independently regulated. The authors also reported that there is reduced HTZ-1 binding on the X chromosomes than autosomes. Sites of HTZ-1 binding on X are similar in amplitude and breadth as on autosomes, indicating that the binding characteristics of HTZ-1 on the X is unchanged, there are simply fewer regions of HTZ-1 binding. The authors concluded that the lower occupancy of HTZ-1 on X was not likely to be of functional significance but merely a reflection of the fact that HTZ-1 is found at promoters of developmentally essential genes of which there are fewer on X. While it is true that the X has fewer genes that result in embryonic lethality when depleted by RNAi [163], this group did not provide any functional data to support this conclusion. Our data actually support a functional role for HTZ-1 depletion on X and this will be discussed thoroughly in Chapter 4.

H2A.Z compartmentalizes the genome

H2A.Z is an evolutionarily ancient protein that has evolved a diverse set of functions. The replacement of canonical H2A with the variant H2A.Z overall imparts structural changes to the nucleosome that can effect chromatin organization in different ways. H2A.Z incorporation into either heterochromatin or euchromatin results in the formation of a specific, functional compartment within the local chromatin environment. Acetylated H2A.Z nucleosome compartments are found at gene promoters, boundary elements, and transcription factor binding sites. These compartments have a high rate of nucleosome turnover, suggesting that their function is to prevent accumulation of silent chromatin marks and keep important regulatory sequences accessible. Acetylation is markedly absent from

H2A.Z found in heterochromatic compartments. Non acetylated H2A.Z nucleosomes form a chromatin fiber that readily condenses through associations between H2A.Z nucleosomes themselves. Condensed H2A.Z fibers have a high affinity for HP1 which may stabilize the clustering of linearly dispersed H2A.Z domains within pericentric heterochromatin and centric heterochromatin to form structural compartments. What ultimately results is the precise organization of the 3-dimensional structure of the centromere in mammals and *Drosophila* required for proper segregation of chromosomes.

The curious case of DPY-30

My work on the role of HTZ-1 in dosage compensation as described in Chapter 4 led us to test whether other chromatin components cooperate with HTZ-1 in this process. As described above, HTZ-1 and H3K4 methylation have been both physically associated in genome-wide localization assays and functionally associated in gene expression regulation and in preventing heterochromatin from spreading in yeast. Interestingly, DPY-30 was previously described to affect DCC localization, similar to what we observe in *htz-1* animals [89]. DPY-30 homologs in other organisms have been characterized as members of H3K4 methylation complexes adding to the possibility that H3K4 methylation functions in dosage compensation. In the following I will briefly describe the complexes responsible for H3K4 methylation, as well as the functions associated with H3K4 methylation that have been described in *C. elegans*.

Like H2A.Z, H3K4 methylation is has been observed in all eukaryotes studied, suggesting it has ancient, conserved roles in chromatin organization. The machinery responsible for H3K4methylation is likewise conserved. *Trithorax (Trx)* in *Drosophila* was the first H3K4methylation component characterized genetically as a positive regulator of homeotic (Hox) gene expression [164]. To better understand the biochemical nature of its gene expression function, studies on the budding yeast *Trx* homolog, *SET1*, were conducted. Set1p contains an RNA recognition motif (RRM) and a Su(var) 3-9/Enhancer of Zeste/trithorax (SET) domain, a domain found in histone methyltransferase enzymes [165]. Set1 was subsequently purified in a macromolecular complex that was characterized to have H3K4-specific methylation activity [166-168]. This complex has been called COMPASS for *com*plex of *p*roteins *as*sociated with *S*et1 and is capable of mono-, di-, and trimethylation of H3K4 [169-171]. There is only one such complex in yeast, but there are several similar complexes in other eukaryotes . Mammals contain both COMPASS-like Set1 complexes (Set1A and Set1B, or collectively referred to as Set1C for Set1 *C*omplexes) and Trithorax-like MLL complexes containing methyltranferase subunits of the mixed lineage leukemia family (MLL1-4) [172-176]. All Set1-like and MLL-like methyltransferases contain a SET domain and Post-set domain at their C-terminus, but the identified domains in the N-terminal regions of these proteins differ. Set1-type proteins all have an N-terminal RRM domain, but MLL proteins (and Trithorax in *Drosophila*) all contain N-terminal plant homeodomains (PHD). The domain structure of Set1 and MLL

proteins has been summarized by Eissenberg and Shilatifard [177] and is shown in figure 1.9.

In addition to the methyltransferase subunit, COMPASS contains seven other proteins that contribute to complex function in methylation [166-168]. These proteins have all been named CPS (for COMPASS) followed by their molecular weight, however, for ease of discussion I will utilize the names of the mammalian orthologs (please refer to Table 5.1 for a list of names in yeast, mammals, and *C. elegans*). WDR5, Wdr82, and RbBP5 all contain numerous WD repeats which commonly function in protein-protein interaction. This implies that these proteins may assist in scaffolding or assembly of the complex. Indeed, WDR5 has been shown to bind directly to both RbBP5 in both yeast and mammalian studies [170, 178] and the methyltransferase subunit (MLL1) in mammals [179] and is required for Set1 stability *in vivo* [170, 171]. RbBP5 binds to Ash2 and a minimal complex containing only these two subunits from mammals has recently been shown to have methyltransferase activity on its own [180]. Additionally, the minimal MLL1 complex required for H3K4me3 *in vitro* contains WDR5, RbBP5 and Ash2L, suggesting that these components form the enzymatic core of H3K4 methylation complexes [181]. Wdr82 is specific to COMPASS or Set1-type complexes and may bind directly to RNAPolII to tether the complex at sites of RNAPolII localization [182]. CXXC1 contains the CXXC domain that is known to bind CpG islands [174]. Structure-function analysis of CXXC1 has revealed that this component functions to target the mammalian COMPASS-like complexes, Set1A and B, to DNA, specifically to euchromatic

regions [183]. Ash2 in yeast (Bre2) contains a SPRY domain (the function of these domains is not known) and is related to *Trx* [167]. In other eukaryotes, Ash2 proteins also contain a PHD finger [184]. SPP1 in yeast contains a PHD finger and binds Bre2/Ash2 forming a structure that has been hypothesized to be similar to the mammalian Ash2 [185]. Finally, the small hDPY-30 protein contains a conserved DPY-30 domain and interacts directly with Ash2 [186]. Based on the crystal structure of the DPY-30 domain, it has been proposed that DPY-30 forms a homodimer that functions to dimerize COMPASS-like complexes [187].

There are several functions that have been linked to H3K4 methylation, a number of which are related to transcription. Genome-wide association studies in yeast have shown that H3K4 methylation is found near the transcription start site of active genes specifically [136, 188-191]. H3K4 methylation appears to drop off within the gene body as trimethylation peaks immediately downstream of the TSS, followed by dimethylation and monomethylation. It has been proposed that this drop-off is due to progressive loss of Set1C from elongating polymerase [189]. Loss of Set1C is dependent on C-Terminal domain Kinase 1 (CTK1), the kinase responsible for phosphorylation of the C-terminal Domain of RNA PolII [188, 192]. This supports the hypothesis that H3K4 methylation drop-off is co-regulated with RNA PolII elongation.

In other eukaryotes such as *Arabidopsis*, *Drosophila*, and mammals, the global pattern of H3K4 methylation is more complex [128, 193-197]. H3K4 methylation has been documented at the promoters of active genes, within gene bodies, in wide domains within developmentally regulated loci, at enhancer

regions, and within pericentric heterochromatin [128, 147, 193-197]. This diverse pattern of H3K4methylation in these organisms may be the result of the activity of the expanded family of Set1 and MLL complexes.

H3K4methylation at the promoter may serve as a binding site for the TFIID component TAF3 suggesting a function in transcription initiation [198]. CHD1 binding to methylated H3K4 suggests a mechanism for the recruitment of elongation and mRNA processing factors to sites of gene expression [199]. Loss of CHD1 results in pre-mRNA splicing defects *in vitro* and *in vivo* and reduced H3K4 methylation by Ash2 depletion has similar effects on splicing. Comparitive profiling of H3K4 mono-, di-, and trimethylation in Arabidopsis demonstrated that H3K4me3 is primarily found at the promoters of highly expressed genes, suggesting that positive regulation of transcription may be imparted largely by this modified form of H3K4 [193].

Trithorax was originally identified as a gene with important roles in *Drosophila* development [164] and mutations in members of H3K4 methyltranferase complexes have developmental phenotypes in mammals, *C. elegans*, and *Arabidopsis* [200-203]. The general function of H3K4 methylation in transcription may certainly contribute to these phenotypes, but it has been specifically linked to developmentally regulated genes at the Hox loci [164, 196, 202-207]. In pluripotent mammalian cells, Hox genes are bivalent as they harbor both H3K4me2/3 and H3K27me3 [208-210]. It has been clearly demonstrated that loss of H3K27me3 leads to ectopic expression of bivalent genes [209, 211, 212], but it has only been recently demonstrated that loss of H3K4me3 prevents

expression [194]. The difficulty in making this connection may be due to the number of complexes responsible for H3K4 methylation in mammals and may also be due to the fact that the overall chromatin environment in pluripotent cells is more conducive to transcription (as review by Meister [213]. In fact, loss of H3K4 methylation does not affect expression of active genes in pluripotent stem cells. It is only upon differentiation that loss of H3K4methylation at bivalent genes results in failure to properly express these genes [194]. Importantly, the genes that fail to activate in this study are genes that are normally bound by Set1C/MLL proteins and are sites that show significant loss of H3K4 methylation.

In addition to playing a role in activation of transcription, H3K4 methylation may serve an important function in transcriptional memory. Above, I described a study where it was reported that M-phase gene silencing involves de-acetylation of H2A.Z at promoters [157]. Hypoacetylated H2A.Z nucleosomes lose all other marks associated with activation, with the exception of H3K4me3. So, H3K4me3 is passed on to the daughter cell and may be important for gene reactivation following telophase.

In *C. elegans*, H3K4 methylation function has been described in vulval development and in aging [214-216]. So far only two H3K4 methyltransferases have been identified in *C. elegans*, SET-2 and SET-16. SET-2 contains an RRM domain and is homologous to Set1-like proteins found in yeast through humans. SET-16 contains PHD fingers in addition to its SET domain placing it in the MLL-family. A Set1-like complex has been identified to genetically function in regulating aging. Loss of *set-2, ash-2,* and *wdr-5* in fertile worms increases

lifespan [216]. Regulation of lifespan by *set-2, ash-2, and wdr-5* specifically requires the presence of fertilized eggs, although the molecular signal from either fertilization or the egg itself is unknown. Vulval development in *C. elegans* is particularly sensitive to changes in chromatin organization [217-219]. An MLL-like complex containing SET-16 is required for proper development of the vulva [214]. Interestingly, the authors did not detect expression changes in the vulval Hox genes that were tested, but rather observed that MLL is required for the expression of an epithelial cell membrane marker called AJM-1. Loss of *ajm-1* expression on its own led to increased RAS signaling, suggesting that MLL affects vulval development via regulation of a cell membrane component.

As mentioned above, DPY-30 is a component of all of the biochemically purified Set1 and MLL complexes [166-168, 220] but it was originally identified as a gene required for *C. elegans* dosage compensation [200]. In *dpy-30* hermaphrodites, the DCC fails to accumulate on the X by IF and ChIP-chip analysis [89, 102]. In the other dosage compensation mutants where the X fails to accumulate on the X chromosome, the DCC signal is lost over time, suggesting that chromatin localization stabilizes the complex [79, 80, 86, 87, 96]. However, in *dpy-30* animals the DCC signal remains high [89, 102] (and Chapter 5). This is similar to the observation made in *htz-1* animals where we did not detect any changes in the DCC signal, we only detected changes in DCC localization [221]. It is unclear as to how DPY-30 functions in DCC localization, but the published characterization of the DCC regulatory component SDC-3, mentioned that SDC-3 signal was specifically lost in *dpy-30* mutants [81]. In that

report the authors hypothesized that the role of DPY-30 in dosage compensation was specifically in the regulation of SDC-3, however there has not been any follow-up work to address this.

dpy-30 male animals also display developmental defects, suggesting that it has functions outside of dosage compensation [200]. Indeed, *dpy-30* can suppress growth defects and lethality of HP1 (heterochromatin 1) mutants and has been proposed to function in conjunction with other Set1/MLL components in antagonizing HP1 [215]. Also, loss of *dpy-30* in *C. elegans* affects global levels of H3K4 methylation and physically interacts with ASH-2 in a reciprocal fashion [102]. These indicate that DPY-30 functions in Set1/MLL complexes in *C. elegans* as described in other eukaryotes.

The question remained as to whether H3K4 methylation contributes to dosage compensation. We were interested specifically in whether DPY-30's role in dosage compensation is related to H3K4methylation and whether H3K4 methylation might function with HTZ-1 in regulating DCC localization. The results of these studies are described in Chapter 5.

How is the *C. elegans* DCC specifically targeted to the X chromosome?

The overall goal of my thesis work has been to help understand the requirements for DCC targeting in dosage compensation. To accomplish this I needed to first understand the restrictions within the complex itself that contribute to its ability to bind chromatin. Described in Chapter 2 is the characterization of CAPG-1, the final identified member of the dosage compensation condensin

complex. My work on this project demonstrated that CAPG-1 is required for the DCC to localize to the X chromosomes and indeed loss of any one of the DCC subunits I tested resulted in failure of DCC loading. I also observed defects in chromosome segration in my CAPG-1 depletion experiments suggesting a role for CAPG-1 in chromosome segregation. We confirmed that CAPG-1 is found in a newly identified condensin that functions in mitosis and meiosis. In Chapter 3, I went on to test whether the chromatin-binding requirements of the mitotic and meiotic condensin are the same as the DC condensin complex.

Next, I wanted to understand how the chromatin environment contributed to X-specific targeting of the DCC. In Chapter 4, I describe the role of *htz-1*, which encodes the *C. elegans* H2A.Z variant, in dosage compensation. The identification of a condensin complex in dosage compensation had led to the hypothesis that the process affects higher order chromosome structure [78], but no one had previously looked at how changes in chromatin organization at the fundamental level of the nucleosome might be involved.

Finally, I wanted to know whether other nucleosomal factors contributed to DCC targeting. I focused on testing H3K4 methylation as it is so often functionally linked with H2A.Z in the literature, and the DCC protein DPY-30 is found in H3K4 methyltransferase complexes in other organisms. I hypothesized that H3K4 methylation contributed to dosage compensation along with H2A.Z and that DPY-30 function in dosage compensation was linked to H3K4 methylation. I tested this hypothesis extensively and the results are described in Chapter 5.

References

1. Sandman, K., S.L. Pereira, and J.N. Reeve, *Diversity of prokaryotic chromosomal proteins and the origin of the nucleosome.* Cellular and molecular life sciences : CMLS, 1998. **54**(12): p. 1350-64.
2. Ouzounis, C.A. and N.C. Kyrpides, *Parallel origins of the nucleosome core and eukaryotic transcription from Archaea.* Journal of molecular evolution, 1996. **42**(2): p. 234-9.
3. Dinger, M.E., G.J. Baillie, and D.R. Musgrave, *Growth phase-dependent expression and degradation of histones in the thermophilic archaeon Thermococcus zilligii.* Molecular microbiology, 2000. **36**(4): p. 876-85.
4. Monneron, A. and W. Bernhard, *Fine structural organization of the interphase nucleus in some mammalian cells.* Journal of ultrastructure research, 1969. **27**(3): p. 266-88.
5. Smetana, K. and F. Hermansky, *A Contribution to the Knowledge of the Ultrastructure of Leukaemic Lymphocytes.* Neoplasma, 1963. **10**: p. 405-11.
6. Felsenfeld, G. and M. Groudine, *Controlling the double helix.* Nature, 2003. **421**(6921): p. 448-53.
7. Rando, O.J. and K. Ahmad, *Rules and regulation in the primary structure of chromatin.* Current opinion in cell biology, 2007. **19**(3): p. 250-6.
8. Morse, R.H., *Transcription factor access to promoter elements.* Journal of cellular biochemistry, 2007. **102**(3): p. 560-70.
9. Carr, A. and M.D. Biggin, *Accessibility of transcriptionally inactive genes is specifically reduced at homeoprotein-DNA binding sites in Drosophila.* Nucleic acids research, 2000. **28**(14): p. 2839-46.
10. Boyle, A.P., et al., *High-resolution mapping and characterization of open chromatin across the genome.* Cell, 2008. **132**(2): p. 311-22.
11. John, S., et al., *Interaction of the glucocorticoid receptor with the chromatin landscape.* Molecular cell, 2008. **29**(5): p. 611-24.
12. Heintzman, N.D., et al., *Histone modifications at human enhancers reflect global cell-type-specific gene expression.* Nature, 2009. **459**(7243): p. 108-12.
13. Li, X.Y., et al., *The role of chromatin accessibility in directing the widespread, overlapping patterns of Drosophila transcription factor binding.* Genome biology, 2011. **12**(4): p. R34.
14. Fakhouri, T.H., et al., *Dynamic chromatin organization during foregut development mediated by the organ selector gene PHA-4/FoxA.* PLoS genetics, 2010. **6**(8).
15. Sinclair, A.H., et al., *A gene from the human sex-determining region encodes a protein with homology to a conserved DNA-binding motif.* Nature, 1990. **346**(6281): p. 240-4.
16. Parkhurst, S.M., D. Bopp, and D. Ish-Horowicz, *X:A ratio, the primary sex-determining signal in Drosophila, is transduced by helix-loop-helix proteins.* Cell, 1990. **63**(6): p. 1179-91.
17. Madl, J.E. and R.K. Herman, *Polyploids and sex determination in Caenorhabditis elegans.* Genetics, 1979. **93**(2): p. 393-402.
18. Hassold, T., et al., *A cytogenetic study of 1000 spontaneous abortions.* Annals of human genetics, 1980. **44**(Pt 2): p. 151-78.
19. Hassold, T.J., *A cytogenetic study of repeated spontaneous abortions.* American journal of human genetics, 1980. **32**(5): p. 723-30.
20. Mao, R., et al., *Primary and secondary transcriptional effects in the developing human Down syndrome brain and heart.* Genome biology, 2005. **6**(13): p. R107.

21. Saran, N.G., et al., *Global disruption of the cerebellar transcriptome in a Down syndrome mouse model.* Human molecular genetics, 2003. **12**(16): p. 2013-9.
22. Csankovszki, G., E.L. Petty, and K.S. Collette, *The worm solution: a chromosome-full of condensin helps gene expression go down.* Chromosome research : an international journal on the molecular, supramolecular and evolutionary aspects of chromosome biology, 2009. **17**(5): p. 621-35.
23. Gupta, V., et al., *Global analysis of X-chromosome dosage compensation.* Journal of biology, 2006. **5**(1): p. 3.
24. Nguyen, D.K. and C.M. Disteche, *Dosage compensation of the active X chromosome in mammals.* Nature genetics, 2006. **38**(1): p. 47-53.
25. Lin, H., et al., *Dosage compensation in the mouse balances up-regulation and silencing of X-linked genes.* PLoS biology, 2007. **5**(12): p. e326.
26. Lyon, M.F., *Gene action in the X-chromosome of the mouse (Mus musculus L.).* Nature, 1961. **190**: p. 372-3.
27. Lyon, M.F., et al., *A Mouse Translocation Suppressing Sex-Linked Variegation.* Cytogenetics, 1964. **15**: p. 306-23.
28. Borsani, G., et al., *Characterization of a murine gene expressed from the inactive X chromosome.* Nature, 1991. **351**(6324): p. 325-9.
29. Brockdorff, N., et al., *Conservation of position and exclusive expression of mouse Xist from the inactive X chromosome.* Nature, 1991. **351**(6324): p. 329-31.
30. Ohhata, T., et al., *Crucial role of antisense transcription across the Xist promoter in Tsix-mediated Xist chromatin modification.* Development, 2008. **135**(2): p. 227-35.
31. Navarro, P., et al., *Molecular coupling of Xist regulation and pluripotency.* Science, 2008. **321**(5896): p. 1693-5.
32. Navarro, P., et al., *Molecular coupling of Tsix regulation and pluripotency.* Nature, 2010. **468**(7322): p. 457-60.
33. Monkhorst, K., et al., *X inactivation counting and choice is a stochastic process: evidence for involvement of an X-linked activator.* Cell, 2008. **132**(3): p. 410-21.
34. Hernandez-Munoz, I., et al., *Stable X chromosome inactivation involves the PRC1 Polycomb complex and requires histone MACROH2A1 and the CULLIN3/SPOP ubiquitin E3 ligase.* Proceedings of the National Academy of Sciences of the United States of America, 2005. **102**(21): p. 7635-40.
35. Zhao, J., et al., *Polycomb proteins targeted by a short repeat RNA to the mouse X chromosome.* Science, 2008. **322**(5902): p. 750-6.
36. Kalantry, S. and T. Magnuson, *The Polycomb group protein EED is dispensable for the initiation of random X-chromosome inactivation.* PLoS genetics, 2006. **2**(5): p. e66.
37. de Napoles, M., et al., *Polycomb group proteins Ring1A/B link ubiquitylation of histone H2A to heritable gene silencing and X inactivation.* Developmental cell, 2004. **7**(5): p. 663-76.
38. Fang, J., et al., *Ring1b-mediated H2A ubiquitination associates with inactive X chromosomes and is involved in initiation of X inactivation.* The Journal of biological chemistry, 2004. **279**(51): p. 52812-5.
39. Sarma, K., et al., *Locked nucleic acids (LNAs) reveal sequence requirements and kinetics of Xist RNA localization to the X chromosome.* Proceedings of the National Academy of Sciences of the United States of America, 2010. **107**(51): p. 22196-201.
40. Heard, E., et al., *Methylation of histone H3 at Lys-9 is an early mark on the X chromosome during X inactivation.* Cell, 2001. **107**(6): p. 727-38.

41. Boggs, B.A., et al., *Differentially methylated forms of histone H3 show unique association patterns with inactive human X chromosomes.* Nature genetics, 2002. **30**(1): p. 73-6.
42. Chadwick, B.P. and H.F. Willard, *Chromatin of the Barr body: histone and non-histone proteins associated with or excluded from the inactive X chromosome.* Human molecular genetics, 2003. **12**(17): p. 2167-78.
43. Kohlmaier, A., et al., *A chromosomal memory triggered by Xist regulates histone methylation in X inactivation.* PLoS biology, 2004. **2**(7): p. E171.
44. Doyen, C.M., et al., *Mechanism of polymerase II transcription repression by the histone variant macroH2A.* Molecular and cellular biology, 2006. **26**(3): p. 1156-64.
45. Costanzi, C., et al., *Histone macroH2A1 is concentrated in the inactive X chromosome of female preimplantation mouse embryos.* Development, 2000. **127**(11): p. 2283-9.
46. Grigoryev, S.A., et al., *Dynamic relocation of epigenetic chromatin markers reveals an active role of constitutive heterochromatin in the transition from proliferation to quiescence.* Journal of cell science, 2004. **117**(Pt 25): p. 6153-62.
47. Zhang, R., et al., *Formation of MacroH2A-containing senescence-associated heterochromatin foci and senescence driven by ASF1a and HIRA.* Developmental cell, 2005. **8**(1): p. 19-30.
48. Csankovszki, G., et al., *Conditional deletion of Xist disrupts histone macroH2A localization but not maintenance of X inactivation.* Nature genetics, 1999. **22**(4): p. 323-4.
49. Kouzarides, T., *Chromatin modifications and their function.* Cell, 2007. **128**(4): p. 693-705.
50. Chaumeil, J., et al., *A novel role for Xist RNA in the formation of a repressive nuclear compartment into which genes are recruited when silenced.* Genes & development, 2006. **20**(16): p. 2223-37.
51. Rego, A., et al., *The facultative heterochromatin of the inactive X chromosome has a distinctive condensed ultrastructure.* Journal of cell science, 2008. **121**(Pt 7): p. 1119-27.
52. Lucchesi, J.C., W.G. Kelly, and B. Panning, *Chromatin remodeling in dosage compensation.* Annual review of genetics, 2005. **39**: p. 615-51.
53. Copps, K., et al., *Complex formation by the Drosophila MSL proteins: role of the MSL2 RING finger in protein complex assembly.* The EMBO journal, 1998. **17**(18): p. 5409-17.
54. Kelley, R.L., et al., *Expression of msl-2 causes assembly of dosage compensation regulators on the X chromosomes and female lethality in Drosophila.* Cell, 1995. **81**(6): p. 867-77.
55. Lyman, L.M., et al., *Drosophila male-specific lethal-2 protein: structure/function analysis and dependence on MSL-1 for chromosome association.* Genetics, 1997. **147**(4): p. 1743-53.
56. Morales, V., et al., *Functional integration of the histone acetyltransferase MOF into the dosage compensation complex.* The EMBO journal, 2004. **23**(11): p. 2258-68.
57. Morales, V., et al., *The MRG domain mediates the functional integration of MSL3 into the dosage compensation complex.* Molecular and cellular biology, 2005. **25**(14): p. 5947-54.
58. Richter, L., J.R. Bone, and M.I. Kuroda, *RNA-dependent association of the Drosophila maleless protein with the male X chromosome.* Genes to cells : devoted to molecular & cellular mechanisms, 1996. **1**(3): p. 325-36.
59. Hilfiker, A., et al., *mof, a putative acetyl transferase gene related to the Tip60 and MOZ human genes and to the SAS genes of yeast, is required for dosage compensation in Drosophila.* The EMBO journal, 1997. **16**(8): p. 2054-60.

60. Gu, W., P. Szauter, and J.C. Lucchesi, *Targeting of MOF, a putative histone acetyl transferase, to the X chromosome of Drosophila melanogaster.* Developmental genetics, 1998. **22**(1): p. 56-64.
61. Smith, E.R., et al., *The drosophila MSL complex acetylates histone H4 at lysine 16, a chromatin modification linked to dosage compensation.* Molecular and cellular biology, 2000. **20**(1): p. 312-8.
62. Alekseyenko, A.A., et al., *High-resolution ChIP-chip analysis reveals that the Drosophila MSL complex selectively identifies active genes on the male X chromosome.* Genes & development, 2006. **20**(7): p. 848-57.
63. Gilfillan, G.D., et al., *Chromosome-wide gene-specific targeting of the Drosophila dosage compensation complex.* Genes & development, 2006. **20**(7): p. 858-70.
64. Kind, J. and A. Akhtar, *Cotranscriptional recruitment of the dosage compensation complex to X-linked target genes.* Genes & development, 2007. **21**(16): p. 2030-40.
65. Kadlec, J., et al., *Structural basis for MOF and MSL3 recruitment into the dosage compensation complex by MSL1.* Nature structural & molecular biology, 2011. **18**(2): p. 142-9.
66. Kaplan, C.D., L. Laprade, and F. Winston, *Transcription elongation factors repress transcription initiation from cryptic sites.* Science, 2003. **301**(5636): p. 1096-9.
67. Mavrich, T.N., et al., *A barrier nucleosome model for statistical positioning of nucleosomes throughout the yeast genome.* Genome research, 2008. **18**(7): p. 1073-83.
68. Robinson, P.J., et al., *30 nm chromatin fibre decompaction requires both H4-K16 acetylation and linker histone eviction.* Journal of molecular biology, 2008. **381**(4): p. 816-25.
69. Shogren-Knaak, M., et al., *Histone H4-K16 acetylation controls chromatin structure and protein interactions.* Science, 2006. **311**(5762): p. 844-7.
70. Core, L.J. and J.T. Lis, *Transcription regulation through promoter-proximal pausing of RNA polymerase II.* Science, 2008. **319**(5871): p. 1791-2.
71. Kelley, R.L., et al., *Epigenetic spreading of the Drosophila dosage compensation complex from roX RNA genes into flanking chromatin.* Cell, 1999. **98**(4): p. 513-22.
72. Meller, V.H., et al., *Ordered assembly of roX RNAs into MSL complexes on the dosage-compensated X chromosome in Drosophila.* Current biology : CB, 2000. **10**(3): p. 136-43.
73. Straub, T., et al., *The chromosomal high-affinity binding sites for the Drosophila dosage compensation complex.* PLoS genetics, 2008. **4**(12): p. e1000302.
74. Alekseyenko, A.A., et al., *A sequence motif within chromatin entry sites directs MSL establishment on the Drosophila X chromosome.* Cell, 2008. **134**(4): p. 599-609.
75. Meyer, B.J. and L.P. Casson, *Caenorhabditis elegans compensates for the difference in X chromosome dosage between the sexes by regulating transcript levels.* Cell, 1986. **47**(6): p. 871-81.
76. Jans, J., et al., *A condensin-like dosage compensation complex acts at a distance to control expression throughout the genome.* Genes & development, 2009. **23**(5): p. 602-18.
77. DeLong, L., L.P. Casson, and B.J. Meyer, *Assessment of X chromosome dosage compensation in Caenorhabditis elegans by phenotypic analysis of lin-14.* Genetics, 1987. **117**(4): p. 657-70.
78. Meyer, B.J., *X-Chromosome dosage compensation.* WormBook : the online review of C. elegans biology, 2005: p. 1-14.
79. Csankovszki, G., et al., *Three distinct condensin complexes control C. elegans chromosome dynamics.* Current biology : CB, 2009. **19**(1): p. 9-19.

80. Chuang, P.T., J.D. Lieb, and B.J. Meyer, *Sex-specific assembly of a dosage compensation complex on the nematode X chromosome.* Science, 1996. **274**(5293): p. 1736-9.
81. Davis, T.L. and B.J. Meyer, *SDC-3 coordinates the assembly of a dosage compensation complex on the nematode X chromosome.* Development, 1997. **124**(5): p. 1019-31.
82. Plenefisch, J.D., L. DeLong, and B.J. Meyer, *Genes that implement the hermaphrodite mode of dosage compensation in Caenorhabditis elegans.* Genetics, 1989. **121**(1): p. 57-76.
83. Nusbaum, C. and B.J. Meyer, *The Caenorhabditis elegans gene sdc-2 controls sex determination and dosage compensation in XX animals.* Genetics, 1989. **122**(3): p. 579-93.
84. Villeneuve, A.M. and B.J. Meyer, *sdc-1: a link between sex determination and dosage compensation in C. elegans.* Cell, 1987. **48**(1): p. 25-37.
85. Meneely, P.M. and W.B. Wood, *An autosomal gene that affects X chromosome expression and sex determination in Caenorhabditis elegans.* Genetics, 1984. **106**(1): p. 29-44.
86. Lieb, J.D., et al., *DPY-26, a link between dosage compensation and meiotic chromosome segregation in the nematode.* Science, 1996. **274**(5293): p. 1732-6.
87. Dawes, H.E., et al., *Dosage compensation proteins targeted to X chromosomes by a determinant of hermaphrodite fate.* Science, 1999. **284**(5421): p. 1800-4.
88. Klein, R.D. and B.J. Meyer, *Independent domains of the Sdc-3 protein control sex determination and dosage compensation in C. elegans.* Cell, 1993. **72**(3): p. 349-64.
89. Hsu, D.R., P.T. Chuang, and B.J. Meyer, *DPY-30, a nuclear protein essential early in embryogenesis for Caenorhabditis elegans dosage compensation.* Development, 1995. **121**(10): p. 3323-34.
90. Yonker, S.A. and B.J. Meyer, *Recruitment of C. elegans dosage compensation proteins for gene-specific versus chromosome-wide repression.* Development, 2003. **130**(26): p. 6519-32.
91. Nonet, M.L. and B.J. Meyer, *Early aspects of Caenorhabditis elegans sex determination and dosage compensation are regulated by a zinc-finger protein.* Nature, 1991. **351**(6321): p. 65-8.
92. Hudson, D.F., K.M. Marshall, and W.C. Earnshaw, *Condensin: Architect of mitotic chromosomes.* Chromosome research : an international journal on the molecular, supramolecular and evolutionary aspects of chromosome biology, 2009. **17**(2): p. 131-44.
93. Csankovszki, G., *Condensin function in dosage compensation.* Epigenetics : official journal of the DNA Methylation Society, 2009. **4**(4): p. 212-5.
94. Blauwkamp, T.A. and G. Csankovszki, *Two classes of dosage compensation complex binding elements along Caenorhabditis elegans X chromosomes.* Molecular and cellular biology, 2009. **29**(8): p. 2023-31.
95. Hodgkin, J., *X chromosome dosage and gene expression in Caenorhabditis elegans: Two unusual dpy genes. Mol. Gen. Genet.*, 1983. **192**: p. 452-458.
96. Lieb, J.D., et al., *MIX-1: an essential component of the C. elegans mitotic machinery executes X chromosome dosage compensation.* Cell, 1998. **92**(2): p. 265-77.
97. Chuang, P.T., D.G. Albertson, and B.J. Meyer, *DPY-27:a chromosome condensation protein homolog that regulates C. elegans dosage compensation through association with the X chromosome.* Cell, 1994. **79**(3): p. 459-74.

98. Csankovszki, G., P. McDonel, and B.J. Meyer, *Recruitment and spreading of the C. elegans dosage compensation complex along X chromosomes.* Science, 2004. **303**(5661): p. 1182-5.
99. McDonel, P., et al., *Clustered DNA motifs mark X chromosomes for repression by a dosage compensation complex.* Nature, 2006. **444**(7119): p. 614-8.
100. Ercan, S., et al., *X chromosome repression by localization of the C. elegans dosage compensation machinery to sites of transcription initiation.* Nature genetics, 2007. **39**(3): p. 403-8.
101. Ercan, S., L.L. Dick, and J.D. Lieb, *The C. elegans dosage compensation complex propagates dynamically and independently of X chromosome sequence.* Current biology : CB, 2009. **19**(21): p. 1777-87.
102. Pferdehirt, R.R., W.S. Kruesi, and B.J. Meyer, *An MLL/COMPASS subunit functions in the C. elegans dosage compensation complex to target X chromosomes for transcriptional regulation of gene expression.* Genes & development, 2011. **25**(5): p. 499-515.
103. Iouzalen, N., J. Moreau, and M. Mechali, *H2A.Zl, a new variant histone expressed during Xenopus early development exhibits several distinct features from the core histone H2A.* Nucleic acids research, 1996. **24**(20): p. 3947-52.
104. Thatcher, T.H. and M.A. Gorovsky, *Phylogenetic analysis of the core histones H2A, H2B, H3, and H4.* Nucleic acids research, 1994. **22**(2): p. 174-9.
105. Suto, R.K., et al., *Crystal structure of a nucleosome core particle containing the variant histone H2A.Z.* Nature structural biology, 2000. **7**(12): p. 1121-4.
106. Thakar, A., et al., *H2A.Z and H3.3 histone variants affect nucleosome structure: biochemical and biophysical studies.* Biochemistry, 2009. **48**(46): p. 10852-7.
107. Chakravarthy, S., et al., *Structural characterization of histone H2A variants.* Cold Spring Harbor symposia on quantitative biology, 2004. **69**: p. 227-34.
108. Weber, C.M., J.G. Henikoff, and S. Henikoff, *H2A.Z nucleosomes enriched over active genes are homotypic.* Nature structural & molecular biology, 2010. **17**(12): p. 1500-7.
109. Clarkson, M.J., et al., *Regions of variant histone His2AvD required for Drosophila development.* Nature, 1999. **399**(6737): p. 694-7.
110. Ridgway, P., et al., *Unique residues on the H2A.Z containing nucleosome surface are important for Xenopus laevis development.* The Journal of biological chemistry, 2004. **279**(42): p. 43815-20.
111. Li, W., et al., *Effects of histone acetylation, ubiquitination and variants on nucleosome stability.* The Biochemical journal, 1993. **296 (Pt 3)**: p. 737-44.
112. Abbott, D.W., et al., *Characterization of the stability and folding of H2A.Z chromatin particles: implications for transcriptional activation.* The Journal of biological chemistry, 2001. **276**(45): p. 41945-9.
113. Zhang, H., D.N. Roberts, and B.R. Cairns, *Genome-wide dynamics of Htz1, a histone H2A variant that poises repressed/basal promoters for activation through histone loss.* Cell, 2005. **123**(2): p. 219-31.
114. Thambirajah, A.A., et al., *H2A.Z stabilizes chromatin in a way that is dependent on core histone acetylation.* The Journal of biological chemistry, 2006. **281**(29): p. 20036-44.
115. Henikoff, S., et al., *Genome-wide profiling of salt fractions maps physical properties of chromatin.* Genome research, 2009. **19**(3): p. 460-9.
116. Flaus, A., et al., *Sin mutations alter inherent nucleosome mobility.* The EMBO journal, 2004. **23**(2): p. 343-53.
117. Li, B., et al., *Preferential occupancy of histone variant H2AZ at inactive promoters influences local histone modifications and chromatin remodeling.* Proceedings of the

National Academy of Sciences of the United States of America, 2005. **102**(51): p. 18385-90.
118. Fan, J.Y., et al., *The essential histone variant H2A.Z regulates the equilibrium between different chromatin conformational states.* Nature structural biology, 2002. **9**(3): p. 172-6.
119. Kumar, S.V. and P.A. Wigge, *H2A.Z-containing nucleosomes mediate the thermosensory response in Arabidopsis.* Cell, 2010. **140**(1): p. 136-47.
120. Fan, J.Y., et al., *H2A.Z alters the nucleosome surface to promote HP1alpha-mediated chromatin fiber folding.* Molecular cell, 2004. **16**(4): p. 655-61.
121. Rangasamy, D., I. Greaves, and D.J. Tremethick, *RNA interference demonstrates a novel role for H2A.Z in chromosome segregation.* Nature structural & molecular biology, 2004. **11**(7): p. 650-5.
122. Krogan, N.J., et al., *Regulation of chromosome stability by the histone H2A variant Htz1, the Swr1 chromatin remodeling complex, and the histone acetyltransferase NuA4.* Proceedings of the National Academy of Sciences of the United States of America, 2004. **101**(37): p. 13513-8.
123. Keogh, M.C., et al., *The Saccharomyces cerevisiae histone H2A variant Htz1 is acetylated by NuA4.* Genes & development, 2006. **20**(6): p. 660-5.
124. Mehta, M., et al., *Individual lysine acetylations on the N terminus of Saccharomyces cerevisiae H2A.Z are highly but not differentially regulated.* The Journal of biological chemistry, 2010. **285**(51): p. 39855-65.
125. Sarcinella, E., et al., *Monoubiquitylation of H2A.Z distinguishes its association with euchromatin or facultative heterochromatin.* Molecular and cellular biology, 2007. **27**(18): p. 6457-68.
126. Chadwick, B.P. and H.F. Willard, *Histone H2A variants and the inactive X chromosome: identification of a second macroH2A variant.* Human molecular genetics, 2001. **10**(10): p. 1101-13.
127. Shia, W.J., B. Li, and J.L. Workman, *SAS-mediated acetylation of histone H4 Lys 16 is required for H2A.Z incorporation at subtelomeric regions in Saccharomyces cerevisiae.* Genes & development, 2006. **20**(18): p. 2507-12.
128. Barski, A., et al., *High-resolution profiling of histone methylations in the human genome.* Cell, 2007. **129**(4): p. 823-37.
129. Cui, K., et al., *Chromatin signatures in multipotent human hematopoietic stem cells indicate the fate of bivalent genes during differentiation.* Cell stem cell, 2009. **4**(1): p. 80-93.
130. Brickner, D.G., et al., *H2A.Z-mediated localization of genes at the nuclear periphery confers epigenetic memory of previous transcriptional state.* PLoS biology, 2007. **5**(4): p. e81.
131. Guillemette, B., et al., *Variant histone H2A.Z is globally localized to the promoters of inactive yeast genes and regulates nucleosome positioning.* PLoS biology, 2005. **3**(12): p. e384.
132. Henikoff, S., *Labile H3.3+H2A.Z nucleosomes mark 'nucleosome-free regions'.* Nature genetics, 2009. **41**(8): p. 865-6.
133. Szenker, E., D. Ray-Gallet, and G. Almouzni, *The double face of the histone variant H3.3.* Cell research, 2011. **21**(3): p. 421-34.
134. Allis, C.D., et al., *hv1 is an evolutionarily conserved H2A variant that is preferentially associated with active genes.* The Journal of biological chemistry, 1986. **261**(4): p. 1941-8.

135. Santisteban, M.S., T. Kalashnikova, and M.M. Smith, *Histone H2A.Z regulats transcription and is partially redundant with nucleosome remodeling complexes.* Cell, 2000. **103**(3): p. 411-22.
136. Adam, M., et al., *H2A.Z is required for global chromatin integrity and for recruitment of RNA polymerase II under specific conditions.* Molecular and cellular biology, 2001. **21**(18): p. 6270-9.
137. Larochelle, M. and L. Gaudreau, *H2A.Z has a function reminiscent of an activator required for preferential binding to intergenic DNA.* The EMBO journal, 2003. **22**(17): p. 4512-22.
138. Dhillon, N., et al., *H2A.Z functions to regulate progression through the cell cycle.* Molecular and cellular biology, 2006. **26**(2): p. 489-501.
139. Millar, C.B., et al., *Acetylation of H2AZ Lys 14 is associated with genome-wide gene activity in yeast.* Genes & development, 2006. **20**(6): p. 711-22.
140. Raisner, R.M., et al., *Histone variant H2A.Z marks the 5' ends of both active and inactive genes in euchromatin.* Cell, 2005. **123**(2): p. 233-48.
141. Yuan, G.C., et al., *Genome-scale identification of nucleosome positions in S. cerevisiae.* Science, 2005. **309**(5734): p. 626-30.
142. Hartley, P.D. and H.D. Madhani, *Mechanisms that specify promoter nucleosome location and identity.* Cell, 2009. **137**(3): p. 445-58.
143. Meneghini, M.D., M. Wu, and H.D. Madhani, *Conserved histone variant H2A.Z protects euchromatin from the ectopic spread of silent heterochromatin.* Cell, 2003. **112**(5): p. 725-36.
144. Brickner, J.H., *Transcriptional memory at the nuclear periphery.* Current opinion in cell biology, 2009. **21**(1): p. 127-33.
145. Hardy, S., et al., *The euchromatic and heterochromatic landscapes are shaped by antagonizing effects of transcription on H2A.Z deposition.* PLoS genetics, 2009. **5**(10): p. e1000687.
146. Lemieux, K., M. Larochelle, and L. Gaudreau, *Variant histone H2A.Z, but not the HMG proteins Nhp6a/b, is essential for the recruitment of Swi/Snf, Mediator, and SAGA to the yeast GAL1 UAS(G).* Biochemical and biophysical research communications, 2008. **369**(4): p. 1103-7.
147. Greaves, I.K., et al., *H2A.Z contributes to the unique 3D structure of the centromere.* Proceedings of the National Academy of Sciences of the United States of America, 2007. **104**(2): p. 525-30.
148. Rangasamy, D., et al., *Pericentric heterochromatin becomes enriched with H2A.Z during early mammalian development.* The EMBO journal, 2003. **22**(7): p. 1599-607.
149. Dhillon, N. and R.T. Kamakaka, *A histone variant, Htz1p, and a Sir1p-like protein, Esc2p, mediate silencing at HMR.* Molecular cell, 2000. **6**(4): p. 769-80.
150. Fingerman, I.M., et al., *Global loss of Set1-mediated H3 Lys4 trimethylation is associated with silencing defects in Saccharomyces cerevisiae.* The Journal of biological chemistry, 2005. **280**(31): p. 28761-5.
151. Venkatasubrahmanyam, S., et al., *Genome-wide, as opposed to local, antisilencing is mediated redundantly by the euchromatic factors Set1 and H2A.Z.* Proceedings of the National Academy of Sciences of the United States of America, 2007. **104**(42): p. 16609-14.
152. Bruce, K., et al., *The replacement histone H2A.Z in a hyperacetylated form is a feature of active genes in the chicken.* Nucleic acids research, 2005. **33**(17): p. 5633-9.

153. Zilberman, D., et al., *Histone H2A.Z and DNA methylation are mutually antagonistic chromatin marks.* Nature, 2008. **456**(7218): p. 125-9.
154. Conerly, M.L., et al., *Changes in H2A.Z occupancy and DNA methylation during B-cell lymphomagenesis.* Genome research, 2010. **20**(10): p. 1383-90.
155. Leach, T.J., et al., *Histone H2A.Z is widely but nonrandomly distributed in chromosomes of Drosophila melanogaster.* The Journal of biological chemistry, 2000. **275**(30): p. 23267-72.
156. Altaf, M., et al., *NuA4-dependent acetylation of nucleosomal histones H4 and H2A directly stimulates incorporation of H2A.Z by the SWR1 complex.* The Journal of biological chemistry, 2010. **285**(21): p. 15966-77.
157. Kelly, T.K., et al., *H2A.Z maintenance during mitosis reveals nucleosome shifting on mitotically silenced genes.* Molecular cell, 2010. **39**(6): p. 901-11.
158. Kobor, M.S., et al., *A protein complex containing the conserved Swi2/Snf2-related ATPase Swr1p deposits histone variant H2A.Z into euchromatin.* PLoS biology, 2004. **2**(5): p. E131.
159. Krogan, N.J., et al., *A Snf2 family ATPase complex required for recruitment of the histone H2A variant Htz1.* Molecular cell, 2003. **12**(6): p. 1565-76.
160. Updike, D.L. and S.E. Mango, *Temporal regulation of foregut development by HTZ-1/H2A.Z and PHA-4/FoxA.* PLoS genetics, 2006. **2**(9): p. e161.
161. Hanai, K., et al., *RSF governs silent chromatin formation via histone H2Av replacement.* PLoS genetics, 2008. **4**(2): p. e1000011.
162. Whittle, C.M., et al., *The genomic distribution and function of histone variant HTZ-1 during C. elegans embryogenesis.* PLoS genetics, 2008. **4**(9): p. e1000187.
163. Reinke, V., et al., *Genome-wide germline-enriched and sex-biased expression profiles in Caenorhabditis elegans.* Development, 2004. **131**(2): p. 311-23.
164. Ingham, P.W., Whittle, R., *Trithorax: a new homeotic mutation of Drosophila melanogaster causing transformations of abdominal and thoracic imaginal segments.* Mol. Gen. Genet., 1980. **179**: p. 607-614.
165. Nislow, C., E. Ray, and L. Pillus, *SET1, a yeast member of the trithorax family, functions in transcriptional silencing and diverse cellular processes.* Molecular biology of the cell, 1997. **8**(12): p. 2421-36.
166. Miller, T., et al., *COMPASS: a complex of proteins associated with a trithorax-related SET domain protein.* Proceedings of the National Academy of Sciences of the United States of America, 2001. **98**(23): p. 12902-7.
167. Roguev, A., et al., *The Saccharomyces cerevisiae Set1 complex includes an Ash2 homologue and methylates histone 3 lysine 4.* The EMBO journal, 2001. **20**(24): p. 7137-48.
168. Nagy, P.L., et al., *A trithorax-group complex purified from Saccharomyces cerevisiae is required for methylation of histone H3.* Proceedings of the National Academy of Sciences of the United States of America, 2002. **99**(1): p. 90-4.
169. Krogan, N.J., et al., *COMPASS, a histone H3 (Lysine 4) methyltransferase required for telomeric silencing of gene expression.* The Journal of biological chemistry, 2002. **277**(13): p. 10753-5.
170. Dehe, P.M., et al., *Protein interactions within the Set1 complex and their roles in the regulation of histone 3 lysine 4 methylation.* The Journal of biological chemistry, 2006. **281**(46): p. 35404-12.
171. Schneider, J., et al., *Molecular regulation of histone H3 trimethylation by COMPASS and the regulation of gene expression.* Molecular cell, 2005. **19**(6): p. 849-56.

172. Cho, Y.W., et al., *PTIP associates with MLL3- and MLL4-containing histone H3 lysine 4 methyltransferase complex.* The Journal of biological chemistry, 2007. **282**(28): p. 20395-406.
173. Hughes, C.M., et al., *Menin associates with a trithorax family histone methyltransferase complex and with the hoxc8 locus.* Molecular cell, 2004. **13**(4): p. 587-97.
174. Lee, J.H. and D.G. Skalnik, *CpG-binding protein (CXXC finger protein 1) is a component of the mammalian Set1 histone H3-Lys4 methyltransferase complex, the analogue of the yeast Set1/COMPASS complex.* The Journal of biological chemistry, 2005. **280**(50): p. 41725-31.
175. Lee, J.H., et al., *Identification and characterization of the human Set1B histone H3-Lys4 methyltransferase complex.* The Journal of biological chemistry, 2007. **282**(18): p. 13419-28.
176. Wu, M., et al., *Molecular regulation of H3K4 trimethylation by Wdr82, a component of human Set1/COMPASS.* Molecular and cellular biology, 2008. **28**(24): p. 7337-44.
177. Eissenberg, J.C. and A. Shilatifard, *Histone H3 lysine 4 (H3K4) methylation in development and differentiation.* Developmental biology, 2010. **339**(2): p. 240-9.
178. Odho, Z., S.M. Southall, and J.R. Wilson, *Characterization of a novel WDR5-binding site that recruits RbBP5 through a conserved motif to enhance methylation of histone H3 lysine 4 by mixed lineage leukemia protein-1.* The Journal of biological chemistry, 2010. **285**(43): p. 32967-76.
179. Southall, S.M., et al., *Structural basis for the requirement of additional factors for MLL1 SET domain activity and recognition of epigenetic marks.* Molecular cell, 2009. **33**(2): p. 181-91.
180. Cao, F., et al., *An Ash2L/RbBP5 heterodimer stimulates the MLL1 methyltransferase activity through coordinated substrate interactions with the MLL1 SET domain.* PloS one, 2010. **5**(11): p. e14102.
181. Dou, Y., et al., *Regulation of MLL1 H3K4 methyltransferase activity by its core components.* Nature structural & molecular biology, 2006. **13**(8): p. 713-9.
182. Lee, J.H. and D.G. Skalnik, *Wdr82 is a C-terminal domain-binding protein that recruits the Setd1A Histone H3-Lys4 methyltransferase complex to transcription start sites of transcribed human genes.* Molecular and cellular biology, 2008. **28**(2): p. 609-18.
183. Tate, C.M., J.H. Lee, and D.G. Skalnik, *CXXC finger protein 1 restricts the Setd1A histone H3K4 methyltransferase complex to euchromatin.* The FEBS journal, 2010. **277**(1): p. 210-23.
184. Steward, M.M., et al., *Molecular regulation of H3K4 trimethylation by ASH2L, a shared subunit of MLL complexes.* Nature structural & molecular biology, 2006. **13**(9): p. 852-4.
185. Takahashi, Y.H., et al., *Regulation of H3K4 trimethylation via Cps40 (Spp1) of COMPASS is monoubiquitination independent: implication for a Phe/Tyr switch by the catalytic domain of Set1.* Molecular and cellular biology, 2009. **29**(13): p. 3478-86.
186. South, P.F., et al., *A conserved interaction between the SDI domain of Bre2 and the Dpy-30 domain of Sdc1 is required for histone methylation and gene expression.* The Journal of biological chemistry, 2010. **285**(1): p. 595-607.
187. Wang, X., et al., *Crystal structure of the C-terminal domain of human DPY-30-like protein: A component of the histone methyltransferase complex.* Journal of molecular biology, 2009. **390**(3): p. 530-7.
188. Xiao, T., et al., *The RNA polymerase II kinase Ctk1 regulates positioning of a 5' histone methylation boundary along genes.* Molecular and cellular biology, 2007. **27**(2): p. 721-31.

189. Krogan, N.J., et al., *Methylation of histone H3 by Set2 in Saccharomyces cerevisiae is linked to transcriptional elongation by RNA polymerase II.* Molecular and cellular biology, 2003. **23**(12): p. 4207-18.
190. Krogan, N.J., et al., *The Paf1 complex is required for histone H3 methylation by COMPASS and Dot1p: linking transcriptional elongation to histone methylation.* Molecular cell, 2003. **11**(3): p. 721-9.
191. Ng, H.H., et al., *Targeted recruitment of Set1 histone methylase by elongating Pol II provides a localized mark and memory of recent transcriptional activity.* Molecular cell, 2003. **11**(3): p. 709-19.
192. Wood, A., et al., *Ctk complex-mediated regulation of histone methylation by COMPASS.* Molecular and cellular biology, 2007. **27**(2): p. 709-20.
193. Zhang, X., et al., *Genome-wide analysis of mono-, di- and trimethylation of histone H3 lysine 4 in Arabidopsis thaliana.* Genome biology, 2009. **10**(6): p. R62.
194. Jiang, H., et al., *Role for Dpy-30 in ES cell-fate specification by regulation of H3K4 methylation within bivalent domains.* Cell, 2011. **144**(4): p. 513-25.
195. Roy, S., et al., *Identification of functional elements and regulatory circuits by Drosophila modENCODE.* Science, 2010. **330**(6012): p. 1787-97.
196. Guenther, M.G., et al., *Global and Hox-specific roles for the MLL1 methyltransferase.* Proceedings of the National Academy of Sciences of the United States of America, 2005. **102**(24): p. 8603-8.
197. Wang, P., et al., *Global analysis of H3K4 methylation defines MLL family member targets and points to a role for MLL1-mediated H3K4 methylation in the regulation of transcriptional initiation by RNA polymerase II.* Molecular and cellular biology, 2009. **29**(22): p. 6074-85.
198. Vermeulen, M., et al., *Selective anchoring of TFIID to nucleosomes by trimethylation of histone H3 lysine 4.* Cell, 2007. **131**(1): p. 58-69.
199. Sims, R.J., 3rd, et al., *Recognition of trimethylated histone H3 lysine 4 facilitates the recruitment of transcription postinitiation factors and pre-mRNA splicing.* Molecular cell, 2007. **28**(4): p. 665-76.
200. Hsu, D.R. and B.J. Meyer, *The dpy-30 gene encodes an essential component of the Caenorhabditis elegans dosage compensation machinery.* Genetics, 1994. **137**(4): p. 999-1018.
201. Alvarez-Venegas, R., et al., *ATX-1, an Arabidopsis homolog of trithorax, activates flower homeotic genes.* Current biology : CB, 2003. **13**(8): p. 627-37.
202. Terranova, R., et al., *Histone and DNA methylation defects at Hox genes in mice expressing a SET domain-truncated form of Mll.* Proceedings of the National Academy of Sciences of the United States of America, 2006. **103**(17): p. 6629-34.
203. Yu, B.D., et al., *Altered Hox expression and segmental identity in Mll-mutant mice.* Nature, 1995. **378**(6556): p. 505-8.
204. Yu, B.D., et al., *MLL, a mammalian trithorax-group gene, functions as a transcriptional maintenance factor in morphogenesis.* Proceedings of the National Academy of Sciences of the United States of America, 1998. **95**(18): p. 10632-6.
205. Ernst, P., et al., *An Mll-dependent Hox program drives hematopoietic progenitor expansion.* Current biology : CB, 2004. **14**(22): p. 2063-9.
206. Glaser, S., et al., *Multiple epigenetic maintenance factors implicated by the loss of Mll2 in mouse development.* Development, 2006. **133**(8): p. 1423-32.
207. Guenther, M.G., et al., *Aberrant chromatin at genes encoding stem cell regulators in human mixed-lineage leukemia.* Genes & development, 2008. **22**(24): p. 3403-8.

208. Bernstein, B.E., et al., *A bivalent chromatin structure marks key developmental genes in embryonic stem cells.* Cell, 2006. **125**(2): p. 315-26.
209. Azuara, V., et al., *Chromatin signatures of pluripotent cell lines.* Nature cell biology, 2006. **8**(5): p. 532-8.
210. Pan, G., et al., *Whole-genome analysis of histone H3 lysine 4 and lysine 27 methylation in human embryonic stem cells.* Cell stem cell, 2007. **1**(3): p. 299-312.
211. Boyer, L.A., et al., *Polycomb complexes repress developmental regulators in murine embryonic stem cells.* Nature, 2006. **441**(7091): p. 349-53.
212. Lee, T.I., et al., *Control of developmental regulators by Polycomb in human embryonic stem cells.* Cell, 2006. **125**(2): p. 301-13.
213. Meister, P., S.E. Mango, and S.M. Gasser, *Locking the genome: nuclear organization and cell fate.* Current opinion in genetics & development, 2011. **21**(2): p. 167-74.
214. Fisher, K., et al., *Methylation and demethylation activities of a C. elegans MLL-like complex attenuate RAS signalling.* Developmental biology, 2010. **341**(1): p. 142-53.
215. Simonet, T., et al., *Antagonistic functions of SET-2/SET1 and HPL/HP1 proteins in C. elegans development.* Developmental biology, 2007. **312**(1): p. 367-83.
216. Li, T. and W.G. Kelly, *A Role for Set1/MLL-Related Components in Epigenetic Regulation of the Caenorhabditis elegans Germ Line.* PLoS genetics, 2011. **7**(3): p. e1001349.
217. Ceol, C.J. and H.R. Horvitz, *A new class of C. elegans synMuv genes implicates a Tip60/NuA4-like HAT complex as a negative regulator of Ras signaling.* Developmental cell, 2004. **6**(4): p. 563-76.
218. Cui, M., E.B. Kim, and M. Han, *Diverse chromatin remodeling genes antagonize the Rb-involved SynMuv pathways in C. elegans.* PLoS genetics, 2006. **2**(5): p. e74.
219. Cui, M., et al., *SynMuv genes redundantly inhibit lin-3/EGF expression to prevent inappropriate vulval induction in C. elegans.* Developmental cell, 2006. **10**(5): p. 667-72.
220. Yokoyama, A., et al., *Leukemia proto-oncoprotein MLL forms a SET1-like histone methyltransferase complex with menin to regulate Hox gene expression.* Molecular and cellular biology, 2004. **24**(13): p. 5639-49.
221. Petty, E.L., et al., *Restricting dosage compensation complex binding to the X chromosomes by H2A.Z/HTZ-1.* PLoS genetics, 2009. **5**(10): p. e1000699.

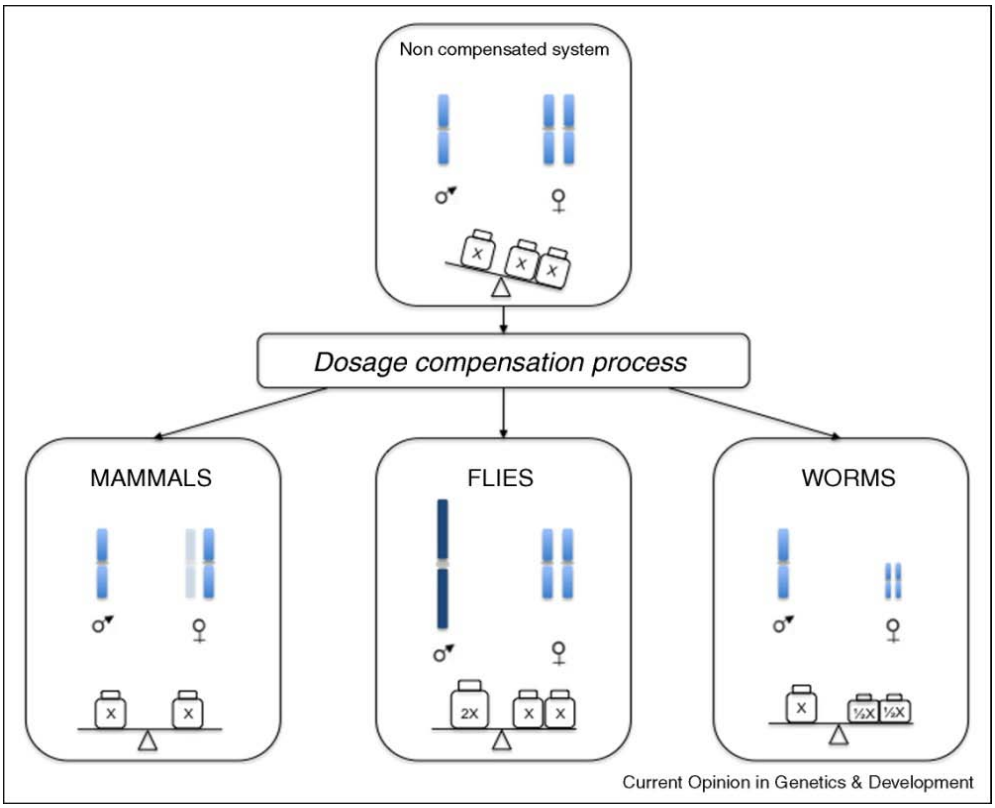

Figure 1.1 The different dosage compensation strategies of mammals, flies, and worms. To equalize X-linked expression between the sexes, mammals inactivate one X in females, flies upregulate the single X in males, and worms down-regulate the two Xs in hermaphrodites. This figure is from Lavarty, Lucci, and Akhtar (2010).

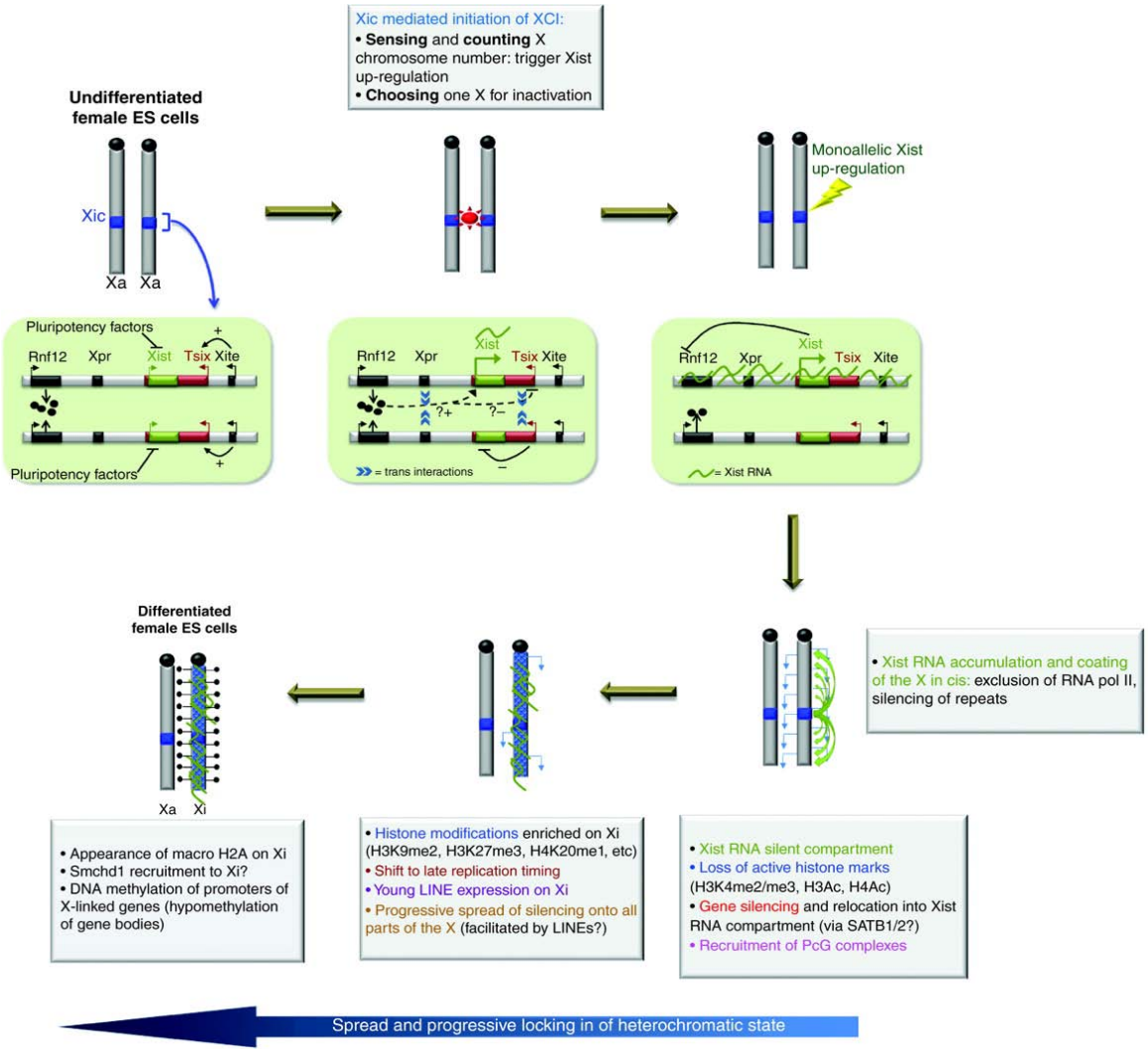

Figure 1.2 Step-wise model of XCI in mammals. In undifferentiated cells, *Xist* is repressed. *Xist* expression triggers inactivation of one of the X chromosomes and this leads to spreading of Xist RNA along the Xi. Changes in histone modifications follow and ultimately, DNA methylation of silenced promoters ensures stable silencing. This figure is from Chow and Heard (2010).

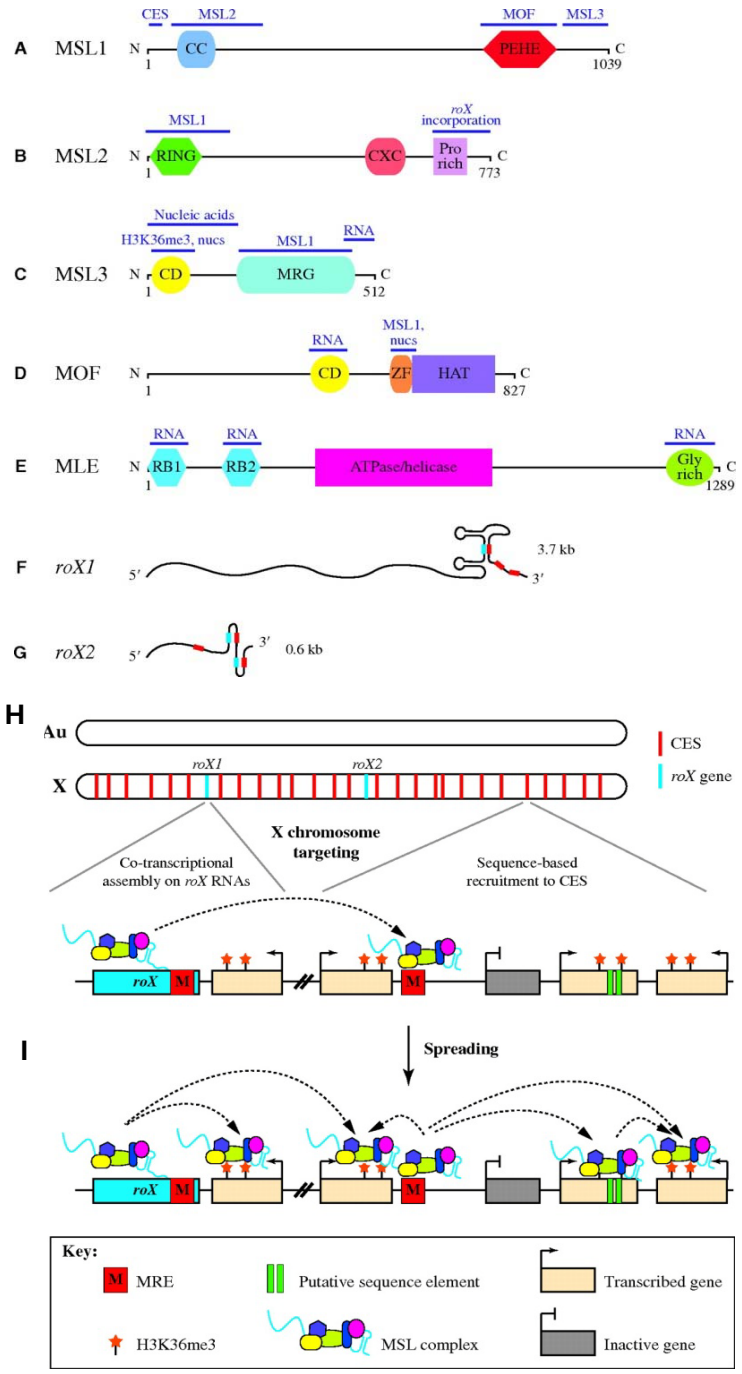

Figure 1.3 MSL complex makeup and targeting in *D. melanogaster* dosage compensation. A-G structures and interaction regions of the MSL complex proteins and *roX* RNAs. H. Initial targeting of MSL sites to chromatin entry sites (CES, also called High Affinity Sites) containing MSL-response elements (MRE) including the *roX* loci, which are required for full assembly of the complex. I. MSL spreads from MREs to active genes, recognized by H3K36me3. Not shown: MSL activity at 3' end of active genes results in H4K16 acetylation and increased rates of transcription. These figures are from Gelbart and Kuroda (2009).

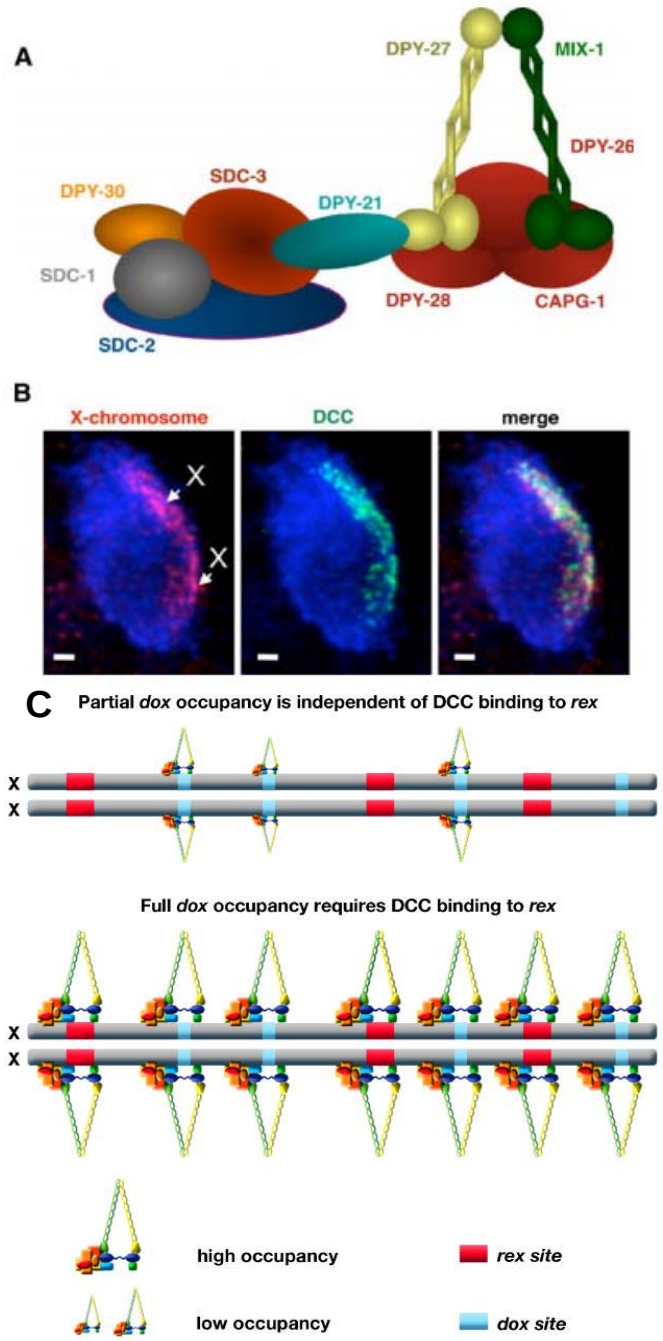

Figure 1.4 The dosage compensation complex (DCC) localizes to both X chromosomes in the hermaphrodite. A. Schematic representation of the full DCC. The five subunits to the left are the regulatory subunits, the five subunits to the right are the Condensin I^{DC} subunits. B. The DCC (green, IF) localizes to the X chromosomes (red, FISH) in hermaphrodite nuclei. A and B were originally published in Csankovszki, Petty, and Collette (2009). C. Full DCC occupancy on the X chromosome relies heavily on the regulatory subcomplex. When either *sdc-2* or *dpy-30* is not expressed, DCC fails to recognize *rex* sites and only some *dox* site binding remains. C was originally published in Meyer (2010).

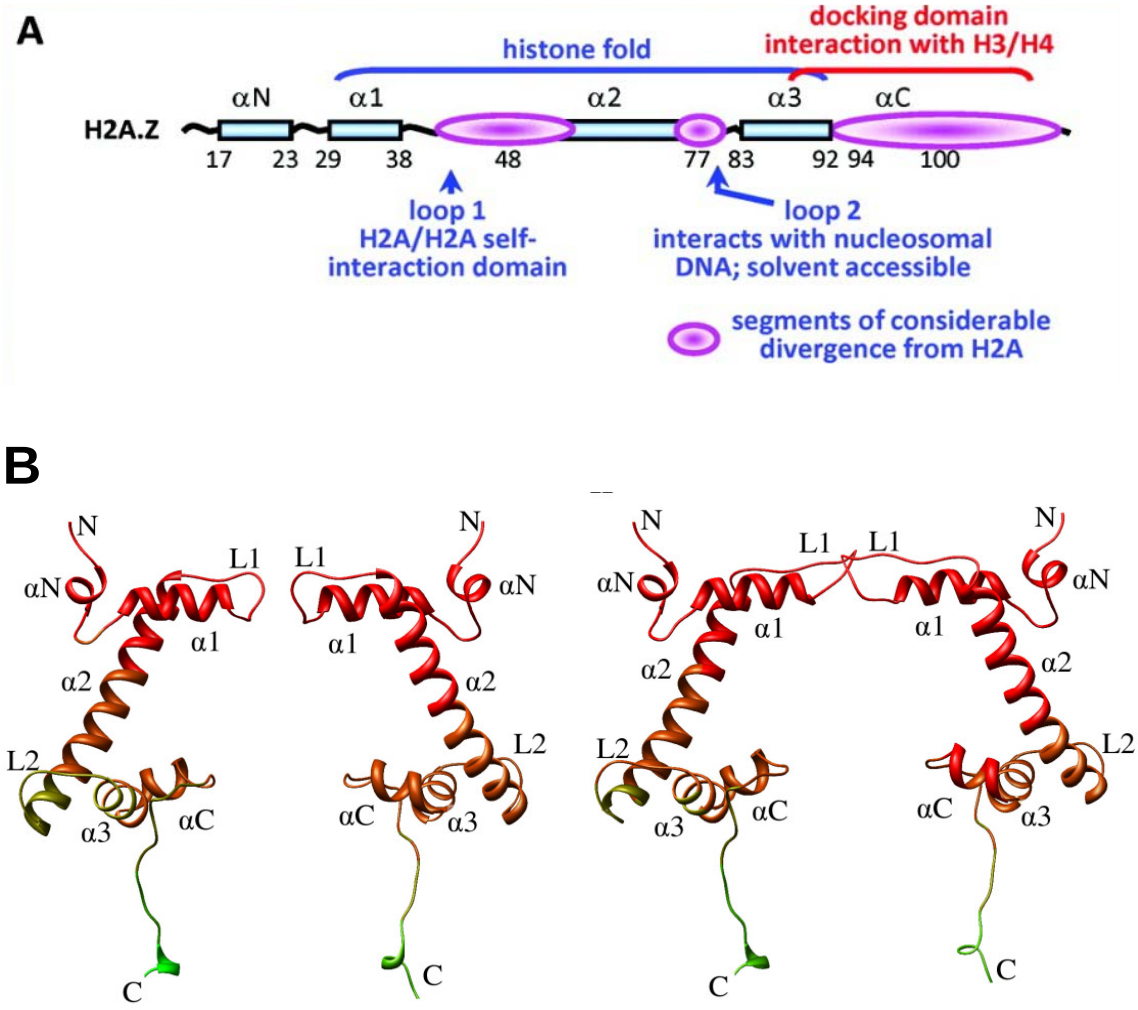

Figure 1.5 Structural differences between H2A and H2A.Z. A. Schematic outlining regions of H2A.Z that are significantly different from H2A published in Thakar et al., (2009) B. Structural models of H2A (left) and H2A.Z (right) published by Ramaswamy and Ioshikhes (2007). Note the predicted increase in L1 interaction between H2A.Z molecules.

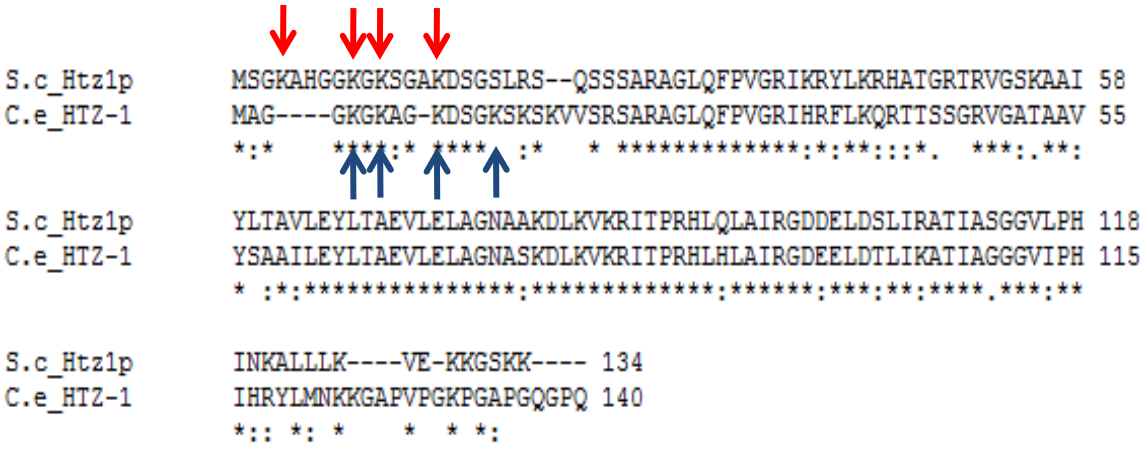

Figure 1.6 H2A.Z acetylation is conserved in *C. elegans*. Alignment of *S. cerevisiae* and *C. elegans* Htz1p and HTZ-1 was perfomed using Clustal W2. Acetylated, N-terminal lysine residues in budding yeast are indicated by the red arrow (Keogh et al., 2006). In collaboration with the Yates lab, we also found that *C. elegans* HTZ-1 is acetylated at several N-terminal residues by mass spectrometry analysis of immunoprecipitated HTZ-1. Three out of four acetylated residues correspond to acetylated residues in budding yeast, including the most frequent site of Htz1p acetylation, K14.

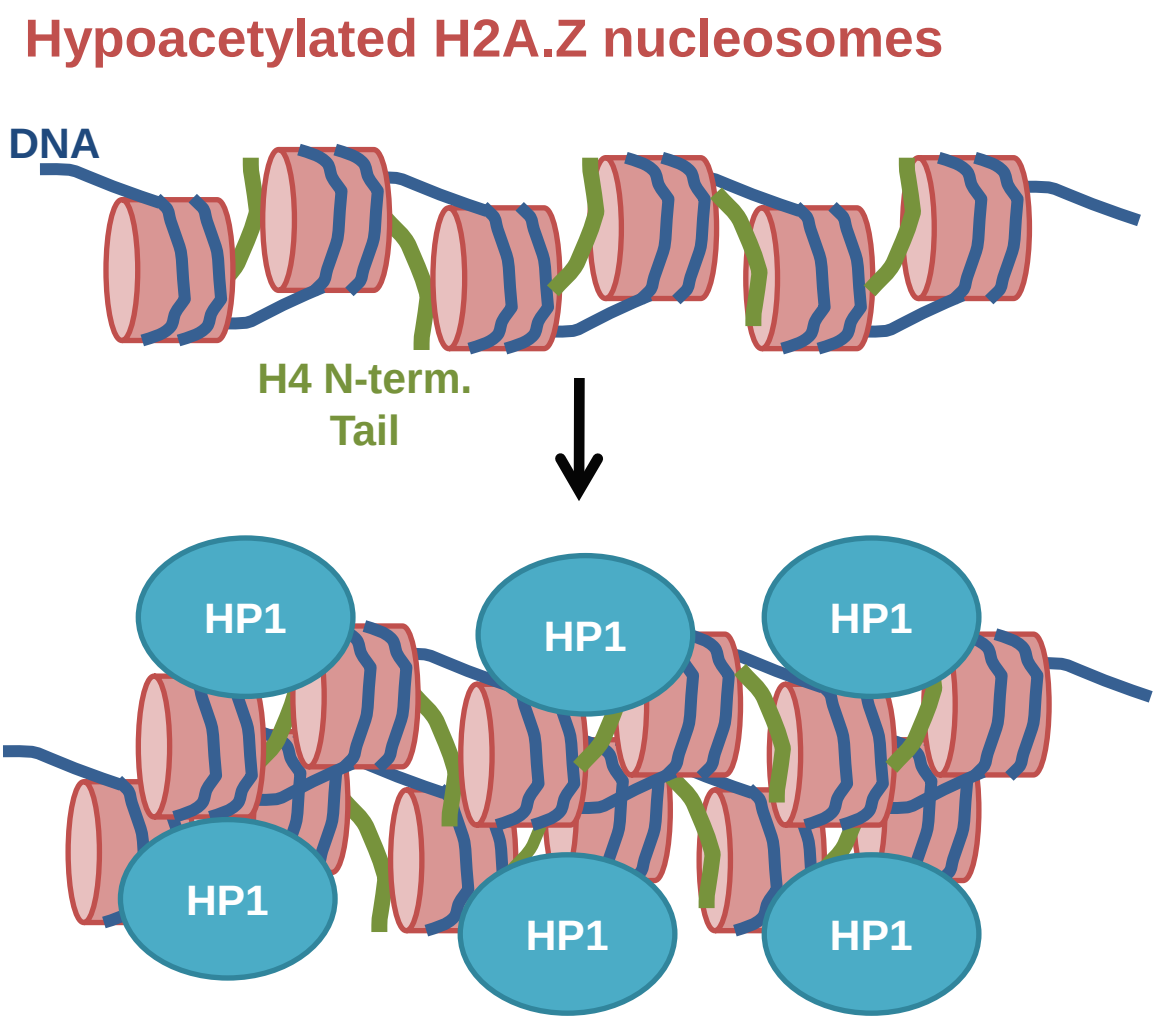

Figure 1.7 Model of heterochromatin formation by hypoacetylated H2A.Z. Basic residues of hypoacetylated H4 N-terminal tail (green) interact with the extended acidic patch of H2A.Z nucleosomes (red). B. H2A.Z nucleosomes readily form higher order intramolecular structures *in vitro.* This, combined with the high affinity of HP1 with condensed H2A.Z fibers may contribute to formation of heterochromatin.

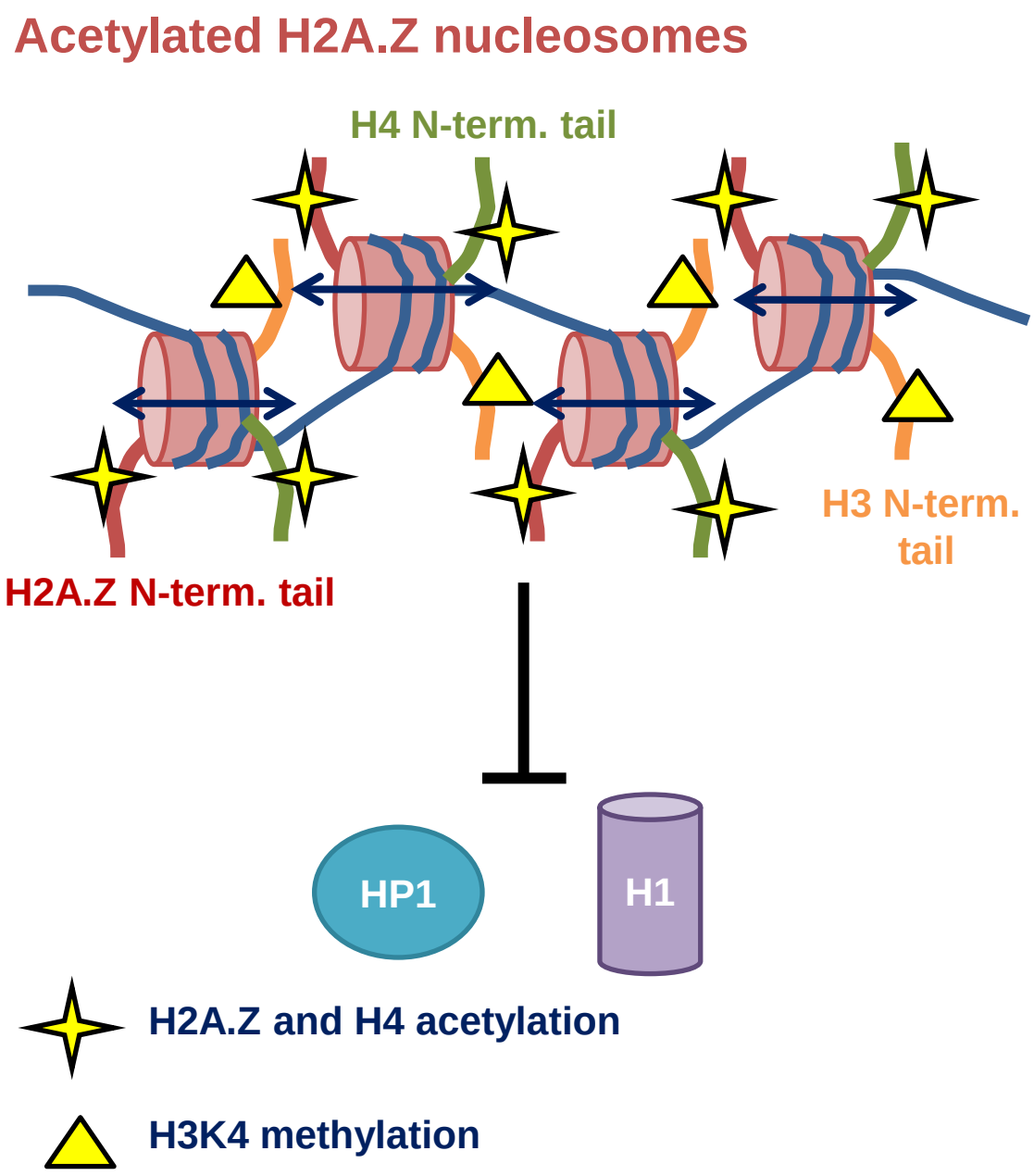

Figure 1.8 Model of euchromatin organization by acetylated H2A.Z. Acetylated H2A.Z is highly coincident with both H3K4methylation and H4K16acetylation. H4 acetylation may reduce the interaction between H4 tail and H2A.Z charge patch preventing higher order assembly required for increased HP1 affinity. The lack of linker histone binding may allow increased mobility of these nucleosomes (indicated by double-headed arrows) which may also result in a more “open” conformation. H2A.Z Acetylation also may contribute to decreased stability of the nucleosome itself. Higher turnover rates may function to prevent silencing marks from accumulating at boundary regions.

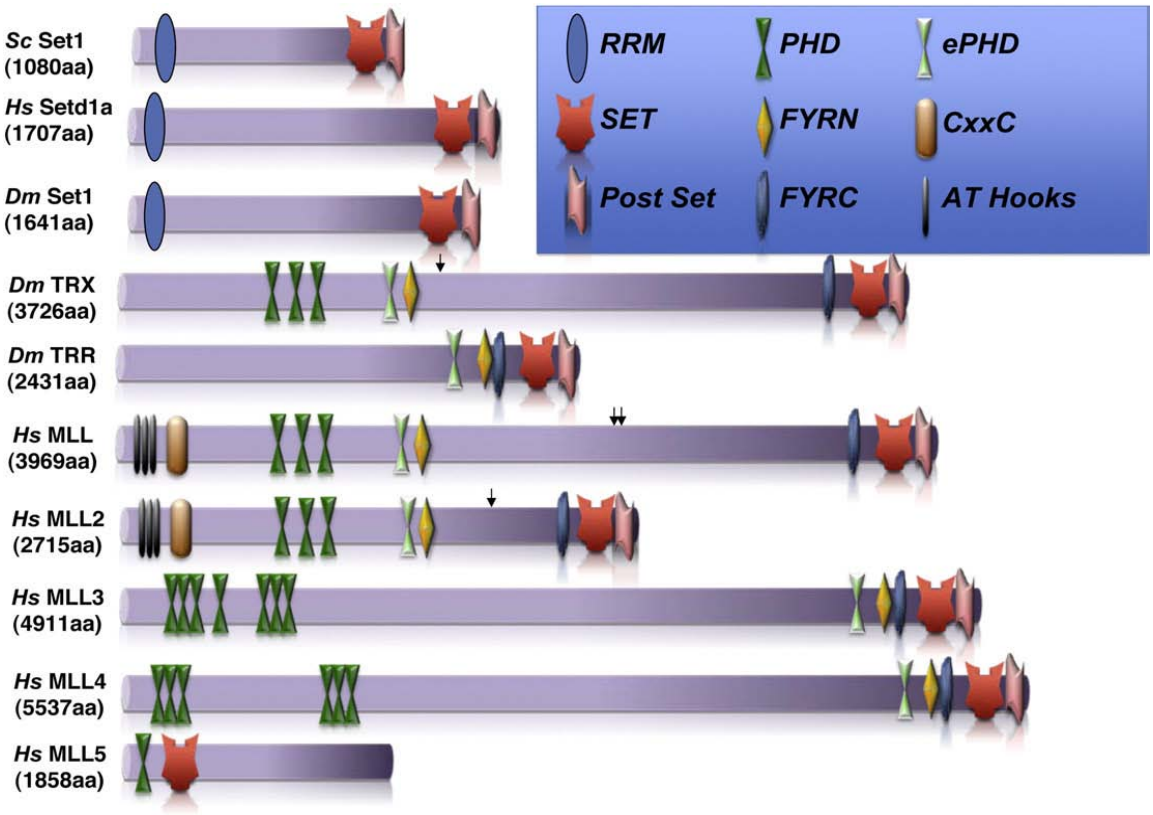

Figure 1.9 Schematic outline of Set1 and MLL domain architecture in budding yeast, fruit fly, and human. Published by Eissenberg and Shilatifard (2010). Set1 family proteins share an N-terminal RRM domain, while the trithorax/MLL family proteins share Plant homeodomains (PHD).

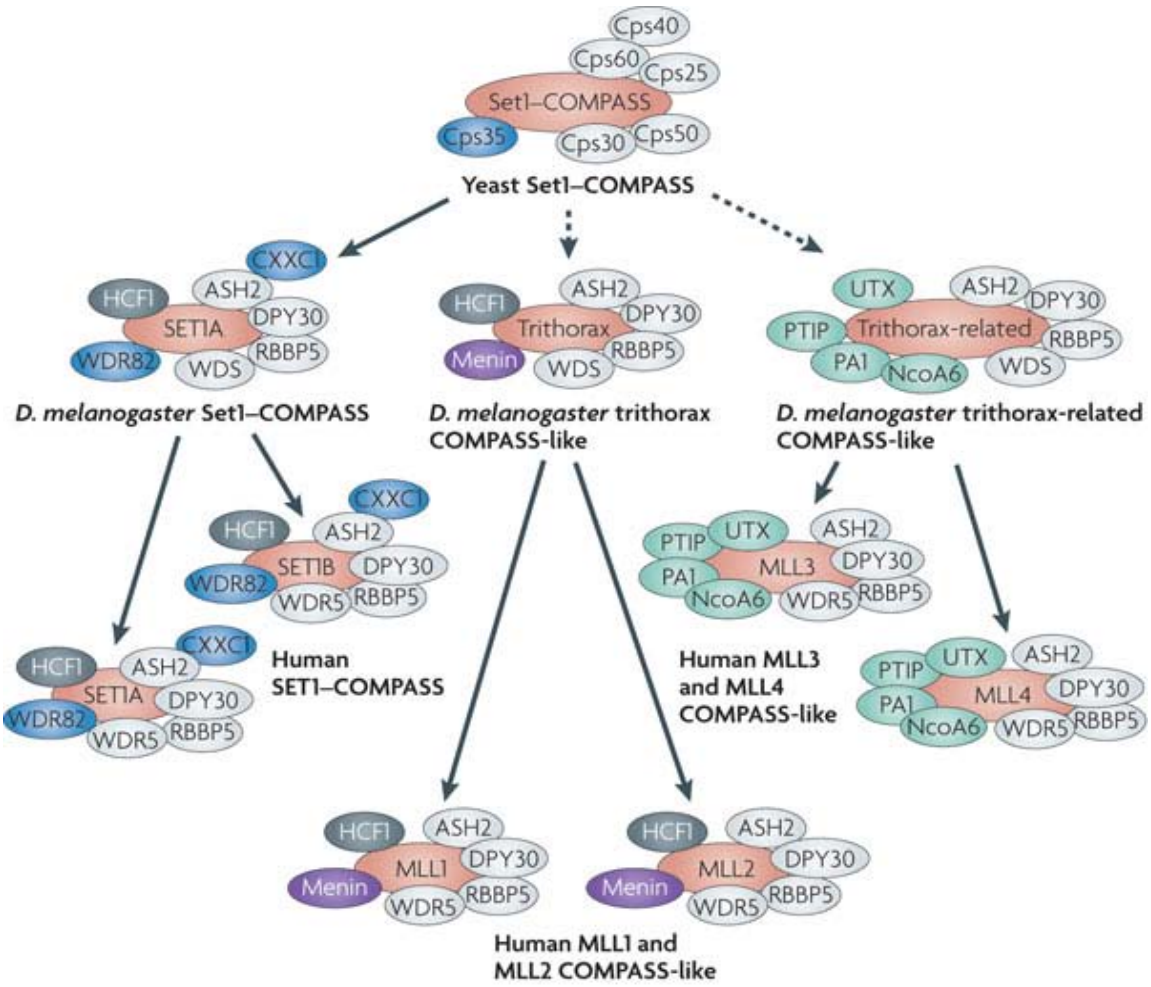

Figure 1.10 Expansion of H3K4 methyltransferase complexes. This figure is from Mohan and Shilatifard, 2010. Complexes are differentiated by the SET-domain containing subunit (red). The light blue proteins are common to all versions of the complexes (Cps40 and 60 together form a structure similar to ASH-2 in *D. melanogaster* and humans). .

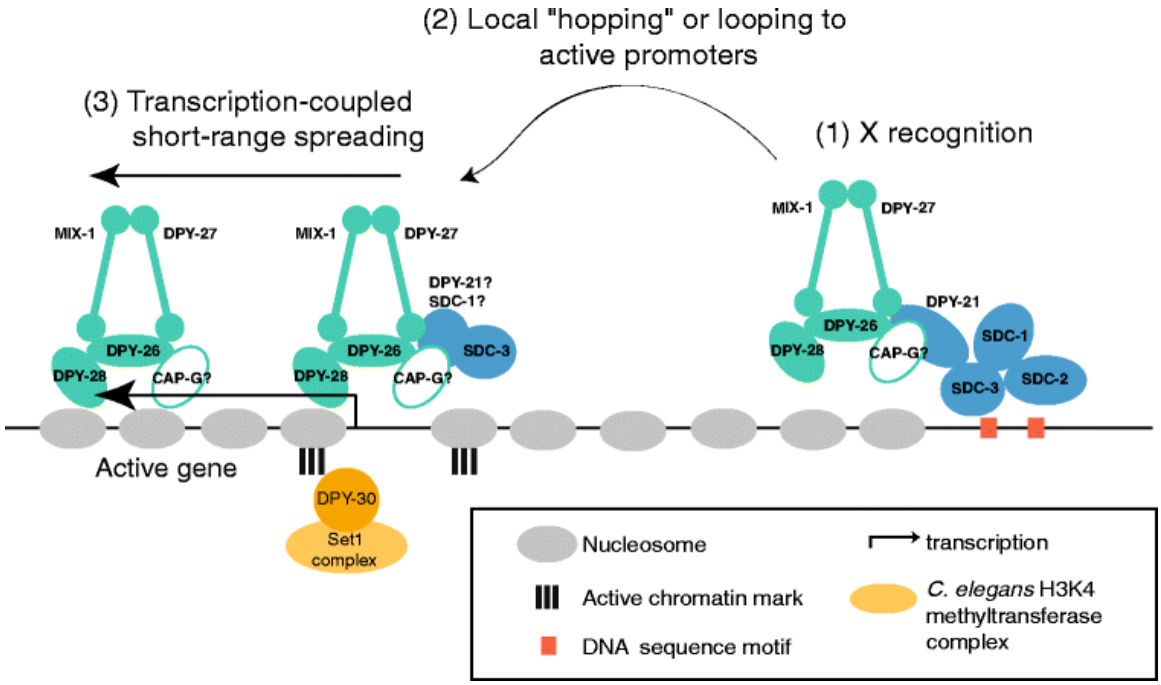

Figure 1.11 Proposed model of a Set1C-dependent role for DPY-30 in *C. elegans* dosage compensation. This model was published by Ercan and Lieb in 2009. The y propose that sequence-driven DCC recognition is followed by sequence-independent “hopping” of the DCC to promoter regions by recognition of DPY-30. DPY-30 is a member of H3K4methyltransferase complexes that are found at the promoters of active genes. This model explains how the DCC might specifically bind active genes.

CHAPTER 2

Three distinct condensin complexes control *C. elegans* chromosome dynamics

This Chapter was published as Csankovszki et al. (2009) in Current Biology as "Three distinct condensin complexes control *C. elegans* chromosome dynamics." I conducted the experiments and image analysis for data shown in 2.5A and B, 2.7A, and 2.11. Figures 2.2, 2.6, 2.9, 2.12, 2.13, 2.14 are the work of G. Csankovszki, K. Collette and our collaborators in the Hagstrom lab. Figures 2.3, 2.4, 2.7 B-E, 2.10 are the work of K. Collette.

Abstract

Condensin complexes organize chromosome structure and facilitate chromosome segregation. Higher eukaryotes have two complexes, condensin I and condensin II, each essential for chromosome segregation. The nematode *Caenorhabditis elegans* was considered an exception, because it has a mitotic condensin II complex but appeared to lack mitotic condensin I. Instead, its condensin I-like complex (here called condensin I^{DC}) dampens gene expression along hermaphrodite X chromosomes during dosage compensation.

Here we report the discovery of a third condensin complex, condensin I, in *C. elegans*. We identify new condensin subunits and show that each complex

has a conserved five-subunit composition. Condensin I differs from condensin I^{DC} by only a single subunit. Yet condensin I binds to autosomes and X chromosomes in both sexes to promote chromosome segregation, while condensin I^{DC} binds specifically to X chromosomes in hermaphrodites to regulate transcript levels. Both condensin I and II promote chromosome segregation, but associate with different chromosomal regions during mitosis and meiosis. Unexpectedly, condensin I also localizes to regions of cohesion between meiotic chromosomes before their segregation.

We demonstrate that condensin subunits in *C. elegans* form three complexes, one that functions in dosage compensation, and two that function in mitosis and meiosis. These results highlight how the duplication and divergence of condensin subunits during evolution may facilitate their adaptation to specialized chromosomal roles, and illustrate the versatility of condensins to function in both gene regulation and chromosome segregation.

INTRODUCTION

Chromosomes must be structurally organized for the proper reading and propagation of genetic information. During interphase, chromatin structure can dictate whether genes are expressed or silenced. During mitosis, duplicated chromosomes must be precisely folded to ensure their accurate segregation into daughter cells. Gene regulation and mitotic chromosome condensation have historically been thought to involve different mechanisms. However, condensin proteins have emerged as important determinants in both processes.

Condensins are conserved protein complexes that bind chromosomes and facilitate chromosome segregation, DNA repair, and gene regulation (reviewed in [1, 2]). Condensin complexes consist of a heterodimer of two SMC (Structural Maintenance of Chromosomes) ATPase subunits (SMC2 and SMC4) and three regulatory subunits referred to as CAPs (Chromosome Associated Polypeptides). While yeasts have a single condensin complex, higher eukaryotes have two: condensin I and condensin II [3-5]. Each contains the same SMC2/4 heterodimer but has a unique set of CAP subunits: CAP-D2, CAP-G, and CAP-H in condensin I, and CAP-D3, CAP-G2, and CAP-H2 in condensin II (Figure 2.1A).

Condensins I and II localize to different chromosome regions and make distinct contributions to chromosome segregation. Condensin II is nuclear, and concentrates on chromosomes when condensation initiates at prophase. In contrast, vertebrate condensin I does not access chromosomes until nuclear envelope breakdown, then becomes enriched within each chromatid in alternating regions from condensin II [3-5]. Condensin II is required for proper kinetics of chromosome condensation at prophase, while condensin I appears to stabilize chromosome rigidity [3-11]. Depletion of each complex individually leads to distinct and characteristic defects in chromosome morphology, while simultaneous depletion of both leads to more severe defects [3-6]. Each complex is required for sister chromatid segregation at anaphase in all organisms tested (reviewed in [1, 2]). How condensins I and II achieve different chromosomal distribution and function is not well understood.

In *C. elegans*, two incomplete condensin complexes have been characterized. A condensin II-like complex performs chromosome segregation functions. Condensin II consists of the SMC4 subunit SMC-4, the SMC2 subunit MIX-1, and the CAP-D3 subunit HCP-6 (Figure 2.1) [7, 9, 12, 13]. Depleting members of this complex impairs prophase condensation, anaphase segregation, and centromere organization in mitosis [7, 9, 11], as well as the restructuring and segregation of chromosomes during meiosis [12]. By contrast, the known condensin I-like complex (condensin I^{DC}) in worms functions in X-chromosome dosage compensation. Condensin I^{DC} binds both hermaphrodite X-chromosomes to downregulate expression two-fold, leading to equal X-linked gene expression levels between XX hermaphrodites and XO males (reviewed in [14]). Condensin I^{DC} shares the SMC2 subunit MIX-1 [13], but contains a unique SMC4 subunit DPY-27 [15], and the condensin I class CAP proteins DPY-28 [16] and DPY-26 [17, 18] (Figure 2.1).

C. elegans condensin I^{DC} appears to have no mitotic function. Except for the shared MIX-1 subunit, mutations in condensin I^{DC} genes were not reported to show mitotic defects in the soma, and while hermaphrodites die due to inappropriately high X-linked gene expression, males carrying these mutations are viable [13, 15-17, 19, 20]. The apparent lack of a mitotic condensin I in *C. elegans* is puzzling, since in all other systems examined, both condensin I and II are essential for mitosis. It has been suggested that during evolution an ancient condensin I lost its mitotic role and became adapted for the specialized function of dosage compensation [2].

However, while the condensin I^{DC} complex per se appears not to function in chromosome segregation, roles for its CAP subunits in germline mitosis and meiosis have been reported. *dpy-26* and *dpy-28* mutant alleles increase non-disjunction of the X in meiosis [17, 19, 20], and *dpy-28* is required for germline mitosis and proper crossover number and distribution during meiotic recombination [16]. These results raise the possibility that these proteins perform chromosome segregation functions independent of their role in condensin I^{DC}.

Here we provide evidence that *C. elegans* does have a mitotic condensin I complex. By identifying new subunits and re-examining existing subunits, we reveal three distinct complexes and characterize their different composition, localization, and function. We demonstrate that the newly identified condensin I complex binds mitotic and meiotic chromosomes and promotes chromosome segregation. Condensins I and I^{DC} share many subunits, clarifying previous indications that some condensin I^{DC} subunits function outside of gene regulation [16, 17, 19, 20]. Condensin I is shown elsewhere (Mets and Meyer, in preparation) to control crossover number and distribution in meiosis. Here we describe different localization and phenotypes of condensin I and II, suggesting distinct functions, and we provide the first comparison in any system of these complexes along holocentric chromosomes and during meiosis. Despite sharing all but one subunit with condensin I, condensin I^{DC} is unique among known condensins, modulating sex- and chromosome-specific gene expression rather than promoting segregation. These results suggest that duplication and divergence of an SMC subunit facilitated the evolutionary adaptation of

mitotic/meiotic condensin I for chromosome-specific gene silencing. This illustrates how chromosome architectural complexes may evolve and diversify their functions to meet the needs of more complex eukaryotic genomes.

RESULTS

A proteomics approach identifies new condensin subunits and suggests three condensin complexes

To identify all *C. elegans* condensin subunits, we performed large-scale immunoprecipitation (IP) from embryo extracts using antibodies against DPY-27, the SMC4 subunit of condensin I^{DC}, or against SMC-4, the SMC4 subunit of condensin II. Four independent IP experiments were analyzed by MudPIT (see methods and supplemental methods) [21]. To eliminate non-specific interactors, we subtracted proteins immunoprecipitated in controls with pre-immune IgG or with an antibody against KLP-7, a mitotic protein that does not associate with SMC-4 or DPY-27 (data not shown). SMC-4 and DPY-27 IPs each recovered a set of interacting condensin subunits that appeared reproducibly and with high total spectrum count (Figure 2.2A).

C. elegans condensin I^{DC} resembles condensin I in other organisms, but functions uniquely in dosage compensation and no CAP-G subunit had been identified by bioinformatics [5] or genetic screens [14]. Proteomics analysis of DPY-27 IPs revealed a previously uncharacterized protein, F29D11.2 that was consistently recovered along with all four known condensin I^{DC} subunits (DPY-27, MIX-1, DPY-28, and DPY-26) (Figure 2.2A). F29D11.2 contains ARM/HEAT motifs, and PSI-BLAST and phylogenetic analyses showed that F29D11.2 shares

homology with CAP-G class subunits (Figure 2.8). F29D11.2 appears to encode the missing CAP-G subunit of condensin I^{DC} (see data below) and we named it *capg-1*. Thus, despite its unusual function, condensin I^{DC} has the subunit composition of a *bona fide* condensin I complex.

SMC-4 IPs recovered SMC-4, MIX-1, and HCP-6, the known members of condensin II, as well as F55C5.4 and KLE-2 (Figure 2.2A). F55C5.4 was shown by PSI-BLAST and phylogenetic analyses (Figure 2.8) to be a CAPG-2 class subunit, consistent with a previous prediction [5]. Based on data below, we conclude that F55C5.4 is the CAP-G2 subunit of condensin II and named it *capg-2*. KLE-2 was previously categorized as a CAP-H2 homolog [5] and a member of the kleisin ("closure") protein family and shown to affect chromosome segregation [18]. Here we demonstrate that KLE-2 interacts with MIX-1/SMC-4, as previously speculated, and is the CAP-H2/kleisin subunit of condensin II. Thus, *C. elegans* has a conserved five-subunit condensin II complex.

To our surprise, the SMC-4 IP recovered not just the set of three CAP II class subunits, but also the three CAP I subunits DPY-26, DPY-28, and CAPG-1 (Figure 2.2A). Thus, we reconsidered the composition of *C. elegans* condensin complexes and hypothesized a three condensin model (Figure 2.1). In our model, *C. elegans* contains not only condensin I^{DC} and condensin II, but also a previously unrecognized condensin I complex, composed of a MIX-1/SMC-4 core and the condensin I CAPs DPY-28, CAPG-1, and DPY-26.

Subunit associations suggest three distinct complexes

To test this model, we raised antibodies against CAPG-1, CAPG-2, and KLE-2 and examined associations among all condensin subunits. We first performed IPs with CAPG-1 and KLE-2 antibodies and analyzed interacting proteins by MudPIT (Figure 2.2A). CAPG-1 IPs recovered all subunits of condensin I^{DC}, consistent with the prediction that it is the missing subunit of this complex. CAPG-1 IPs also recovered SMC-4, but not class II CAPs, consistent with CAPG-1 and SMC-4 forming a complex that is distinct from condensin II. The KLE-2 IPs recovered CAPG-2 and known subunits of condensin II, supporting the prediction that KLE-2 and CAPG-2 are subunits of this complex (Figure 2.2A). KLE-2 IPs did not pull down DPY-27 or class I CAPs, confirming that KLE-2 is a subunit of condensin II but not condensin I^{DC} or I.

To further test subunit interactions, we performed IPs of each of the nine condensin subunits and analyzed them on Western blots probed with a battery of condensin subunit antibodies (Figures 2.2B and C). The SMC2 homolog MIX-1 interacted with each SMC4 class subunit and with both class I and II CAPs, consistent with MIX-1 participating in all complexes. SMC-4 interacted with both class I and class II CAPs, consistent with SMC-4 being shared between condensin I and condensin II. DPY-27 interacted with MIX-1 and class I CAPs, but not SMC-4 or class II CAPs, consistent with it being unique to condensin I^{DC}. Finally, each CAP subunit interacted with the two others in its class, but CAP subunits of different classes never interacted. This result suggests that CAP

subunits of different classes do not “swap,” and that each condensin complex contains a complete set of either class I CAPs or class II CAPs.

These data support our three condensin model. In *C. elegans*, as in other metazoans, a single set of SMC2/4 core proteins (MIX-1/SMC-4) interacts with three class I CAPs to form condensin I or with three class II CAPs to form condensin II. Unlike other metazoans, *C. elegans* has an additional SMC4 class protein, DPY-27, which is used to form condensin I^{DC}, a complex highly related to condensin I but with a unique role in dosage compensation.

Three condensins localize to chromosomes in distinct patterns

We used immunofluorescence to compare chromosome association patterns of the condensin complexes throughout the cell cycle and development. DPY-27 was used to indicate condensin I^{DC}, KLE-2 was used to indicate condensin II, and CAPG-1 patterns not shared by DPY-27 were presumed to represent condensin I localization.

In early hermaphrodite embryos, before dosage compensation initiates, DPY-27 appears diffusely nuclear in interphase and absent from mitotic chromosomes (Figure 3.3) [15]. In contrast, CAPG-1 associates with mitotic chromosomes in a discontinuous coating pattern (Figure 3.3), similar to DPY-26 and DPY-28 [16, 17]. The three class I CAPs share this pattern and they co-localize on mitotic chromosomes (Figure 2.10). This class I CAP pattern differs from the “outlining” of condensed chromosomes by KLE-2 (Figure 3.3), a pattern observed for other condensin II subunits and coincident with centromere proteins along the outer face of *C. elegans* holocentric chromosomes [7, 10-12, 16]. The

three class II CAPs share this pattern and they co-localize, while there is little overlap between class I and class II CAP patterns (Figure 2.10).

In mid-stage hermaphrodite embryos undergoing dosage compensation, condensin I^{DC} localizes to two nuclear sub-regions, the X chromosomes [13, 15-17]. Both DPY-27 and CAPG-1 localized to X (Figures 2.3 and 2.10). However, during mitosis CAPG-1 localized not only in two bright foci, but also along all condensed chromosomes, an additional localization not shared by DPY-27 (Figure 2.3). We observed this pattern for all class I CAPs and suggest it reflects their dual roles: they associate with X chromosomes in hermaphrodites as part of condensin I^{DC} and with all mitotic chromosomes in both sexes as part of condensin I. Consistent with this interpretation, “mitotic coating” but not the two bright foci of CAPG-1 localization were observed in male embryos (Figure 2.3). In contrast, condensin II subunits appeared at low or background levels during interphase, showing bright “centromere-like outlining” of mitotic chromosomes in both early and late embryos of both sexes (Figure 2.3) [7, 10-12]. The distinct localization patterns observed for DPY-27, class I CAPs and class II CAPs are consistent with the existence of three separate complexes.

Since SMC-4 and MIX-1 participate in both condensin I and II, they should exhibit a hybrid localization pattern. These proteins show the bright condensin II “outlining” pattern, as reported [7, 12, 16], but not a condensin I “coating” pattern distinguishable from background during mitosis (data not shown). The condensin I pattern may be difficult to visualize in the presence of intense condensin II localization. Alternatively, the three class I CAP subunits might form a sub-

complex lacking SMC subunits, comparable to the 11S sub-complex in *Xenopus* egg extracts [22]. However, during meiosis we clearly observed SMC-4 and MIX-1 in a hybrid pattern (see below and Figure 2.4), as predicted if they were shared between two different holo-complexes.

Condensin I and II associate with meiotic chromosomes in distinct patterns

We next analyzed condensin localization during meiosis. Condensin I^{DC} proteins are maternally contributed to embryos and accumulate in oocytes, which are arrested at prophase of meiosis I [14, 15, 23]. Like DPY-27, CAPG-1 accumulated in the oocyte nucleoplasm (Figure 2.4A). Unlike DPY-27, CAPG-1 was present throughout the germline (Figure 2.4 and data not shown), as are DPY-26 and DPY-28 [16, 17], presumably reflecting condensin I localization. In contrast to the condensin I^{DC} or condensin I patterns, KLE-2 localizes within each sister chromatid in oocytes (Figure 2.4A), as do other condensin II subunits [12].

We examined later meiotic stages in spermatocytes and fertilized oocytes undergoing meiotic divisions (Figure 2.4A). DPY-27 was not detected at this stage of meiosis. Class II CAPs appeared within each sister chromatid during meiosis I prophase and metaphase, and meiosis II metaphase. In contrast, class I CAPs surrounded chromosomes at prophase of meiosis I. Strikingly, class I CAP immunostaining became restricted to the interface between aligned homologous chromosomes during metaphase of meiosis I and to the region between sister chromatids at metaphase of meiosis II (Figure 2.4A and data not shown). These locations correspond to the last points of contact between homologs (meiosis I) and sister chromatids (meiosis II), where the mitotic/meiotic

kinase AIR-2/AuroraB promotes the release of cohesion by phosphorylation of the meiotic cohesin subunit REC-8 [9, 24]. This localization pattern raises the possibility that condensin I contributes to the separation of chromosomes during meiosis.

MIX-1 and SMC-4 showed a hybrid pattern of chromosomal association corresponding to class I and class II CAP patterns (Figure 2.4B). Part of the MIX-1 pattern overlaps with the pattern of CAPG-1 (class I CAP), surrounding chromosomes at meiotic prophase and localizing between them at metaphase of meiosis I and II. Another part of the MIX-1 pattern did not overlap with CAPG-1, localizing instead within sister chromatids in the pattern of class II CAP subunits (Figure 2.4B). These results are consistent with SMC-4 and MIX-1 being core subunits in both condensin I and condensin II.

As a member of condensin I^{DC}, CAPG-1 mediates X dosage compensation

Next, we investigated the functional consequences of depleting condensin subunits. Condensin I^{DC} binds X chromosomes in an all-or-none fashion so that inactivating one subunit disrupts localization of the others [13, 16, 17, 25]. Indeed, CAPG-1 association with hermaphrodite X chromosomes was not detected in *capg-1, dpy-26, dpy-28*, or *dpy-27* mutant animals (Figure 2.5A). Reciprocally, association of DPY-27, MIX-1, or DPY-26 with X chromosomes was not observed in *capg-1* mutant or RNAi depleted animals (Figure 2.5B). Like other condensin I^{DC} subunits, CAPG-1 localization to X depended on *sdc-2* and *sdc-3*, and SDC-3 localization to X was reduced in *capg-1* RNAi animals (Figure

2.11). SDC-2 and SDC-3 are non-condensin proteins that associate with condensin I^{DC} to confer sex-specificity to dosage compensation [14, 23, 26].

Next we asked whether *capg-1* depletion influenced strains sensitized to perturbations in dosage compensation. Mutations in *sex-1* cause partial disruption of dosage compensation [27, 28] and low embryonic lethality, which can be enhanced by depleting genes required for dosage compensation [29]. Indeed, the 15% embryonic lethality in *sex-1(y263)* mutants fed control vector was increased to about 90% in those fed dsRNA targeting *dpy-27, dpy-28, dpy-26,* or *capg-1* (Figure 2.5C). A second assay used a *xol-1(y9) sex-1(y263)* mutant strain, in which loss of *xol-1* function inappropriately triggers dosage compensation in males, leading to male lethality that can be rescued by depleting dosage compensation genes [28, 30]. We found that RNAi depletion of *dpy-27, dpy-28, dpy-26,* or *capg-1* in this background rescued a large proportion of male progeny (Figure 2.5C). Thus, in two genetic assays *capg-1* depletion appears to disrupt dosage compensation. Together, these results indicate that CAPG-1 functions as a member of condensin I^{DC} to regulate X-linked gene expression in hermaphrodites.

As components of condensin II, CAPG-2 and KLE-2 mediate chromosome condensation and segregation

We tested whether CAPG-2 and KLE-2 function like other subunits of condensin II. We depleted each subunit individually by injection plus feeding RNAi and live imaged chromosomes visualized by GFP::histone H2B (see methods). CAPG-2 depleted chromosomes failed to condense and individualize

at mitotic prophase, as with depletion of any other condensin II subunit (Figures 2.6 and 2.12A) [7, 9-12, 18]. CAPG-2 and KLE-2 depletion also impaired chromosome segregation during meiosis (Figures 2.6A and 2.12B). These phenotypes are consistent with CAPG-2 and KLE-2 being subunits of condensin II, and with a more limited previous analysis [18].

To determine how condensin II impacts development, we characterized deletion mutants *smc-4(tm1868), capg-2(tm1833), kle-2(tm1823),* and *kle-2(ok1151).* They have a common homozygous phenotype, becoming uncoordinated, sick, sterile adults, with protruding vulvae and withered tails (data not shown). Similar phenotypes are observed in *mix-1(mn29)* homozygotes [13] or when animals carrying the temperature-sensitive mutation *hcp-6(mr17)* are shifted to non-permissive temperature at early larval stages [11]. Such defects are typical of mutated cell division genes. Early cell divisions are allowed by maternal-origin product, but as it diminishes, mitoses fail in late-dividing tissues. Indeed, homozygous adults mutant for each condensin II subunit exhibited abnormal connections between nuclei in late-dividing cell types like ventral nerve cord (Figure 2.12C), gut, and germline (Figure 2.6B), which likely reflect failed mitotic chromosome segregation. Condensin II is also required for proper germline formation, as the germline was extremely under-proliferated and contained only a small patch of abnormal nuclei in mutants (Figure 2.6B).

These studies extend previous analysis of condensin II, show common developmental abnormalities caused by mutating members of this complex, and provide new data supporting that CAPG-2 and KLE-2 are condensin II subunits.

Condensin I subunits promote mitotic and meiotic chromosome segregation

We next determined the functions of the newly identified condensin I complex. We reasoned that condensin I functions could be derived by determining depletion phenotypes observed for all three subunits shared between condensin I and I^{DC} (DPY-28, CAPG-1, and DPY-26), but not observed upon depleting the condensin I^{DC}-specific subunit DPY-27.

In several different settings, depletion of DPY-28, CAPG-1, and DPY-26 caused chromosome segregation defects, while DPY-27 depletion did not. Worms grown to adulthood on RNAi food targeting *dpy-28, capg-1*, or *dpy-26* showed inappropriate chromatin bridges between nuclei in many tissues. This defect was most easily scored in gut cell nuclei, which become polyploid after their divisions. While most gut nuclei in control or *dpy-27* RNAi fed worms were completely separated, many gut nuclei in *dpy-28, capg-1*, or *dpy-26* RNAi fed worms appear connected by a thin “bridge” of DNA (Figure 2.7A and B). Segregation defects caused by class I CAP depletion are unlikely to result from impaired dosage compensation or karyotype-specific defects, since they are observed in XX hermaphrodites (dosage compensation active) as well as XO males and XO hermaphrodites (dosage compensation inactive) (Figure 2.7B, Figure 2.13B).

To follow mitosis in real time, we extended RNAi feeding for two generations in a strain carrying GFP::histone H2B and filmed F2 embryos. Control and *dpy-27* depleted chromosomes separated fully at anaphase,

whereas chromosomes depleted of *dpy-28, capg-1*, or *dpy-26* remained connected by DNA strands (Figure 2.7C, Figure 2.13A). The anaphase segregation defect caused by depleting condensin I subunits was weaker, but similar to that caused by condensin II depletion (Figure 2.12). We confirmed that condensin II localizes normally to mitotic chromosomes in these condensin I-depleted F2 embryos (Figure 2.14A). Thus, the observed mitotic defects result from condensin I depletion and not from condensin II mislocalization.

To test whether condensin I depletion leads to aneuploidy, we depleted *capg-1* using two generation RNAi feeding and analyzed adult and embryonic nuclei by FISH using a 5S rDNA probe (Figure 2.7D). Most nuclei in controls had two fluorescent signals indicating diploidy, or one signal, presumably representing two un-resolvable foci. However, several nuclei in *capg-1* RNAi treated embryos or adult nerve cord had more than two signals, indicating aneuploidy (Figure 2.7D). Earlier FISH analysis of SMC-4 depleted nuclei uncovered similar, albeit more severe, defects [7].

Meiotic chromosome segregation defects also occurred after RNAi of *dpy-28, capg-1*, or *dpy-26*, but not *dpy-27*. Time-lapse analysis of animals carrying GFP::histone H2B after two generations of feeding control or *dpy-27* RNAi showed normal completion of two meiotic divisions, producing two polar bodies and a separate oocyte pronucleus. But in animals depleted of *dpy-28, capg-1*, or *dpy-26*, the oocyte pronucleus often remained connected to the second polar body (Figure 2.7E), reflecting meiosis II chromosome segregation failure. We could not determine whether condensin I is required for meiosis I: we failed to

observe meiosis I defects but we suspect this could be attributed to incomplete depletion of the complex by RNAi (Figure 2.14B).

Finally, we analyzed phenotypes caused by mutating genes encoding condensin I subunits. Mutations in *dpy-26* and *dpy-28* cause near complete hermaphrodite-specific maternal-effect lethality, but males are viable [19, 20]. The deletion mutant *capg-1(tm1514)* is more severe, and both sexes of homozygous mutant progeny from heterozygous mothers arrest as uncoordinated, sick, sterile adults with numerous bridged nuclei, unusually large or small nuclei, and under-proliferated germlines (data not shown). These phenotypes resemble those caused by condensin II subunit mutations. Why RNAi depletion of each class I CAP subunit produces equivalent phenotypes but mutations show differing severities is unclear, and may require additional alleles to resolve. Nevertheless, the surviving hermaphrodite and male progeny of *dpy-26, capg-1,* or *dpy-28* mutant mothers showed chromosome segregation defects in many tissues, while *dpy-27* mutants did not (scored for gut nuclei, Figure 2.13B), confirming that condensin I promotes mitotic chromosome segregation. Moreover, combining condensin I and II hypomorphic mutations caused more severe nuclear defects than either single mutant alone (Figure 2.15), as observed in other organisms [3-6], suggesting that both condensin I and II contribute to chromosome segregation. Because condensin I RNAi depletion produces weaker mitotic defects than condensin II depletion, and because *dpy-26* and *dpy-28* males are viable, while condensin II subunit mutants are lethal, it seems that condensin II function predominates.

DISCUSSION

Evolution of diverse condensin complexes

Condensins I and II are conserved complexes that ensure the accurate segregation of chromosomes during cell division [1, 2]. In *C. elegans*, incomplete condensin I-like and condensin II-like complexes had been identified [7, 12, 14]. Previous studies, extended here with RNAi and mutant analysis of all subunits, indicated that *C. elegans* condensin II is required for prophase chromosome condensation and anaphase segregation, conserved condensin II activities [7, 12]. In contrast, the previously identified condensin I-like complex, condensin I^{DC}, seemed not to function in chromosome segregation, but instead to modulate chromosome- and sex-specific gene expression [14]. Moreover, despite extensive genetic screens and homology searches, the CAP-G subunit of condensin I^{DC} was missing. It had therefore been suggested that *C. elegans* condensin I lost its mitotic function during the course of evolution and was converted to the specialized function of dosage compensation. One speculation was that holocentric chromosomes might not demand condensin I activity for segregation [2].

Our discovery of condensin I changes the basis for this viewpoint. We show that *C. elegans* contains both conserved condensin I and II complexes, each with a typical suite of five subunits, and that both promote chromosome segregation. The main difference between *C. elegans* and other organisms is a second SMC4 class protein, DPY-27, the only subunit that distinguishes condensin I^{DC} from condensin I. Thus, our findings indicate that mitotic condensin

I was not lost, but that the duplication and divergence of an SMC4 subunit allowed the ancestral mitotic condensin I to be adapted for dosage compensation. A related example is subunit paralogs that distinguish mitotic from meiotic versions of the cohesin SMC complex [31].

Roles of condensin I and II in chromosome segregation

How condensin I and II contribute differently to chromosome structure and function remains unclear. We show that in worms, depletion of either complex causes defects in chromosome segregation in multiple tissues and times in development. Differences in chromosomal distributions and depletion phenotypes suggest each complex has specialized functions. RNAi mediated depletion of condensin I or II each caused segregation defects, but only condensin II depletion caused prophase condensation defects, as in vertebrate cells [3, 6]. Condensin I depletion generally caused less severe phenotypes than condensin II depletion, with the exception of the strong *capg-1(tm1514)* deletion allele. It is conceivable that CAPG-1 has some functions independent of condensin I and I^{DC}.

We observed enhanced phenotypes when hypomorphic alleles of condensin I and II CAP subunits were combined, as seen in other systems [5, 6]. Yet a deletion allele of the SMC-4 subunit, which is shared between condensin I and II, appears no more severe than deletion alleles of condensin II CAP subunits alone (Figures 2.6 and 2.12). Together, these results suggest that condensin II plays a more critical role in mitosis and development than condensin

I in *C. elegans*, and may explain why condensin I had not been identified prior to this study.

Differential distribution of condensin I and II on holocentric chromosomes during mitosis and meiosis

The balance of condensin I and II distribution and activity has been speculated to influence the different chromosome shapes in different organisms [2, 5]. Most model organisms have chromosomes with distinct arms and a discrete centromere (monocentric organization), and condensin I and II show alternating distribution within the core of each sister chromatid arm, with enrichment of condensin II at the centromere [3-5]. Our study is the first to compare condensin I and II on chromosomes with an extended centromere (holocentric organization). Condensin I is broadly distributed on mitotic chromosomes internal to condensin II, which is restricted to the outer face of each sister chromatid coincident with the extended centromere, consistent with previous studies of individual subunits [7, 10-12, 16, 17]. Perhaps the different pattern of condensins on holocentric chromosomes indicates an underlying difference in the placement or structure of the holocentric chromatid core, thought to be the scaffold around which loop domains are arranged. Despite major differences, the non-overlapping distribution of condensin I and II and the enrichment of condensin II at the centromere are conserved. The more extreme difference in condensin I versus II localization on holocentrics makes an ideal setting in which to study how localization differences are dictated. Future

genome-wide chromatin IP studies could yield further insight into differential functions by mapping DNA elements bound by each complex.

Our studies also provide the first evidence in any organism for differences in condensin I and condensin II localization during meiosis. While condensin II localizes within the core of meiotic sister chromatids ([12] and this work), *C. elegans* condensin I localizes to the region between paired homologs at meiosis I and between sister chromatids at meiosis II. This contrasts with its broad distribution along mitotic chromosomes and with the localization of condensin I in other species to the internal core of sister chromatids during meiosis [32, 33]. *C. elegans* condensin I enrichment corresponds to regions where cohesion between homologs (meiosis I) or sisters (meiosis II) is maintained until anaphase. A speculation is that condensin I contributes to the proper formation and/or release of cohesion during the meiotic divisions. Previous studies have implicated condensin in mediating cohesion [34] and releasing cohesin [3, 35]. It is interesting to note that AIR-2, the *C. elegans* homolog of the Aurora B kinase, also localizes between homologs at meiosis I and between sisters at meiosis II, and is required for proper release of a meiotic subunit of cohesin [9, 24].

Condensin function in chromosome segregation and gene regulation

An unresolved question is how differences between condensin complexes are specified. In principle, functional differences could be due to differences in biochemical activity, regulation, or chromosomal targeting. Although condensin I is known to have ATP-dependent supercoiling and DNA compaction activities [36-38], it is currently unknown whether these activities are shared by condensin

II. We previously demonstrated supercoiling activity in SMC-4 immunoprecipitates [7]. That preparation, in light of the current study, contained both condensin I and II, making the source of supercoiling activity ambiguous. Gene regulation by condensin I^{DC} may also require an ATP-dependent process, because lesions in the ATP binding domain of *dpy-27* and *mix-1* impair dosage compensation [13, 15].

For condensins I and I^{DC}, a difference in one subunit has a profound effect on function, converting a mitotic complex into a gene regulatory complex. Interestingly, condensin I and II subunits in other organisms have been implicated in gene regulation. Condensin I subunits in *S. cerevisiae* function in silencing at the mating type locus [39], rDNA silencing [40] and tRNA-gene mediated silencing [41]. In *Drosophila*, condensin I subunits participate in repression of transgenes inserted in heterochromatin [42, 43]. A murine condensin II (CAP-G2) subunit antagonizes activation of reporter genes [44]. Even the bacterial SMC complex has roles in both chromosome partitioning and gene regulation, implying that these are ancient linked roles [45]. A common alteration of chromosome structure could conceivably underlie both chromosome preparation for mitosis, and down-regulation of gene expression. Continued comparative studies of condensin complexes are likely to shed light on the links between chromosome segregation and gene regulation.

EXPERIMENTAL PROCEDURES

See Supplemental Data for MuDPIT, phylogenetic analysis, strains, genetic assays, antibody information, and image collection.

Protein analysis. Small-scale IPs and western blotting were performed as described [12].Large-scale protein extract preparation and IPs for MudPIT were scaled-up versions of this protocol.

Microscopy. Antibody staining of embryos and dissected adults was performed as described in protocol #21 in [46]. To distinguish between older male and hermaphrodite embryos, we co-stained embryos with antibodies to SDC-3, which only localizes to the X chromosomes of hermaphrodites. DNA staining of whole worms was performed by treating with Carnoy's fixative, re-hydrating in 1x M9 buffer, and mounting in ProLong anti-fade containing DAPI. FISH was performed as in protocol #25 in [46]. Time-lapse imaging of mitotic and meiotic chromosome segregation was performed on animals carrying GFP::histone H2B. These were dissected with a syringe needle on a 2% agar pad in 1x M9 buffer and covered gently with a coverslip. Z stacks were acquired with a Perkin Elmer spinning disk confocal microscope every 20s with ~0.75s exposure and 2x2 binning. For fluorescent image collection details see supplemental data.

RNA interference

RNA interference by feeding was performed using the Ahringer lab RNAi feeding library [47].

<u>One generation RNAi feeding</u> (as in Figure 2.7A & B, Figure 2.11B & C)

L1 stage larvae were placed on plates seeded with bacteria expressing dsRNA corresponding to the gene being knocked down and grown to adulthood ("PO" generation adults).

Two generation RNAi feeding (as in Figure 2.7C & D, Figure 2.12A)

PO adults from above were transferred to fresh RNAi plates, allowed to lay eggs, and these progeny ("F1" generation) were grown to adulthood and examined. Where stated, embryos from mothers of this F1 generation ("F2" generation embryos) were examined.

RNAi injection plus feeding (as in Figure 2.6A, Figure 2.11A)

dsRNA corresponding to a region of each gene encoding a predicted condensin II subunit was prepared by in vitro transcription and injected into young hermaphrodites. These were recovered onto plates seeded with the corresponding RNAi food and examined 48 hours later.

ACKNOWLEDGMENTS

We thank the Japanese National BioResource Project, the C. elegans Gene Knockout Consortium, and the C. elegans Genetics Center for strains. This work was supported by National Institutes of Health grants (RO1 GM076378 to K.H., R01 GM079533 to G.C., and RO1 GM30702 to BJM), an allocation from American Cancer Society Institutional Research Grant (IRG 93-033 to K.H.), the Worcester Foundation for Biomedical Research (to K.H.), the Biological Sciences Scholars Program at the University of Michigan (to G.C.), and Predoctoral Training in Genetics, NIH T32 GM07544 (to E.P and K.C.). BJM is an Investigator of the Howard Hughes Medical Institute.

REFERENCES

1. Belmont, A.S. (2006). Mitotic chromosome structure and condensation. Curr Opin Cell Biol *18*, 632-638.
2. Hirano, T. (2005). Condensins: organizing and segregating the genome. Curr Biol *15*, R265-275.
3. Hirota, T., Gerlich, D., Koch, B., Ellenberg, J., and Peters, J.M. (2004). Distinct functions of condensin I and II in mitotic chromosome assembly. J Cell Sci *117*, 6435-6445.
4. Ono, T., Fang, Y., Spector, D.L., and Hirano, T. (2004). Spatial and temporal regulation of Condensins I and II in mitotic chromosome assembly in human cells. Mol Biol Cell *15*, 3296-3308.
5. Ono, T., Losada, A., Hirano, M., Myers, M.P., Neuwald, A.F., and Hirano, T. (2003). Differential contributions of condensin I and condensin II to mitotic chromosome architecture in vertebrate cells. Cell *115*, 109-121.
6. Gerlich, D., Hirota, T., Koch, B., Peters, J.M., and Ellenberg, J. (2006). Condensin I stabilizes chromosomes mechanically through a dynamic interaction in live cells. Curr Biol *16*, 333-344.
7. Hagstrom, K.A., Holmes, V.F., Cozzarelli, N.R., and Meyer, B.J. (2002). C. elegans condensin promotes mitotic chromosome architecture, centromere organization, and sister chromatid segregation during mitosis and meiosis. Genes Dev *16*, 729-742.
8. Hudson, D.F., Vagnarelli, P., Gassmann, R., and Earnshaw, W.C. (2003). Condensin is required for nonhistone protein assembly and structural integrity of vertebrate mitotic chromosomes. Dev Cell *5*, 323-336.
9. Kaitna, S., Pasierbek, P., Jantsch, M., Loidl, J., and Glotzer, M. (2002). The aurora B kinase AIR-2 regulates kinetochores during mitosis and is required for separation of homologous Chromosomes during meiosis. Curr Biol *12*, 798-812.
10. Maddox, P.S., Portier, N., Desai, A., and Oegema, K. (2006). Molecular analysis of mitotic chromosome condensation using a quantitative time-resolved fluorescence microscopy assay. Proc Natl Acad Sci U S A *103*, 15097-15102.
11. Stear, J.H., and Roth, M.B. (2002). Characterization of HCP-6, a C. elegans protein required to prevent chromosome twisting and merotelic attachment. Genes Dev *16*, 1498-1508.
12. Chan, R.C., Severson, A.F., and Meyer, B.J. (2004). Condensin restructures chromosomes in preparation for meiotic divisions. J Cell Biol *167*, 613-625.
13. Lieb, J.D., Albrecht, M.R., Chuang, P.T., and Meyer, B.J. (1998). MIX-1: an essential component of the C. elegans mitotic machinery executes X chromosome dosage compensation. Cell *92*, 265-277.
14. Meyer, B.J. (2005). X-Chromosome dosage compensation. In Wormbook, The *C. elegans* Research Community, ed. (doi/10.1895/wormbook.1.8.1, http://www.wormbook.org).

15. Chuang, P.T., Albertson, D.G., and Meyer, B.J. (1994). DPY-27:a chromosome condensation protein homolog that regulates C. elegans dosage compensation through association with the X chromosome. Cell *79*, 459-474.
16. Tsai, C.J., Mets, D.G., Albrecht, M.R., Nix, P., Chan, A., and Meyer, B.J. (2008). Meiotic crossover number and distribution are regulated by a dosage compensation protein that resembles a condensin subunit. Genes Dev *22*, 194-211.
17. Lieb, J.D., Capowski, E.E., Meneely, P., and Meyer, B.J. (1996). DPY-26, a link between dosage compensation and meiotic chromosome segregation in the nematode. Science *274*, 1732-1736.
18. Schleiffer, A., Kaitna, S., Maurer-Stroh, S., Glotzer, M., Nasmyth, K., and Eisenhaber, F. (2003). Kleisins: a superfamily of bacterial and eukaryotic SMC protein partners. Mol Cell *11*, 571-575.
19. Hodgkin, J. (1983). X chromosome dosage and gene expression in Caenorhabditis elegans: Two unusual dumpy genes. Mol Gen Genet *192*, 452-458.
20. Plenefisch, J.D., DeLong, L., and Meyer, B.J. (1989). Genes that implement the hermaphrodite mode of dosage compensation in Caenorhabditis elegans. Genetics *121*, 57-76.
21. Delahunty, C.M., and Yates, J.R., 3rd (2007). MudPIT: multidimensional protein identification technology. Biotechniques *43*, 563, 565, 567 passim.
22. Kimura, K., and Hirano, T. (2000). Dual roles of the 11S regulatory subcomplex in condensin functions. Proc Natl Acad Sci U S A *97*, 11972-11977.
23. Dawes, H.E., Berlin, D.S., Lapidus, D.M., Nusbaum, C., Davis, T.L., and Meyer, B.J. (1999). Dosage compensation proteins targeted to X chromosomes by a determinant of hermaphrodite fate. Science *284*, 1800-1804.
24. Rogers, E., Bishop, J.D., Waddle, J.A., Schumacher, J.M., and Lin, R. (2002). The aurora kinase AIR-2 functions in the release of chromosome cohesion in Caenorhabditis elegans meiosis. J Cell Biol *157*, 219-229.
25. Chuang, P.T., Lieb, J.D., and Meyer, B.J. (1996). Sex-specific assembly of a dosage compensation complex on the nematode X chromosome. Science *274*, 1736-1739.
26. Davis, T.L., and Meyer, B.J. (1997). SDC-3 coordinates the assembly of a dosage compensation complex on the nematode X chromosome. Development *124*, 1019-1031.
27. Carmi, I., Kopczynski, J.B., and Meyer, B.J. (1998). The nuclear hormone receptor SEX-1 is an X-chromosome signal that determines nematode sex. Nature *396*, 168-173.
28. Miller, L.M., Plenefisch, J.D., Casson, L.P., and Meyer, B.J. (1988). xol-1: a gene that controls the male modes of both sex determination and X chromosome dosage compensation in C. elegans. Cell *55*, 167-183.

29. Gladden, J.M., Farboud, B., and Meyer, B.J. (2007). Revisiting the X:A signal that specifies Caenorhabditis elegans sexual fate. Genetics *177*, 1639-1654.
30. Rhind, N.R., Miller, L.M., Kopczynski, J.B., and Meyer, B.J. (1995). xol-1 acts as an early switch in the C. elegans male/hermaphrodite decision. Cell *80*, 71-82.
31. Revenkova, E., and Jessberger, R. (2006). Shaping meiotic prophase chromosomes: cohesins and synaptonemal complex proteins. Chromosoma *115*, 235-240.
32. Viera, A., Gomez, R., Parra, M.T., Schmiesing, J.A., Yokomori, K., Rufas, J.S., and Suja, J.A. (2007). Condensin I reveals new insights on mouse meiotic chromosome structure and dynamics. PLoS ONE *2*, e783.
33. Yu, H.G., and Koshland, D.E. (2003). Meiotic condensin is required for proper chromosome compaction, SC assembly, and resolution of recombination-dependent chromosome linkages. J Cell Biol *163*, 937-947.
34. Lam, W.W., Peterson, E.A., Yeung, M., and Lavoie, B.D. (2006). Condensin is required for chromosome arm cohesion during mitosis. Genes Dev *20*, 2973-2984.
35. Yu, H.G., and Koshland, D. (2005). Chromosome morphogenesis: condensin-dependent cohesin removal during meiosis. Cell *123*, 397-407.
36. Kimura, K., and Hirano, T. (1997). ATP-dependent positive supercoiling of DNA by 13S condensin: a biochemical implication for chromosome condensation. Cell *90*, 625-634.
37. Kimura, K., Rybenkov, V.V., Crisona, N.J., Hirano, T., and Cozzarelli, N.R. (1999). 13S condensin actively reconfigures DNA by introducing global positive writhe: implications for chromosome condensation. Cell *98*, 239-248.
38. Strick, T.R., Kawaguchi, T., and Hirano, T. (2004). Real-time detection of single-molecule DNA compaction by condensin I. Curr Biol *14*, 874-880.
39. Bhalla, N., Biggins, S., and Murray, A.W. (2002). Mutation of YCS4, a budding yeast condensin subunit, affects mitotic and nonmitotic chromosome behavior. Mol Biol Cell *13*, 632-645.
40. Machin, F., Paschos, K., Jarmuz, A., Torres-Rosell, J., Pade, C., and Aragon, L. (2004). Condensin regulates rDNA silencing by modulating nucleolar Sir2p. Curr Biol *14*, 125-130.
41. Haeusler, R.A., Pratt-Hyatt, M., Good, P.D., Gipson, T.A., and Engelke, D.R. (2008). Clustering of yeast tRNA genes is mediated by specific association of condensin with tRNA gene transcription complexes. Genes Dev *22*, 2204-2214.
42. Cobbe, N., Savvidou, E., and Heck, M.M. (2006). Diverse mitotic and interphase functions of condensins in Drosophila. Genetics *172*, 991-1008.
43. Dej, K.J., Ahn, C., and Orr-Weaver, T.L. (2004). Mutations in the Drosophila condensin subunit dCAP-G: defining the role of condensin for chromosome condensation in mitosis and gene expression in interphase. Genetics *168*, 895-906.

44. Xu, Y., Leung, C.G., Lee, D.C., Kennedy, B.K., and Crispino, J.D. (2006). MTB, the murine homolog of condensin II subunit CAP-G2, represses transcription and promotes erythroid cell differentiation. Leukemia *20*, 1261-1269.
45. Dervyn, E., Noirot-Gros, M.F., Mervelet, P., McGovern, S., Ehrlich, S.D., Polard, P., and Noirot, P. (2004). The bacterial condensin/cohesin-like protein complex acts in DNA repair and regulation of gene expression. Mol Microbiol *51*, 1629-1640.
46. Shaham, S.e. (2006). Methods in cell biology. In Wormbook, The *C. elegans* Research Community, ed. (doi/10.1895/wormbook.1.8.1, http://www.wormbook.org).
47. Kamath, R.S., and Ahringer, J. (2003). Genome-wide RNAi screening in Caenorhabditis elegans. Methods *30*, 313-321.

A

	Human Condensin I	*C. elegans* Condensin I^{DC}	*C. elegans* Condensin I
SMC	SMC 2/hCAP-E	MIX-1	MIX-1
SMC	SMC 4/hCAP-C	DPY-27	SMC-4
CAP I	hCAP-D2	DPY-28	DPY-28
CAP I	hCAP-G	CAPG-1	CAPG-1
CAP I	hCAP-H	DPY-26	DPY-26
	Human Condensin II	***C. elegans* Condensin II**	
SMC	SMC 2/hCAP-E	MIX-1	
SMC	SMC 4/hCAP-C	SMC-4	
CAP II	hCAP-D3	HCP-6	
CAP II	hCAP-G2	CAPG-2	
CAP II	hCAP-H2	KLE-2	

B

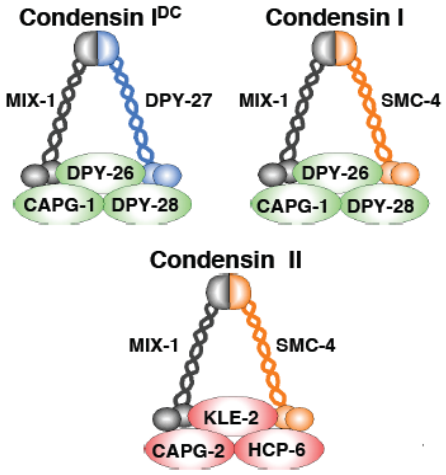

Figure 2.1 The three condensin model. (A) *C. elegans* condensin subunits and their human homologs. We propose that *C. elegans* has three condensin complexes of the composition shown. Condensin I and II share the same SMC2 and SMC4 subunits but associate with either class I or class II CAP subunits, respectively. Condensin I^{DC} differs from condensin I only by its unique SMC4 subunit, DPY-27. (B) Cartoon depicting the three proposed complexes.

A

Identity	Gene name	Gene	DPY-27	SMC-4	KLE-2	CAPG-1	KLP-7
SMC							
SMC2	*mix-1*	M106.1	95	456	99	1034	0
SMC4	*smc-4*	F35G12.8	0	351	77	684	0
SMC4	*dpy-27*	R13G10.1	128	0	0	616	0
CAP I							
CAP-D2	*dpy-28*	Y39A1B.3	47	222	0	1133	0
CAP-G	*capg-1*	F29D11.2	39	131	0	1020	0
CAP-H	*dpy-26*	C25G4.5	30	209	0	895	0
CAP II							
CAP-D3	*hcp-6*	Y110A7A.1	0	203	127	3	0
CAP-G2	*capg-2*	F55C5.4	0	111	79	0	0
CAP-H2	*kle-2*	C29E4.2	0	131	156	0	0

B

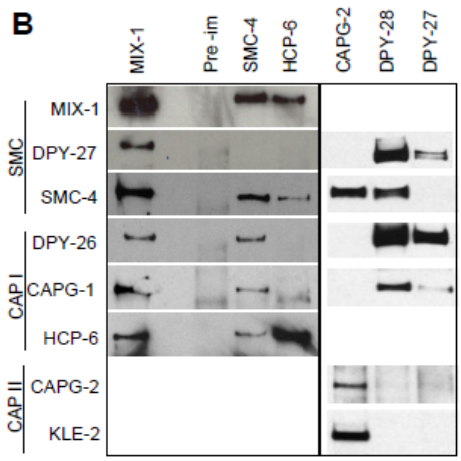

C

	SMC			CAP I			CAP II		
	MIX-1	SMC-4	DPY-27	DPY-28	CAPG-1	DPY-26	HCP-6	CAPG-2	KLE-2
SMC									
MIX-1	+	+	+		+		+		
SMC-4	+	+	-	+	+	+	+	+	+
DPY-27	+	-	+	+	+	+	-	-	-
CAP I									
DPY-28		+	+	+	+	+	-	-	-
CAP-G1	+	+	+	+	+	+	-	-	-
DPY-26	+	+	+	+	+	+	-	-	-
CAP II									
HCP-6	+	+	-	-		-	+	+	+
CAP-G2		+	-	-	-	-	+	+	+
KLE-2		+	-	-	-	-	+	+	+

Figure 2.2 Condensin subunit interactions identified by immunoprecipitation. (A) Immunoprecipitation (IP) from embryo extracts with antibodies against DPY-27, SMC-4, KLE-2, CAPG-1 and KLP-7 (control) were analyzed by MudPIT mass spectrometry. Numbers indicate the total mass spectra collected in three (KLE-2) or four (all others) IP samples corresponding to each protein indicated on the left. (B and C) IP reactions from embryo extracts using antibodies against condensin subunits were performed and analyzed on Western blots probed with an array of antibodies. Pre-immune IP (Pre-im) is shown as control. Selected western blots are shown in (B); summary of all IPs analyzed is shown in (C). "+": subunit was detected in the IP, "–" subunit was not detected in the IP, blank cell: interaction was not scored.

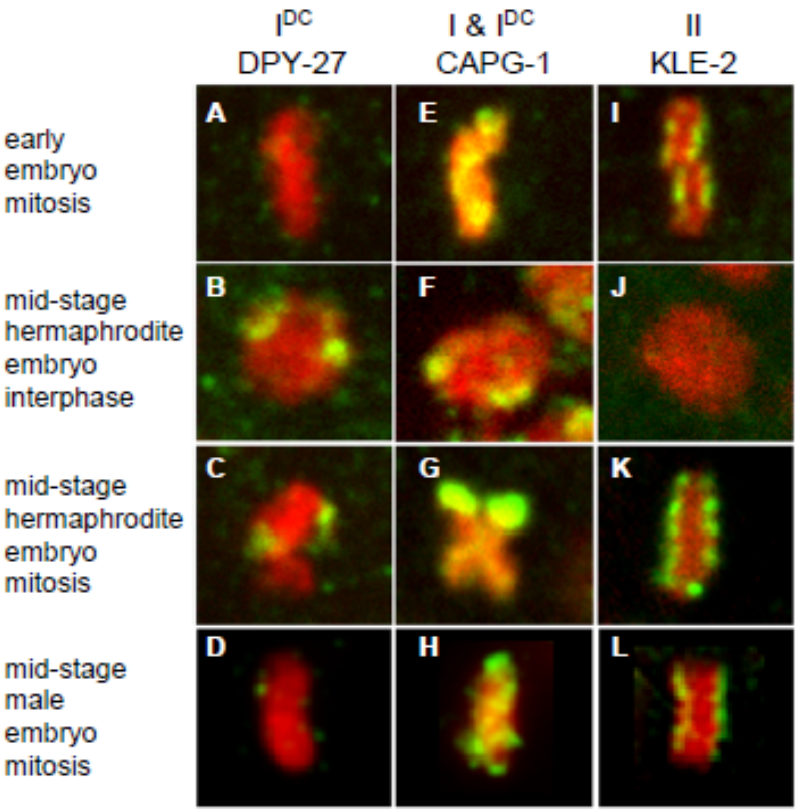

Figure 2.3 Condensin I localizes to mitotic chromosomes in a pattern distinct from condensin I^{DC} or condensin II. Anti-DPY-27 antibody was used to indicate the subcellular localization of condesin I^{DC}, anti-CAPG-1 to indicate both condensin I and condensin I^{DC}, and anti-KLE-2 to indicate condensin II. Condensin I^{DC} does not associate with mitotic chromosomes in early stage hermaphrodite embryos (A), or in male embryos (D), but associates with the two hermaphrodite X chromosomes after the onset of dosage compensation, both during interphase (B) and during mitosis (C). CAPG-1 staining not shared by DPY-27 indicates that condensin I localizes to mitotic chromosomes in both hermaphrodites (E) and males (H). Once dosage compensation initiates in hermaphrodite embryos CAPG-1 localizes to the X chromosomes in interphase, as part of condensin I^{DC} (F). During mitosis CAPG-1 localizes to two bright X foci (as part of condensin I^{DC}) and less intensely to other chromosomes (as part of condensin I) (G). Condensin II shows no distinct pattern during interphase (J), and a centromere-like pattern on mitotic chromosomes in both hermaphrodites (I, K) and males (L). Antibody in green, DNA in red, merge in yellow.

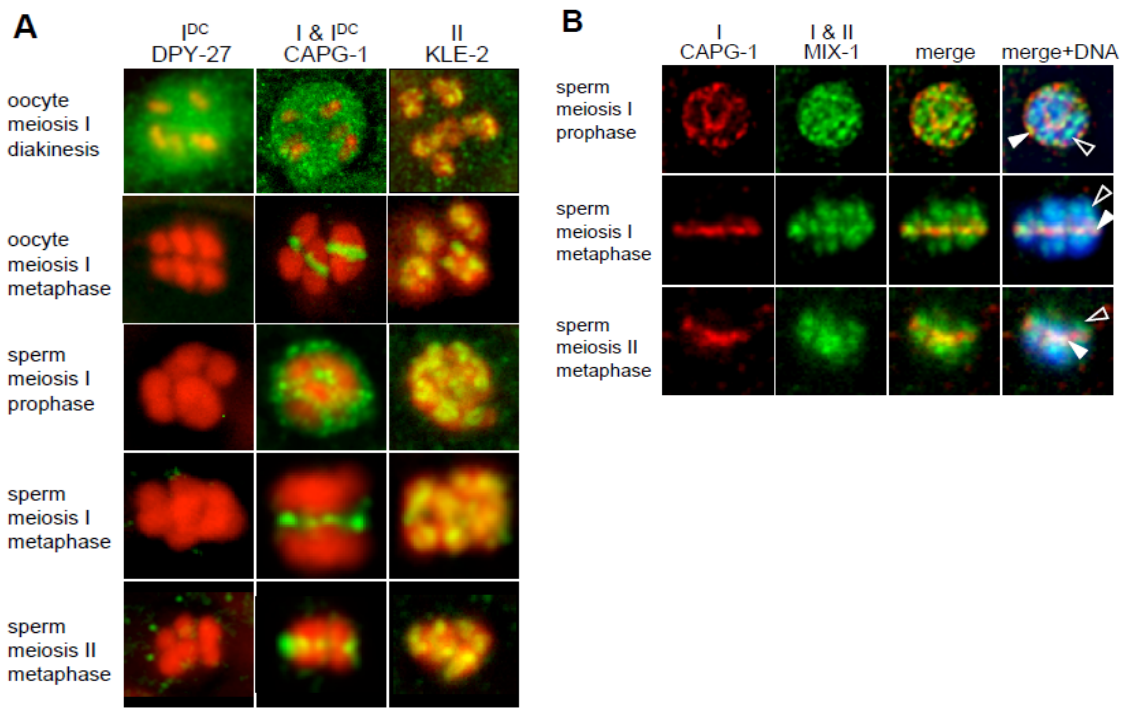

Figure 2.4 Condensin I localizes to meiotic chromosomes in a pattern distinct from condensin I^{DC} or condensin II. (A) Anti-DPY-27 antibody was used to indicate the localization of condesin I^{DC}, anti-CAPG-1 to indicate condensin I and condensin I^{DC}, and anti-KLE-2 to indicate condensin II. DPY-27 was detected in the nucleoplasm of mature oocytes, but not at other stages of meiosis. CAPG-1 staining indicates that condensin I surrounds chromosomes in prophase then localizes to the interface between homologs (meiosis I) or sister chromatids (meiosis II). In contrast, KLE-2 staining indicates that condensin II localizes to the core of each sister chromatid. Antibody in green, DNA in red, merge in yellow. (B) MIX-1 localization is a hybrid of condensin I and condensin II patterns. MIX-1 (green) partially colocalizes with CAPG-1 (red, representing condensin I) on sperm chromosomes (blue). MIX-1 and CAPG-1 co-localize surrounding chromosomes in meiosis prophase I, between homologs in metaphase I and between sisters at metaphase II (filled arrows). In addition, MIX-1 localizes to the chromosome core at each stage (open arrows), a pattern resembling condensin II and not shared by CAPG-1.

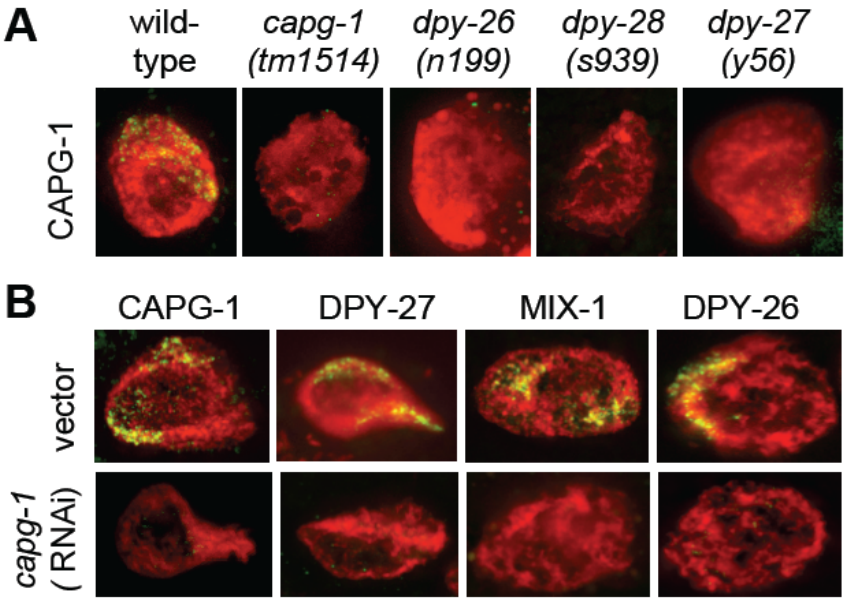

C

RNAi construct	wild-type % lethality	*sex-1(y263)* % lethality	*xol-1(y9) sex-1(y263)* %male rescue
vector	0.7	15	<1
dpy-27	1.7	92	40
dpy-28	0.7	89	60
dpy-26	0	93	33
capg-1	0.8	91	60

Figure 2.5 CAPG-1 functions in dosage compensation. (A) CAPG-1 (green) localizes to X chromosomes in wild-type hermphrodites, but not in animals carrying mutated subunits of condensin I^{DC}. (B) Condensin I^{DC} subunits (green) localize to hermaphrodite X chromosomes in control vector RNAi animals, but not in animals fed RNAi targeting *capg-1*. Shown are intestinal nuclei (red) of adult hermaphrodites. (C) Genetic assays testing dosage compensation function. Feeding RNAi targeting condensin I^{DC} subunits was minimally lethal in wild-type embryos, and enhanced lethality in the *sex-1* mutant background. By contrast, *xol-1 sex-1* males die due to inappropriate activation of dosage compensation, but can be rescued by RNAi depletion of a condensin I^{DC} subunit. In both assays, *capg-1* RNAi yields results similar to RNAi of other condensin I^{DC} subunits. % lethality was calculated as dead progeny/total progeny x100. Male rescue was calculated as # males/expected number of males x 100. At least 200 animals were scored for RNAi of each gene.

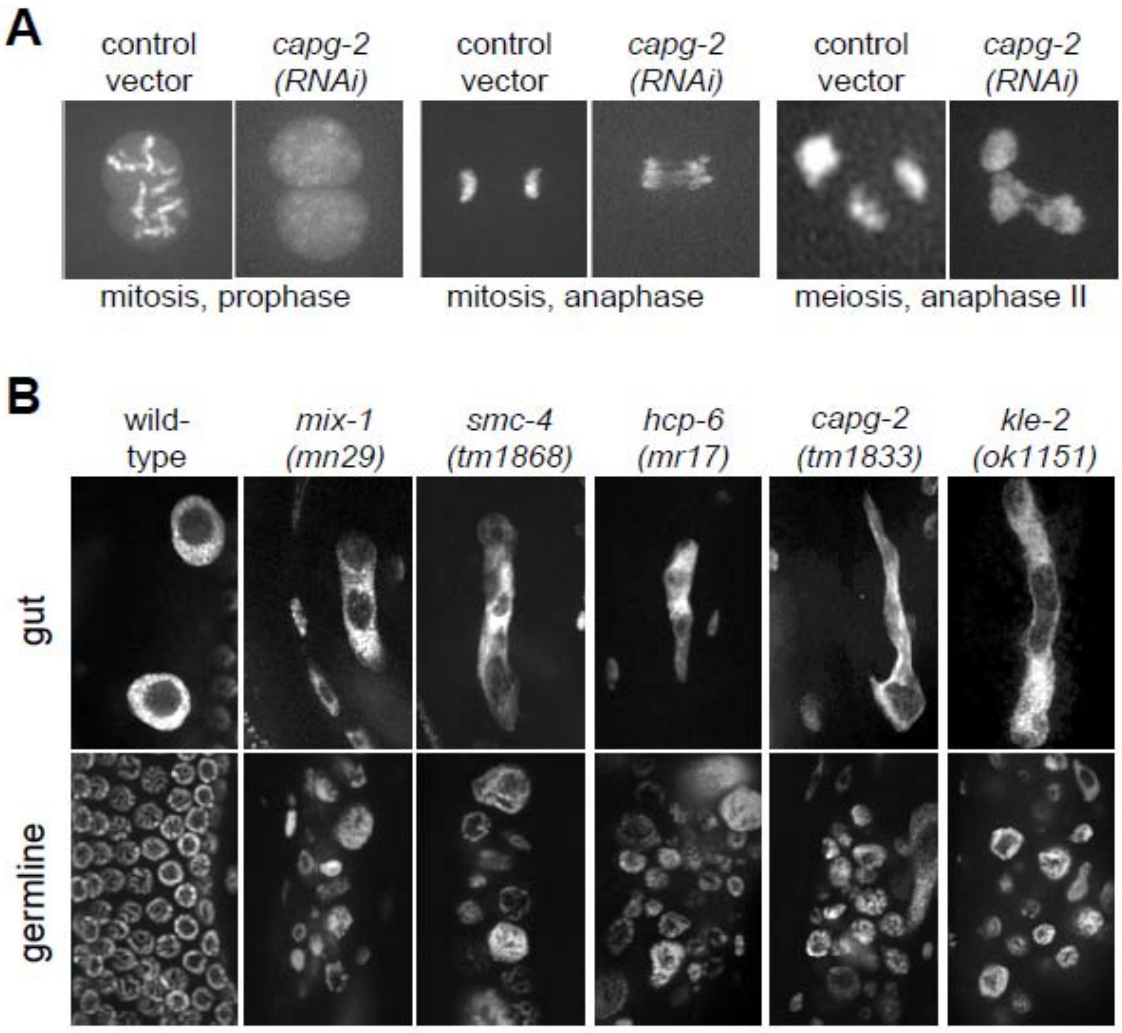

Figure 2.6 Depleting each condensin II subunit results in common chromosomal and developmental defects. (A) Images from time-lapse movies of control or *capg-2* RNAi-depleted worms carrying a GFP::histone H2B transgene. At the first embryonic mitosis, *capg-2* depleted chromosomes fail to condense into distinct rod shapes during prophase (left). At anaphase, *capg-2* depleted chromosomes fail to separate completely and abnormal DNA connections are observed (middle). Separating chromatids during meiosis anaphase II also show abnormal DNA connections in *capg-2* depleted animals (right). (B) Wild-type or homozygous condensin II subunit mutant adult hermaphrodites, stained with DNA dye. Gut nuclei (top row) are separated in wild-type, but often connected in condensin II subunit mutants. Germline nuclei (bottom row) are uniformly sized and evenly spaced in wild-type. Condensin II subunit mutants have fewer germline nuclei, which are abnormally sized and unevenly distributed.

Figure 2.7 Condensin I is required for mitotic and meiotic chromosome segregation (A) Gut nuclei from adults raised since hatching on bacteria expressing control vector or dsRNA against the subunit indicated. Gut nuclei (stained for DNA) are normally separated in control or *dpy-27* RNAi treated animals, but abnormally connected after depleting condensin I subunits *dpy-28*, *capg-1*, and *dpy-26*. (B) Quantification of defects shown in (A), scored in hermaphrodites (magenta), males (blue), and a mutant situation with half XO hermaphrodites and half XX hermaphrodites (*tra-2(e2531),* purple). Percentage calculated as the number of gut nuclei with an obvious connection/total gut nuclei x 100. Standard deviation from three experiments is shown. In comparison to control vector by Fisher's exact test , *dpy-27* $p > 0.2$ in each sex (not significant); for *dpy-28*, *capg-1*, and *dpy-26* each $p < 0.0001$ (significant). (C) Still images from time-lapse movies of the first mitosis in F2 embryos after two generations of RNAi feeding in a GFP:histone H2B strain. Chromosome segregation errors characterized by DNA strands between separating sets of chromosomes were observed with *dpy-28*, *capg-1*, and *dpy-26* RNAi but not with control or *dpy-27* RNAi depletion. (D) FISH analysis of nuclei from mid-stage (about 100-cell) embryos (top) or adult nerve cord cells (bottom) using a 5S rDNA probe. After two generations of RNAi feeding, progeny of animals fed control vector contain diploid nuclei with two signals. Only 3 of 15 vector treated embryos contained nuclei with more than two spots, and in each case, it was limited to a single nucleus within the embryo. By contrast, 14 of 16 *capg-1* RNAi-fed progeny contained aneuploid nuclei with more than two signals (arrow). In adults, nuclei in control worms had two signals, indicating diploidy. Only 1 of 8 control treated animals had a nucleus with more than two signals. By contrast, 12 of 13 *capg-1* RNAi treated worms had nuclei with multiple signals, indicating aneuploidy (arrow) (E) Meiosis II after two generations of RNAi feeding in a GFP:histone H2B strain. The two meiotic divisions produce two small polar bodies and a separated oocyte pronucleus in control treated animals. When condensin I subunit DPY-26 is depleted, the second polar body often fails to segregate from the oocyte pronucleus.

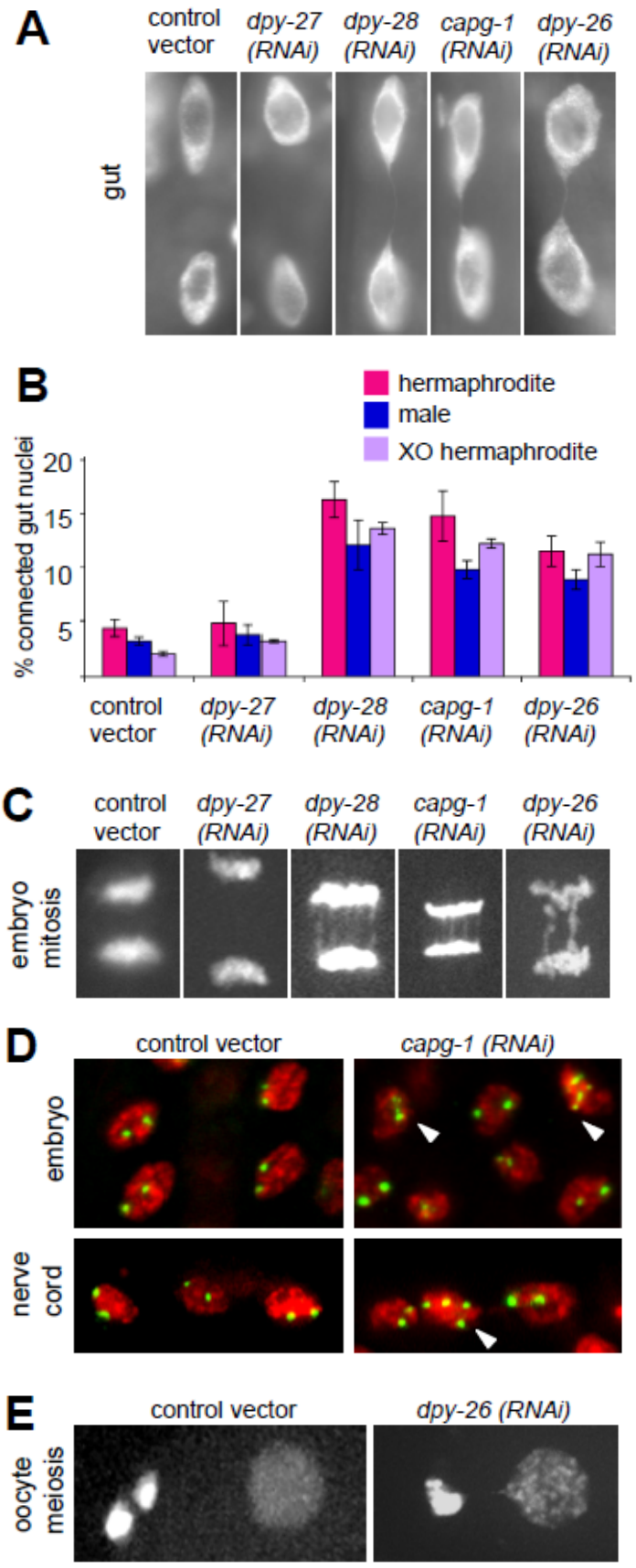
A
control vector
dpy-27 (RNAi)
dpy-28 (RNAi)
capg-1 (RNAi)
dpy-26 (RNAi)
gut
B
hermaphrodite
male
XO hermaphrodite
% connected gut nuclei
20
15
10
5
control vector
dpy-27 (RNAi)
dpy-28 (RNAi)
capg-1 (RNAi)
dpy-26 (RNAi)
C
control vector
dpy-27 (RNAi)
dpy-28 (RNAi)
capg-1 (RNAi)
dpy-26 (RNAi)
embryo mitosis
D
control vector
capg-1 (RNAi)
embryo
nerve cord
E
control vector
dpy-26 (RNAi)
oocyte meiosis

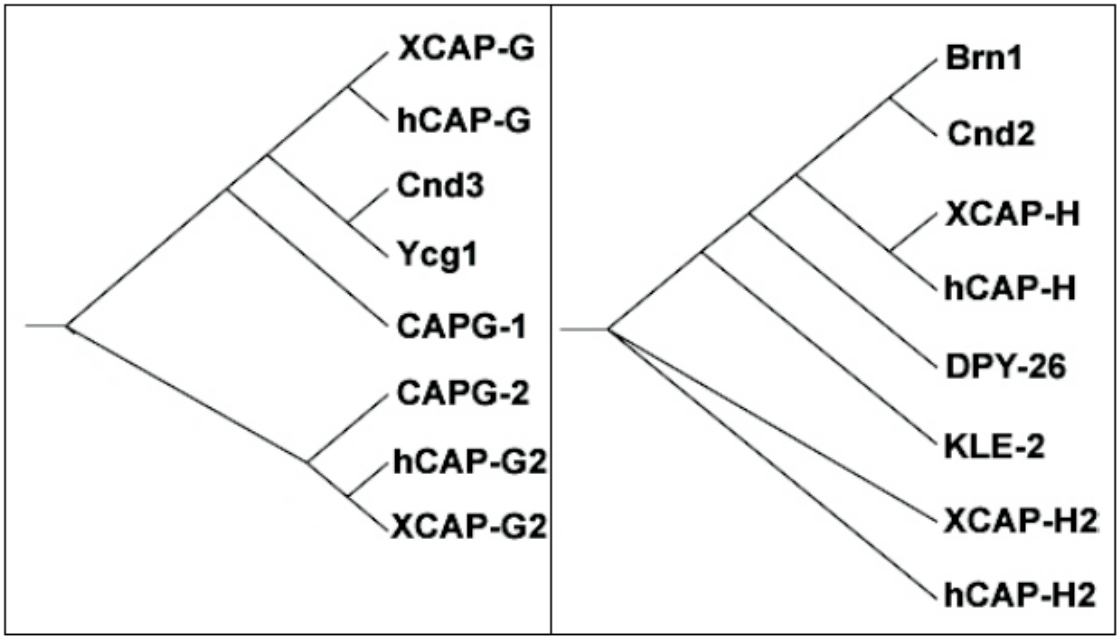

Figure 2.8 *C. elegans CAPG-1 is more closely related to CAP-G proteins, while CAPG-2 is* more closely related to CAP-G2 proteins. Similarly, while DPY-26 is related to CAP-H proteins, KLE-2 is more closely related to CAP-H2 proteins. Phylogenetic analysis of CAP-D2/D3 proteins was reported in Chan et al., 2004. Together these analyses show that the CAP subunits of *C. elegans condensin IDC and* condensin I belong to the CAP I class, and the CAP subunits of condensin II belong to the CAP II class.

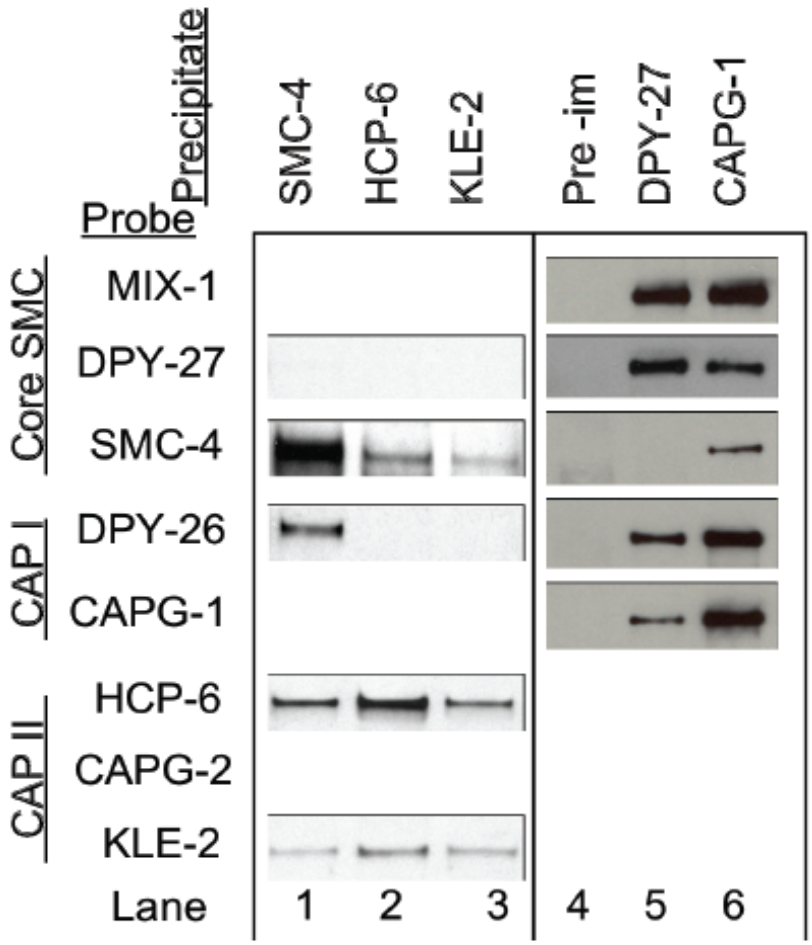

Figure 2.9 IP-western analysis confirms condensin interactions detected by mass spectrometry. Immunoprecipitation (IP) reactions from embryo extracts using antibodies against condensin subunits were performed, listed at the top. Each IP was analyzed on Western blots probed with an array of antibodies, listed on the left.

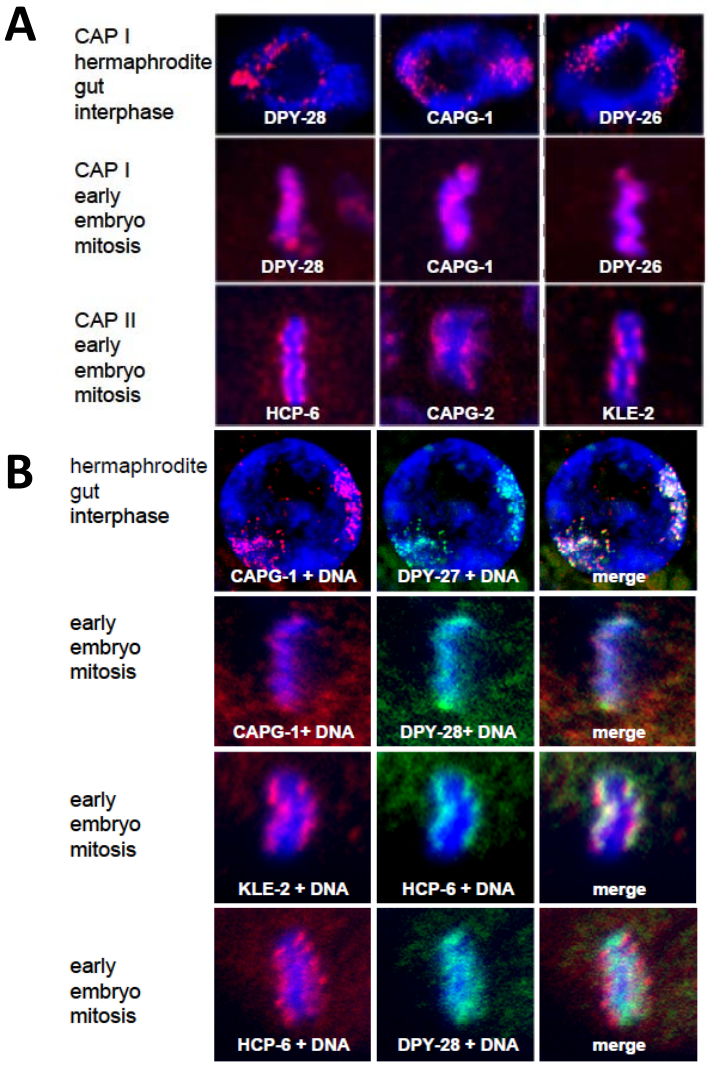

Figure 2.10 All three CAP subunits of each class show the same localization patterns. A. The three class I CAP subunits (DPY-28, CAPG-1, and DPY-26) associate with hermaphrodite interphase nuclei in the sub-regions occupied by the X chromosomes (top row) and coat mitotic chromosomes at the metaphase plate of early embryos (middle row). The three class II subunits (HCP-6, CAPG-2, and KLE-2) all show similar centromere-enriched pattern on mitotic chromosomes at the metaphase plate (bottom row). Antibody in red, DNA in blue, merge in pink. B .CAPG-1 (red) colocalizes with condensin IDC subunit DPY-27 (green) on X chromosomes of interphase intestinal nuclei of hermaphrodites and with condensin I subunit DPY-28 on mitotic chromosomes of early embryos. KLE-2 (red) colocalizes with condensin II subunit HCP-6 (green) on the outer face of mitotic chromosomes of early embryos. Bottom row: Condensin II subunit HCP-6 (red) localizes to outer face of the metaphase plate, while condensin I subunit DPY-28 (green) associates non-uniformly with chromosomes in a diffuse manner, with minimal overlap between the two complexes. DNA in blue.

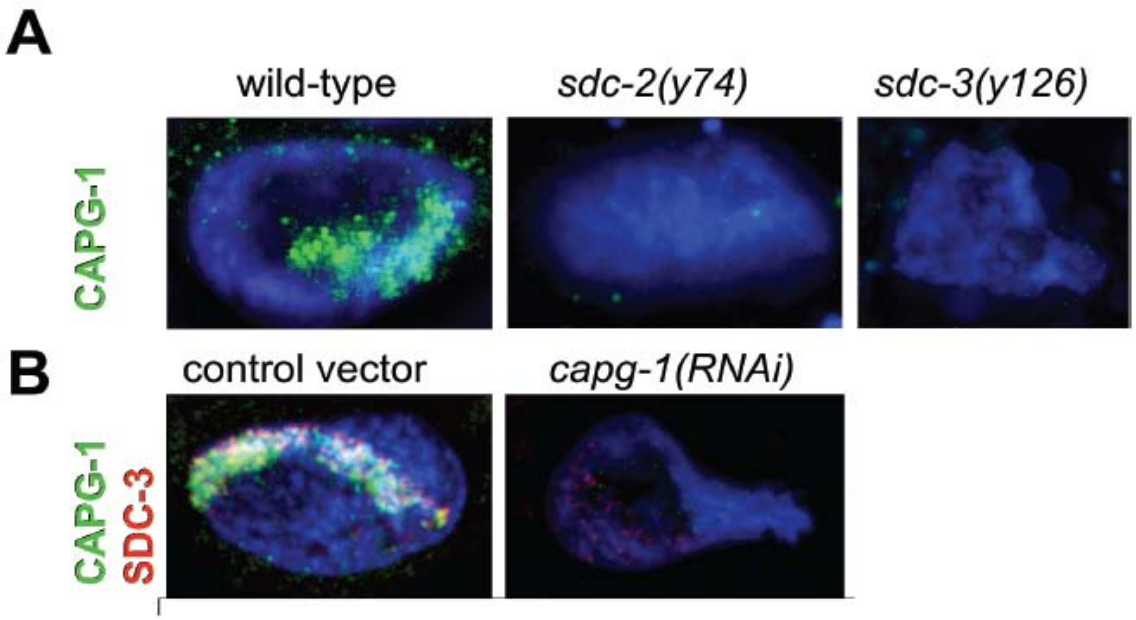

Figure 2.11 CAPG-1 shows X chromosome binding relationships with SDC proteins. (A) CAPG-1 (green) localizes to hermaphrodite X chromosomes in wild type animals, but not in animals carrying mutations in *sdc-2 or sdc-3, genes required* for both sex-determination and dosage compensation. (B) *capg-1 RNAi does not* eliminate, but greatly reduces, staining by SDC-3 specific antibodies (red). DNA in blue.

Figure 2.12 Common chromosomal and developmental defects result from depletion of each condensin II subunit. (A) Three frames from time-lapse movies of the first embryonic mitosis in a strain carrying GFP:histone H2B to visualize chromosomes. RNAi-mediated depletion of each condensin II subunit was achieved by combining dsRNA injection and RNAi feeding into the adult hermaphrodite parent. In control treated animals, condensation during prophase occurs normally and chromosomes adopt distinct rod shapes (top left). In contrast, identical disorganized chromosome morphology is observed after depleting each condensin II subunit (top row). Chromosomes depleted of condensin II subunits condense to a fair degree by metaphase (middle row), but depletion of each subunit causes a similar failure in anaphase segregation and DNA bridges are apparent (bottom row). (B) Images from timelapse movies of meiosis II in a GFP:histone H2B strain after two generations of RNAi feeding. In each panel the first polar body (one set of homologs from meiosis I) is visible at the top left, and segregating chromosomes at anaphase II are visible bottom right. In control treated animals the sets of chromosomes are completely separated (left). Depletion of either *capg-2 or kle-2 leads to* incompletely separated meiotic chromosomes, as previously reported for *hcp-6* depletion. (C) Nerve cell nuclei visualized by DAPI staining are uniformly sized and evenly spaced in wild-type. Mutant alleles of each condensin II subunit exhibit a common defect in which two or more of these nuclei appear fused, presumably from failed chromosome segregation in the prior mitosis.

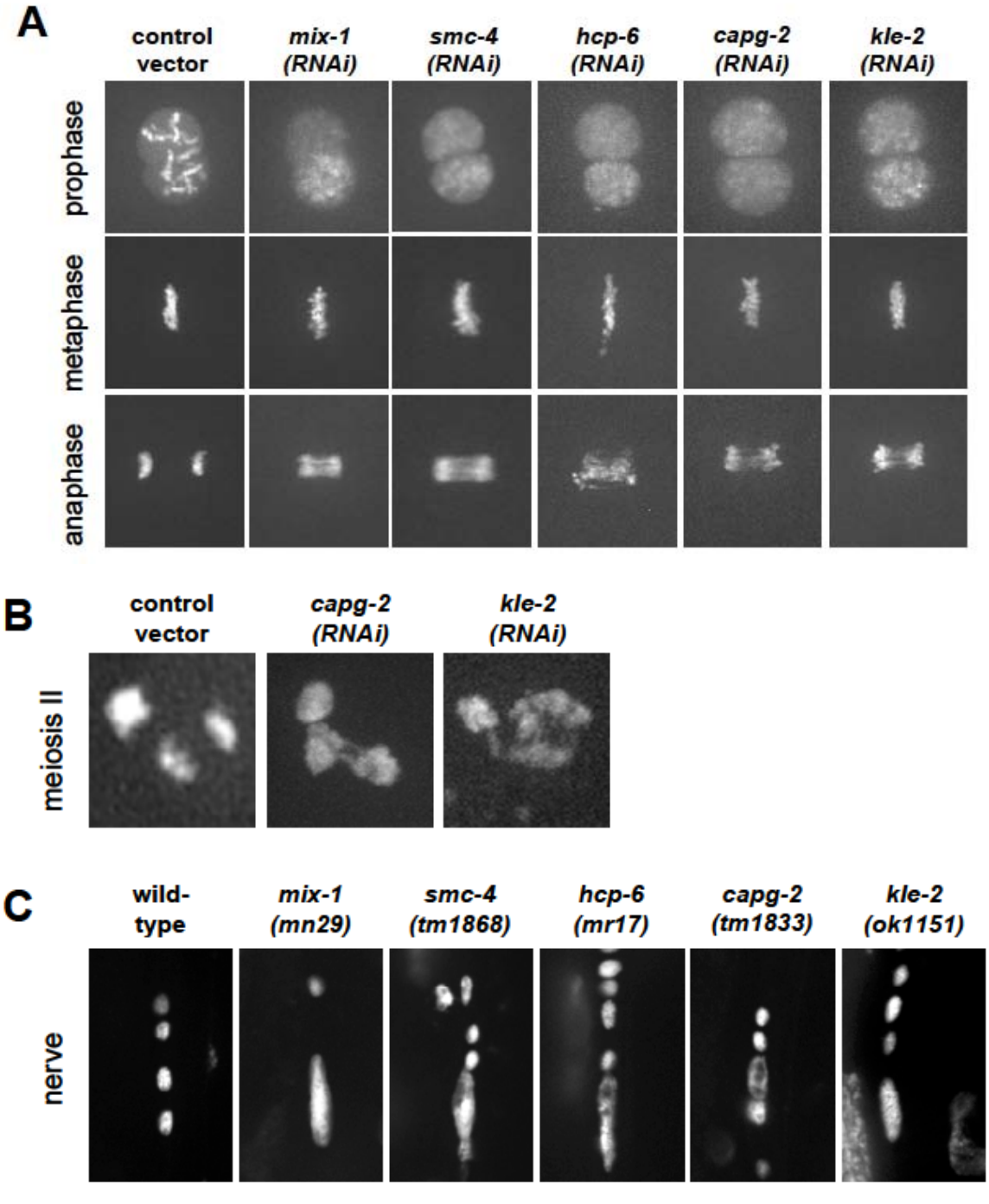
A
control vector
mix-1 (RNAi)
smc-4 (RNAi)
hcp-6 (RNAi)
capg-2 (RNAi)
kle-2 (RNAi)
prophase
metaphase
anaphase
B
control vector
capg-2 (RNAi)
kle-2 (RNAi)
meiosis II
C
wild-type
mix-1 (mn29)
smc-4 (tm1868)
hcp-6 (mr17)
capg-2 (tm1833)
kle-2 (ok1151)
nerve

Figure 2.13 Mutational or RNAi-mediated depletion of class I CAP subunits, but not of *dpy-27, shows chromosome separation defects*. (A) Two generations of RNAi feeding with control empty vector or dsRNA targeting *dpy-27, dpy-28, capg-1, or dpy-26 were performed in a strain carrying* GFP:histone H2B and mitotic chromosomes were visualized in their early stage embryos. The percent of total anaphases in which chromosomes appeared connected by DNA bridges (see Figure 7C) were scored. Depletion of the condensin IDC specific subunit *dpy-27* was not significantly different from control vector while *dpy-28, capg-1, or dpy-26* depletion showed a high percentage of failed anaphases. (B) Wild-type and mutant adult hermaphrodites (magenta) and males (blue) were stained with DNA dye and scored for the percentage of connected gut nuclei. *capg-1(tm1514)* homozygotes were scored from heterozygous mothers, while all other strains were scored as homozygotes from homozygous mothers. This generation of *dpy-27(y56)* hermaphrodites do not live to adulthood so only males were scored, and showed a low percentage of connected gut nuclei as in wild-type. In contrast, a high percent of abnormally connected nuclei were observed in both sexes in strains carrying mutations in each class I CAP subunit. For all cases in both A and B, *dpy-27* depletion was not significantly different from vector or wild-type ($p>0.1$) while *dpy-28, capg-1, or dpy-26* depletion was significantly different ($p<0.0001$) by Fisher's exact test.

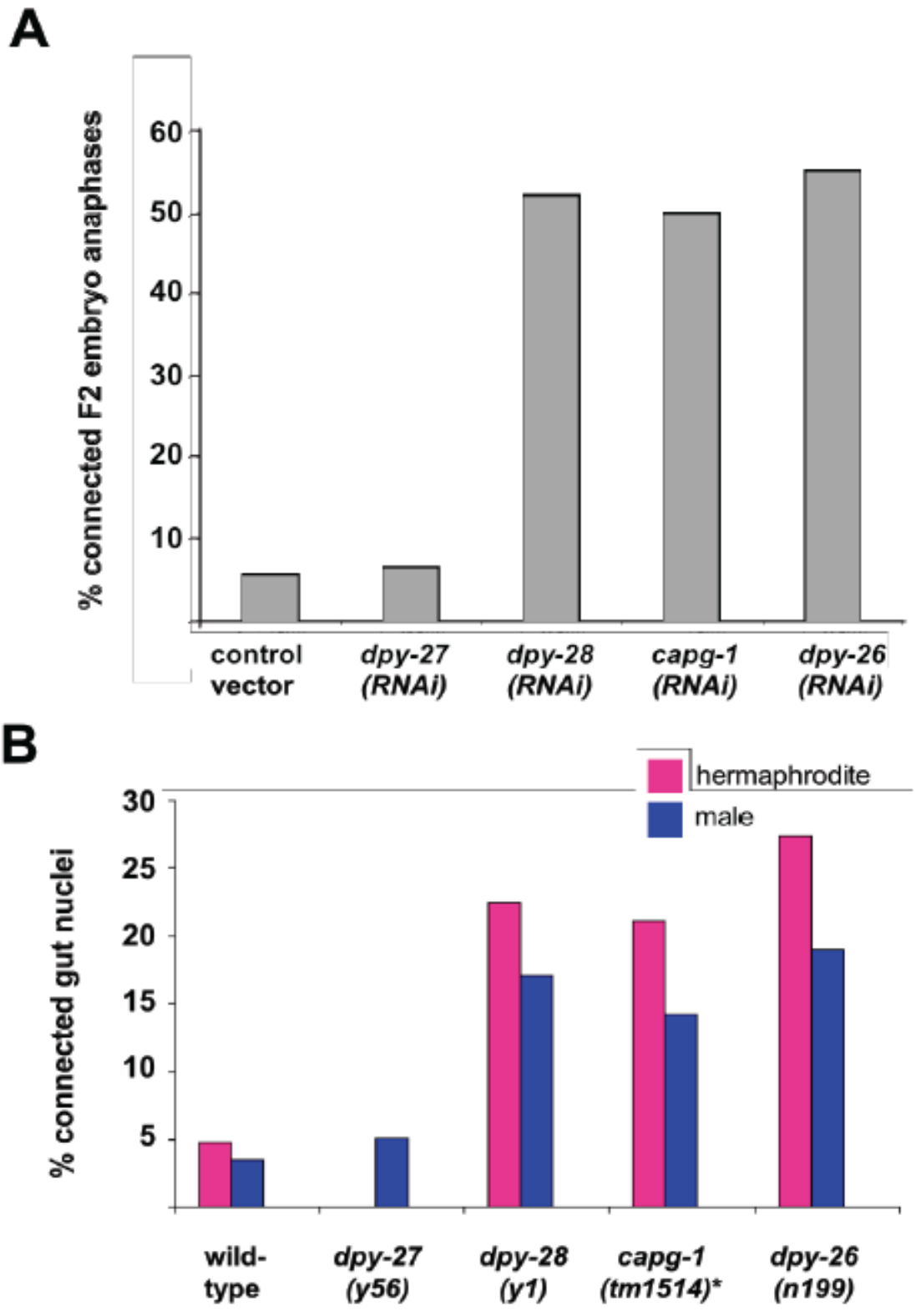
A
% connected F2 embryo anaphases
60
50
40
30
20
10
control vector
dpy-27 (RNAi)
dpy-28 (RNAi)
capg-1 (RNAi)
dpy-26 (RNAi)
B
% connected gut nuclei
hermaphrodite
male
30
25
20
15
10
5
wild-type
dpy-27 (y56)
dpy-28 (y1)
capg-1 (tm1514)*
dpy-26 (n199)

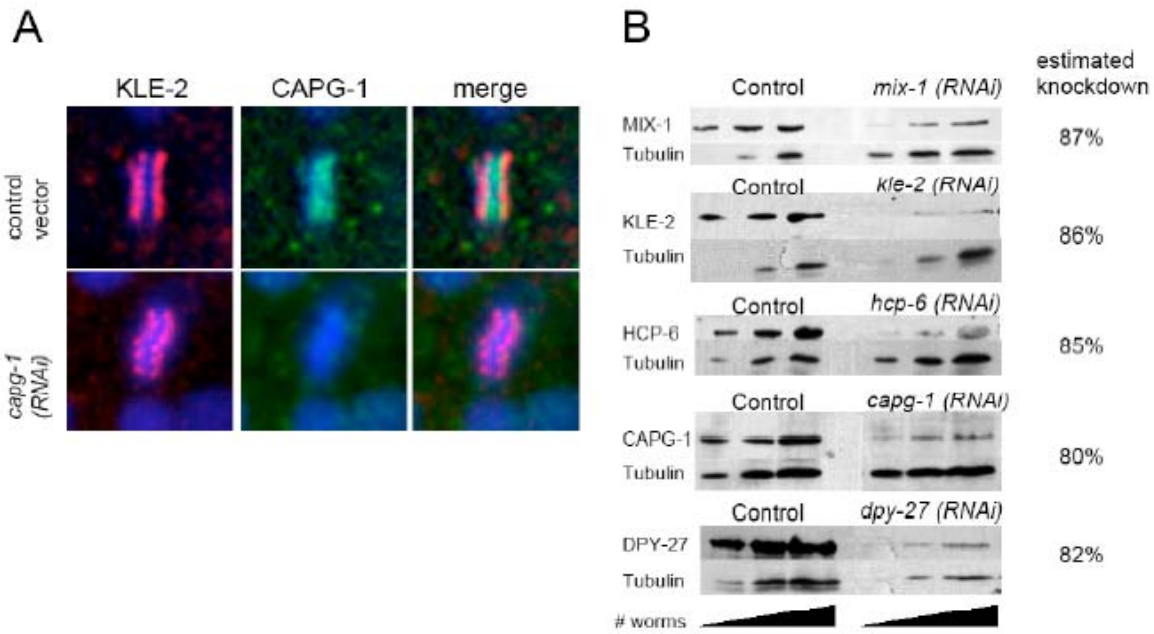

Figure 2.14 Condensin I depletion does not disrupt condensin II localization during mitosis, and RNAi feeding produces substantial but not complete depletion. (A) Metaphase chromosomes from young F2 embryos after two generations of control vector RNAi or *capg-1* RNAi feeding. Embryos were stained with antibodies specific to KLE-2 and CAPG-1. After *capg-1* RNAi, CAPG-1 protein *is* below the level of detection by immunofluorescence, but KLE2 patterns (presumably reflecting condensin II localization) are unaltered. (B) Western blot analysis of the extent of depletion in adults after one-generation (*mix-1, kle-2, hcp-6) or two-generation (capg-1, dpy-27) feeding RNAi (see* methods). Pixel intensity of the targeted subunit was quantified relative to a tubulin control for each of three different concentrations of loaded worms. Intensities were plotted, and a rough estimate of knockdown from the lane that appeared to be in a linear range is shown. Each subunit appears to be knocked down to a similar degree by RNAi feeding, with substantial but not complete depletion. Independent replicates of some subunit RNAi treatments were quantified and give roughly similar levels of knockdown (data not shown).

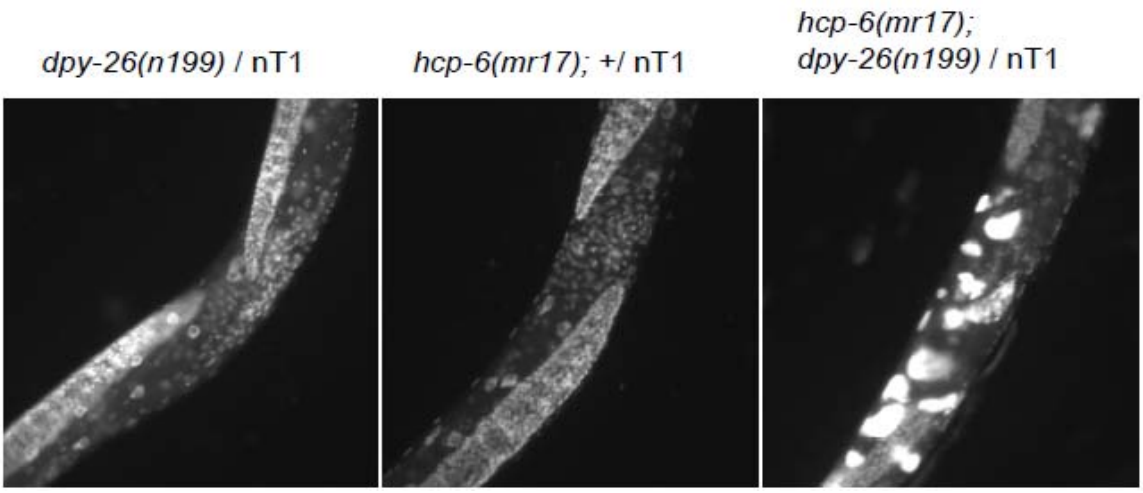

Figure 2.15 Double depletion of a class I and a class II CAP is more severe than either single depletion. Adult hermaphrodites stained with DNA dye, showing the central body region between the two gonad arms. Animals heterozygous for the class I CAP allele *dpy-26(n199) or homozygous for the class II CAP temperature-sensitive allele hcp-6(mr17) show normal nuclear appearance at the permissive temperature of* 15o. In contrast, animals carrying both mutations show severe defects in nuclear morphology at the permissive temperature. For example, double mutants have a greater proportion of connected gut nuclei than either single (data not shown), and in the germline produce what appear to be large, polyploid nuclei. These may represent endomitotic oocytes that underwent repeated rounds of DNA replication without division. Endomitotic oocytes can result from several types of defects, including a failure in meiosis or oocyte maturation. Such endomitotic oocytes are observed, but to a lesser extent, in homozygous *dpy-26(n199)* animals or those depleted of condensin I CAPs by two-generation RNAi feeding (data not shown). nT1 is a translocation chromosome used as a genetic balancer for the *dpy-26 allele and is present in each strain for consistency.*

CHAPTER 3

Different roles for Aurora B in condensin targeting during mitosis and meiosis

This chapter has been accepted to Journal of Cell Science pending revisions. I completed the experiments and imaging shown in Figures 3.10, 3.12 and 3.13. N. Golenberg and J. Bembeneck developed the CAPG-1-GFP transgenic strain and completed the live imaging shown in 3.1C and 3.4B. K. Collette completed all other work.

Abstract

Condensin complexes are essential for mitotic and meiotic chromosome segregation. The two condensin complexes (I and II) in metazoans occupy distinct chromosomal domains and perform non-redundant functions. How the complexes are targeted to distinct regions is not known. We analyzed the timing and regulation of condensin targeting in mitosis and meiosis in the worm *C. elegans*. Despite the differences in mitotic and meiotic chromosome behavior, we uncovered several conserved features. During both mitosis and meiosis, condensin II loads onto chromosomes in early prophase and condensin I at entry into prometaphase. During both mitosis and meiosis, the kinase Aurora B/AIR-2

affects the targeting of condensin I, but not condensin II. However, the role AIR-2 plays in condensin I targeting during these processes is different. In mitosis, AIR-2 activity is required for chromosomal association of condensin I. By contrast during meiosis, AIR-2 is not required for condensin I chromosomal association, but it provides cues for correct spatial targeting of the complex.

Introduction

Condensin is a five-subunit complex that functions in the formation, compaction and segregation of mitotic and meiotic chromosomes [1, 2]. Condensin has been isolated in eukaryotic organisms ranging from yeast to humans. Two Structural Maintenance of Chromosome (SMC) subunits of the SMC2 and SMC4 classes form the enzymatic core of the complex. In addition, condensin contains three regulatory Chromosome Associated Polypeptide (CAP) proteins. While yeast has a single condensin complex, higher eukaryotes possess two, condensins I and II, with condensin I being more homologous to the single yeast condensin [3-5]. Condensins I and II have identical SMC proteins, and distinct, yet similar CAP components: CAP-G, -D2 and -H in condensin I, and CAP-G2, -D3 and -H2 in condensin II.

In mammalian cells, condensins I and II associate with chromosomes at different times, condensin II early in prophase and condensin I after nuclear envelope breakdown (NEBD). The two complexes also occupy distinct domains on mitotic chromosomes and perform non-redundant functions [3-5].

How the two condensin complexes are targeted to distinct chromosomal domains in mitosis is not known. Studies in yeast identified *cis*-acting sites that

play a role in targeting the single yeast condensin to chromosomes [6]. If *cis*-acting elements also play a role in condensin targeting in metazoans, the elements must be different for the two condensin complexes to target them to distinct domains. Alternatively, differential targeting may be achieved by trans-acting factors differentially regulating the two complexes. One candidate for such a regulator is the mitotic kinase and chromosomal passenger complex (CPC) member Aurora B. In some experimental systems, Aurora B depletion had no effect on the chromosomal targeting of condensin(s) [4, 7, 8]. However, in other studies depletion of Aurora B lead to defects in loading of the single yeast condensin in fission yeast [9], and defects of condensin I loading in *Drosophila* [10], *Xenopus* [11], and HeLa cells [12]. Interestingly, condensin II in HeLa cells was unaffected [12], indicating that Aurora B may preferentially affect condensin I targeting in mitosis.

We are using *C. elegans* as a model system to study how reshuffling condensin subunits creates distinct, yet related, complexes with different temporal and spatial association on chromosomes, resulting in distinct functions. *C. elegans* chromosomes are holocentric, and the kinetochores assemble along the entire length of chromosomes, rather than being localized to a single site as on monocentric chromosomes. Despite this difference, chromosomal proteins and their functions are conserved between worms and other eukaryotes [13]. *C. elegans* also has two mitotic/meiotic condensin complexes, and an additional, third condensin, condensin I^{DC}, which functions in the hermaphrodite and X-chromosome-specific process of dosage compensation [14, 15]. The two mitotic

complexes have identical SMC subunits, SMC-4 and MIX-1, and distinct sets of CAP proteins, and condensin I and condensin I^{DC} only differ in their SMC4 subunits (Table 1). While condensins I and II associate with all chromosomes, condensin I^{DC} binds only the X chromosomes in hermaphrodites to downregulate expression two-fold, equalizing X-linked product in XX hermaphrodites and XO males [14].

Some aspects of condensin loading onto mitotic chromosomes are conserved between monocentric mammalian chromosomes and holocentric worm chromosomes. In both systems, condensin II is enriched at the centromeres [4, 16, 17]. *C. elegans* AIR-2/AuroraB was also reported to affect chromosomal association of SMC proteins MIX-1 and SMC-4, components of both condensins I and II[16, 18]. However, in a different study, recruitment of SMC-4 and the condensin II subunit CAPG-2 appeared unaffected by depletion of AIR-2 [19]. These *C. elegans* studies were conducted before the identification of two distinct mitotic complexes. Since SMC proteins are common to condensins I and II, it remains to be determined whether AIR-2/Aurora B is needed for recruitment of one or both condensins.

Compared to mitosis, relatively little is known about condensin distribution and regulation in meiosis. In *C. elegans* meiosis, the two condensin complexes associate with chromosomal domains different from the domain they occupy in mitosis. During meiosis, condensin II localizes to an interior domain within sister chromatids, while condensin I is found between homologs in meiosis I and between sister chromatids in meiosis II [14]. The differences between mitotic and

meiotic localization patterns likely reflect differences in chromosome behavior during these processes. These differences also raise the question whether recruitment mechanisms are comparable between mitosis and meiosis.

The differences between mitotic and meiotic chromosome behavior arise from the unique events during meiosis I, when homologs are separated while sister chromatids stay together. In monocentric organisms the centromere plays a central role in the coordination of these meiotic activities (reviewed in [20]). In meiosis I, cohesion between sister centromeres is preserved, while cohesion along chromosome arms is released to allow separation of homologs. At the same time, cohesion at the centromeres ensures that microtubules attached to sister kinetochores connect to the same pole, while microtubules attached to kinetochores of homologs are attached to opposite poles to establish tension [21].

On the holocentric chromosomes of worms the lack of a localized centromere necessitates coordination of meiotic events in a different manner (reviewed in [22]). During worm meiosis, the site of the crossover, and not a localized region of centromeric CENP-A containing chromatin, ultimately determines the plane of chromosome orientation and the site of cohesion release [23, 24]. Worm chromosomes typically have a single site of crossover, located in an off-center position. During meiosis I prophase, paired homologs (bivalents) are restructured into cross-shaped figures, in which the short arm corresponds to the region between the crossover and the closer chromosome end, and the long arm corresponds to the region between the crossover and the more distant

chromosome end [24, 25]. During metaphase, the short arms of bivalents are lined up along the metaphase plate and the long arms point toward opposite poles. Cohesin along the short arm will be released during meiosis I to separate homologs, and the remaining cohesin will be released in meiosis II to separate sisters (see Fig. 3.3). Since the crossover can happen at either end of the chromosome, the identity of short and long arms is different for the same chromosome in different meioses.

During worm meiosis condensin I is restricted to the short arm of bivalents I [14]. Since the short arm can correspond to either end of the chromosome, condensin I is targeted to different DNA sequences in different meioses. This observation makes it unlikely that *cis*-acting DNA elements provide the primary targeting cue. A more likely targeting signal originates from other chromosomal proteins localizing to the same region. Interestingly, AIR-2/AuroraB, the protein implicated in condensin targeting during mitosis in various systems, also localizes to the short arm of bivalents [18, 26]. How AIR-2/AuroraB activity influence condensin loading in meiosis has not been addressed.

In this study we investigated the timing and regulation of condensin recruitment in mitosis and meiosis in *C. elegans* with particular attention to the role of AIR-2/Aurora B. We found that the need for Aurora B for correct condensin I targeting is conserved between mitosis and meiosis, but the exact role AIR-2 plays differs between the two processes.

Results

Condensin I and II are loaded onto chromosomes at distinct times in mitosis

Since condensin I and II are loaded onto chromosomes at different times in mammalian cells [3-5], we set out to determine the timing of condensin loading during *C. elegans* mitosis using immunofluorescence microscopy (IF). In mammalian cells, NEBD marks the entry into prometaphase. By contrast, in *C. elegans* nuclear pore complexes (NPCs) break down in prometaphase, but the nuclear envelope does not fully disassemble until anaphase [27]. We monitored the breakdown of NPCs using an antibody (mAb414) which recognizes a subset of nucleoporins [28]. Using our fixation conditions, the NPC signal greatly diminishes by prometaphase in embryos of all stages, as judged by chromosome morphology and microtubule staining (Fig. 3.1 and data not shown). To investigate the timing of condensin loading onto chromosomes, we used antibodies against CAPG-1, DPY-26, or DPY-28 to mark condensin I, and antibodies against HCP-6 or KLE-2 to mark condensin II (see Table 1). CAPG-1, DPY-26 and DPY-28 are components of both condensin I and condensin I^{DC}. However, condensin I^{DC} is absent from mitotic chromosomes in early embryos, therefore mitotic chromosomal association patterns can be attributed to condensin I [14].

In early prophase only condensin II associated with chromosomes. Condensin I loaded onto chromosomes after NPC disassembly in prometaphase (Fig. 3.1). These data indicate that the timing of condensin loading onto

chromosomes appears to be conserved between worm and mammalian mitotic cells. From prometaphase to anaphase, the spatial patterns of condensins I and II were is different, with condensin II in a centromere-like pattern[16, 17], and condensin I diffusely coating all chromosomes (Fig. 3.1A). At anaphase, condensin I remains associated with chromosomes, but weak condensin I signal was also seen colocalizing with microtubules at the spindle midzone, using both IF and live imaging of GFP-tagged CAPG-1 (Fig. 3.1B, C, Supp. Movie 1). Similar metaphase patterns were observed for the other condensin I CAP subunits DPY-26 and DPY-28 (Fig. 3.10A). Furthermore, the chromosomal association of CAPG-1 is dependent on the presence of DPY-26 and DPY-28 (Fig 3.10B), indicating that the condensin I CAP subunits associate with mitotic chromosomes as a complex.

AIR-2 is needed for mitotic recruitment of condensin I but not condensin II

The condensin I pattern on mitotic chromosomes resembles the distribution of AIR-2, the Aurora B homolog in *C. elegans* [29]. Indeed, IF experiments demonstrated colocalization during metaphase between CAPG-1 and AIR-2 (Fig. 3.1D) and between CAPG-1 and the chromatin mark deposited by AIR-2 (H3S10Ph) (Fig 3.2A). During anaphase, the weak condensin I “fibers” are also co-incident with AIR-2 (Fig. 3.1D). By contrast, condensin II staining overlaps only minimally with H3S10Ph (Fig. 3.2A). The colocalization between AIR-2 and condensin I, as well as the requirement for Aurora B for condensin I loading in yeast, flies, and mammals [9-12], prompted us to examine whether AIR-2 is needed for condensin recruitment in *C. elegans* mitosis.

To deplete AIR-2 in mitotic cells, hermaphrodite worms homozygous for a temperature sensitive mutation, *air-2(or207)* [30], were shifted to the restrictive temperature and their progeny was analyzed using IF. For control, wild type worms were subjected to the same temperature shift. We used anti-CAPG-1 to mark condensin I, anti-HCP-6 to mark condensin II, anti-H3S10Ph to assess efficiency of AIR-2 depletion, and anti-tubulin as a staining control and to mark mitotic cells. We restricted our analysis to metaphase, at which point both condensin complexes are normally associated with chromosomes. On metaphase figures with no detectable H3S10Ph staining, chromosomal condensin I is lost or greatly reduced (14 out of 18 nuclei) (Fig. 3.2B). We attribute the weak condensin I staining on some metaphase figures to residual AIR-2 activity which likely remains even after shifting to the restrictive temperature. By contrast, 29 out of 29 wild type control metaphases showed condensin I coating the chromosomes. These results suggest that AIR-2 is required for condensin I recruitment in mitosis in worms. We then tested whether AIR-2 is also required for condensin II recruitment. On most (25 out of 37) mitotic figures with no detectable H3S10Ph, condensin II levels appeared to be comparable to wild type controls, while on the remaining figures condensin II levels appeared reduced, but not absent (Fig. 3.2B). 20 out of 20 wild type control metaphases exhibited centromeric condensin II staining. These results indicate that AIR-2 is not needed for condensin II recruitment to chromosomes. We conclude that, similar to what was observed in mammalian cells [12], Aurora

B is required for the recruitment of worm condensin I but not condensin II in mitosis.

Since Aurora B functions during mitosis, it is not expected to influence interphase condensin functions. Consistently, and despite similarities in subunit composition, AIR-2 only affects mitotic targeting of condensin I, but not interphase targeting of condensin I^{DC}. Condensin I^{DC} localization appeared normal on X chromosomes in interphase nuclei of AIR-2-depleted worms (Fig. 3.11). These results indicate that the condensin I CAP subunits are targeted to chromosomes both in an AIR-2 dependent manner (as part of condensin I), and in an AIR-2 independent manner (as part of condensin I^{DC}).

Condensin I and II associate with meiotic chromosomes at distinct times

We next investigated chromosomal targeting of condensin complexes during meiosis in worms. In the *C. elegans* germline, syncitial nuclei are organized in a temporal-spatial array of meiotic stages [31] (Fig. 3.3A). Pre-meiotic nuclei are followed by transition zone (leptotene/ zygotene) where pairing and alignment of homologs begin. In pachytene, homologs are synapsed via the synaptonemal complex (SC). During late pachytene and diplotene, the SC disassembles, and chromosome pairs are condensed and restructured into compact bivalents (Figure 3.3B) [24, 25, 32, 33]. In hermaphrodites, oocytes arrest at diakinesis with homolog pairs organized into six bivalents. The most proximal oocyte, referred to as -1, undergoes maturation followed by fertilization [34]. After fertilization, the oocyte-derived nucleus completes meiosis giving rise

to two polar bodies and the haploid maternal pronucleus. Finally, the oocyte-derived and sperm-derived pronuclei fuse to form a diploid zygotic nucleus.

To characterize the timing of condensin loading onto chromosomes during oocyte meiosis, we compared CAPG-1 (condensin I) and HCP-6 (condensin II) patterns in the hermaphrodite germline and fertilized embryos. While HCP-6 staining was apparent by early diplotene, as reported previously [25], chromosomal association of CAPG-1 was not seen until late diakinesis. During meiosis, NEBD occurs in the -1 oocyte at the time of maturation, immediately preceding fertilization [34]. To monitor NEBD, we used antibodies against the NPC. Indeed, we observed strong CAPG-1 staining only after, but not before, NEBD in the -1 oocytes, while HCP-6 staining is apparent both before and after NEBD (Figure 3.4A). These results indicate that the timing of condensin loading is conserved between mitosis and meiosis in *C. elegans.* After NEBD, once both condensin complexes are associated with meiotic chromosomes, they occupy distinct domains and the patterns do not overlap. Condensin I is found at the interface between homologs marked by reduced DAPI staining ("DAPI-free zone"), while condensin II localizes to sister chromatids throughout meiosis (Fig. 3.4A). During both anaphase I and anaphase II, much of condensin I relocates from chromosomes to microtubules, which are located predominantly between separating chromosomes on the acentrosomal meiotic spindle (Fig. 3.4 B and C, Supp. Movie 2).

Before NEBD in oocytes, CAPG-1 is present in the nucleus, but it does not associate with chromosomes. The intensity of nucleoplasmic staining diminishes

after NEBD, representing diffusion of the protein into the much larger volume of the oocyte (Fig. 3.4A). The same pattern is also seen for the unique condensin I^{DC} subunit DPY-27 and therefore represents the loading of condensin I^{DC} into oocytes in preparation for dosage compensation in fertilized embryos [14, 35]. We used two methods to ensure that the diffuse nuclear staining is not obscuring chromosomal CAPG-1 association. First, we used detergent extraction to reduce nucleoplasmic CAPG-1 staining to background levels. In extracted oocytes, chromosomal association of CAPG-1 was still not observed before NEBD, even though chromosomal staining after NEBD remained comparable to unextracted nuclei (Fig. 3.3A). Second, to reduce condensin I^{DC} levels in oocytes, we examined worms carrying a partial loss-of-function mutation in *dpy-27(y57).* In these worms, nucleoplasmic staining of CAPG-1 in oocytes is greatly reduced, corresponding to a reduction in condensin I^{DC}, but chromosomal association is still only detected after NEBD (Fig. 3.3B). Based on these results, we conclude that maximal enrichment of CAPG-1 on chromosomes occurs after NEBD in the -1 diakinesis oocyte.

Condensin I localizes to the short arms of bivalents, where cohesion between the exchanged parts of sister chromatids holds homologs together. Viewed from the side, it appears as a straight line intersecting the bivalent along its shorter axis. However, viewed from the end, CAPG-1 appears as a ring around the center of the bivalent (Fig. 3.4D), a pattern that has also been seen for AIR-2 and the chromokinesin KLP-19 [36, 37]. This ring-like appearance was observed both in mature oocytes and in fertilized embryos in metaphase of

meiosis I as well as at the sister chromatid interface in meiosis II (Fig. 3.4D). This ring-shaped domain transforms into a linker structures between chromosomes in anaphase to drive chromosome separation [36], and condensin I continues to colocalize with these structures (Fig. 3.4C).

To investigate whether all condensin I CAP subunits associate with chromosomes in a similar pattern, we performed IF using anti-DPY-26 and anti-DPY-28 antibodies. We observed DPY-26 and DPY-28 at the DAPI-free zone at the short arms of diakinesis bivalents and also at the chromosome interface in fertilized embryos (Fig. 3.13A and B). CAPG-1 localization depends on the presence of DPY-26 and DPY-28, since in *dpy-26(n199)* and in *dpy-28(s939)* oocytes (Fig. 3.13C and D), or upon RNAi depletion of DPY-26 or DPY-28 (data not shown) the short arm staining of CAPG-1 is undetectable. Therefore, the condensin I CAP subunits appear to localize to the short arm as a complex.

Unique features of the male germline

For comparison, we also observed condensin localization in the male germline (Fig. 3.5A). Since condensin I^{DC} is absent in males, all CAP subunit staining can be attributed to condensin I. In the male germline, following pachytene, chromosomes rapidly condense, proceed through diplotene, karyosome, and diakinesis and undergo meiotic divisions to form sperm [38]. Both condensins I and II begin to accumulate in nuclei by late pachytene/diplotene, a stage before NEBD. At the karyosome stage, a stage unique to the male germline in worms [38], condensin I forms a halo and is excluded from regions occupied by DNA. By contrast, condensin II is clearly

associating with chromosomes. We investigated the timing of chromosomal association of condensin I in the male germline with respect to NEBD using the NPC-specific antibody (Fig. 3.5B). Prior to NEBD, during diplotene and karyosome and early diakinesis, condensin I is present in the nucleus, but it is excluded from DNA. Chromosomal enrichment is not seen until after NEBD. We conclude that the timing of chromosomal association is conserved between the male and hermaphrodite germlines.

From diakinesis on, condensin I and condensin II localization in oocyte and sperm meioses appears similar (Fig. 3.5A). Condensin I is between aligned homologs (late diakinesis and metaphase I), and between sisters (metaphase II), while condensin II remains associated with sister chromatids throughout. Interestingly, condensin I behavior in sperm and oocytes differs at anaphase. In oocytes, condensin I colocalizes with microtubules between separating chromosomes during anaphase (Fig. 3.4C). In sperm, microtubules are not detected between separating chromosomes, and, condensin I is absent from this region (Fig 3.5B).

AIR-2 restricts condensin I to the short arm of the bivalent

The chromosomal association patterns of condensin complexes are dissimilar in mitosis and meiosis. However, in both cases, condensin I localization closely parallels that of AIR-2, while condensin II occupies a distinct domain (Figs. 3.1 and 3.4). This observation, coupled with the finding that condensin I requires AIR-2 for mitotic chromosomal association, prompted us to investigate the potential role for AIR-2 in condensin recruitment in meiosis.

To deplete AIR-2 levels during meiosis, we used RNAi in the *air-2* temperature sensitive mutants shifted to the restrictive temperature, and we limited our analysis to oocytes in which H3S10Ph levels were reduced to below the level of detection by IF. For control, wild type worms were shifted to the same temperature. In control oocytes after NEBD, we observed condensin I at the short arm of the bivalent, while condensin II associated with the four sister chromatids (Fig. 3.6B). In AIR-2 depleted oocytes, condensin II staining on the four sister chromatids was discernable, despite the somewhat disorganized structure of the bivalent (compare DAPI images of control and AIR-2 depleted bivalents). Similar results were obtained with condensin II subunits HCP-6 (Fig. 3.6B) and KLE-2 (data not shown). By contrast, condensin I appeared mislocalized. CAPG-1 occupied a cross shape as though localizing to both arms of the bivalents (Fig. 3.6B). Note however that bivalents in AIR-2-depleted oocytes do not have a distinct DAPI-free zone at the short arm. Rather faint DAPI-light lines appear along the condensin I occupied domain (Fig. 3.6B). Taken together, similar to mitosis, AIR-2 influences the chromosomal localization of condensin I, but not condensin II, during meiosis. However, unlike in mitosis, AIR-2 is not needed to load condensin I onto chromosomes in meiosis, indicating that AIR-2, or H3S10Ph, is unlikely to serve as a direct recruiter of condensin I.

AIR-2 provides spatial cues for Condensin I targeting in meiosis

In worms, crossovers divide bivalents into highly asymmetric structures, with AIR-2 at short arms. The AIR-2 occupied domain dictates not only the plane of cohesin release [18, 26], but also the plane of chromosome orientation. At

metaphase I, the short arms are lined up at the metaphase plate, while the long arms are parallel to spindle microtubules [37, 39]. To further investigate how condensin I is targeted to the short arm, we analyzed mutant backgrounds in which the activity of AIR-2 is not restricted to this specialized domain or in which this domain does not exist due to lack of chiasma formation.

HTP-1 is a HORMA domain protein that assumes a reciprocal localization pattern with respect to AIR-2 and is restricted to the long arm of bivalents (Fig. 3.3B) [33]. In *htp-1(gk174)* oocytes, autosomes do not pair with their homologs due to a defect in early meiosis, and exist as ten univalents. However, in some oocytes, the two X chromosomes form a bivalent. These rare bivalents lose their asymmetric features, many appear less elongated than wild type, and AIR-2 localizes a cross shape on both bivalent arms [33]. We observed AIR-2 spreading on some, but not all *htp-1(gk174)* bivalents. On bivalents with a cross-shaped AIR-2 domain, CAPG-1 also spread onto both arms of the bivalent, while bivalents that do not show spread of AIR-2 also did not show spread of CAPG-1 (Fig. 3.7A). Interestingly, the H3S10Ph domain spread out all over the bivalent, over a much larger domain than that occupied by AIR-2, perhaps reflecting transient AIR-2 association at these regions (Fig. 3.7B). However, condensin I spreading is only observed in the more restricted domain occupied by AIR-2. These data indicate that stable AIR-2 association with chromosomes may be sufficient to guide condensin I localization, but H3S10Ph is not.

LAB-1 is a worm-specific chromosomal protein containing a PP1 phosphatase interaction domain. During meiotic prophase I, LAB-1 exhibits

localization patterns similar to HTP-1 (Fig. 3.3B), and it antagonizes AIR-2 activity along the long arms of bivalents [32]. Complete loss of LAB-1 disrupts chromosome pairing and chiasma formation, and oocytes lacking LAB-1 contain twelve univalents, rather than six bivalents. To assess the effects of LAB-1 loss on condensin I loading to bivalents, we used RNAi to partially deplete LAB-1 such that most oocytes still contained six bivalents. Similar to the HTP-1 depleted oocytes, in some LAB-1 depleted oocytes AIR-2 localizes to both arms of bivalents [32] and appears to be in a cross-shape. When AIR-2 is seen on both arms, we observe expansion of CAPG-1 onto both arms, and when AIR-2 is limited to the short arm, CAPG-1 remains at this domain as well (Fig. 3.7A). Again, expansion of the H3S10Ph domain is more pronounced than that of the AIR-2 domain (Fig. 3.7B). However, while expansion of the AIR-2 domain is sufficient to cause spreading of condensin I, expansion of H3S10Ph domain is not.

We next analyzed mutant backgrounds in which homologs are not held together in meiosis I, and instead of six bivalents they form twelve univalents. Therefore, there is no homolog interface to which both AIR-2 and condensin I would be normally targeted. In the *spo-11(ok79)* background, chiasmata do not form due to a defect in double strand break formation [40]. Since crossover are required for the orderly asymmetric organization of bivalents, in *spo-11* mutants AIR-2 and HTP-1 are localized in a stochastic, rather than orderly manner. By diplotene/diakinesis they acquire mutually exclusive localization patterns, with some *spo-11* univalents staining only with HTP-1, and others only with AIR-2 [24,

33]. We observed AIR-2 localization on about half of the *spo-11(ok79)* univalents and CAPG-1 and AIR-2 always colocalized (Fig 3.8A). These results indicate that crossover formation is not necessary for condensin I targeting to chromosomes, and that AIR-2 is sufficient to dictate the spatial distribution of condensin I, even when AIR-2 localization is stochastic. Note that in some univalents, AIR-2 and condensin I colocalize along a faint DAPI-free zone intersecting the univalent. Most univalents had H3S10Ph staining of varying intensity, but condensin I only localized to those with most intense staining, presumably reflecting stable AIR-2 association (Fig. 3.8B).

In *rec-8(ok978)* mutants, sister chromatids are held together by REC-8 paralogs COH-3 and COH-4 until anaphase I, forming 12 univalents. *rec-8* univalents biorient at metaphase I, and sisters will prematurely separate toward opposite spindle poles at anaphase I [41]. Unlike on *spo-11* univalents, AIR-2 consistently localizes to a prominent DAPI-free zone between sisters on all twelve *rec-8* univalents, and H3S10Ph intensity is uniform among univalents. In these oocytes, condensin I and AIR-2 co-localized between sister chromatids, similar to what we observe in wild type meiosis II (Fig. 3.8A). Taken together, our data suggest that although AIR-2 is not required for recruitment of condensin I, it provides spatial cues that determine the localization of condensin I on meiotic chromosomes. AIR-2, an important determinant of bivalent asymmetry and chromosome orientation, is also responsible for guiding condensin I to the chromosomal domain which will be aligned at the metaphase plate, whether on

wild type meiosis I bivalents, wild type meiosis II sister chromatids, or *rec-8* mutant meiosis I univalents.

Discussion

Timing of condensin loading to chromosomes in mitosis and meiosis

Meiosis includes a prolonged prophase I during which homologous chromosomes pair, synapse and exchange genetic material. By contrast, prophase in mitosis is relatively brief. Despite these differences, condensin complexes load at analogous time points: condensin II as chromosomes begin to condense in early prophase and condensin I in prometaphase. This time point in worm oocytes coincides with maturation and fertilization. The timing of condensin I and II recruitment in mitosis is conserved between worms and mammals [4], raising the possibility that it is also conserved in meiosis in all metazoans. Consistent with that, condensin I loads onto chromosomes by prometaphase in mouse spermatocytes [42]. Condensin II or NEBD were not analyzed in this study.

What triggers condensin I loading at NEBD/prometaphase is unclear. All components of condensin I are present in the nucleoplasm prior to NEBD, yet they do not associate with chromosomes. This is particularly apparent in the male germline, where condensin CAP subunit staining cannot be attributed to the presence of condensin I^{DC}. Aurora B activity and H3S10Ph staining is also apparent on both mitotic and meiotic chromosomes prior to prometaphase, excluding the possibility that H3S10 phosphorylation triggers condensin I

assembly. Future studies will be needed to determine how the timing of condensin I loading is coordinated with other cell cycle events.

Mitotic recruitment of condensin complexes

Similar to what was observed in mammalian cells [12], AIR-2 depletion in worms disrupts efficient recruitment of condensin I to mitotic chromosomes, but condensin II recruitment is unaffected. It remains unclear whether this reflects a direct recruitment by the kinase or its chromatin mark H3S10Ph, or alternatively, it reflects a need for an AIR-2 mediated change in chromatin structure. Our results also resolve previous conflicting data in the field. Previous studies concluded that AIR-2 is required for loading of SMC proteins MIX-1 and SMC-4 (shared between condensins I and II) onto mitotic chromosomes [16, 18]. However, a different study failed to detect a noticeable change in SMC-4 and CAPG-2 (condensin II CAP subunit) recruitment [19]. We suggest that the observed reduced recruitment of SMC-4 and MIX-1 upon AIR-2 depletion reflects a loss of condensin I from chromosomes. Since condensin II recruitment is unaffected, its subunits remain on chromosomes. Our results also explain the findings that MIX-1 function before prometaphase is AIR-2 independent, yet its chromosomal association in metaphase is (at least partially) AIR-2 dependent [18]. Prior to prometaphase, MIX-1 (as part of condensin II) associates with chromosomes in an AIR-2-independent manner and facilitates chromosome condensation. By contrast, after prometaphase, MIX-1 (as part of condensin I) associates with chromosomes in an AIR-2-dependent manner.

Meiotic recruitment of condensin complexes

Despite the differences in mitotic and meiotic chromosome architecture, condensin I occupies the same domains as AIR-2 in both processes (this study), and condensin II colocalizes with centromeric protein CENP-A in both processes [16, 17, 25]. Consistently, AIR-2 is required for condensin I recruitment in mitosis and for correct condensin I localization in meiosis, but not for condensin II targeting in either process. By contrast, CENP-A is needed for recruitment of condensin II in mitosis, but not during meiosis [17, 25]. The fact that condensin II can load onto meiotic chromosomes in the absence of CENP-A, is consistent with CENP-A function being dispensable during *C. elegans* meiosis [23].

While our data is consistent with AIR-2 serving as a direct recruiter for condensin I in mitosis, it plays a different role in meiosis. During meiosis, condensin I can associate with chromosome in the absence of AIR-2, but without targeting cues from AIR-2, it localizes to both bivalent arms. Interestingly, we observed similar spreading of condensin I in oocytes in which the AIR-2 domain is expanded, indicating that when present, AIR-2 is sufficient to dictate condensin I localization. Consistent with that, condensin I also colocalizes with AIR-2 on *spo-11* univalents (where AIR-2 distribution is stochastic), and at the sister chromatid interface on bioriented *rec-8* univalents.

The more limited localization of AIR-2 compared to the broader distribution of H3S10Ph in the *lab-1(RNAi)* and the *htp-1(gk174)* backgrounds is reminiscent of what was observed for some histone modifying enzymes and their modification in the context of gene silencing [43-45] or activation [46, 47]. It is unclear whether

it represents a transient spreading of AIR-2 to phosphorylate H3S10 in a broader region, or transient looping of other chromosomal territories into the AIR-2 occupied domain for modification. In any case, H3S10Ph was not sufficient to mislocalize condensin I. Only where AIR-2 was detectable by IF, could we see a spreading of the condensin I occupied domain.

Is the role of Aurora B in condensin I targeting during meiosis conserved?

Aurora B regulates many events to coordinate cell division, including kinetochore microtubule attachements, chromosome orientation, cohesion release and cytokinesis. Most of these functions are conserved between monocentric and holocentric organisms, with some important differences in meiosis (Fig 3.9). On monocentric chromosomes Aurora B is needed for coorientation of sister kinetochores and biorientation of kinetochores of homologs by destabilizing improper kinetochore-microtubule attachments at the centromeres [48, 49]. In holocentric organisms like *C. elegans*, localized centromeres are lacking, and instead the location of crossover determines which end of the chromosome will form the short arm of the bivalent [24], which in turn determines the plane of chromosome orientation [37, 39]. In both monocentric and in holocentric organisms, Aurora B is located in an ideal position to monitor homolog biorientation and sister co-orientation: at the centromeres in monocentric organisms and at the bivalent short arm in holocentric organisms.

However, the role of Aurora B in the regulation of sister chromatid cohesin during meiosis I is different in monocentric and holocentric organisms. During meiosis I, sister chromatid cohesion is preserved at centromeres of monocentric

chromosomes and at the long arm of holocentric chromosomes, while cohesion is released along chromatid arms of monocentric chromosomes and the short arm of holocentric bivalents. In monocentric organisms Aurora B promotes preservation of cohesion at centromeres [49-51]. By contrast, in worms, AIR-2/AuroraB functions to promote cohesion release at the short arm [18, 26].

In monocentric organisms the activities that orient chromosomes and those that maintain connections between sisters during meiosis are located at the same place, at the centromere. By contrast, in holocentric organisms these activities are located at opposite domains: chromosome orientation is achieved by activities along the short arms of bivalents, while preservation of connection between sisters is achieved along the long arm [26, 32, 33]. These spatial differences likely explain why Aurora B evolved different roles with respect to regulation of cohesion in these organisms. Given the similarities and differences in Aurora B functions in monocentric and holocentric organisms, it will be interesting to determine which aspects of condensin I regulation by Aurora B are conserved in meiosis in monocentric organisms.

Materials and Methods

C. elegans strains: All strains were maintained as described [52] and grown at 20°C, unless indicated otherwise. Strains include N2 Bristol strain (wild type), EKM28 (CAPG-1::GFP genotype), EU630 *air-2(or207ts)*I, WH371 *unc119(ed3); ojIs50* [*Ppie-1:: GFP:: air-2 unc-119* (+)], VC666 *rec-8*(*ok 978*) IV/ nT1[*qIs51*](IV; V), TY0420 *dpy-27*(y57)III, TY3837 *dpy-28(s939)*III/ qC1, and TY4341 *dpy-26*(n199) unc-30(e191)/ nT1(G)IV;V, EKM21 *spo-11(ok79) IV/*nT1(G) IV;V,

EKM22 *htp-1(gk174)IV/*nT1(G) IV;V, AV307 *syp-1(me17)*V/nT1[*unc-?(n754) let-? qIs50*] IV;V.

For analysis of AIR-2 deficiency, *air-2 (or207ts*) L4 worms were shifted to 25 ^{0}C for 24 h.

Antibodies

Primary antibodies: rabbit α-CAPG-1[14]; rabbit α-KLE-2, α-DPY-26 and αDPY-28 (Kirsten Hagstrom [U Mass Worchester] [14]), rabbit α-HCP-6 (Raymond Chan [U Michigan] [25]), rabbit α-AIR-2 (Jill Schumacher [U Texas, MD Anderson Cancer Center] [29]), mouse α-H3S10Ph (6G3) (Cell Signaling Technology), mouse α-NPC [mab414] (Abcam), mouse α - alpha- tubulin (DM1A) (Sigma), chicken anti-GFP (Fisher). Secondary antibodies: FITC or cy3 conjugated donkey anti-rabbit, goat anti-chicken, and donkey anti-mouse (Jackson Immunoresearch).

RNA interference

RNAi by feeding was performed as described [53]. To generate an RNAi construct for *air-2*, a genomic region was PCR amplified (using primers catgctcgagtggacatttccatgtagcga and gatcaagcttggggttagacgattgggaa), digested with Xho I and Hind III cloned into the DT7 vector [53]. For *lab-1* RNAi, bacterial cultures were grown at 37^{0}C for 20 hours and induced with IPTG for two hours prior to plating; for *air-2* RNAi, 50 mL bacterial cultures were grown at 37^{0}C for 20 hours, induced with IPTG for two hours, pelleted and resuspended in 500μL of fresh LB broth and plated as a concentrated bacterial lawn. RNAi was initiated at the L1 stage. L4 worms were transferred to plates, and allowed to produce

progeny (F1) for 24 hours. F1 worms were processed 24 hours post L4 for IF. To deplete AIR-2 in meiosis, *air-2(or207ts)* hermaphrodites were grown on AIR-2 RNAi plates at 25^0C from L1 to adulthood. Control experiments were performed using the same conditions as RNAi experiments.

Immunostaining

Adult worms were dissected in 1X sperm salts (50 mM PIPES pH7, 25 mM KCl, 1 mM $MgSO_4$, 45 mM NaCl, 2 mM $CaCl_2$), fixed in 2% paraformaldehyde in 1X sperm salts for five minutes and frozen on dry ice for ten minutes. Slides were washed three times for ten minutes each in PBS/0.1% Triton (PBST) before incubation with 30μL of diluted primary antibody in a humid chamber, overnight at room temperature (RT). Double labeling of samples was performed with all primary antibodies simultaneously during this overnight incubation. Slides were then washed three times, ten minutes each, with PBST, incubated for one hour with 30μL diluted secondary antibody at 37^0C, washed again twice for ten minutes each with PBST, and once for ten minutes with PBST plus DAPI. Slides were mounted with Vectashield (Vector Labs). For colocalization studies of Condensin I and AIR-2, rabbit CAPG-1 and rabbit AIR-2 antibodies were directly labeled using the Zenon Rabbit IgG labeling kit (Molecular Probes) according to manufacturers instructions.

Detergent extraction: Nucleoplasmic proteins were extracted from oocytes by dissecting adults in 1X sperm salts plus 1 % Triton, and processed as above.

Methanol-acetone fixation (Fig 3.13A): Adult hermaphrodites were dissected in 1X sperm salts, and frozen on dry ice for ten minutes. The slides were fixed for

one minute each in methanol followed by acetone at -20^{0}C. Slides were washed three times for ten minutes each in PBST, before incubation with primary antibody.

Embryos were obtained from hermaphrodites by bleaching, fixed with Finney fixative (2% paraformaldehyde, 18% methanol, 10mM PIPES pH 7.5, 60 mM KCl, 8 mM NaCl, 2.6 mM EGTA, 0.4 mM spermidine, 0.16 mM spermine, 0.4% β-mercaptoethanol), frozen at -80^{0}C for 20 minutes, thawed, fixed for 20 minutes at RT, and washed in PBST for 15 minutes. Samples were incubated with primary antibody overnight at RT. Embryos were washed three times (15 minutes each) in PBST, and incubated overnight with secondary antibody at RT. This incubation was followed by two PBST washes and a third wash in PBST plus DAPI. Embryos were mounted on slides with Vectashield.

Images were captured using a Hamamatsu ORCA-ERGA CCD camera on an Olympus BX61 motorized X-drive microscope using a 60X PlanApo oil immersion objective with a NA of 1.42. Images were captured in Z stacks with planes at 0.2μm intervals and deconvolved and projected with 3i Slidebook software. Adobe Photoshop was used for image assembly.

Acknowledgements

We thank Raymond Chan, Kentaro Nabeshima, Kirsten Hagstrom, Martha Snyder, Laura Custer, Michael Wells, and Joshua Bembenek for comments on the manuscript, and Uchita Patel and Emily Laughlin for technical help. The work was supported by NIH grant RO1 GM079533 to G.C. and Predoctoral Training in Genetics, NIH T32 GM07544 to E. P. and K.C. Some nematode strains were

provided by the Caenorhabditis Genetics Center, which is funded by the NIH National Center for Research Resources (NCRR).

References

1. Hirano, T., *Condensins: organizing and segregating the genome.* Curr Biol, 2005. **15**(7): p. R265-75.
2. Hudson, D.F., K.M. Marshall, and W.C. Earnshaw, *Condensin: Architect of mitotic chromosomes.* Chromosome Res, 2009. **17**(2): p. 131-44.
3. Hirota, T., et al., *Distinct functions of condensin I and II in mitotic chromosome assembly.* J Cell Sci, 2004. **117**(Pt 26): p. 6435-45.
4. Ono, T., et al., *Spatial and temporal regulation of Condensins I and II in mitotic chromosome assembly in human cells.* Mol Biol Cell, 2004. **15**(7): p. 3296-308.
5. Ono, T., et al., *Differential contributions of condensin I and condensin II to mitotic chromosome architecture in vertebrate cells.* Cell, 2003. **115**(1): p. 109-21.
6. D'Ambrosio, C., et al., *Identification of cis-acting sites for condensin loading onto budding yeast chromosomes.* Genes Dev, 2008. **22**(16): p. 2215-27.
7. Losada, A., M. Hirano, and T. Hirano, *Cohesin release is required for sister chromatid resolution, but not for condensin-mediated compaction, at the onset of mitosis.* Genes Dev, 2002. **16**(23): p. 3004-16.
8. MacCallum, D.E., et al., *ISWI remodeling complexes in Xenopus egg extracts: identification as major chromosomal components that are regulated by INCENP-aurora B.* Mol Biol Cell, 2002. **13**(1): p. 25-39.
9. Petersen, J. and I.M. Hagan, *S. pombe aurora kinase/survivin is required for chromosome condensation and the spindle checkpoint attachment response.* Curr Biol, 2003. **13**(7): p. 590-7.
10. Giet, R. and D.M. Glover, *Drosophila aurora B kinase is required for histone H3 phosphorylation and condensin recruitment during chromosome condensation and to organize the central spindle during cytokinesis.* J Cell Biol, 2001. **152**(4): p. 669-82.
11. Takemoto, A., et al., *Analysis of the role of Aurora B on the chromosomal targeting of condensin I.* Nucleic Acids Res, 2007. **35**(7): p. 2403-12.
12. Lipp, J.J., et al., *Aurora B controls the association of condensin I but not condensin II with mitotic chromosomes.* J Cell Sci, 2007. **120**(Pt 7): p. 1245-55.
13. Maddox, P.S., et al., *"Holo"er than thou: chromosome segregation and kinetochore function in C. elegans.* Chromosome Res, 2004. **12**(6): p. 641-53.
14. Csankovszki, G., et al., *Three distinct condensin complexes control C. elegans chromosome dynamics.* Curr Biol, 2009. **19**(1): p. 9-19.

15. Mets, D.G. and B.J. Meyer, *Condensins regulate meiotic DNA break distribution, thus crossover frequency, by controlling chromosome structure.* Cell, 2009. **139**(1): p. 73-86.
16. Hagstrom, K.A., et al., *C. elegans condensin promotes mitotic chromosome architecture, centromere organization, and sister chromatid segregation during mitosis and meiosis.* Genes Dev, 2002. **16**(6): p. 729-42.
17. Stear, J.H. and M.B. Roth, *Characterization of HCP-6, a C. elegans protein required to prevent chromosome twisting and merotelic attachment.* Genes Dev, 2002. **16**(12): p. 1498-508.
18. Kaitna, S., et al., *The aurora B kinase AIR-2 regulates kinetochores during mitosis and is required for separation of homologous Chromosomes during meiosis.* Curr Biol, 2002. **12**(10): p. 798-812.
19. Maddox, P.S., et al., *Molecular analysis of mitotic chromosome condensation using a quantitative time-resolved fluorescence microscopy assay.* Proc Natl Acad Sci U S A, 2006. **103**(41): p. 15097-102.
20. Sakuno, T. and Y. Watanabe, *Studies of meiosis disclose distinct roles of cohesion in the core centromere and pericentromeric regions.* Chromosome Res, 2009. **17**(2): p. 239-49.
21. Sakuno, T., K. Tada, and Y. Watanabe, *Kinetochore geometry defined by cohesion within the centromere.* Nature, 2009. **458**(7240): p. 852-8.
22. Schvarzstein, M., S.M. Wignall, and A.M. Villeneuve, *Coordinating cohesion, co-orientation, and congression during meiosis: lessons from holocentric chromosomes.* Genes Dev, 2010. **24**(3): p. 219-28.
23. Monen, J., et al., *Differential role of CENP-A in the segregation of holocentric C. elegans chromosomes during meiosis and mitosis.* Nat Cell Biol, 2005. **7**(12): p. 1248-55.
24. Nabeshima, K., A.M. Villeneuve, and M.P. Colaiacovo, *Crossing over is coupled to late meiotic prophase bivalent differentiation through asymmetric disassembly of the SC.* J Cell Biol, 2005. **168**(5): p. 683-9.
25. Chan, R.C., A.F. Severson, and B.J. Meyer, *Condensin restructures chromosomes in preparation for meiotic divisions.* J Cell Biol, 2004. **167**(4): p. 613-25.
26. Rogers, E., et al., *The aurora kinase AIR-2 functions in the release of chromosome cohesion in Caenorhabditis elegans meiosis.* J Cell Biol, 2002. **157**(2): p. 219-29.
27. Lee, K.K., et al., *C. elegans nuclear envelope proteins emerin, MAN1, lamin, and nucleoporins reveal unique timing of nuclear envelope breakdown during mitosis.* Mol Biol Cell, 2000. **11**(9): p. 3089-99.
28. Davis, L.I. and G. Blobel, *Identification and characterization of a nuclear pore complex protein.* Cell, 1986. **45**(5): p. 699-709.
29. Schumacher, J.M., A. Golden, and P.J. Donovan, *AIR-2: An Aurora/Ipl1-related protein kinase associated with chromosomes and midbody microtubules is required for polar body extrusion and cytokinesis in Caenorhabditis elegans embryos.* J Cell Biol, 1998. **143**(6): p. 1635-46.

30. Severson, A.F., et al., *The aurora-related kinase AIR-2 recruits ZEN-4/CeMKLP1 to the mitotic spindle at metaphase and is required for cytokinesis.* Curr Biol, 2000. **10**(19): p. 1162-71.
31. Schedl, T., *Developmental genetics of the germ line*, in *C. elegans II*, D.L. Riddle, et al., Editors. 1997, Cold Spring Harbor Laboratory Press: Cold Spring Harbor, NY. p. 241-270.
32. de Carvalho, C.E., et al., *LAB-1 antagonizes the Aurora B kinase in C. elegans.* Genes Dev, 2008. **22**(20): p. 2869-85.
33. Martinez-Perez, E., et al., *Crossovers trigger a remodeling of meiotic chromosome axis composition that is linked to two-step loss of sister chromatid cohesion.* Genes Dev, 2008. **22**(20): p. 2886-901.
34. McCarter, J., et al., *On the control of oocyte meiotic maturation and ovulation in Caenorhabditis elegans.* Dev Biol, 1999. **205**(1): p. 111-28.
35. Chuang, P.T., D.G. Albertson, and B.J. Meyer, *DPY-27:a chromosome condensation protein homolog that regulates C. elegans dosage compensation through association with the X chromosome.* Cell, 1994. **79**(3): p. 459-74.
36. Dumont, J., K. Oegema, and A. Desai, *A kinetochore-independent mechanism drives anaphase chromosome separation during acentrosomal meiosis.* Nat Cell Biol, 2010. **12**(9): p. 894-901.
37. Wignall, S.M. and A.M. Villeneuve, *Lateral microtubule bundles promote chromosome alignment during acentrosomal oocyte meiosis.* Nat Cell Biol, 2009. **11**(7): p. 839-44.
38. Shakes, D.C., et al., *Spermatogenesis-specific features of the meiotic program in Caenorhabditis elegans.* PLoS Genet, 2009. **5**(8): p. e1000611.
39. Albertson, D.G. and J.N. Thomson, *Segregation of holocentric chromosomes at meiosis in the nematode, Caenorhabditis elegans.* Chromosome Res, 1993. **1**(1): p. 15-26.
40. Dernburg, A.F., et al., *Meiotic recombination in C. elegans initiates by a conserved mechanism and is dispensable for homologous chromosome synapsis.* Cell, 1998. **94**(3): p. 387-98.
41. Severson, A.F., et al., *The axial element protein HTP-3 promotes cohesin loading and meiotic axis assembly in C. elegans to implement the meiotic program of chromosome segregation.* Genes Dev, 2009. **23**(15): p. 1763-78.
42. Viera, A., et al., *Condensin I reveals new insights on mouse meiotic chromosome structure and dynamics.* PLoS ONE, 2007. **2**(1): p. e783.
43. Kahn, T.G., et al., *Polycomb complexes and the propagation of the methylation mark at the Drosophila ubx gene.* J Biol Chem, 2006. **281**(39): p. 29064-75.
44. Papp, B. and J. Muller, *Histone trimethylation and the maintenance of transcriptional ON and OFF states by trxG and PcG proteins.* Genes Dev, 2006. **20**(15): p. 2041-54.
45. Schwartz, Y.B., et al., *Genome-wide analysis of Polycomb targets in Drosophila melanogaster.* Nat Genet, 2006. **38**(6): p. 700-5.

46. Gelbart, M.E., et al., *Drosophila MSL complex globally acetylates H4K16 on the male X chromosome for dosage compensation.* Nat Struct Mol Biol, 2009. **16**(8): p. 825-32.
47. Parker, D.S., et al., *Wingless signaling induces widespread chromatin remodeling of target loci.* Mol Cell Biol, 2008. **28**(5): p. 1815-28.
48. Hauf, S., et al., *Aurora controls sister kinetochore mono-orientation and homolog bi-orientation in meiosis-I.* EMBO J, 2007. **26**(21): p. 4475-86.
49. Monje-Casas, F., et al., *Kinetochore orientation during meiosis is controlled by Aurora B and the monopolin complex.* Cell, 2007. **128**(3): p. 477-90.
50. Resnick, T.D., et al., *INCENP and Aurora B promote meiotic sister chromatid cohesion through localization of the Shugoshin MEI-S332 in Drosophila.* Dev Cell, 2006. **11**(1): p. 57-68.
51. Yu, H.G. and D. Koshland, *The Aurora kinase Ipl1 maintains the centromeric localization of PP2A to protect cohesin during meiosis.* J Cell Biol, 2007. **176**(7): p. 911-8.
52. Brenner, S., *The genetics of Caenorhabditis elegans.* Genetics, 1974. **77**(1): p. 71-94.
53. Kamath, R.S., et al., *Systematic functional analysis of the Caenorhabditis elegans genome using RNAi.* Nature, 2003. **421**(6920): p. 231-7.

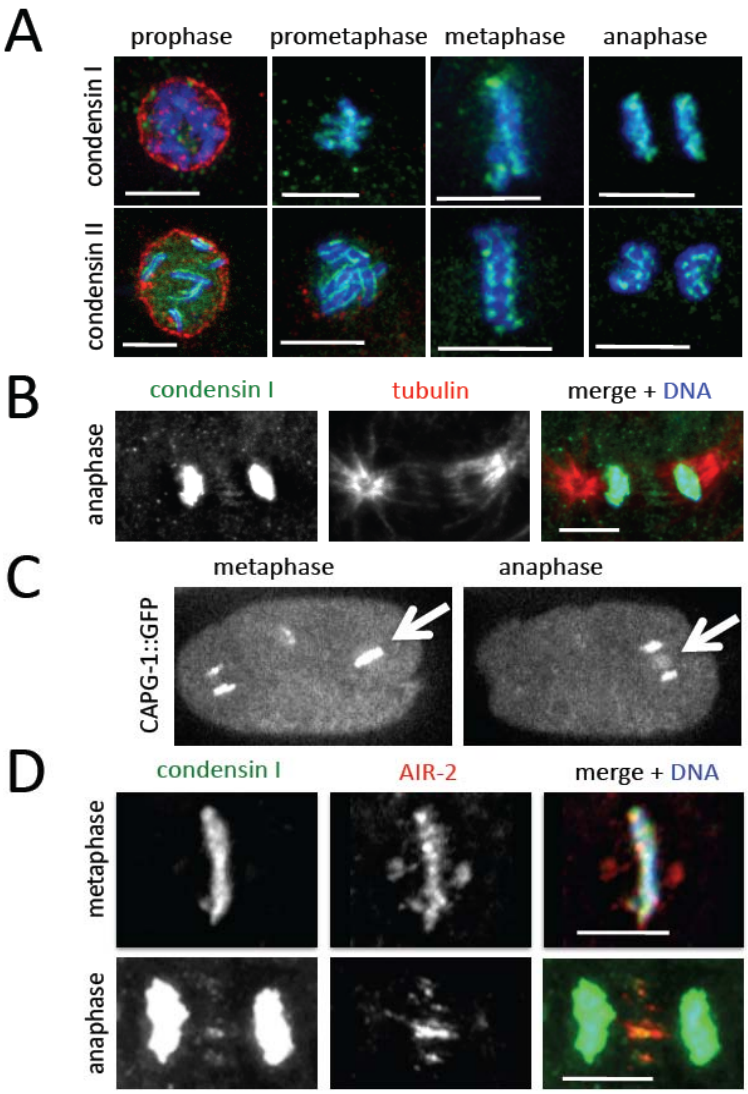

Figure 3.1 Condensin I and II during mitosis. (A) In early prophase, condensin I (CAPG-1, green) is not detected on chromosomes, while condensin II (HCP-6, green) localizes to the centromeres. From prometaphase on, condensin I discontinuously coats mitotic chromosomes and condensin II maintains its centromere-enriched localization. Nuclear pore complex staining is shown in red, DAPI in blue. **(B)** Longer exposure of an anaphase figure reveals condensin I (CAPG-1, green) staining on spindle midzone microtubules (red). **(C)** Live imaging of CAPG-1::GFP in an 8-cell embryo reveals similar patterns of chromosomal association at metaphase and spindle localization during anaphase (arrows). **(D)** Condensin I (CAPG-1, green) and AIR-2 (red) colocalize on mitotic chromosomes at metaphase. At anaphase, AIR-2 dissociates from DNA and localizes to the spindle midzone. Condensin I remains on DNA, but also colocalizes at the midzone with AIR-2. Scale bar = 5μm

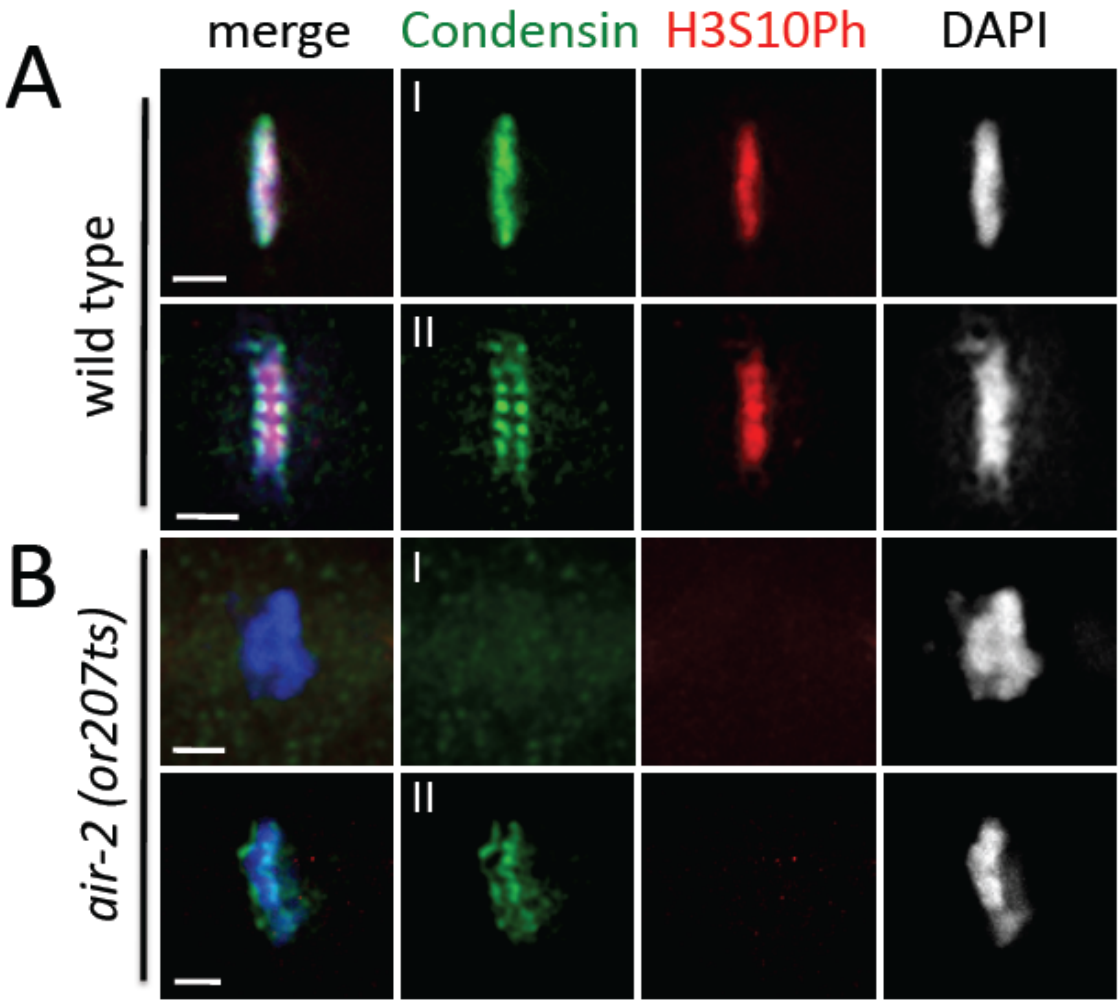

Figure 3.2 Condensin I, but not II, depends on AIR-2 for mitotic recruitment. (A) On wild type metaphase chromosomes, condensin I (CAPG-1, green) and the AIR-2 dependent modification H3S10Ph (red) colocalize on the chromosomes, but condensin II (HCP-6, green) does not overlap with H3S10Ph. **(B)** In AIR-2-depleted embryos, the H3S10Ph signal is undetectable, condensin I is not recruited to metaphase chromosomes, but condensin II recruitment is less affected. Scale bar = 2 μm

Figure 3.3 (A) A diagram of the adult hermaphrodite gonad. Nuclei enter meiosis in the transition zone (TZ, leptotene and zygotene), and proceed through pachytene, diplotene, and diakinesis prior to fertilization. Sperm are stored in the spermatheca (sp). The most proximal oocyte is designated -1. Oocytes move through the spermatheca, are fertilized and then complete meiotic divisions (MI and MII). A set of homologs is extruded as the first polar body (PB1) during MI, and a set of sister chromatids is extruded as the second polar body (PB2) during MII. Oocyte pronucleus (O), sperm-derived pronucleus (S). **(B)** Meiotic chromosomes are extensively restructured between pachytene and diakinesis. During pachytene, replicated chromosomes are held together by the SC (i). A single off-center crossover divides the paired homologs into two domains. At pachytene exit, HTP-1 and LAB-1 are retained between the crossover and the more distant chromosome end, and SYP-1 is retained between the crossover and the closer chromosome end. AIR-2 is recruited to the domain where SYP-1 is retained (ii). The AIR-2 bound domain becomes the short arm, and the HTP-1/LAB-1 bound domain becomes the long arm of the bivalent (iii). Bivalents undergo extensive condensation (iv and v). At metaphase of meiosis I, bioriented bivalents are aligned with their long arms parallel to spindle microtubules and the AIR-2 occupied domain at the metaphase plate (spindle pole axis indicated by arrows) (v). In meiosis I, AIR-2 promotes cohesion loss at the short arm and homologs move away from each other. In meiosis II, the AIR-2 occupied domain at the sister chromatid interface is aligned at the metaphase plate and sister chromatids become bioriented and eventually separated (vi).

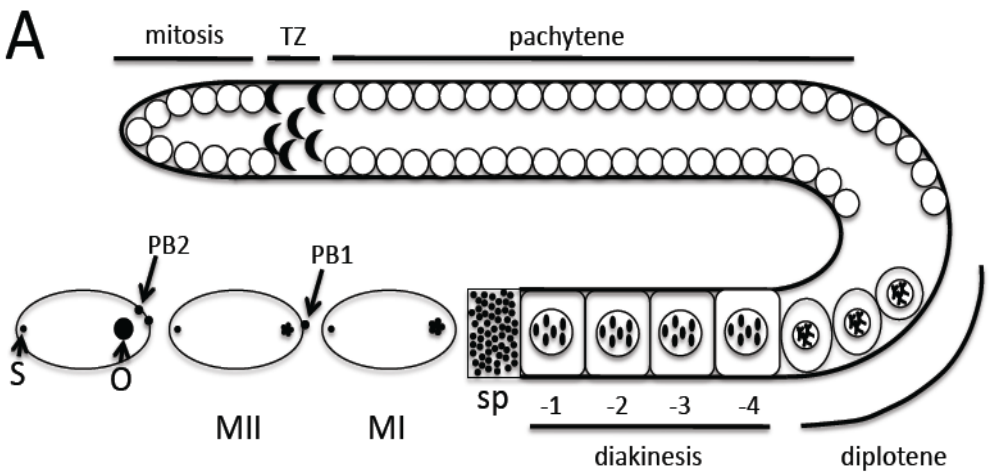
A
mitosis
TZ
pachytene
PB2
PB1
S
O
MII
MI
sp
-1
-2
-3
-4
diakinesis
diplotene

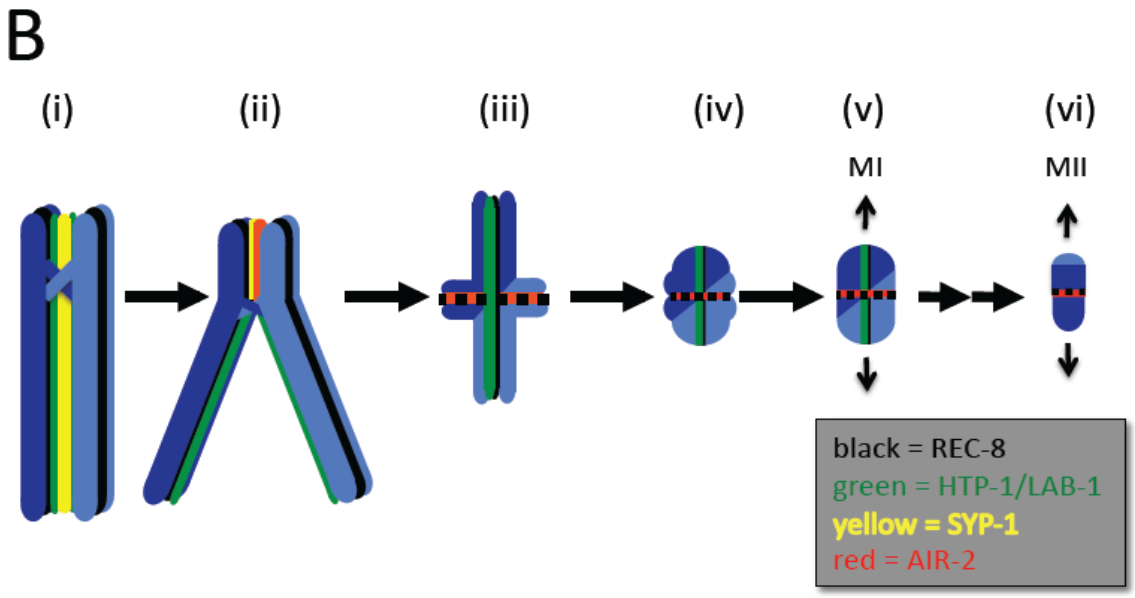
B
(i)
(ii)
(iii)
(iv)
(v)
(vi)
MI
MII
black = REC-8
green = HTP-1/LAB-1
yellow = SYP-1
red = AIR-2

Figure 3.4 Condensin I and II in oocyte meiosis. **(A)** Condensin I (CAPG-1, green) associates with the short arm of bivalents only after NEBD in the -1 oocyte. During metaphase I, condensin I localizes between homologous chromosome pairs, at anaphase I it is seen between separating homologs, at metaphase II between sister chromatids and on the polar body (PB). Condensin II (HCP-6, green) associates with chromosomes prior to NEBD and remains at the core of sister chromatids throughout meiosis. Nuclear pore complex is shown in red, DAPI in blue. **(B)** Live imaging of CAPG-1::GFP showing condensin I on chromosomes and between separating chromosomes in a fertilized oocyte undergoing meiosis I. **(C)** Condensin I (CAPG-1, green) and either tubulin (top, red) or AIR-2 (bottom, red) localization patterns. During acentrosomal meiosis, poleward microtubules disassemble after metaphase and are seen primarily between separating chromosomes during anaphase. Condensin I colocalizes with microtubules during anaphase I and anaphase II. Condensin I also colocalizes with AIR-2 at the metaphase plate, and on the anaphase I spindle **(D)** Enlarged images of a diakinesis bivalent (meiosis I), a pair of sister chromatids during meiosis 2. Viewed from the side, condensin I (CAPG-1, green) and AIR-2 (red) appear as a line between chromosomes. Viewed from the end, they appear as a ring encircling the chromosomes. Scale bar = 2 μm (A, C) and 1 μm (D).

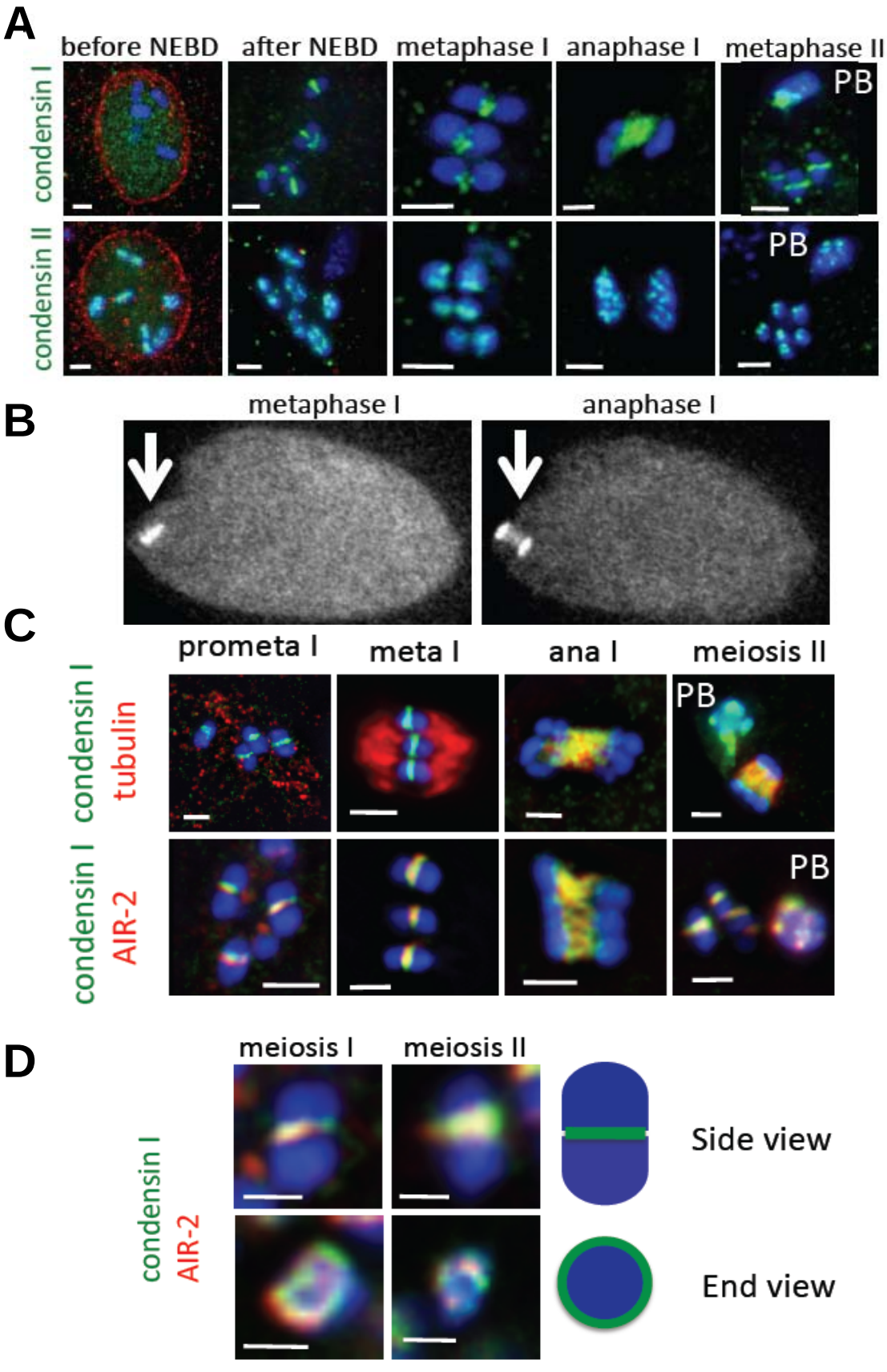
A
before NEBD
after NEBD
metaphase I
anaphase I
metaphase II
condensin I
condensin II
PB
PB
B
metaphase I
anaphase I
C
prometa I
meta I
ana I
meiosis II
condensin I
tubulin
condensin I
AIR-2
PB
PB
D
meiosis I
meiosis II
condensin I
AIR-2
Side view
End view

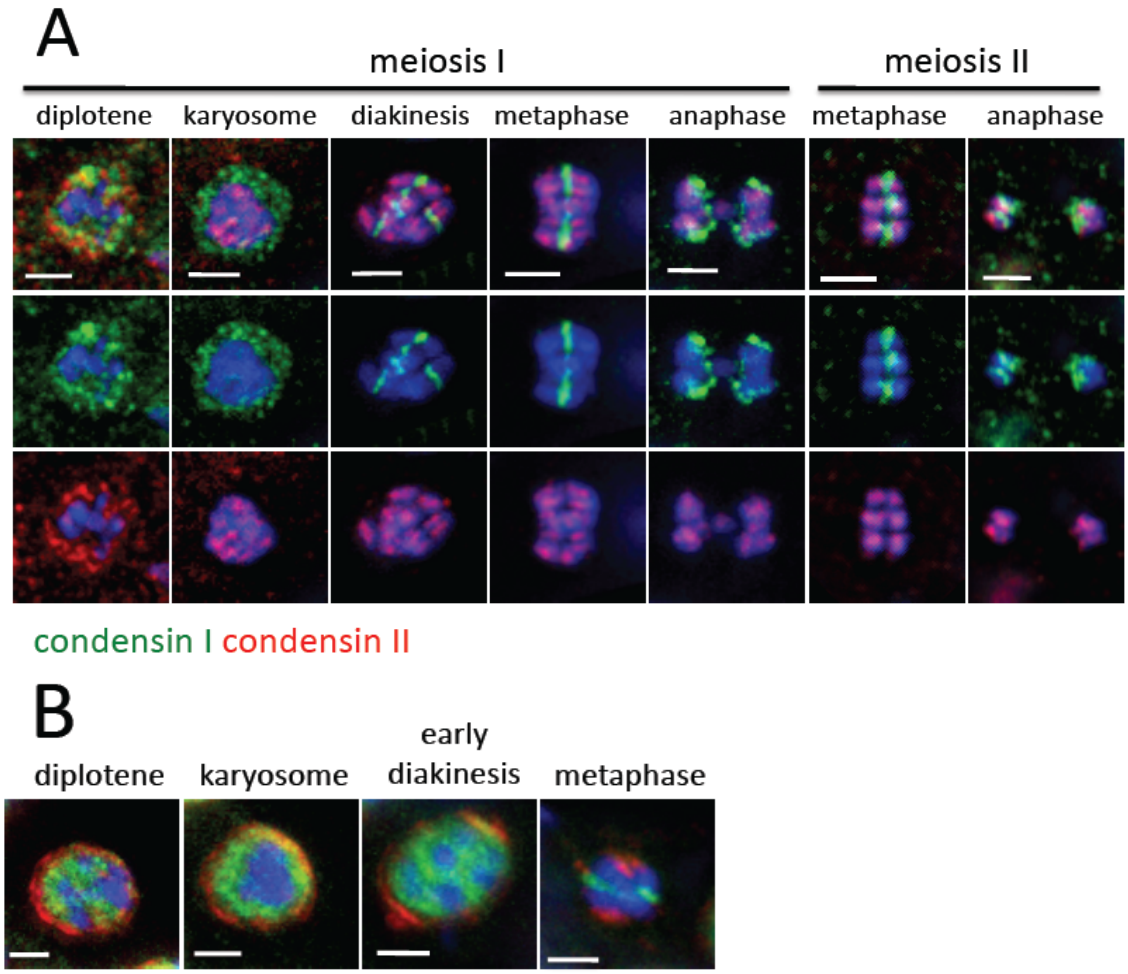

Figure 3.5 Condensin I and condensin II in sperm meiosis (A) Images taken from dissected male gonads co-stained with antibodies specific to condensin I (CAPG-1, green) and condensin II (KLE-2, red). Condensin I is visible in pachytene, karyosome, and early diakinesis nuclei surrounding, but not on, chromosomes, while condensin II associates with chromosomes by late pachytene/early diplotene. Condensin I localizes to the short arms of bivalents in late diakinesis and metaphase I, to the inner edges of separating chromosomes in anaphase I, between sister chromatids in metaphase II and to the inner edges of separating chromatids in anaphase II. Throughout all stages, condensin II associates with sister chromatids. **(B)** Condensin I (CAPG-1, green) is seen inside the nucleus prior to NEBD, but does not associate with chromosomes until after NEBD. NPC is shown in red, DAPI in blue. **(C)** CAPG-1 (green), tubulin (red), and AIR-2 (red) are not prominent between separating chromosomes during anaphase I in sperm meiosis. Sperm meiosis in L4 larval hermaphrodite is shown for tubulin, and male for AIR-2 staining. Scale bar = 2 μm.

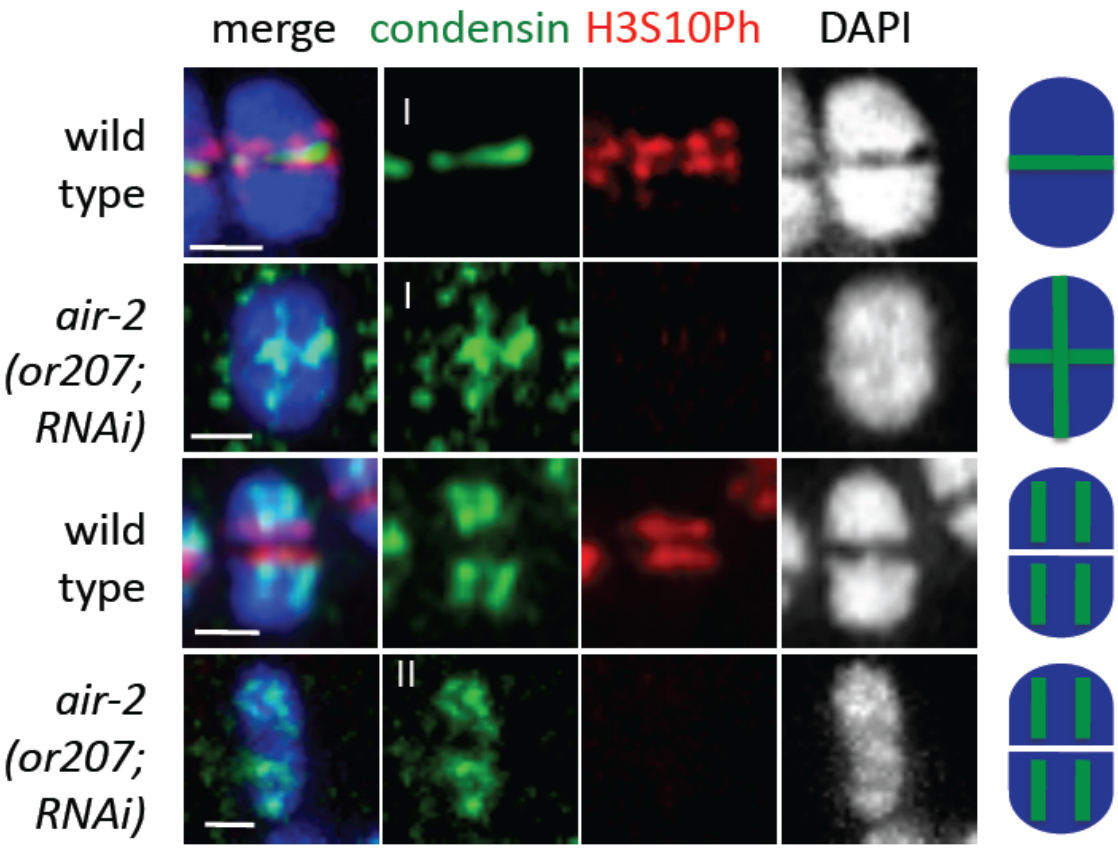

Figure 3.6 AIR-2 activity is needed for correct targeting of condensin I, but not condensin II, in meiosis. Enlarged bivalents from oocytes after NEBD. On control bivalents, condensin I (CAPG-1, green) is restricted to the short arm, and H3S10Ph (red) is seen on both sides of the condensin I domain. In AIR-2-depleted oocytes, the H3S10Ph signal is absent, and condensin I mislocalizes to both arms of the bivalents and appears in a cross shape. By contrast, chromosomal association of condensin II (HCP-6, green) appears similar on control and AIR-2-depleted bivalents. DAPI is shown in blue and gray. Scale bar = 1μm.

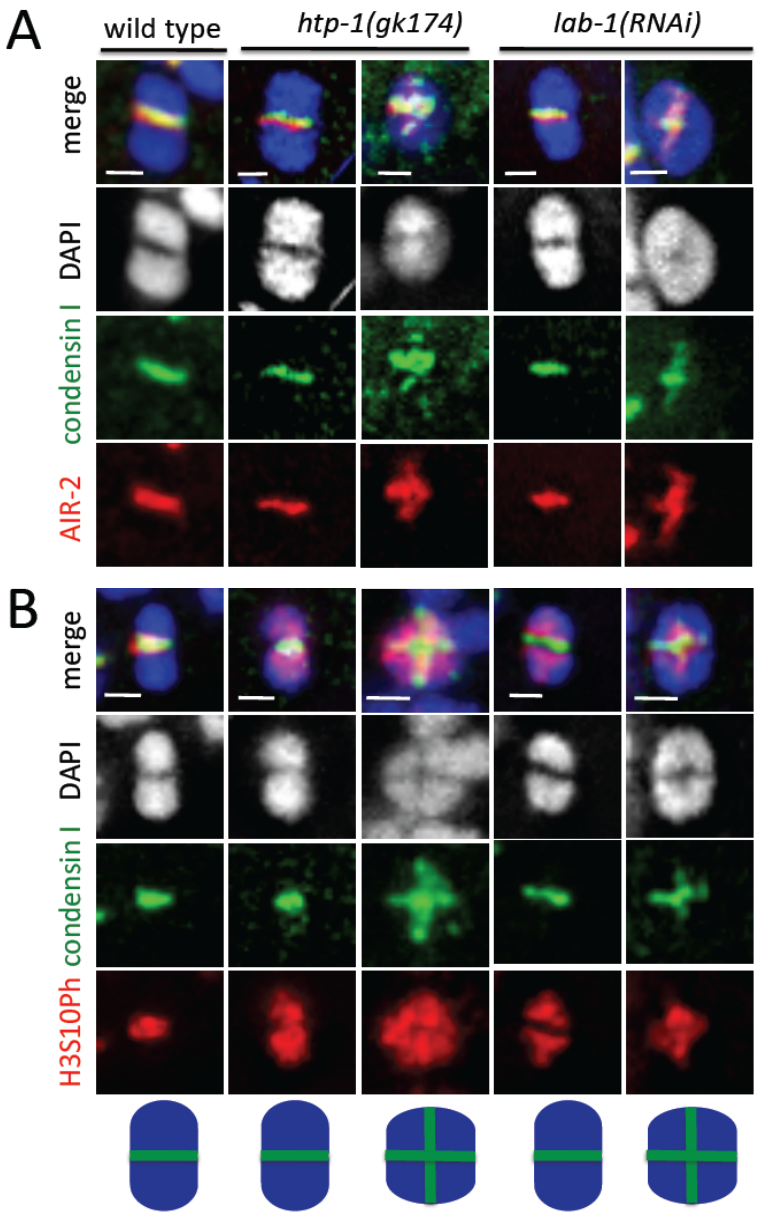

Figure 3.7 Spreading of condensin I and AIR-2 on meiotic bivalents. Enlarged bivalents from oocytes after NEBD, stained with antibodies specific to CAPG-1 (green) and either AIR-2 (red) **(A)** or H3S10Ph (red) **(B)**. On wild type bivalents, condensin I, AIR-2 and H3S10Ph localize to the short arm. On some *htp-1(gk174)* and *lab-1(RNAi)* bivalents, H3S10Ph spreads to cover the bivalent surface, but AIR-2 either remains at the short arm or spreads to both arms. When AIR-2 spreads away from the short arm, condensin I follows AIR-2 and extends onto the long arm. When AIR-2 remains restricted to the short arm, condensin I also remains restricted to this region. Spreading of condensin I and AIR-2 is most pronounced on more rounded and less asymmetric bivalents.

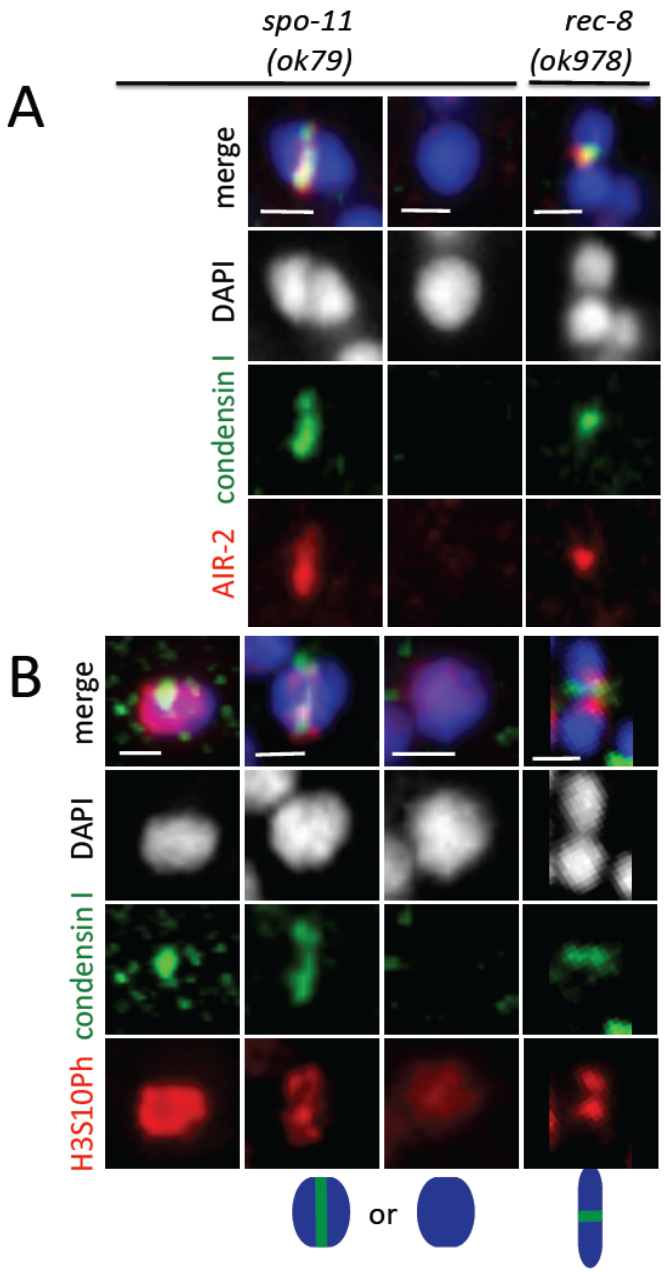

Figure 3.8 Condensin I localization on meiosis I univalents. Enlarged univalents from oocytes after NEBD, stained with antibodies specific to CAPG-1 (green) and either AIR-2 (red) **(A)** or H3S10Ph (red) **(B).** On some *spo-11* univalents, condensin I (CAPG-1) and AIR-2 colocalize to a DAPI-light line, while on others neither condensin I nor AIR-2 are found. Most *spo-11* univalents have H3S10Ph staining of varying intensity, and condensin I only localizes to those with brighter H3S10Ph staining. On all *rec-8* univalents, condensin I and AIR-2 colocalize at the interface between sister chromatids and H3S10Ph forms a boundary on either side of condensin I. Scale bar = 1 μm

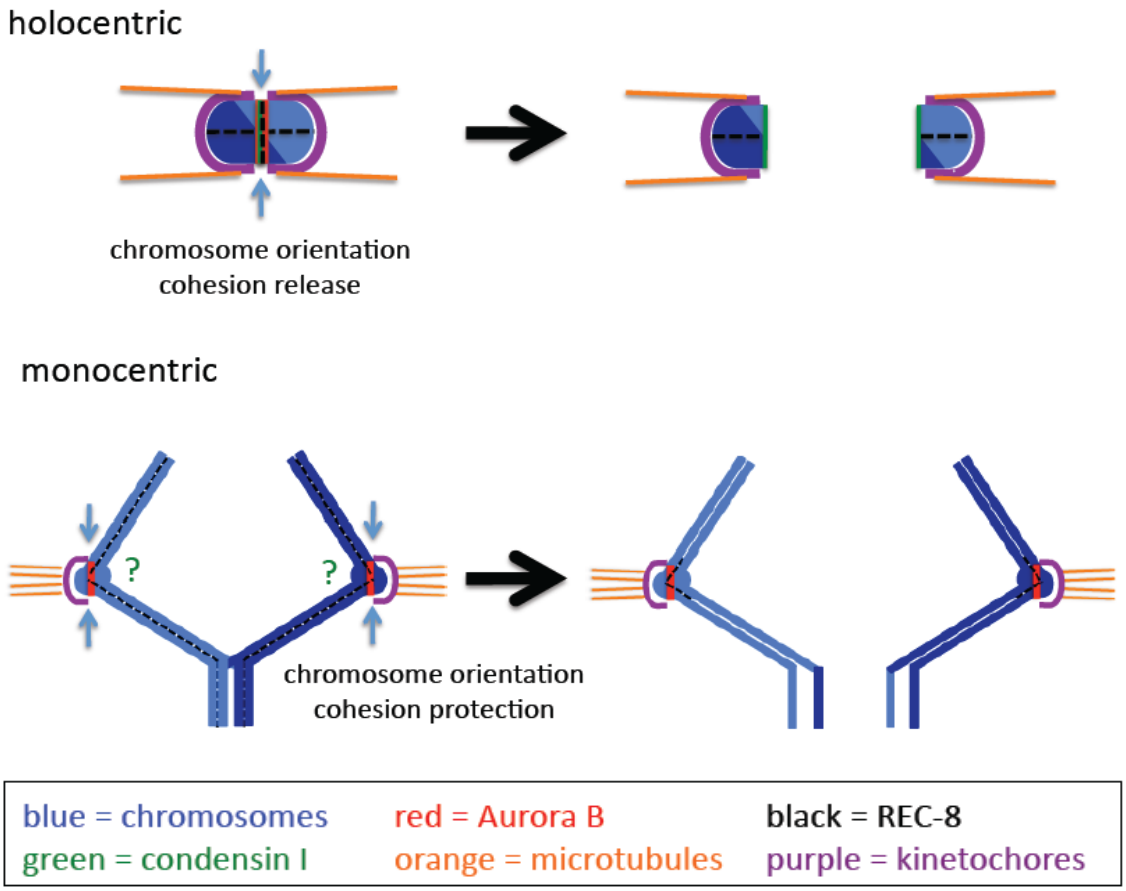

Figure 3.9 Model for AIR-2 activity on monocentric and holocentric chromosomes during meiosis I. On holocentric chromosomes, AIR-2 is in an ideal position at the short arm of the bivalent to promote both homolog biorientation and sister coorientation by ensuring that microtubules do not cross the AIR-2 zone, thereby keeping sisters together and homologs apart. The AIR-2 zone is also the region where sister chromatid cohesion must be released in meiosis I to allow homolog separation. At the short arm of bivalents, AIR-2 activity is also needed to restrict condensin I to the short arm of the bivalent. On monocentric chromosomes, Aurora B is enriched at the inner centromere and promotes homolog biorientation and sister coorientation. This zone of Aurora B activity is where centromeric cohesion must be protected in meiosis I. The role of Aurora B in condensin I and II targeting in meiosis in monocentric organisms is not known.

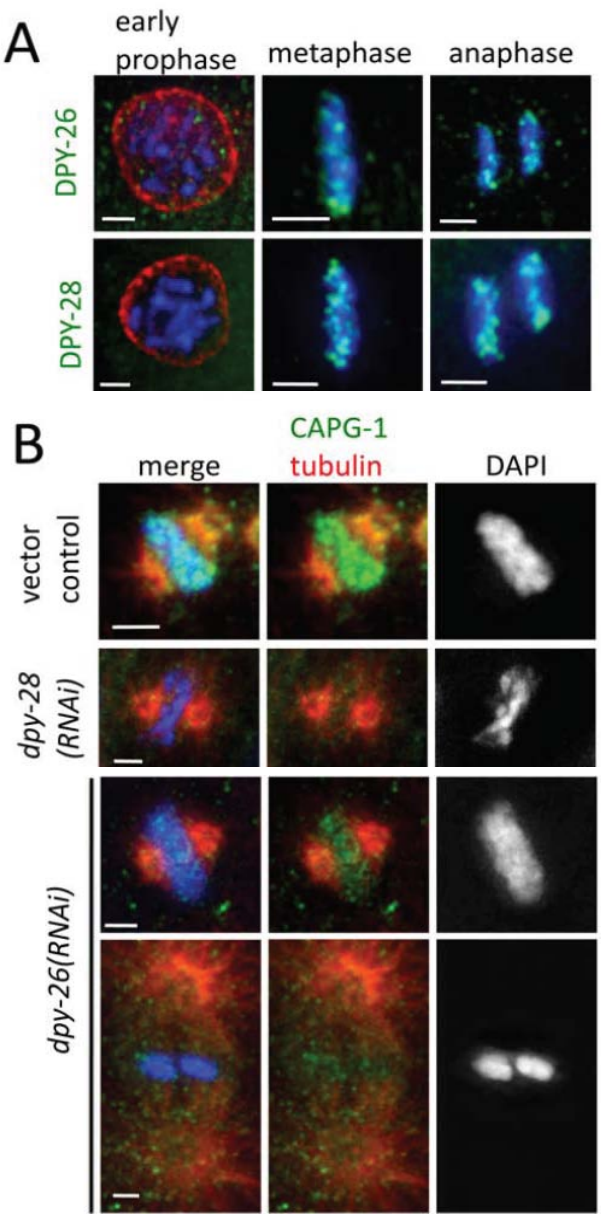

Figure 3.10 The CAP subunits of Condensin I associate with mitotic chromosomes as a complex. (A) Similar to CAPG-1, DPY-26 and DPY-28 (green) also associate with mitotic chromosomes prometaphase through anaphase, but not in early prophase. Nuclear pore complex is shown in red, DAPI in blue. (B) In the absence of DPY-26 or DPY-28, CAPG-1 no longer associates with mitotic chromosomes. Metaphase plates from young embryos are shown, CAPG-1 in green, tubulin in red. In DPY-28-depleted embryos, CAPG-1 binding to mitotic chromosomes is undetectable, while in DPY-26-depleted embryos, CAPG-1 staining is reduced (top row) or absent (bottom row). DAPI is shown in blue and gray. Scale bar =2μm.

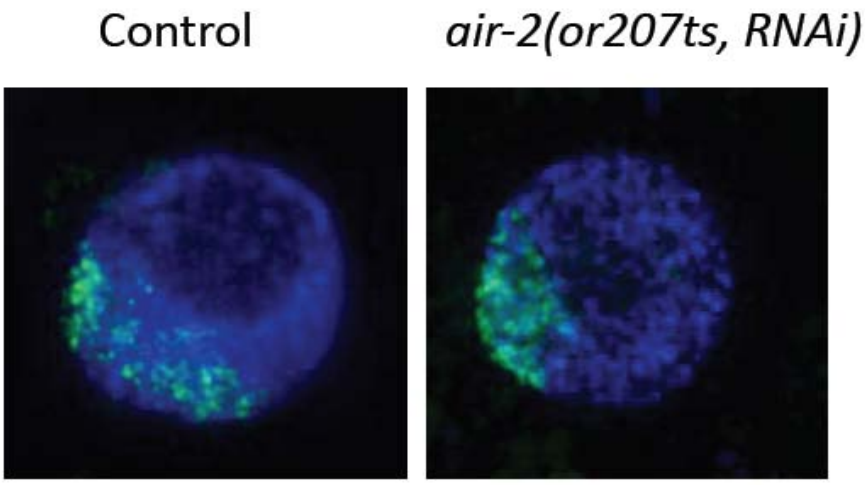

Figure 3.11 Condensin I^{DC} is unaffected by AIR-2 depletion. X-chromosome localization of CAPG-1 (green) is unperturbed in AIR-2 depleted somatic (intestinal) nuclei of adult worms. DAPI is shown in blue. Scale bar=5μm.

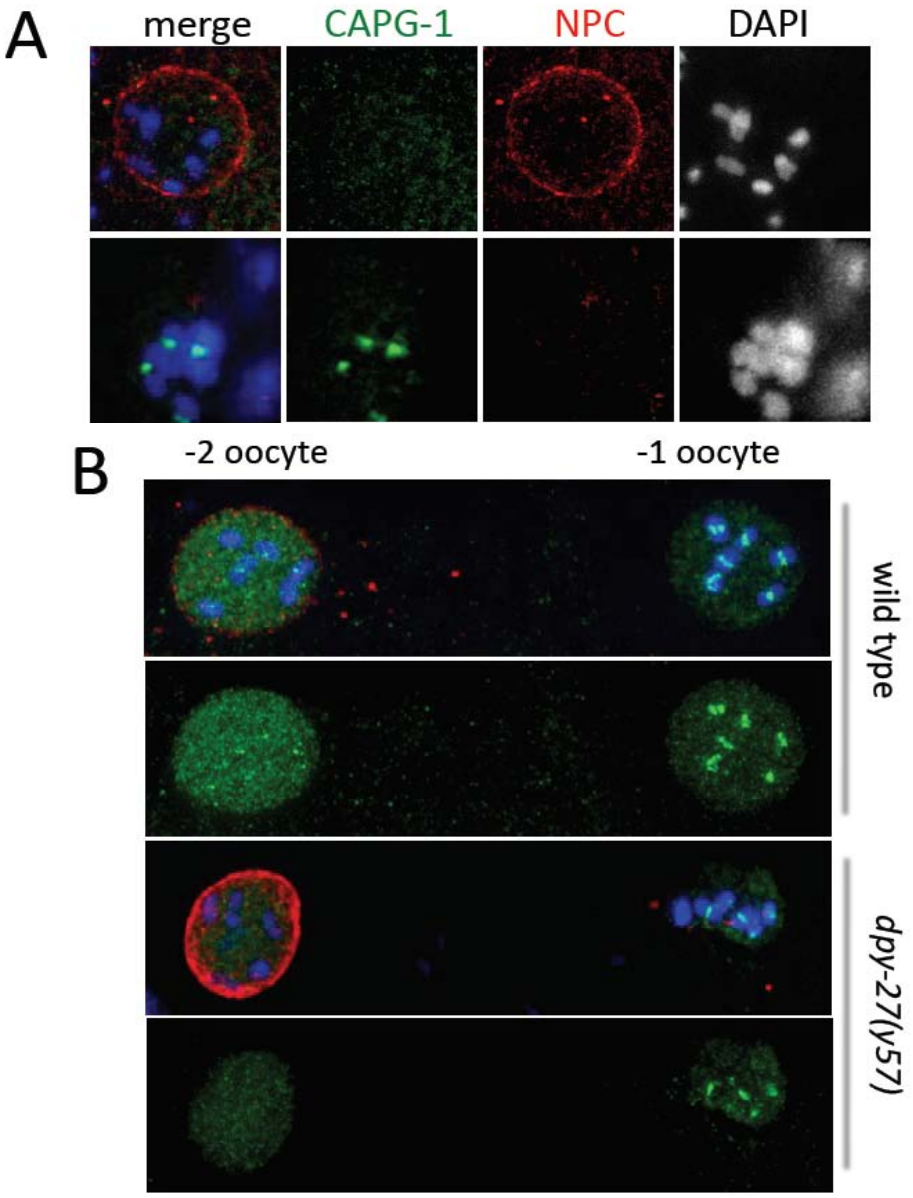

Figure 3.12 Nucleoplasmic background does not mask chromosomal association of Condensin I prior to NEBD. (A) Nucleoplasmic CAPG-1 (green) staining is reduced after detergent extraction, but short arm localization of condensin I is not visible before NEBD (top row). Short arm localization of CAPG-1 is detected after NEBD even in extracted nuclei (bottom row). Nuclear pore complex (NPC) is shown in red. (B) In *dpy-27(y57)* mutants, nucleoplasmic staining of condensin IDC is reduced. In this background, we do not detect chromosomal association of CAPG-1 before NEBD (-2 oocyte), but easily detect it after NEDB (-1 oocyte). DAPI is shown in blue and gray. Scale bar=5μm.

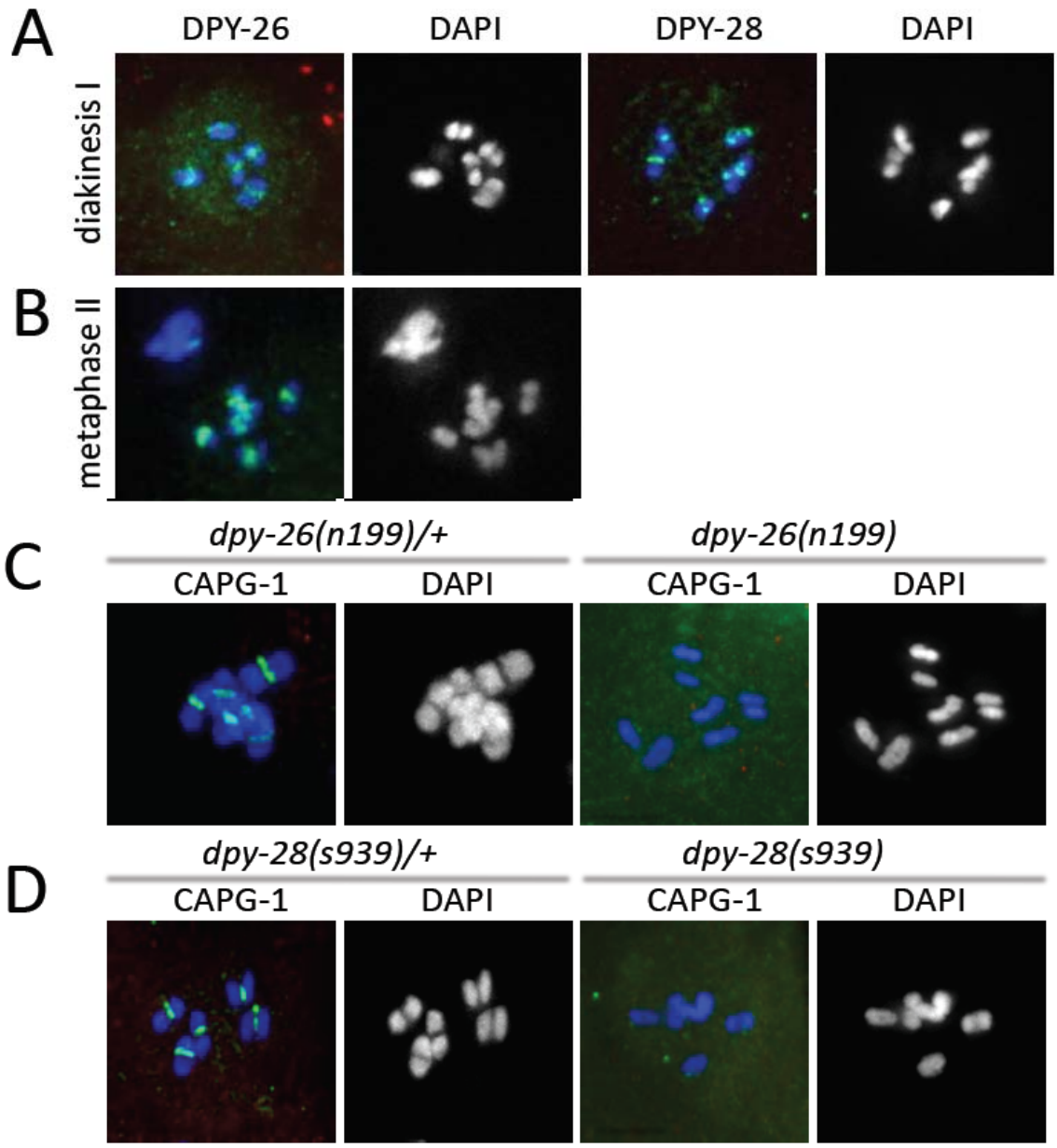

Figure 3.13 The CAP subunits of condensin I associate with meiotic chromosomes as a complex. (A) DPY-26 and DPY-28 (green) localize to the short arms of diakinesis bivalents after NEBD. Methanol/acetone fixed oocytes are shown. (B) DPY-26 localizes to the interface between sister chromatids in metaphase of meiosis II. Methanol acetone fixed embryo is shown. (C and D) Short arm association of CAPG-1 (green) depends on the presence of DPY-26 and DPY-28. In *dpy-26(n199)* (C) and in *dpy-28(s939)* (D) mutants, CAPG-1 localization to the short arm is no longer detected. Oocytes after NEBD are shown, NPC staining is red, DAPI is blue and gray. Heterozygotes are shown as controls. Scale bar=5μm.

CHAPTER 4

Restricting Dosage Compensation Complex binding to the X chromosomes by H2A.Z/HTZ-1

This chapter was published in PLoS Genetics in 2009. K. Collette contributed to Figure 1 A and B and A. Cohen contributed to Figure 1A. I completed all other work.

Abstract

Dosage compensation ensures similar levels of X-linked gene products in males (XY or XO) and females (XX), despite their different numbers of X-chromosomes. In mammals, flies, and worms, dosage compensation is mediated by a specialized machinery that localizes to one or both of the X chromosomes in one sex resulting in a change in gene expression from the affected X chromosome(s). In mammals and flies, dosage compensation is associated with specific histone posttranslational modifications and replacement with variant histones. Until now, no specific histone modifications or histone variants have been implicated in *C. elegans* dosage compensation.

Taking a candidate approach, we have looked at specific histone modifications and variants on the *C. elegans* dosage compensated X chromosomes. Using RNAi-based assays, we show that reducing levels of the histone H2A variant, H2A.Z (HTZ-1 in *C. elegans*), leads to partial disruption of dosage compensation. By immunofluorescence, we have observed that HTZ-1 is under-represented on the dosage compensated X chromosomes but not on the non-dosage compensated male X chromosome. We find that reduction of HTZ-1 levels by RNA interference (RNAi) and mutation results in only a very modest change in dosage compensation complex protein levels. However, in these animals, the X-chromosome specific localization of the complex is partially disrupted, with some nuclei displaying DCC localization beyond the X-chromosome territory. We propose a model in which HTZ-1, directly or indirectly, serves to restrict the dosage compensation complex to the X chromosome by acting as or regulating the activity of an autosomal repellant.

Author Summary

In organisms where females have two X-chromosomes and males only have one, a mechanism called dosage compensation ensures that both sexes receive the same amount of information from their X-chromosomes. Disruption of dosage compensation leads to lethality in the affected sex. While the precise mechanisms of dosage compensation differ between organisms, changes to the structure of the X-chromosomes are involved in each case. The DNA of all chromosomes is packaged into a complex protein-DNA structure called chromatin. The most basic level of packaging involves wrapping DNA around a

group of small proteins called histones. In both mammals and flies, dosage compensation is associated with specific changes to the histones on the dosage compensated X-chromosome. Until now, no such change has been associated with dosage compensation in worms. Here we present evidence that the histone variant HTZ-1/H2A.Z plays a role in dosage compensation in the worm. Specifically, we suggest that HTZ-1 functions to ensure that only the X-chromosomes, and not the other chromosomes, are subjected to dosage compensation. This suggests that despite different mechanisms, one common theme of dosage compensation is a change at the level of the histones associated with the chromosomal DNA.

Introduction

Many species- such as humans, mice, flies, and worms- utilize a chromosome-based mechanism to establish sex. This results in a difference in sex chromosome number between the sexes that, left uncorrected, puts one sex at a great selective disadvantage. In order to combat this, these organisms employ a second mechanism to ensure that the same amount of sex chromosome-linked gene expression occurs in both sexes. This mechanism is called dosage compensation [1-4].

In flies and mammals, specific posttranslational histone modifications and/or replacement of core histones with variants are key features of the dosage compensated X chromosomes [5]. Dosage compensation in flies is brought about by the MSL (*m*ale-*s*pecific-*l*ethal) complex that localizes to the single X chromosome in males resulting in a two-fold increase in gene expression [6, 7].

The MSL complex is made up of at least five proteins (MSL1 [8], MSL2 [9], MSL3 [10], MLE [11], and MOF [12]), and one of two non-coding RNAs (roX 1 and roX2, *R*NA *o*n the *X* [13, 14]). The hypertranscribed male X is enriched for histone H4 lysine 16 acetylation (H4K16ac) [15]. MOF (*m*ales-absent *o*n the *f*irst) places the H4K16ac mark on the male X and this function is essential for dosage compensation [16-18]. In mammals, one of the two female X chromosomes is transcriptionally inactivated [3]. The inactive X is targeted for silencing by the non-coding RNA, Xist in mice [19, 20], XIST in humans [21], that coats the inactive X chromosome [22]. This is followed by chromosome-wide histone H3 lysine 27 tri-methylation (H3K27me3) by Polycomb repressor complex 2 (PRC2) [23], and histone H2A and H2A.Z mono-ubiquitylation by Polycomb repressor complex 1 (PRC1) [24, 25]. On the inactive X chromosome, there is also an enrichment of histone H3 lysine 9 dimethylation (H3K9me2) [26] and an enrichment of the histone variant macroH2A [27]. However, other modifications and variants are specifically under-represented on the inactive X: di-, and trimethylation of histone H3 lysine 4 (H3K4me) [26, 28], dimethylation of histone H3 arginine 17 (H3R17me2) and H3 lysine 36 (H3K36me2)[29], acetylation of the N-terminal tails of histones H2A, H3 and H4 [30-32], and the phosphorylated form of macroH2A1 [33]. These and other modifications are thought to be vital for the resulting essential change in X-linked gene expression in male flies and female mammals.

In *C. elegans*, dosage compensation is achieved by the dosage compensation complex (DCC), which binds both X chromosomes in

hermaphrodites to downregulate gene expression two-fold [2]. DPY-27 [34], MIX-1 [35], DPY-26 [36], DPY-28 [37], and CAPG-1 [38] form a condensin-like complex, condensin I^{DC}. SDC-2 [39], SDC-3 [40], and DPY-30 [41] are thought to be responsible for recruitment of the condensin-like complex, as well as DPY-21 [39] and SDC-1 [42, 43], to the X chromosomes in hermaphrodites. All DCC proteins, except for SDC-2, are supplied maternally to the oocyte, and are initially present in both male and hermaphrodite embryos [2]. SDC-2 is not contributed maternally, expressed only in hermaphrodites and is thought to confer both sex-specificity and X-chromosome specificity to dosage compensation [39]. The DCC initially binds to *rex* (*r*ecruitment *e*lements on the *X*) sites, which represent sites of DCC enrichment on the X chromosome, and spreads in *cis* along the lengths of both X chromosomes in the hermaphrodite [44-47]. As a result, gene expression from the two hermaphrodite X chromosomes is down-regulated by half, thus limiting X-linked gene products to levels produced in XO males [48]. Condensin complexes are well known for their roles in affecting chromosome architecture during mitosis and meiosis [49], so it is believed that the DCC may be altering the overall organization of the X chromosomes to dampen gene expression during interphase. A chromosome-wide architectural change by the DCC condensin may require or lead to specific modifications to the basic organizational unit of chromatin, the nucleosome. However, no nucleosomal changes, such as posttranslational modification of histones or histone variants, have been previously implicated to play a role in *C. elegans* dosage compensation.

While in somatic cells of hermaphrodites the X chromosome is subject to dosage compensation, in the postembryonic germ line of both sexes the X is subject to a distinct form of chromosome-wide regulatory process: global repression throughout meiosis in males and during early meiosis in hermaphrodites [50]. The *m*aternal *e*ffect *s*terility (MES) proteins mediate silencing of the germ line X chromosome and their function is required for germ line viability [50-52]. Three of the *mes* genes (*mes-2*, *mes-3*, and *mes-6*) encode proteins that function together in a PRC2-like complex, which localizes to the germ line X-chromosome(s) and leads to enrichment of H3 lysine 27 trimethylation on the X [53-56]. By contrast, an additional MES protein, MES-4, localizes only to the autosomes and not X, and its function is necessary for germ line X silencing [51, 57]. Additionally, the silenced germ line X chromosomes show a significant depletion of activating marks such as acetylation of the N terminal tail of histone H4 and methylation of lysine 4 on H3 [50, 58].

From studies of dosage compensation in other organisms and of germ line X chromosome silencing in *C. elegans*, there are many well-documented links between different forms of chromosome-wide gene regulation and specific nucleosome characteristics. This led us to explore whether we might find a similar link between *C. elegans* dosage compensation and nucleosome composition. We were interested to see if any histone modifications or histone variants play a functional role in dosage compensation in worms. In this paper we report on the role of the *C. elegans* histone H2A.Z variant (HTZ-1).

The histone variant H2A.Z is conserved from yeast to humans and has been implicated in diverse biological processes. Interestingly, depending on its histone partner in the nucleosome core particle, H2A.Z can either stabilize or destabilize the nucleosome [59]. When partnered with histone H3, the H2A.Z-containing nucleosome becomes more stable, but when partnered with the histone variant H3.3, the nucleosome becomes destabilized. Unstable H2A.Z/H3.3. nucleosomes may function to poise genes for activation. Consistently, studies in several organisms implicate H2A.Z in various aspects of transcription activation. In *Tetrahymena*, hv1/H2A.Z associates with the transcriptionally active macronucleus [60-62]. Genome-wide localization studies in yeast [63-66], worms [67], flies [68], plants [69], and humans [70], revealed that H2A.Z preferentially localizes to 5' ends of genes, consistent with a role in transcription activation. Loss of Htz1 has been shown to diminish RNA Pol II binding to promoters, slow the activation of regulated genes, or prevent rapid reactivation of recently repressed genes [66, 71, 72]. A role of HTZ-1 to poise genes for rapid activation has also been observed in a study of the *C. elegans* H2A.Z homolog, HTZ-1 [73].

However, H2A.Z also localizes to regulatory regions not corresponding to promoters to exert other functions. In budding yeast, Htz1 also functions at boundary elements to protect genes from heterochromatinization by antagonizing the spread of silencing complexes [74]. This antisilencing functions at the global level, not just locally [75]. Consistent with an antisilencing role, in plants, H2A.Z antagonizes DNA methylation [69]. H2A.Z also localizes to insulator elements in

chicken [76], and to functional regulatory elements in human cells [70]. It has been proposed that in this context, the presence of an H2A.Z/H3.3 labile nucleosome prevents the spreading of heterochromatic marks [59].

On the other hand, H2A.Z also plays a role in heterochromatin formation. In this context, H2A.Z most likely partners with H3 to form stable nucleosomes [59]. In mammals and in flies, H2A.Z associates with pericentric heterochromatin and interacts with heterochromatin protein HP1 [77-80]. Mammalian H2A.Z also becomes incorporated into the inactive XY body following meiosis [81]. However, H2A.Z is significantly underrepresented and differentially modified on the mammalian inactive X chromosome in somatic cells, indicating that H2A.Z enrichment is not a general feature of all heterochromatin [25, 79, 82]. Consistent with that, H2A.Z is not enriched at heterochromatic chromocenters in plants [69, 83].

Here we show that in *C. elegans* the histone variant H2A.Z/HTZ-1 functions in dosage compensation. Consistent with previous reports [67], we find that HTZ-1 is under-represented on the dosage compensated X chromosomes in somatic nuclei of hermaphrodites. However, we do not observe HTZ-1 depletion on the non-dosage compensated X chromosome in male somatic nuclei. We also see an underrepresentation of HTZ-1 on the silent X chromosomes of both male and hermaphrodite germ nuclei. Partial depletion of HTZ-1 does not lead to an overall decrease in DCC protein levels. Instead we see mislocalization of the DCC away from the X chromosomes and onto autosomes. These results reveal an HTZ-1-dependent activity that serves to repel the DCC away from autosomes.

We propose that HTZ-1 plays a role in dosage compensation by directly or indirectly restricting binding of the DCC to the X chromosomes.

Results

HTZ-1 function promotes dosage compensation

To search for chromatin modifiers involved in worm dosage compensation, we utilized two RNAi-based assays in a genetic background sensitized for detecting disturbances in dosage compensation. We tested genes encoding *C. elegans* homologs of histone variants, genes implicated in modifying chromatin via posttranslational histone modifications (such as acetylation or methylation) or chromatin remodeling [84], as well as genes annotated to contain chromo-, bromo- or SET domains (Wormbase [http://www.wormbase.org], release WS201).

The first assay was completed in the *sex-1(y263)* mutant background. *sex-1* functions genetically as an X signal element by repressing *xol-1*, the master switch regulating both sex-determination and dosage compensation [85, 86]. In addition, *sex-1* plays a role downstream of *xol-1*, promoting dosage compensation in hermaphrodites [87]. In *sex-1(y263)* mutant hermaphrodites, dosage compensation is partially impaired, resulting in 15-30% embryonic lethality. In these worms, partial loss-of-function due to feeding RNAi of a gene important for dosage compensation leads to increased lethality [87]. A second genetic assay was based on the rescue of males that inappropriately turn on dosage compensation due to a *xol-1(y9)* mutation. Expression of *xol-1* in males is essential to prevent dosage compensation of the single X chromosome [88].

Mutations in *xol-1* are male lethal due to ectopic dosage compensation, leading to abnormally low levels of X-linked gene expression. The *sex-1(y263)* mutation partially weakens dosage compensation, as described above. *xol-1(y9) sex-1(y263)* males die, but they can be rescued by feeding RNAi of dosage compensation genes [38, 87]. To ensure a consistent proportion of males in our test strain, we perform these assays in a strain that also carries the *him-8(e1489)* allele. Mutations in *him-8* cause X chromosome nondisjunction in meiosis and results in a predictable 38% of XO progeny each generation [89].

RNAi of DCC components show near complete *sex-1* lethality and results in 33-60% rescue of *him-8(e1489)*; *xol-1(y9) sex-1(y263)* males in these two assays [38]. One candidate, the histone variant *htz-1* (*C. elegans* H2A.Z homolog) showed a similar genetic interaction. RNAi in the wild type background leads to little to no lethality, while *htz-1* RNAi in the *sex-1(y263)* background leads to near complete embryonic lethality (Figure 4.1A). In the *him-8(e1489); xol-1(y9) sex-1(y263)* background, RNAi of the histone variant *htz-1* resulted in over 15% rescue (Figure 4.1B). To ensure that these phenotypes are not caused by general disruption to chromatin, we also tested two genes encoding H3.3 histone variants (*his-71* and *his-72*) [90], and genes encoding linker histones [*his-24* (H1.1), *hil-3* (H1.3), *hil-4* (H1.4), *hil-5* (H1.5), *hil-6* (H1.6), and *hil-7* (H1.Q)] [91]. RNAi of these genes did not show similar genetic interactions. RNAi of many other chromatin factors also failed to result in significant male rescue (for a complete list, see Table S1). The chromatin remodeling enzyme *isw-1*, and the

histone deacetylase *let-418* are shown as examples (Figure 4.1B). We conclude that depletion of HTZ-1 leads to disruption of dosage compensation.

HTZ-1 is underrepresented on hermaphrodite X chromosomes but not the male X chromosome

A previous study found that in worms HTZ-1 preferentially localizes to promoters, as in other organisms [67]. Furthermore, fewer peaks of HTZ-1 incorporation were found on the X chromosome, as compared to autosomes. The authors attribute this difference to the relative lack of developmentally important genes on the X chromosome, rather than a direct role in dosage compensation [67]. Our RNAi data above indicates that HTZ-1 function is needed for wild type levels of dosage compensation, but does not address whether this role is direct or indirect. That is, *htz-1* may directly regulate some aspect of DCC function, or *htz-1* may indirectly affect dosage compensation by regulating expression of known or unknown dosage compensation genes. To begin to distinguish between these possibilities, we analyzed the distribution of HTZ-1 in male and hermaphrodite nuclei. We reasoned that if HTZ-1 functions in dosage compensation, its distribution in the nucleus may be different in males (dosage compensation inactive) and hermaphrodites (dosage compensation active).

To analyze HTZ-1 distribution, we took advantage of a strain expressing a YFP-HTZ-1 fusion protein, or used an HTZ-1 specific antibody. The specificity of our HTZ-1 antibody is demonstrated by recognition of a protein of the predicted size on western blots and reduction of signal after HTZ-1 depletion on both western blots and by immunofluorescence (IF) (Figure 4.9). We marked the X-

chromosome territory with an antibody specific to DPY-27 (marks the X chromosomes in hermaphrodites only) or X-paint fluorescent *in situ* hybridization (FISH) (to mark the X chromosomes in both sexes). Consistent with a previous report [67], we observed reduced HTZ-1 staining on the dosage compensated X chromosomes in mid-to-late stage hermaphrodite embryos after the onset of dosage compensation by DPY-27/HTZ-1 IF (Figure 4.2A and 4.2B), and combined X-Paint FISH/HTZ-1 IF (Figure 4.2C). We also observed reduced levels of YFP-HTZ-1 in the territory of the X-chromosomes in transgenic hermaphrodite embryos (Figure 4.10). However, in males we did not observe a decrease in HTZ-1 staining intensity in the X chromosome territory of somatic nuclei (Figure 4.2C). These results indicate that reduced HTZ-1 levels are specific to dosage compensated X chromosomes and not a general feature of X chromosomes in both sexes in adult animals.

HTZ-1 depletion does not lead to a decrease in DCC protein levels

The results of the genetic assays and localization assays appeared contradictory: reduced *htz-1* expression disrupts dosage compensation, yet the protein itself is depleted on the dosage compensated X chromosomes. Therefore, we wanted to explore how dosage compensation is affected in *htz-1* depleted animals. If HTZ-1 functions in dosage compensation indirectly (by regulating expression of dosage compensation genes) we would predict to see a decrease in DCC protein levels upon HTZ-1 depletion. We analyzed worms carrying the *htz-1* deletion allele *tm2469* that removes 345 of 885 base pairs from *htz-1* and likely represents a null allele. *htz-1(tm2469)* homozygous progeny of

heterozygous mothers (m^+z^-) develop into healthy adults but are sterile, as reported [67]. However, the *tm2469* deletion appears to affect expression of not just *htz-1*, but the neighboring gene as well (Figure 4.11). It was therefore important to obtain HTZ-1-depleted worms using an alternate method and to confirm that phenotypes are due to HTZ-1 depletion, and not depletion of the neighboring gene product. As an alternative method, we depleted HTZ-1 levels by feeding worms bacteria expressing double stranded RNA corresponding to *htz-1*. As a control, worms were fed bacteria carrying an empty vector. Feeding RNAi in wild type animals greatly reduced HTZ-1 as detected both by immunofluorescence and quantitative Western blot analyses (89% reduction) (Figure 4.3B and Figure 4.9).

To investigate the possibility that HTZ-1 depletion leads to a decrease in DCC protein levels, we quantified protein levels by western blotting of HTZ-1 depleted and control animals. Although HTZ-1 levels were clearly reduced after *htz-1* RNAi, we did not observe a dramatic change in DCC protein levels (Figure 4.3A and 4.3C). Levels of DPY-27 and CAPG-1 show a very slight decrease while MIX-1, DPY-26, and DPY-28 show very slight increases after *htz-1* RNAi. Our results suggest that, HTZ-1 reduction does not lead to a significant defect in overall DCC protein levels. However, we cannot exclude the possibility that the timing of DCC gene expression is changed (delayed) in HTZ-1 depleted cells, as was observed for genes involved in foregut development [73]. It is also possible that a small amount HTZ-1 that remains after feeding RNAi is sufficient for DCC

gene expression, but more complete HTZ-1 depletion would result in a significant decrease in DCC protein levels.

SDC-2, the primary determinant of hermaphrodite fate, is the only DCC protein whose expression in the zygote is essential [39]. The remaining DCC proteins are maternally loaded into the oocyte and this maternal load is sufficient to carry out dosage compensation in the developing embryo. Therefore, it was important to determine whether *sdc-2* transcript levels are affected after HTZ-1 depletion. We analyzed *sdc-2* mRNA levels in HTZ-1 depleted and control animals by reverse transcription followed by quantitative polymerase chain reaction (RT-qPCR) and observed no significant change in *sdc-2* expression (Figure 4.3D). We conclude that the changes observed in DCC protein and RNA levels are not likely to be sufficient to explain the observed requirement for HTZ-1 to maintain wild type levels of dosage compensation.

DCC localization is disrupted in HTZ-1 depleted animals

An alternative possibility is that HTZ-1 has a more direct role in dosage compensation by affecting DCC localization or function. To explore this possibility, we used immunofluorescence to observe DCC localization in HTZ-1-depleted worms. The DCC was clearly present in nuclei of *htz-1(RNAi)* animals, again suggesting that HTZ-1 depletion does not lead to a significant reduction in DCC protein levels. However, the territory occupied by the DCC in these nuclei was significantly more diffuse in appearance than in wild type nuclei (Figure 4.4).

We hypothesized that the diffuse appearance of the DCC reflected mislocalization of the DCC away from the X chromosome. To observe DCC

localization relative to X chromosomes, we combined DCC immunofluorescence with X-paint FISH in *htz-1(RNAi)* (Figure 4.4) and mutant (Figure 4.5) animals. We used intestinal nuclei because they are 32-ploid, allowing for easier visualization of sub-nuclear regions by FISH [92]. To determine the degree of colocalization between X-Paint and DPY-27 signals we determined Pearson's correlation coefficient (R_r) values (see Materials and Methods). An R_r value of +1 indicates a complete and positive correlation between two signals within a region of interest while a value of 0 indicates no linear relationship between the two signals.

In vector control RNAi animals we observed that the DCC was highly restricted to the X chromosomes and the mean R_r was 0.65±0.14. R_r was greater than 0.5 in the vast majority of nuclei observed (88%), and only a minority of nuclei had R_r values between 0.5 and 0.2 (~12%). No correlation values of less than 0.2 were observed in these animals. Representative nuclei and corresponding R_r are shown in Figure 4.4A. By contrast, after *htz-1* RNAi, the mean R_r for *htz-1* RNAi nuclei was 0.44±0.20, significantly lower than control (p=5.79E-8). The majority of nuclei (58%) had DPY-27/X-paint correlation values below 0.5, and 27% of nuclei had values below the lowest value observed in the control. Representative *htz-1*(RNAi) nuclei and corresponding R_r values are shown in Figure 4.4B. A summary of DPY-27/X-Paint colocalization quantification after vector and *htz-1* RNAi is shown in Figure 4.4C.

DCC mislocalization was also observed in intestinal nuclei of homozygous *htz-1(tm2469)* hermaphrodite progeny of heterozygous mothers (m+z-) (Figure

4.5) and in HTZ-1-depleted embryos (Figure 4.12). The mislocalization phenotype observed in *htz-1(tm2469)* (Figure 4.5) mutant animals was very similar to the observations made after *htz-1* RNAi. In wild-type hermaphrodites only 5% of nuclei observed had R_r values below 0.5, but a majority of *htz-1(tm2469)* nuclei (59%) had values below 0.5. Additionally, 45% of nuclei observed had values below the lowest value observed in wild-type nuclei (Figure 4.5B and 4.5C). We also analyzed HTZ-1-depleted embryos after the 50-cell stage in development (after the onset of dosage compensation). We observed 16% of *htz-1*–depleted embryos with a diffuse nuclear DCC localization pattern (as opposed to 2% of vector RNAi control embryos), confirming that DCC mislocalization is not tissue specific (Figure 4.12).

Finally, we analyzed DCC distribution in nuclei of *ssl-1 (n4077)* mutant animals. *ssl-1* encodes a homolog of Swr1, the catalytic subunit of Swr1-com, the complex responsible for exchanging H2A for H2A.Z [93-96]. Consistent with this function, *ssl-1(n4077)* m+z- homozygous animals have reduced HTZ-1 staining (Figure 4.5A). In *ssl-1(n4077)* hermaphrodites, 43% of nuclei observed had R_r values below 0.5, similar to what we observe after *htz-1* RNAi and in *htz-1(tm2469)* animals. Also, 33% of *ssl-1* nuclei had R_r values below the lowest value observed in wild type nuclei, confirming that reduced HTZ-1 disrupts the localization of DCC to the X chromosomes (Figure 4.5B and 4.5C). Together, these results strongly suggest that HTZ-1, a protein more abundant on autosomes, is important for restricting localization of the DCC to the X chromosomes.

DCC localization to autosomes upon HTZ-1 depletion

The portion of DCC which is not associated with the X chromosome appears nonetheless bound to chromatin. When we combined X-Paint FISH/DPY-27 IF with a protocol previously shown to extract nucleoplasmic proteins [97], we were unable to remove the non-X associated DCC within intestinal nuclei of *htz-1* RNAi animals (Figure 4.6A). This suggests that the non-X associated DCC is associated with autosomal chromatin.

To confirm DCC association with autosomes, we analyzed prophase chromosomes in both vector control and *htz-1* depleted embryos. We reasoned that individualized mitotic chromosomes would allow for more conspicuous visualization of DCC localization. To mark mitotic nuclei, embryos were co-stained with α-Phospho-Histone H3 Serine 10. In control embryos, DCC localization was largely restricted to two chromosomes in prophase nuclei. After *htz-1* RNAi, however, 32% of prophase nuclei had low-level DCC staining on more than two chromosomes (Figure 4.6B). These data indicate that the DCC associates not only with the X chromosome, but also with autosomes in HTZ-1-depleted animals. Taken together, these results suggest the existence of an HTZ-1 dependent autosomal repellent activity. In wild type animals, this activity restricts localization of the DCC to the X chromosome. Loss of *htz-1* reduces the efficiency of this repellant, allowing the DCC to bind other chromosomes.

HTZ-1 levels are also reduced on the X chromosomes in the male and hermaphrodite germ lines

In different organisms, H2A.Z has been observed to be either enriched in silent chromatin, (such as mammalian and *Drosophila* centromeres [77-80], or the XY sex body in the mammalian germ line [81]) or depleted in silent chromatin (such as heterochromatic chromocenters in plants [69, 83], or the transcriptionally inactive micronucleus in *Tetrahymena* [60-62]). Dosage compensation in worms is thought to involve two-fold downregulation of gene expression, but not complete silencing [2]. To explore whether HTZ-1 localizes to silent chromatin in worms, we examined its distribution in the germ line, where the X chromosomes are subject to chromosome-wide silencing by a mechanism unrelated to dosage compensation [50]. In the male germ line, the single X chromosome is subject to meiotic silencing of unpaired chromatin and is silent throughout meiosis. In the hermaphrodite germ line, the paired X chromosomes are silent during early meiosis, but become transcriptionally active in later stages [50]. To test HTZ-1 levels on the silent X chromosome in the germ line, we performed immunofluorescence experiments on dissected male and hermaphrodite gonads. To distinguish the X from autosomes we used antibodies specific to MES-4, H3K27me3, or H4K16ac, all of which have been used in previous studies to distinguish the X from autosomes in the germ line. MES-4, a SET-Domain protein, is enriched on autosomes and markedly depleted from the X chromosome in the germ line [51, 57]. Conversely, H3K27me3 is enriched on the silent X chromosomes in the germ line [53]. In the male germ line, H4K16ac

is present on autosomes but absent from the unpaired X chromosome [50]. We found that HTZ-1 levels are much lower on the X chromosomes than on autosomes in both male and hermaphrodite germ lines (Figure 4.7). Thus, underrepresentation of HTZ-1 appears to be a general feature of both types of chromosome-wide repression in the worm: two-fold downregulation by dosage compensation and complete meiotic silencing. The possible involvement of HTZ-1 in germ line X chromosome silencing will be explored elsewhere.

DISCUSSION

Dosage compensation in *C. elegans* is accomplished by the DCC, a complex of proteins that binds the two X chromosomes in hermaphrodites to down-regulate expression of genes two-fold. In this study we report on the role of the histone variant H2A.Z/HTZ-1 in this process. HTZ-1 is less abundant on the dosage compensated X chromosomes in hermaphrodites but is found at higher levels on autosomes and X chromosomes in male somatic cells. When *htz-1* expression is reduced, levels of DCC proteins do not change. However, binding of the DCC is no longer restricted to the X chromosomes and dosage compensation is impaired.

Models for HTZ-1 function in dosage compensation

One of the intriguing challenges in the study of dosage compensation is to understand how the DCC machinery is able to specifically target the X chromosomes for regulation. Our studies indicate that when HTZ-1 is depleted, the DCC appears to be no longer targeted correctly to the X chromosome. Rather than binding solely to the X chromosomes, the complex now binds

autosomes as well. These results reveal that the normal function of HTZ-1 (or an HTZ-1 regulated factor) includes keeping the DCC away from autosomes. Previous studies indicated that specific DCC binding sites on the X chromosome, so-called *rex* sites (*r*ecruiting *e*lement on *X*), are important for attracting the DCC to the X chromosome ([44-47]). Taken together, these data suggest that positive forces (X-specific recruitment elements that attract the DCC) and negative forces (autosomal chromatin that repels the DCC) cooperate to discriminate the X from autosomes (Figure 4.8).

The mechanism of how HTZ-1 restricts DCC localization is unclear. We will consider three possible models. First, HTZ-1 may serve as a direct regulator of DCC binding. Targeting of the DCC to the X chromosome is believed to be a two-step process. The complex initially binds to an estimated 200 *rex* sites, followed by dispersal to numerous so-called *dox* sites (*d*ependent *o*n *X*) or "way stations" [44, 46, 47, 98]. *Rex* sites coincide with the highest peaks of DCC binding and are characterized by the presence and clustering of short sequence motifs called MEX motifs [46, 47, 99]. MEX motifs are slightly enriched on the X chromosome, but are also present on autosomes [46]. In principle, HTZ-1 can affect either DCC targeting to *rex* sites, or dispersal to *dox* sites, or both.

It should be pointed out that this model is different from the interpretation of the HTZ-1 localization data presented in [67]. Using high-resolution analysis of HTZ-1 binding, the authors showed that a subset of DCC peaks on the X chromosome coincide with HTZ-1 peaks. One way to reconcile their data and ours is to point out that the DCC/HTZ-1 overlap tends to be at promoters (DCC

dox sites), and less so at the highest peaks of DCC binding (DCC foci or *rex* sites) [67]. Therefore, if HTZ-1 is a negative regulator of DCC binding, it is more likely that HTZ-1 affects the targeting step to *rex* sites, but not the dispersal step to *dox* sites. Another way to reconcile the data in the two studies is to suggest that HTZ-1 at *dox* sites is modified posttranslationally (see below) in such a way that permits DCC binding. According to this model, MEX motifs attract DCC to the X chromosome, whereas HTZ-1 negatively regulates DCC recruitment to *rex* sites. If a MEX motif-containing sequence is not bound by HTZ-1 the DCC will be recruited. However, if a MEX motif-containing sequence is bound by HTZ-1, the DCC will be prevented from binding. From sites of entry, the DCC then may be dispersed to *dox* sites in a sequence and HTZ-1 independent manner. When HTZ-1 levels are reduced by RNAi or mutation, the DCC will be able to bind all MEX motif containing sites, whether they are on the autosomes or on the X chromosome. Ectopic DCC binding to autosomes will reduce the amount of DCC binding to the X chromosomes, and dosage compensation will be impaired as a result. To test this model, it will be important to observe DCC binding patterns genome-wide at high resolution upon *htz-1* depletion and to determine whether ectopic DCC binding sites contain a DNA sequence motif similar to MEX motifs.

An alternative possibility is that changes in the higher order chromatin organization imposed by HTZ-1 determine whether the DCC is able to bind the chromosome. H2A.Z has been reported to alter the nucleosome surface, affect recruitment of other chromatin components, and thereby modulate higher order features of the chromatin fiber [77]. High levels of HTZ-1 on the autosomes may

result in alterations in the overall structure of the chromatin fiber, which preclude DCC binding. Low levels of HTZ-1 on the X chromosome would allow DCC binding. Upon reduction of HTZ-1 levels, general disruption of higher order chromatin folding would allow the DCC to bind both the X and the autosomes. According to this model, the changes in chromatin fiber folding are a direct consequence of HTZ-1 levels on the chromosome. However, the model does not require complete mutually exclusive binding of the DCC and HTZ-1 at high resolution, and therefore does not conflict with the data in [67].

Finally, HTZ-1 may regulate expression of a DCC component, or another gene needed for proper DCC localization. While HTZ-1 is an obvious candidate for the DCC-repelling activity, it should be noted that in principle another HTZ-1-regulated protein could also perform this function. Our evidence, as yet, does not support this model, as we do not observe a change in DCC protein levels or *sdc-2* RNA levels when *htz-1* expression is reduced. In addition, most DCC proteins are loaded into oocytes, and this maternal load of DCC proteins is sufficient for healthy development. Therefore, it is unlikely that the observed dosage compensation defects in m+z- *htz-1* mutant animals are due to defects in transcription of DCC genes. However, it remains possible that HTZ-1 plays more subtle roles in regulating the exact levels and timing of expression of dosage compensation genes. Nonetheless, the difference in HTZ-1 levels in male and hermaphrodite X chromosomes (Figure 4.2C) argue for a more direct role for HTZ-1 in the hermaphrodite specific-process of dosage compensation. High-

resolution analysis of HTZ-1 binding to the male X chromosome may help distinguish between the models presented above.

HTZ-1 depletion on the X chromosome

A question that remains unanswered is how HTZ-1 is specifically targeted to autosomes, or conversely, how the X chromosomes become depleted of HTZ-1. The small number of developmentally important genes on the X chromosome relative to autosomes can certainly contribute to this difference [67]. However, this model does not explain why the male X in adult animals does not appear to be depleted of HTZ-1 at the chromosomal level (Figure 4.2C). The X chromosome in the both the male and hermaphrodite germ lines is subject to silencing [50-52], and it is possible that the chromosome maintains some memory of this silencing after fertilization. Such effects have been seen on the sperm-derived X chromosome [100]. The differences between the sperm derived X (which only hermaphrodite embryos receive) and the oocyte-derived X (which both males and hermaphrodites receive) may contribute to the sex-specific differences in observed X-linked HTZ-1 levels. Comparison of HTZ-1 dynamics in male and hermaphrodite embryos in early development will be an important future area of investigation.

Different HTZ-1 pools for different functions

It is important to keep in mind that dosage compensation is a chromosome-wide gene regulation mechanism that is super-imposed on the unique transcriptional programs of individual X-linked genes. While HTZ-1 levels on the dosage compensated X chromosomes are reduced overall, the protein is

not completely absent. Indeed, HTZ-1 binds to the promoter of an X-linked dosage compensated gene, *myo-2*, and is needed for its proper temporal activation [73]. It is possible that a pool of HTZ-1 functions at promoters, including promoters on the X chromosome, to promote timely regulation of gene expression. Superimposed on that is the global repression of the X chromosome by the DCC. Thus, HTZ-1 may perform a double role: it regulates genes both individually (by binding to promoters) and chromosome-wide (by regulating DCC binding).

Different pools of HTZ-1 may differ in their histone partners and/or the level of posttranslational modifications. Unlike yeast (where the only histone H3 is most similar to H3.3), worms possess both H3 and H3.3 [90]. Therefore, in principle, one population of HTZ-1 in worms is able to form labile nucleosomes, while another population can form stable nucleosomes. Furthermore, both populations can be modified by various posttranslational modifications, increasing the number of potentially different ways in which HTZ-1 can affect genome activity. Consistent with this idea, acetylation of the N-terminal tail of Htz1 is necessary for the anti-silencing property of Htz1 in *S. cerevisiae*, as unacetylatable Htz1 shows no change in localization to anti-silenced genes, but Sir complex spreading and decreased expression of anti-silenced genes is observed [101]. Htz1 is also subject to C-terminal SUMOylation. SUMO-Htz1 is implicated in directing chromosomes with persistent double-strand breaks to re-localize to the nuclear periphery in budding yeast [102]. Posttranslational modification of H2A.Z has also been observed in mammalian dosage

compensation [25]. H2A.Z is under-represented on the inactive X in female mouse nuclei, but the small population of remaining H2A.Z is specifically mono-ubiquitylated by the Ring1b E3 ligase as part of the Polycomb repressor complex 1 (PRC1). Ring1b is also responsible for mono-ubiquitylation of histone H2A in X inactivation [24]. Although it is not currently understood how mono-ubiquitylation of H2A and H2A.Z function in X inactivation, the fact that this modification is largely specific to the inactive X suggests an important role. It is highly likely that *C. elegans* HTZ-1 is subject to posttranslational modification and it will be important to address how these modifications affect its role both in dosage compensation and in other processes.

Barriers to repressor complex binding

The proposed role of HTZ-1 in dosage compensation is similar to that of two proteins shown to function in germ line X-chromosome silencing in *C. elegans*. The gene encoding MES-4 was originally identified in a forward genetic screen with several other genes whose mutations led to the same *mes* phenotype (*m*aternal *e*ffect *s*terility) [51]. MES-2, MES-3 and MES-6, are the protein products of the other genes identified, and these form a Polycomb repressor-like complex that is responsible for enriching the X chromosomes with the silencing H3K27me3 mark [53]. Surprisingly, MES-4, a histone H3 lysine 36 methyltransferase (HMT), localizes to autosomes, not the X, and yet it has been shown to be important for germ line X-chromosome silencing [51, 57]. MRG-1, an ortholog of the mammalian mortality factor related protein MRG15, is the second autosome-enriched protein that has been shown to play a role in germ

line X chromosome silencing [103]. In both *mes-4* and *mrg-1* mutants, de-silencing of X-linked genes is observed. It has been proposed that the activities of MES-4 and MRG-1 on autosomes prevent the binding of a repressor protein or complex and help limit repressor binding to the X chromosomes. The proposed mode of action of MRG-1 and MES-4 in germ line X chromosome silencing is similar to the model of HTZ-1 function in dosage compensation we have proposed.

Our model describing HTZ-1 as an autosomal DCC barrier is also similar to the role of Htz1 in yeast in blocking the spread of silencing complexes into euchromatic regions adjacent to telomeres [74]. In *htz1Δ* cells, the Sir proteins spread into these regions, leading to silencing of genes. Recent evidence has shown that loss of Htz1 leads to ectopic Sir complex localization that is not limited to immediate anti-silenced regions, but, rather, is found throughout the genome [75]. Thus, Htz1p in yeast may serve a global, not just a local, anti-silencing function, similar to our proposed model of HTZ-1 action in worms. Furthermore, in *Arabidopsis*, H2A.Z also plays a global antisilencing role by protecting DNA from methylation [69]. When H2A.Z incorporation is compromised, DNA methylation expands into regions once protected by H2A.Z-containing nucleosomes. Therefore, a function for H2A.Z in the protection against transcriptional repression may be a widely conserved role for this histone variant.

Htz1 functions in parallel with other nucleosomal elements to prevent heterochromatic spreading. The Set1 complex is responsible for histone H3 lysine 4 methylation (H3K4me) and also has an anti-silencing function [104]. A

recent study found that Set1 and Htz1 cooperate to mediate global antisilencing in yeast [75]. This raises the possibility that there are other nucleosomal modifications or elements that might function in X-chromosome DCC restriction in parallel with HTZ-1 in *C. elegans.*

Materials and Methods

Strains and alleles

All strains used were maintained as described [105]. Strains include: N2 Bristol strain (wild type), TY2384 *sex-1(y263)* X; TY4403 *him-8(e1489)* IV*; xol-1(y9) sex-1(y263)* X*;* EKM11 *htz-1(tm2469)* IV*/nT1(qIs51)* IV,V*;* MT12963 *ssl-1(n4077)III/eT1* (III;V); SM1353 *cha-1(p1182)* IV*; pxEx214(HTZ-1promoter::YFP::HTZ-1 + HTZ-1promoter::CFP::LacI +pRF4)* [73].

RNA interference

E. coli HT115 bacteria expressing double stranded RNA for *htz-1*, *dpy-27*, *capg-1*, *his-71* (coding region), *his-24, hil-3, hil-4, hil-5, hil-6, hil-7, isw-1* or vector (polylinker), were used for feeding RNAi using the Ahringer feeding RNAi clones [106]. To generate RNAi vectors for *let-418* and the 3' UTR of *his-71* and *his-72*, the regions were PCR amplified, digested with Bam HI and Bgl II (*let-418*) or Bgl II and Not I (*his-71* and *his-72*), and cloned into the DT7 vector as described [106]. The following primers were used for amplification:

his-71 3'-UTR

cgaagatctcgtgcataaacgttgagctg and gagcggccgccatgcacgctgttcaaaaac

his-72 3'-UTR

cgaagatctagctccatcaccaattctcg and gagcggccggcgtggaatatagttgct

let-418

catgggatccttgccgctcctcattcaact and gtacagatctgacgatgtgcacgagagaaa

RNAi in N2 was initiated at the L1-L2 stage. Adults were then transferred to new RNAi plates to produce progeny for 24 hours. For IF/FISH, western, and RT-PCR analysis, RNAi progeny were processed 24 hours post-L4. To score embryonic lethality in the *sex-1* strain, adult animals were allowed to lay eggs for 24 hours and the number of embryos laid was counted. The next day the number of dead embryos and larvae were counted and the percentage of embryonic lethality was calculated by dividing number of dead embryos by the total number of embryos laid. To score male rescue in *him-8(e1489) IV; xol-1(y9) sex-1(y263) X*, adult animals were allowed to lay eggs for 24 hours. When adult animals were removed from the RNAi plates, the number of embryos laid was counted. Three days later the number of male progeny on each plate was counted. Male viability was calculated by dividing the number of male progeny observed by the expected number of males. The *him-8(e1489)* mutation reproducibly results in 38% male self-progeny [89], so the expected number of males was determined to be 38% of total embryos laid. Male rescue = Number of males/(total embryos x 0.38). All RNAi was conducted at 20°C.

Immunostaining

Rabbit and rat α-HTZ-1 antibodies were raised against the C-terminal 19 amino acids (NKKGAPVPGKPGAPGQGPQ) and affinity purified. Polyclonal rat α-HTZ-1 was used at a dilution of 1:500, polyclonal rabbit α-HTZ-1 at a dilution of 1:100 for immunofluorescence. Other primary antibodies used are: polyclonal rabbit α-

DPY-27 at a dilution of 1:100 [38], polyclonal rabbit α-MES-4 (Susan Strome [UC Santa Cruz], [57]) at 1:100, rabbit antiserum α-acetyl-histone H4 (Lys16) (Upstate) at 1:100, rabbit polyclonal α-trimethyl-histone H3 (Lys27) (Upstate) at 1:500, and mouse monoclonal α-phospho-histone H3S10 (6G3) (Cell Signaling Technology) at 1:500. Secondary antibodies used are: Fluorescein (FITC) conjugated donkey α-rabbit (Jackson ImmunoResearch) and Cy3 conjugated donkey α-rabbit IgG (Jackson ImmunoResearch) both at a dilution of 1:100. Embryos were stained as described [34]. Adult animals were dissected and stained as described [44]. In adults, somatic non-intestinal nuclei near the cut site (vulval area) were observed. Images were captured with a Hamamatsu ORCA-ERGA CCD camera mounted on an Olympus BX61 motorized X-drive microscope using a 60X oil immersion objective. Captured images were deconvolved using 3i Slidebook imaging software. Projected images were taken at 0.2μm intervals through samples. Adobe Photoshop was used for assembling images.

Fluorescent *in situ* hybridization

FISH probe templates were generated by degenerate oligonucleotide primed PCR to amplify purified yeast artificial chromosome DNA. The labeled X-paint probe was prepared and used as described [44]. Hybridization was performed on adult animals (24 hours post-L4) with or without previous RNAi treatment. For X-paint hybridization followed by DPY-27 immunostaining, sample and probe were denatured at 95°C for 3 minutes. For X-paint hybridization followed by HTZ-1 immunostaining, sample and probe were denatured at 78-80°C for 8-10

minutes in a Hybaid OmniSlide *in situ* Thermal Cycler System (Thermo Scientific). Imaging was conducted as described above.

Quantification of colocalization

3i Slidebook imaging software was used to measure colocalization of DPY-27 (FITC) and X-Paint (Cy3) signals on images obtained as described above. A FITC mask was set for each nucleus z-stack and the correlation between signals was calculated within this mask by the software. The FITC:Cy3 correlation coefficient was recorded and used as an indication of colocalization between DPY-27 and X-Paint.

Detergent extraction

Detergent extraction of nucleoplasmic protein from dissected nuclei was performed by dissecting animals in 1X sperm salts plus 1% Triton detergent [97]. Dissected animals were then processed for either Fluorescent *in situ* hybridization or immunofluorescence.

Western Blot Analysis

For each treatment described, 100 animals (all 24 hours post-L4) were picked into 1XM9, washed, and incubated for ten minutes at 95°C in 19µl SDS-PAGE loading dye (0.1M Tris-HCl pH 6.8, 75M Urea, 2% SDS, Bromophenol Blue for color) plus 1µl β-mercaptoethanol. The treated samples were then loaded into either 6% acrylamide (for detection of DPY-27, MIX-1, DPY-26, DPY-28, and CAPG-1) or 15% acrylamide gels (for detection of HTZ-1). SDS-PAGE was performed and protein was transferred onto nitrocellulose. The following antibodies and dilutions were used: rabbit α-HTZ-1 at 1:500, rabbit α-DPY-27 at

1:500, rabbit α-CAPG-1 at 1:500 [38], rabbit α-DPY-28 (gift of K. Hagstrom) at 1:500, rabbit α-DPY-26 (gift of K. Hagstrom) at 1:5000, rabbit α-MIX-1 (gift of R. Chan) at 1:500, mouse monoclonal α- α-Tubulin (Sigma) at 1:1000, LI-COR IRDye 800CW Conjugated Goat (polyclonal) □-Mouse IgG at 1:10000, LI-COR IRDye 800CW Conjugated Goat (polyclonal) □-Rabbit IgG at 1:10000. Blots were scanned and band intensities were quantified using an Odyssey Infrared Imaging System (LI-COR Biosciences). Protein levels for DCC proteins and HTZ-1 were normalized to α-tubulin. Relative protein levels after *htz-1* RNAi were calculated by dividing the normalized *htz-1* RNAi level by normalized vector RNAi level.

RT-PCR

Trizol (Invitrogen) was used to extract RNA from all samples. Worms were washed from RNAi plates or normal OP50 plates 24 hours post L4, washed with M9 and stored at -80°C until extraction. For RNA extraction, samples were thawed on ice and tissue was homogenized by grinding using a microcentrifuge tube pestle. Tissue was ground in three 60-second intervals and re-frozen in liquid nitrogen between each interval. During the final 60-second interval, 250µl of Trizol was added to the tube, and when completed, another 250 µl was added for a total volume of 500µl Trizol and the standard protocol was used to extract RNA from the homogenized samples (Invitrogen). DNA-Free kit (Applied Biosystems) was used to digest remaining DNA contamination.

Reverse transcription (RT) reactions were performed utilizing the High Capacity cDNA Reverse Transcription Kit with RNase Inhibitor (Applied Biosystems). 1µl of DNase-treated RNA was used in each RT reaction.

PCR was used to observe relative levels of *htz-1*, R08C7.10, and *act-1* (actin) expression levels. The following primers were used with a 60°C annealing temperature:

act-1: gctatgttccagccatccttc and aagagcggtgatttccttctg

htz-1: tggctggaggaaaaggaaag and aacgatggatgtgtgggatg

R08C7.10: gtagaccaaaccagccagca and agcgccttgacgatacttttt

Real-time PCR analysis

Real-time PCR analysis was conducted as described [98]. The following primers were used with an annealing temperature of 59°C:

act-1: same as above

htz-1: gcgctgccatcctcgaat and gggctcccttcttgttcatc

sdc-2: ggaaacaagaccgacaggaa and gatgcaatagtacacgccaaatc

Relative *htz-1* and *sdc-1* expression levels were calculated using the Pfaffl method [107] incorporating the PCR efficiency for each primer set as determined by a 10-fold dilution series for each primer set in each reaction. Reactions were conducted in triplicate per experiment. Data shown are resulting averages from three experiments.

Acknowledgements

We thank S. Strome for the α-MES-4 antibody, S. Mango for the SM1353 YFP-HTZ-1 strain, K. Hagstrom for the α-DPY-26 and -28 antibodies, R. Chan for the

α-MIX-1 antibody, the *Caenorhabditis* Genetics Center for strains, and S. Mitani (National BioResource Project, Japan) for the *htz-1(tm2469)/+* deletion strain. We also thank Mohamed Taki for assistance with the RNAi assays, B. Kelly, Jason Lieb, R. Chan, and K. Nabeshima for helpful comments and suggestions.

References

1. Mendjan S, Akhtar A (2007) The right dose for every sex. Chromosoma 116(2): 95-106.
2. Meyer BJ (2005) X-Chromosome dosage compensation. In: *The C. elegans* Research Community, editor. WormBook: doi/10.1895/wormbook.1.8.1, http://wormbook.org.
3. Payer B, Lee JT (2008) X Chromosome Dosage Compensation: How Mammals Keep the Balance. Annu Rev Genet 42: 733-772.
4. Straub T, Becker PB (2007) Dosage compensation: the beginning and end of generalization. Nat Rev Genet 8(1): 47-57.
5. Lucchesi JC, Kelly WG, Panning B (2005) Chromatin Remodeling in Dosage Compensation. Annu Rev Genet.
6. Hamada FN, Park PJ, Gordadze PR, Kuroda MI (2005) Global regulation of X chromosomal genes by the MSL complex in Drosophila melanogaster. Genes Dev 19(19): 2289-2294.
7. Straub T, Gilfillan GD, Maier VK, Becker PB (2005) The Drosophila MSL complex activates the transcription of target genes. Genes Dev 19(19): 2284-2288.
8. Palmer MJ, Mergner VA, Richman R, Manning JE, Kuroda MI *et al*. (1993) The male-specific lethal-one (msl-1) gene of Drosophila melanogaster encodes a novel protein that associates with the X chromosome in males. Genetics 134(2): 545-557.
9. Zhou S, Yang Y, Scott MJ, Pannuti A, Fehr KC *et al*. (1995) Male-specific lethal 2, a dosage compensation gene of Drosophila, undergoes sex-specific regulation and encodes a protein with a RING finger and a metallothionein-like cysteine cluster. Embo J 14(12): 2884-2895.
10. Gorman M, Franke A, Baker BS (1995) Molecular characterization of the male-specific lethal-3 gene and investigations of the regulation of dosage compensation in Drosophila. Development 121(2): 463-475.
11. Kuroda MI, Kernan MJ, Kreber R, Ganetzky B, Baker BS (1991) The maleless protein associates with the X chromosome to regulate dosage compensation in Drosophila. Cell 66(5): 935-947.
12. Gu W, Szauter P, Lucchesi JC (1998) Targeting of MOF, a putative histone acetyl transferase, to the X chromosome of Drosophila melanogaster. Dev Genet 22(1): 56-64.
13. Amrein H, Axel R (1997) Genes expressed in neurons of adult male Drosophila. Cell 88(4): 459-469.

14. Meller VH, Wu KH, Roman G, Kuroda MI, Davis RL (1997) roX1 RNA paints the X chromosome of male Drosophila and is regulated by the dosage compensation system. Cell 88(4): 445-457.
15. Turner BM, Birley AJ, Lavender J (1992) Histone H4 isoforms acetylated at specific lysine residues define individual chromosomes and chromatin domains in Drosophila polytene nuclei. Cell 69(2): 375-384.
16. Akhtar A, Becker PB (2000) Activation of transcription through histone H4 acetylation by MOF, an acetyltransferase essential for dosage compensation in Drosophila. Mol Cell 5(2): 367-375.
17. Hilfiker A, Hilfiker-Kleiner D, Pannuti A, Lucchesi JC (1997) mof, a putative acetyl transferase gene related to the Tip60 and MOZ human genes and to the SAS genes of yeast, is required for dosage compensation in Drosophila. Embo J 16(8): 2054-2060.
18. Kind J, Vaquerizas JM, Gebhardt P, Gentzel M, Luscombe NM *et al*. (2008) Genome-wide analysis reveals MOF as a key regulator of dosage compensation and gene expression in Drosophila. Cell 133(5): 813-828.
19. Borsani G, Tonlorenzi R, Simmler MC, Dandolo L, Arnaud D *et al*. (1991) Characterization of a murine gene expressed from the inactive X chromosome. Nature 351(6324): 325-329.
20. Brockdorff N, Ashworth A, Kay GF, Cooper P, Smith S *et al*. (1991) Conservation of position and exclusive expression of mouse Xist from the inactive X chromosome. Nature 351(6324): 329-331.
21. Brown CJ, Ballabio A, Rupert JL, Lafreniere RG, Grompe M *et al*. (1991) A gene from the region of the human X inactivation centre is expressed exclusively from the inactive X chromosome. Nature 349(6304): 38-44.
22. Clemson CM, McNeil JA, Willard HF, Lawrence JB (1996) XIST RNA paints the inactive X chromosome at interphase: evidence for a novel RNA involved in nuclear/chromosome structure. J Cell Biol 132(3): 259-275.
23. Plath K, Fang J, Mlynarczyk-Evans SK, Cao R, Worringer KA *et al*. (2003) Role of histone H3 lysine 27 methylation in X inactivation. Science 300(5616): 131-135.
24. de Napoles M, Mermoud JE, Wakao R, Tang YA, Endoh M *et al*. (2004) Polycomb group proteins Ring1A/B link ubiquitylation of histone H2A to heritable gene silencing and X inactivation. Dev Cell 7(5): 663-676.
25. Sarcinella E, Zuzarte PC, Lau PN, Draker R, Cheung P (2007) Monoubiquitylation of H2A.Z distinguishes its association with euchromatin or facultative heterochromatin. Mol Cell Biol 27(18): 6457-6468.
26. Boggs BA, Cheung P, Heard E, Spector DL, Chinault AC *et al*. (2002) Differentially methylated forms of histone H3 show unique association patterns with inactive human X chromosomes. Nat Genet 30(1): 73-76.
27. Costanzi C, Pehrson JR (1998) Histone macroH2A1 is concentrated in the inactive X chromosome of female mammals. Nature 393(6685): 599-601.
28. Chadwick BP, Willard HF (2003) Chromatin of the Barr body: histone and non-histone proteins associated with or excluded from the inactive X chromosome. Hum Mol Genet 12(17): 2167-2178.

29. Chaumeil J, Okamoto I, Guggiari M, Heard E (2002) Integrated kinetics of X chromosome inactivation in differentiating embryonic stem cells. Cytogenet Genome Res 99(1-4): 75-84.
30. Belyaev N, Keohane AM, Turner BM (1996) Differential underacetylation of histones H2A, H3 and H4 on the inactive X chromosome in human female cells. Hum Genet 97(5): 573-578.
31. Boggs BA, Connors B, Sobel RE, Chinault AC, Allis CD (1996) Reduced levels of histone H3 acetylation on the inactive X chromosome in human females. Chromosoma 105(5): 303-309.
32. Jeppesen P, Turner BM (1993) The inactive X chromosome in female mammals is distinguished by a lack of histone H4 acetylation, a cytogenetic marker for gene expression. Cell 74(2): 281-289.
33. Bernstein E, Muratore-Schroeder TL, Diaz RL, Chow JC, Changolkar LN *et al*. (2008) A phosphorylated subpopulation of the histone variant macroH2A1 is excluded from the inactive X chromosome and enriched during mitosis. Proc Natl Acad Sci U S A 105(5): 1533-1538.
34. Chuang PT, Albertson DG, Meyer BJ (1994) DPY-27:a chromosome condensation protein homolog that regulates C. elegans dosage compensation through association with the X chromosome. Cell 79(3): 459-474.
35. Lieb JD, Albrecht MR, Chuang PT, Meyer BJ (1998) MIX-1: an essential component of the C. elegans mitotic machinery executes X chromosome dosage compensation. Cell 92(2): 265-277.
36. Lieb JD, Capowski EE, Meneely P, Meyer BJ (1996) DPY-26, a link between dosage compensation and meiotic chromosome segregation in the nematode. Science 274(5293): 1732-1736.
37. Tsai CJ, Mets DG, Albrecht MR, Nix P, Chan A *et al*. (2008) Meiotic crossover number and distribution are regulated by a dosage compensation protein that resembles a condensin subunit. Genes Dev 22(2): 194-211.
38. Csankovszki G, Collette K, Spahl K, Carey J, Snyder M *et al*. (2009) Three distinct condensin complexes control C. elegans chromosome dynamics. Curr Biol 19(1): 9-19.
39. Dawes HE, Berlin DS, Lapidus DM, Nusbaum C, Davis TL *et al*. (1999) Dosage compensation proteins targeted to X chromosomes by a determinant of hermaphrodite fate. Science 284(5421): 1800-1804.
40. Davis TL, Meyer BJ (1997) SDC-3 coordinates the assembly of a dosage compensation complex on the nematode X chromosome. Development 124(5): 1019-1031.
41. Hsu DR, Chuang PT, Meyer BJ (1995) DPY-30, a nuclear protein essential early in embryogenesis for Caenorhabditis elegans dosage compensation. Development 121(10): 3323-3334.
42. Chu DS, Dawes HE, Lieb JD, Chan RC, Kuo AF *et al*. (2002) A molecular link between gene-specific and chromosome-wide transcriptional repression. Genes Dev 16(7): 796-805.

43. Villeneuve AM, Meyer BJ (1987) sdc-1: a link between sex determination and dosage compensation in C. elegans. Cell 48(1): 25-37.
44. Csankovszki G, McDonel P, Meyer BJ (2004) Recruitment and spreading of the C. elegans dosage compensation complex along X chromosomes. Science 303(5661): 1182-1185.
45. Ercan S, Giresi PG, Whittle CM, Zhang X, Green RD *et al*. (2007) X chromosome repression by localization of the C. elegans dosage compensation machinery to sites of transcription initiation. Nat Genet 39(3): 403-408.
46. Jans J, Gladden JM, Ralston EJ, Pickle CS, Michel AH *et al*. (2009) A condensin-like dosage compensation complex acts at a distance to control expression throughout the genome. Genes Dev 23(5): 602-618.
47. McDonel P, Jans J, Peterson BK, Meyer BJ (2006) Clustered DNA motifs mark X chromosomes for repression by a dosage compensation complex. Nature 444(7119): 614-618.
48. Meyer BJ, Casson LP (1986) Caenorhabditis elegans compensates for the difference in X chromosome dosage between the sexes by regulating transcript levels. Cell 47(6): 871-881.
49. Hirano T (2005) Condensins: organizing and segregating the genome. Curr Biol 15(7): R265-275.
50. Kelly WG, Schaner CE, Dernburg AF, Lee MH, Kim SK *et al*. (2002) X-chromosome silencing in the germ line of C. elegans. Development 129(2): 479-492.
51. Fong Y, Bender L, Wang W, Strome S (2002) Regulation of the different chromatin states of autosomes and X chromosomes in the germ line of C. elegans. Science 296(5576): 2235-2238.
52. Garvin C, Holdeman R, Strome S (1998) The phenotype of mes-2, mes-3, mes-4 and mes-6, maternal-effect genes required for survival of the germ line in Caenorhabditis elegans, is sensitive to chromosome dosage. Genetics 148(1): 167-185.
53. Bender LB, Cao R, Zhang Y, Strome S (2004) The MES-2/MES-3/MES-6 complex and regulation of histone H3 methylation in C. elegans. Curr Biol 14(18): 1639-1643.
54. Holdeman R, Nehrt S, Strome S (1998) MES-2, a maternal protein essential for viability of the germ line in Caenorhabditis elegans, is homologous to a Drosophila Polycomb group protein. Development 125(13): 2457-2467.
55. Korf I, Fan Y, Strome S (1998) The Polycomb group in Caenorhabditis elegans and maternal control of germ line development. Development 125(13): 2469-2478.
56. Xu L, Fong Y, Strome S (2001) The Caenorhabditis elegans maternal-effect sterile proteins, MES-2, MES-3, and MES-6, are associated in a complex in embryos. Proc Natl Acad Sci U S A 98(9): 5061-5066.
57. Bender LB, Suh J, Carroll CR, Fong Y, Fingerman IM *et al*. (2006) MES-4: an autosome-associated histone methyltransferase that participates in silencing the X chromosomes in the C. elegans germ line. Development 133(19): 3907-3917.

58. Reuben M, Lin R (2002) Germ line X chromosomes exhibit contrasting patterns of histone H3 methylation in Caenorhabditis elegans. Dev Biol 245(1): 71-82.
59. Jin C, Felsenfeld G (2007) Nucleosome stability mediated by histone variants H3.3 and H2A.Z. Genes Dev 21(12): 1519-1529.
60. Allis CD, Richman R, Gorovsky MA, Ziegler YS, Touchstone B *et al*. (1986) hv1 is an evolutionarily conserved H2A variant that is preferentially associated with active genes. J Biol Chem 261(4): 1941-1948.
61. Stargell LA, Bowen J, Dadd CA, Dedon PC, Davis M *et al*. (1993) Temporal and spatial association of histone H2A variant hv1 with transcriptionally competent chromatin during nuclear development in Tetrahymena thermophila. Genes Dev 7(12B): 2641-2651.
62. Wenkert D, Allis CD (1984) Timing of the appearance of macronuclear-specific histone variant hv1 and gene expression in developing new macronuclei of Tetrahymena thermophila. J Cell Biol 98(6): 2107-2117.
63. Guillemette B, Bataille AR, Gevry N, Adam M, Blanchette M *et al*. (2005) Variant histone H2A.Z is globally localized to the promoters of inactive yeast genes and regulates nucleosome positioning. PLoS Biol 3(12): e384.
64. Li B, Pattenden SG, Lee D, Gutierrez J, Chen J *et al*. (2005) Preferential occupancy of histone variant H2AZ at inactive promoters influences local histone modifications and chromatin remodeling. Proc Natl Acad Sci U S A 102(51): 18385-18390.
65. Raisner RM, Hartley PD, Meneghini MD, Bao MZ, Liu CL *et al*. (2005) Histone variant H2A.Z marks the 5' ends of both active and inactive genes in euchromatin. Cell 123(2): 233-248.
66. Zhang H, Roberts DN, Cairns BR (2005) Genome-wide dynamics of Htz1, a histone H2A variant that poises repressed/basal promoters for activation through histone loss. Cell 123(2): 219-231.
67. Whittle CM, McClinic KN, Ercan S, Zhang X, Green RD *et al*. (2008) The genomic distribution and function of histone variant HTZ-1 during C. elegans embryogenesis. PLoS Genet 4(9): e1000187.
68. Mavrich TN, Jiang C, Ioshikhes IP, Li X, Venters BJ *et al*. (2008) Nucleosome organization in the Drosophila genome. Nature 453(7193): 358-362.
69. Zilberman D, Coleman-Derr D, Ballinger T, Henikoff S (2008) Histone H2A.Z and DNA methylation are mutually antagonistic chromatin marks. Nature.
70. Barski A, Cuddapah S, Cui K, Roh TY, Schones DE *et al*. (2007) High-resolution profiling of histone methylations in the human genome. Cell 129(4): 823-837.
71. Adam M, Robert F, Larochelle M, Gaudreau L (2001) H2A.Z is required for global chromatin integrity and for recruitment of RNA polymerase II under specific conditions. Mol Cell Biol 21(18): 6270-6279.
72. Brickner DG, Cajigas I, Fondufe-Mittendorf Y, Ahmed S, Lee PC *et al*. (2007) H2A.Z-mediated localization of genes at the nuclear periphery confers epigenetic memory of previous transcriptional state. PLoS Biol 5(4): e81.

73. Updike DL, Mango SE (2006) Temporal regulation of foregut development by HTZ-1/H2A.Z and PHA-4/FoxA. PLoS Genet 2(9): e161.
74. Meneghini MD, Wu M, Madhani HD (2003) Conserved histone variant H2A.Z protects euchromatin from the ectopic spread of silent heterochromatin. Cell 112(5): 725-736.
75. Venkatasubrahmanyam S, Hwang WW, Meneghini MD, Tong AH, Madhani HD (2007) Genome-wide, as opposed to local, antisilencing is mediated redundantly by the euchromatic factors Set1 and H2A.Z. Proc Natl Acad Sci U S A 104(42): 16609-16614.
76. Bruce K, Myers FA, Mantouvalou E, Lefevre P, Greaves I *et al*. (2005) The replacement histone H2A.Z in a hyperacetylated form is a feature of active genes in the chicken. Nucleic Acids Res 33(17): 5633-5639.
77. Fan JY, Rangasamy D, Luger K, Tremethick DJ (2004) H2A.Z alters the nucleosome surface to promote HP1alpha-mediated chromatin fiber folding. Mol Cell 16(4): 655-661.
78. Greaves IK, Rangasamy D, Ridgway P, Tremethick DJ (2007) H2A.Z contributes to the unique 3D structure of the centromere. Proc Natl Acad Sci U S A 104(2): 525-530.
79. Rangasamy D, Berven L, Ridgway P, Tremethick DJ (2003) Pericentric heterochromatin becomes enriched with H2A.Z during early mammalian development. Embo J 22(7): 1599-1607.
80. Swaminathan J, Baxter EM, Corces VG (2005) The role of histone H2Av variant replacement and histone H4 acetylation in the establishment of Drosophila heterochromatin. Genes Dev 19(1): 65-76.
81. Greaves IK, Rangasamy D, Devoy M, Marshall Graves JA, Tremethick DJ (2006) The X and Y chromosomes assemble into H2A.Z-containing [corrected] facultative heterochromatin [corrected] following meiosis. Mol Cell Biol 26(14): 5394-5405.
82. Chadwick BP, Willard HF (2001) Histone H2A variants and the inactive X chromosome: identification of a second macroH2A variant. Hum Mol Genet 10(10): 1101-1113.
83. Deal RB, Topp CN, McKinney EC, Meagher RB (2007) Repression of flowering in Arabidopsis requires activation of FLOWERING LOCUS C expression by the histone variant H2A.Z. Plant Cell 19(1): 74-83.
84. Cui M, Han M (2007) Roles of chromatin factors in C. elegans development. WormBook: 1-16.
85. Carmi I, Kopczynski JB, Meyer BJ (1998) The nuclear hormone receptor SEX-1 is an X-chromosome signal that determines nematode sex. Nature 396(6707): 168-173.
86. Carmi I, Meyer BJ (1999) The primary sex determination signal of Caenorhabditis elegans. Genetics 152(3): 999-1015.
87. Gladden JM, Farboud B, Meyer BJ (2007) Revisiting the X:A signal that specifies Caenorhabditis elegans sexual fate. Genetics 177(3): 1639-1654.

88. Miller LM, Plenefisch JD, Casson LP, Meyer BJ (1988) xol-1: a gene that controls the male modes of both sex determination and X chromosome dosage compensation in C. elegans. Cell 55(1): 167-183.
89. Hodgkin J, Horvitz HR, Brenner S (1979) Nondisjunction Mutants of the Nematode CAENORHABDITIS ELEGANS. Genetics 91(1): 67-94.
90. Ooi SL, Priess JR, Henikoff S (2006) Histone H3.3 variant dynamics in the germ line of Caenorhabditis elegans. PLoS Genet 2(6): e97.
91. Jedrusik MA, Schulze E (2001) A single histone H1 isoform (H1.1) is essential for chromatin silencing and germ line development in Caenorhabditis elegans. Development 128(7): 1069-1080.
92. Hedgecock EM, White JG (1985) Polyploid tissues in the nematode Caenorhabditis elegans. Dev Biol 107(1): 128-133.
93. Kobor MS, Venkatasubrahmanyam S, Meneghini MD, Gin JW, Jennings JL *et al*. (2004) A protein complex containing the conserved Swi2/Snf2-related ATPase Swr1p deposits histone variant H2A.Z into euchromatin. PLoS Biol 2(5): E131.
94. Krogan NJ, Baetz K, Keogh MC, Datta N, Sawa C *et al*. (2004) Regulation of chromosome stability by the histone H2A variant Htz1, the Swr1 chromatin remodeling complex, and the histone acetyltransferase NuA4. Proc Natl Acad Sci U S A 101(37): 13513-13518.
95. Krogan NJ, Keogh MC, Datta N, Sawa C, Ryan OW *et al*. (2003) A Snf2 family ATPase complex required for recruitment of the histone H2A variant Htz1. Mol Cell 12(6): 1565-1576.
96. Mizuguchi G, Shen X, Landry J, Wu WH, Sen S *et al*. (2004) ATP-driven exchange of histone H2AZ variant catalyzed by SWR1 chromatin remodeling complex. Science 303(5656): 343-348.
97. Chan RC, Severson AF, Meyer BJ (2004) Condensin restructures chromosomes in preparation for meiotic divisions. J Cell Biol 167(4): 613-625.
98. Blauwkamp TA, Csankovszki G (2009) Two classes of dosage compensation complex binding elements along Caenorhabditis elegans X chromosomes. Mol Cell Biol 29(8): 2023-2031.
99. Ercan S, Lieb JD (2009) C. elegans dosage compensation: a window into mechanisms of domain-scale gene regulation. Chromosome Res 17(2): 215-227.
100. Bean CJ, Schaner CE, Kelly WG (2004) Meiotic pairing and imprinted X chromatin assembly in Caenorhabditis elegans. Nat Genet 36(1): 100-105.
101. Babiarz JE, Halley JE, Rine J (2006) Telomeric heterochromatin boundaries require NuA4-dependent acetylation of histone variant H2A.Z in Saccharomyces cerevisiae. Genes Dev 20(6): 700-710.
102. Kalocsay M, Hiller NJ, Jentsch S (2009) Chromosome-wide Rad51 spreading and SUMO-H2A.Z-dependent chromosome fixation in response to a persistent DNA double-strand break. Mol Cell 33(3): 335-343.
103. Takasaki T, Liu Z, Habara Y, Nishiwaki K, Nakayama J *et al*. (2007) MRG-1, an autosome-associated protein, silences X-linked genes and protects

germ line immortality in Caenorhabditis elegans. Development 134(4): 757-767.
104. Krogan NJ, Dover J, Khorrami S, Greenblatt JF, Schneider J *et al*. (2002) COMPASS, a histone H3 (Lysine 4) methyltransferase required for telomeric silencing of gene expression. J Biol Chem 277(13): 10753-10755.
105. Brenner S (1974) The genetics of Caenorhabditis elegans. Genetics 77(1): 71-94.
106. Ahringer JE (2005) Reverse genetics. In: The *C. elegans* Research Community, editor. Wormbook: doi/10.1895/wormbook.1.8.1, http://www.wormbook.org.
107. Pfaffl MW (2001) A new mathematical model for relative quantification in real-time RT-PCR. Nucleic Acids Res 29(9): e45.

Table 4.1. RNAi of the following genes did not result in significant (> 10%) male rescue.

locus	gene name	description
Y17G7B.2	ash-2	homolog of Drosophila Ash2, member of histone acetyltransferase complex
F25D7.3	blmp-1	zinc finger and SET domain containing protein
R10E11.1	cbp-1	homolog of mammalian CBP/p300 histone acetyltransferase
T14G8.1	chd-3	SNF2 family member, contain chromo domain
F20D12.1	csr-1	Argonaute protein required for chromosome segregation
ZK783.4	flt-1	PHD and bromo domain containing protein
M04B2.3	gfl-1	TFIIF transcription factor
C46A5.9	hcf-1	putative subunit of COMPASS histone methyltransferase complex
C08B11.2	hda-2	class I histone deacetylase
C10E2.3	hda-4	class II histone deacetylase
F22F1.1	hil-3	H1.3 histone
C18G1.5	hil-4	H1.4 histone
B0414.3	hil-5	H1.5 histone
F59A7.4	hil-6	H1.6 histone
C01B10.5	hil-7	H1.Q histone
M163.3	his-24	H1.1 histone
F45E1.6	his-71	H3.3 histone variant
Y49E10.6	his-72	H3.3 histone variant
K08H2.6	hpl-1	Heterochromatin protein 1 homolog
K01G5.2	hpl-2	Heterochromatin protein 1 homolog
F37A4.8	isw-1	homolog of chromatin remodeling ATPase ISW1
F26F12.7	let-418	homolog of Mi-2/CHD3, subunit of NURD complex
F11A10.1	lex-1	similar to yeast Yta7p, contains bromo domain
F42A9.2	lin-49	zinc finger and bromo domain containing protein
F42A9.2	lin-49	zinc finger and bromo domain containing protein
T12F5.4	lin-59	SET domain containing protein
T08D10.2	lsd-1	homolog of histone demethylase LSD1
C01G8.9	lss-4	ARID/BRIGHT DNA binding domain containing protein
M04B2.1	mep-1/gei-2	putative NURD/CHD complex subunit
R06A4.7	mes-2	Homolog of Enhancer of zeste, contains SET domain
F54C1.3	mes-3	member of the Polycomb-like repressive complex
Y2H9A.1	mes-4	SET domain containing protein, germline development
C09G4.5	mes-6	homolog of Drosophila extra sex combs, interacts with MES-2
R05D3.11	met-2	H3K36 and H3K9 methylation
Y37D8A.9	mrg-1	homolog of mammalian MRG15, contains chromodomain
VC5.4	mys-1	MYST family histone acetyltransferase
K03D10.3	mys-2	MYST family histone acetyltransferase, similar to MOF

C34B7.4	mys-4	MYST family histone acetyltransferase
C26C6.1	pbrm-1	similar to human polybromo 1
Y47G6A.6	pcaf-1	PCAF/GCN5-like histone acetyltransferase
F02E9.4	pqn-28	SIN3 homolog
C01G5.2	prg-2	Piwi subfamily Argonaute protein, germ-line stem cell division
F01G4.1	psa-4	SWI2/SNF2 ortholog
C47E12.4	pyp-1	similar to Drosophila NURF-38 and human PPA1
K07A1.11	rba-1	nucleosome remodeling factor, subunit CAF1
B0205.3	rpn-10	implicated in histone ubiquitination
ZK20.5	rpn-12	implicated in histone ubiquitination
T26A5.7	set-1	SET domain containing protein
F34D6.4	set-11	H3K9 methyltransferase homolog
K09F5.5	set-12	H3K9 methyltransferase homolog
R11E3.4	set-15	SET domain containing protein, germline development
T12D8.1	set-16	zinc finger and SET domain containing protein
T21B10.5	set-17	SET domain containing protein, similar to human PRDM11 and PRDM7
W01C8.3	set-19	SET domain containing protein
C26E6.9	set-2	SET domain containing protein
Y32F6A.1	set-22	SET domain containing protein
Y41D4B.12	set-23	SET domain containing protein
C07A9.7	set-3	similar to human SMYD4, contains SET domain
C32D5.5	set-4	H4K20 methyltransferase homolog
C47E8.8	set-5	SET domain containing protein
C49F5.2	set-6	H3K9 methyltransferase homolog
F02D10.7	set-8	paralog of histone methyltransferase MES-4
F15E6.1	set-9	PHD-zinc finger and SET domain containing protein
K12C11.2	smo-1	SUMO
R07E5.3	snfc-5	ortholog of SWI/SNF subunit SNF5
C50E10.4	sop-2	SAM domain, member of Polycomb group
Y40B1B.6	spr-5	homolog of histone demethylase LSD1
W04A8.7	taf-1	homolog of TAF250, histone acetyltransferase
C14B1.4	tag-125	homolog of histone methyltransferase subunit WDR5
C01H6.7	tag-298	Bromo domain containing protein
ZK856.13	tag-315	RNA Pol III transcription factor TFIIIC
Y119C1B.8	tag-332	bromodomain containing protein
C47D12.1	trr-1	TRRAP-like histone acetyltransferase complex subunit homolog
D2013.9	ttll-2/set-7	putative tubulin polyaminoacid ligase
D2096.8	D2096.8	similar to nucleosome assembly protein NAP-1
F32E10.2	F32E10.2	HP-1 like and chromo domain containing protein
F32E10.6	F32E10.6	chromo domain containing protein
F52B11.1	F52B11.1	PHD finger, SynMuv suppressor
F59E12.1	F59E12.1	bromodomain containing protein

H06O01.2	H06O01.2	putative chromodomain helicase, similar to human CHD1
H20J04.2	H20J04.2	similar to chromatin remodeling complex WSTF-ISWI large subunit
K06A5.1	K06A5.1	chromo domain containing protein
K08F4.2	K08F4.2	SynMuv suppressor, involved in germline silencing
Y37D8A.11	Y37D8A.11	chromo domain containing protein
F54E12.2	F54E12.2	RNA Pol II termination factor TTF2-like
ZK1127.3	ZK1127.3	putative subunit of TPI60/NuA4 histone acetyltransferase complex
ZK1127.7	ZK1127.7	DNA gyrase/topoisomerase
T09A5.8	T09A5.8	chromo domain containing protein
T12E12.2	T12E12.2	chromo domain containing protein
T23B12.1	T23B12.1	Polycomb-like PHD zinc finger protein
Y57G11C.19	Y57G11C.19	chromo domain containing protein
C50A2.2	C50A2.2	chromo domain containing protein
CD4.7	CD4.7	putative SWR1/SCRAP complex member

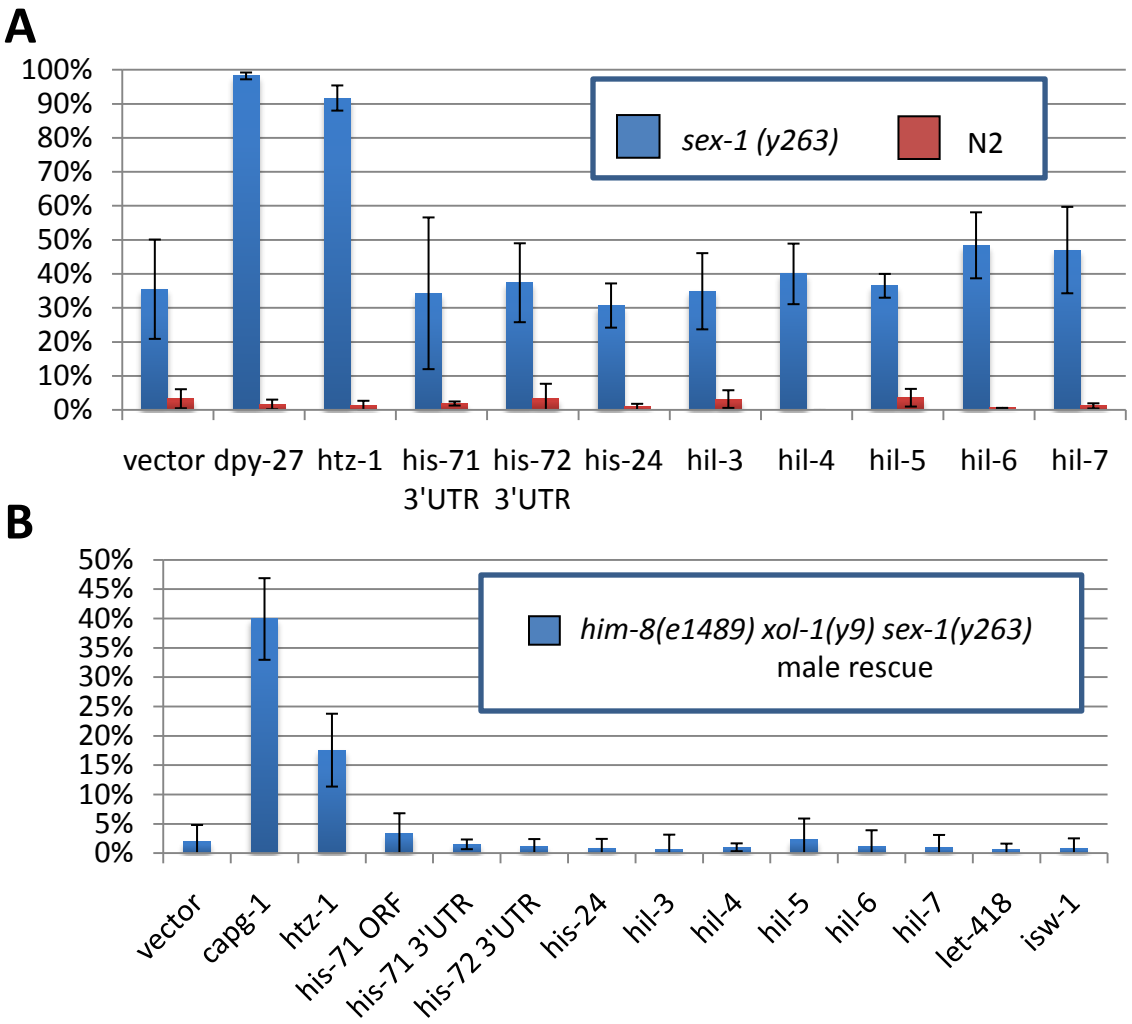

Figure 4.1 HTZ-1 function is needed for dosage compensation
(A) Embryonic lethality caused by feeding RNAi in wild type (N2) and *sex-1(y263)* X hermaphrodite worms. RNAi of both *dpy-27* (n_{N2}= 1173; n_{sex-1}= 566) and *htz-1* (n_{N2}= 1292; n_{sex-1}= 385) leads to synergistic embryonic lethality in the *sex-1* mutant background that is significantly different from levels observed after vector RNAi (n_{N2}= 459; n_{sex-1}= 504) ($p=1.84\times10^{-5}$, and $p=4.9\times10^{-5}$ respectively). RNAi of *his-71* (3'-UTR, n_{N2}=1901 ;n_{sex-1}=1037), *his-72* (3'-UTR, n_{N2}=2821; n_{sex-1}=1381), *his-24* (n_{N2}=438; n_{sex-1}=933), *hil-3* (n_{N2}=378; n_{sex-1}=682), *hil-4* (n_{N2}=412; n_{sex-1}=853), *hil-5* (n_{N2}=440; n_{sex-1}=1083) , *hil-6* (n_{N2}=350; n_{sex-1}=481) , or *hil-7* (n_{N2}=413; n_{sex-1}=882) does not significantly affect *sex-1* embryonic lethality compared to vector. (B) Male survival caused by feeding RNAi in *him-8(e1489) IV; xol-1(y9) sex-1(y263)* X worms. Both *capg-1* (n=771) and *htz-1* (n=1337) RNAi rescue a significant proportion of males ($p=5.2\times10^{-6}$ and $p=3.8\times10^{-4}$ respectively) compared to vector (n=1245). RNAi of *his-71* (coding region, n=623), *his-71* (3'-UTR, n=1786), *his-72* (3'-UTR, n=639), *his-24* (n=633), *hil-3* (n=810), *hil-4* (n=1332), *hil-5* (n=1847), *hil-6* (n=1139), and *hil-7* (n=868), *isw-1*(n=1004), or *let-418* (n=1313) does not lead to significant male rescue. Error bars indicate standard deviation for four experiments. Asterisks indicate a p value of less than 0.05 by student's T-test analysis comparing vector and experimental RNAi data.

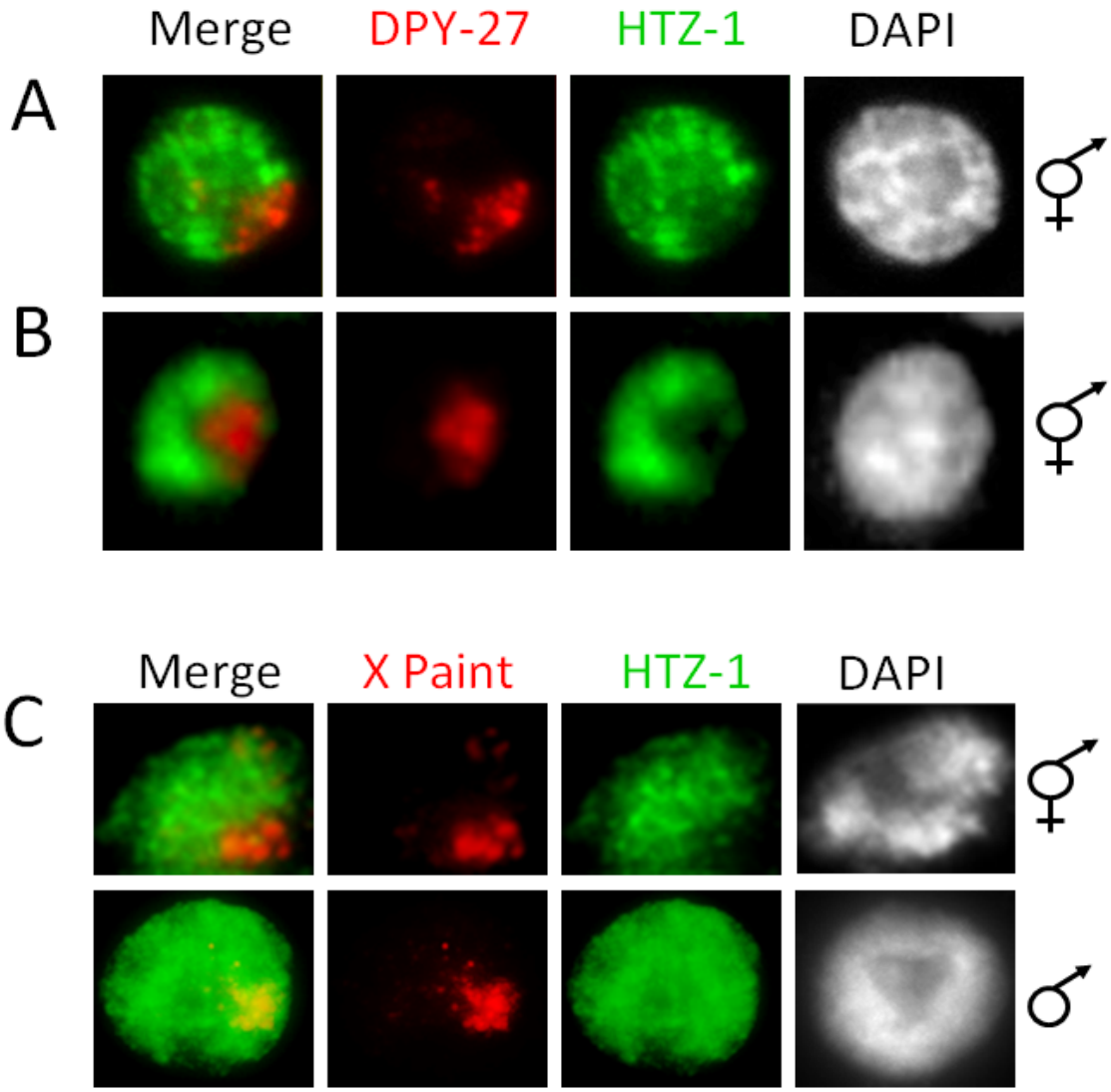

Figure 4.2 HTZ-1 depletion on dosage compensated X chromosomes. HTZ-1 and DPY-27 localization by IF in hermaphrodite adult somatic nucleus (A) and embryonic nucleus after the onset of dosage compensation (B). HTZ-1 (green) staining is reduced in the region containing the X chromosomes, as marked by DPY-27 (red) staining. (C) HTZ-1 localization by IF (green) and X-Chromosome labeling by FISH (red) in adult hermaphrodite (top) and male (bottom) somatic nuclei. HTZ-1 staining is reduced on the hermaphrodite X chromosomes but not on the male X chromosome.

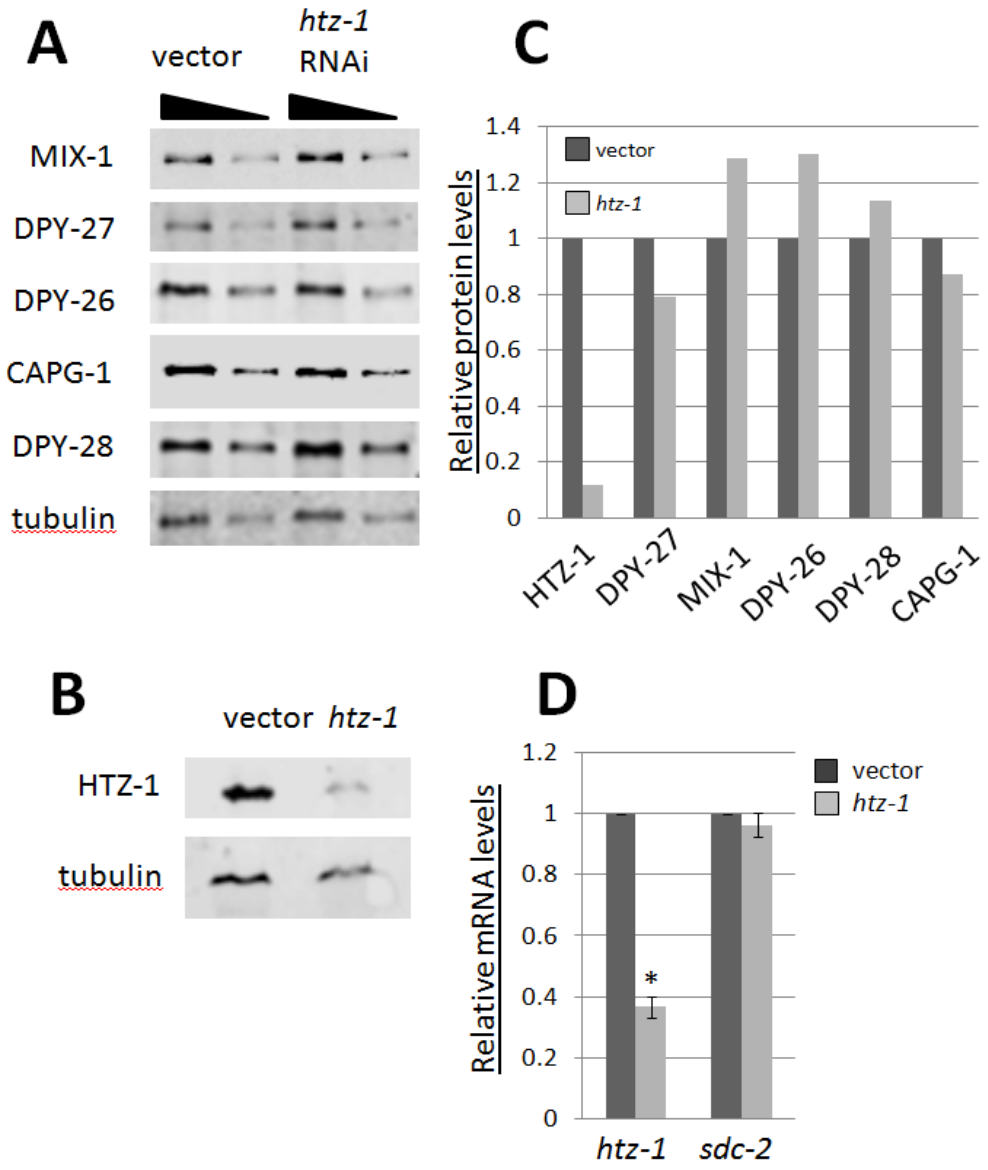

Figure 4.3 *htz-1* RNAi does not significantly decrease DCC levels. HTZ-1 levels were reduced by feeding RNAi in wild type worms. (A and B) An equal number of control vector and *htz-1* RNAi adult animals were collected for quantitative western blot analysis to observe levels of HTZ-1, MIX-1, DPY-27, DPY-26, CAPG-1, DPY-28 and α-Tubulin (loading control) after RNAi treatment. Band intensities were quantified and normalized to tubulin (C). RNAi significantly reduces HTZ-1 levels, but no significant decrease was seen in levels of DCC subunits. Vector and *htz-1* RNAi adults were also collected for RT-qPCR analysis (D). *htz-1* expression is significantly reduced in *htz-1* animals ($p=3.1x10^{-6}$), but there is no significant difference in *sdc-2* expression between vector and *htz-1* RNAi animals.

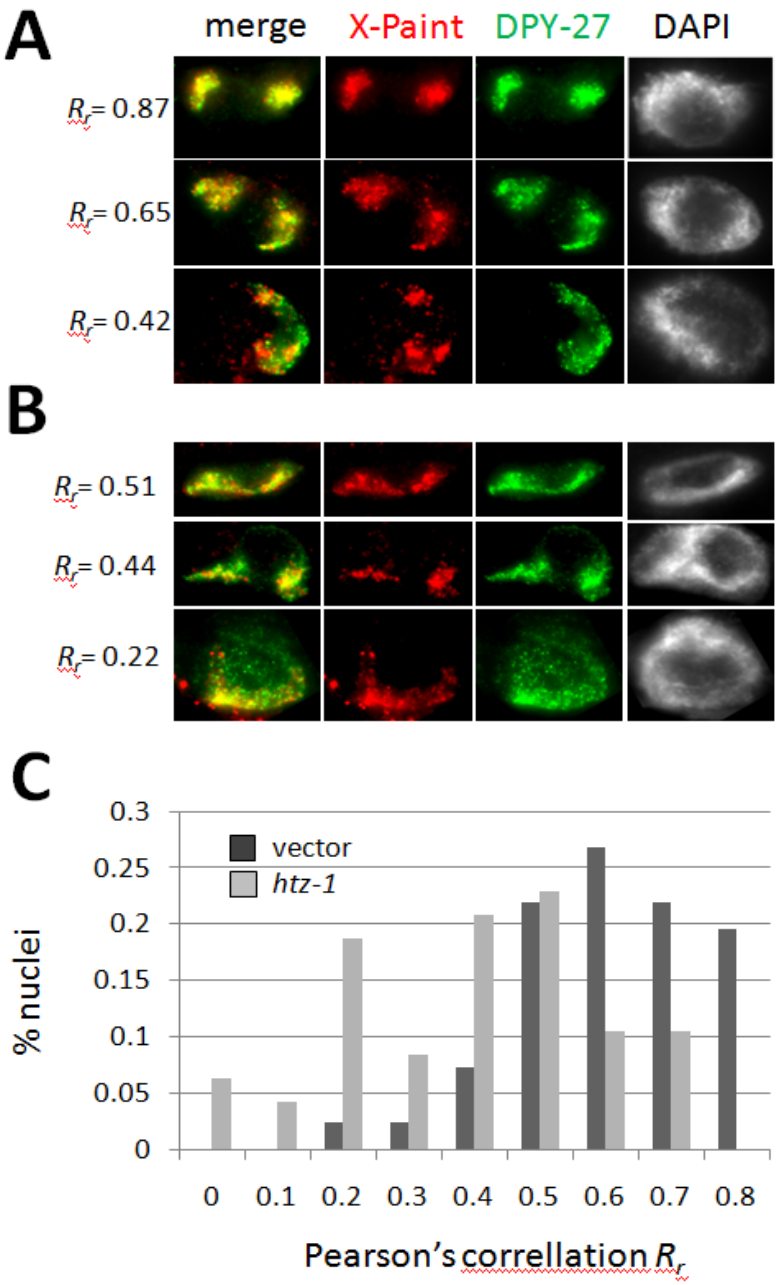

Figure 4.4 HTZ-1 depletion disrupts DCC restriction to the X chromosomes. Adult hermaphrodite intestinal nuclei were stained with α-DPY-27 (green), X-paint FISH probe (red) and DAPI (gray). (**A**) Representative nuclei observed after vector RNAi treatment. (B) Representative nuclei observed after *htz-1* RNAi treatment. (**C**) Summary of quantification of DPY-27 colocalization with the X chromosomes following vector and *htz-1* RNAi treatment. After vector RNAi, the average R_r value from three independent experiments was 0.65±0.14 (n=41). After *htz-1* RNAi, the average value from three independent experiments was reduced to 0.44±0.2 (n=48).

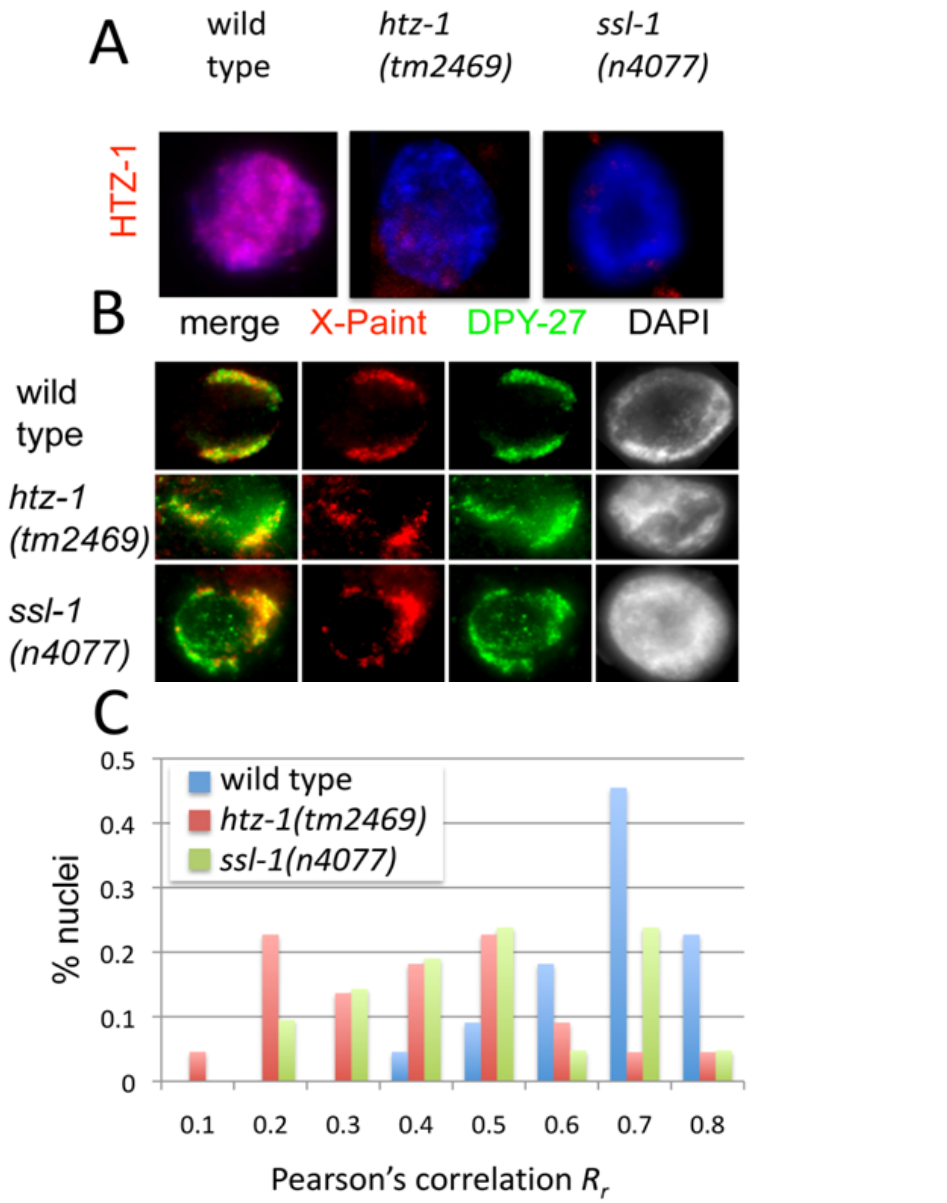

Figure 4.5 DCC mislocalization in *htz-1(tm2469)* and *ssl-1(n4077)* adult hermaphrodites. (A) HTZ-1 (red) and DAPI (blue) staining in wild-type, *htz-1(tm2469)* m+z- and *ssl-1(n4077)* m+z- adult hermaphrodite intestinal nuclei. HTZ-1 levels are reduced in *htz-1(tm2469)*m+z- and *ssl-1(n4077)* m+z- adult hermaphrodites. (B) Representative wild type (R_r=0.67) , *htz-1(tm2469)*m+z- (R_r =0.18) and *ssl-1(n4077)* m+z- (R_r =0.33) adult hermaphrodite intestinal nuclei stained with α-DPY-27 (green), X-paint FISH probe (red) and DAPI (grayscale). (C) Summary of quantification of DPY-27 colocalization with the X chromosomes observed in wild type (mean R_r =0.70, n=22), *htz-1(tm2469)*m+z- (mean R_r =0.45, n=22) and *ssl-1(n4077)* m+z- (mean R_r =0.54, n=21) adult hermaphrodite intestinal nuclei.

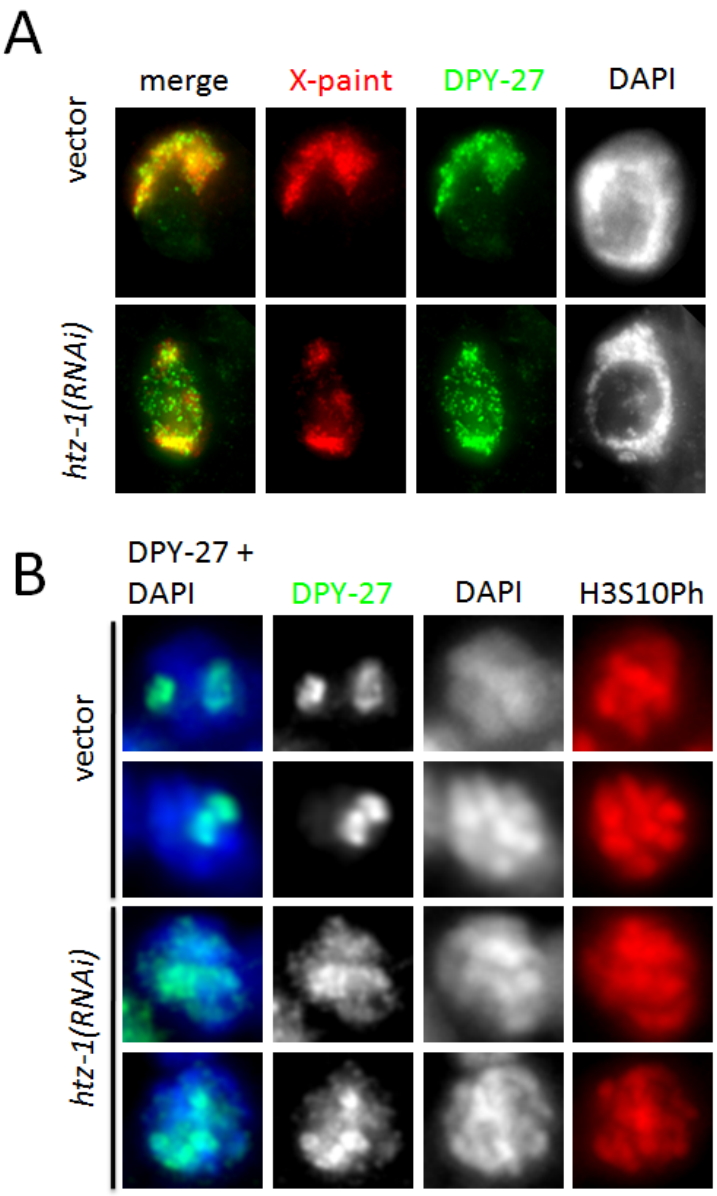

Figure 4.6 DCC associates with autosomes in HTZ-1-depleted cells. (A) DPY-27 (green) and X-chromosome (red) localization in vector and *htz-1* RNAi treated hermaphrodite adult intestinal nuclei after detergent extraction of nucleoplasmic proteins. DCC staining not in association with the X chromosomes remains after detergent extraction in *htz-1* RNAi animals. (B) DPY-27 (green) localization to prophase chromosomes (DAPI, blue) in vector and *htz-1* RNAi treated embryonic nuclei (>50 cell stage). DPY-27 staining to more than two chromosomes is observed in 32% of *htz-1(RNAi)* prophase nuclei (n= 63) but only observed in 11% of vector prophase nuclei (n=57). Mitotic nuclei were identified using an antibody that recognizes H3S10Ph (red).

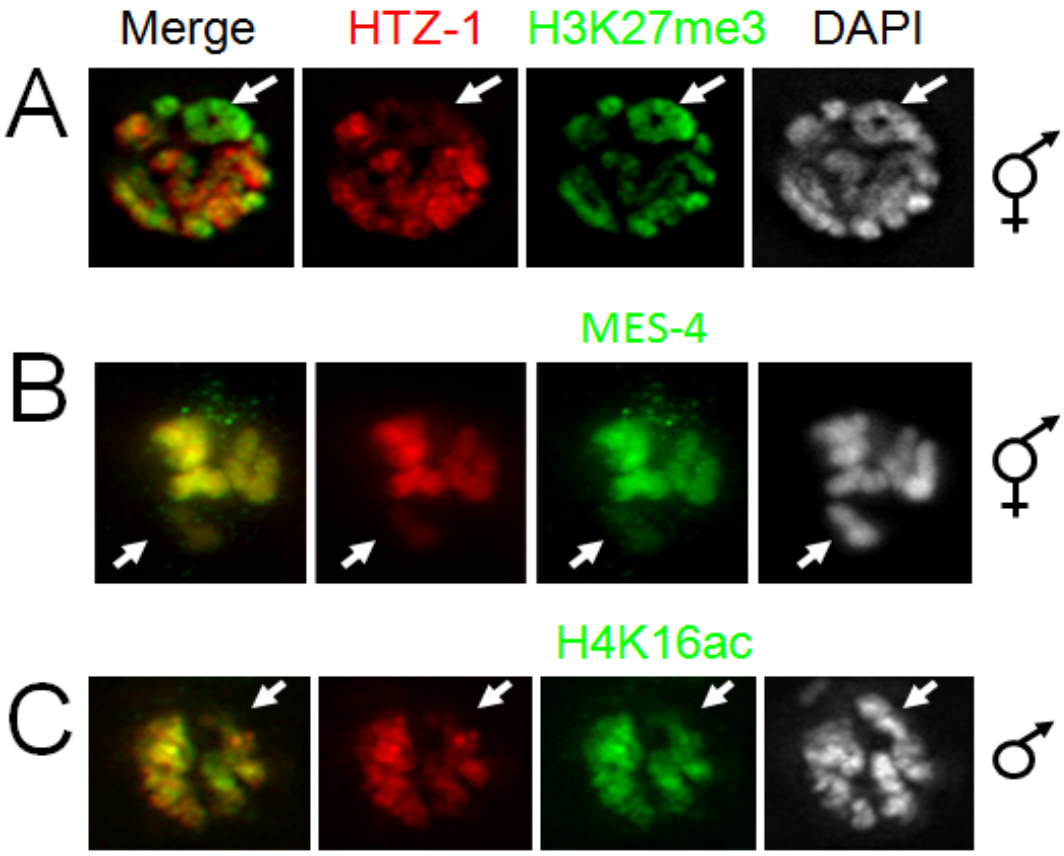

Figure 4.7 HTZ-1 is underrepresented on the silent X chromosomes of male and hermaphrodite germ lines. (**A**) Hermaphrodite germ nucleus in pachytene of prophase I of meiosis stained with antibodies specific to H3K27me3 (a mark enriched on the X, green), HTZ-1 (red), and DAPI (grayscale). (**B**) Hermaphrodite germ nucleus in diplotene of prophase I co-stained for MES-4 (enriched on autosomes, green), HTZ-1 (red), and DAPI (grayscale). (**C**) Male germ nucleus in pachytene of prophase I co-stained for H4K16ac (enriched on autosomes, green), HTZ-1 (red) and DAPI (grayscale). In all cases, HTZ-1 levels are lower on the X chromosome (arrows) than on autosomes.

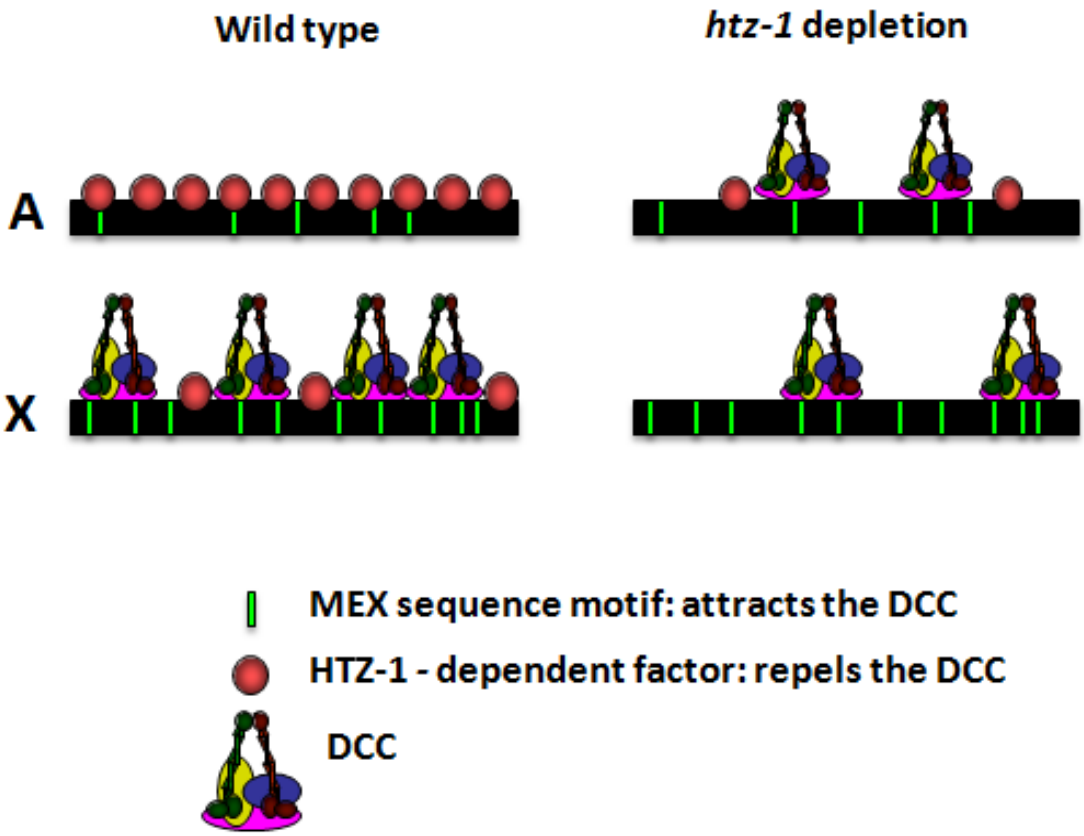

Figure 4.8. Model for HTZ-1 function in dosage compensation. DNA sequence motifs, which are enriched on the X chromosome (X), attract the DCC. HTZ-1, or a factor/activity dependent on HTZ-1, is enriched on autosomes (A) and repels the DCC. As a consequence of these two forces, in wild type cells the DCC is greatly enriched on the X chromosomes. However, when HTZ-1 levels are low, the DCC is now able to bind both the X chromosomes and the autosomes. Ectopic DCC binding on autosomes titrates the complex away from the X chromosomes and impairs dosage compensation.

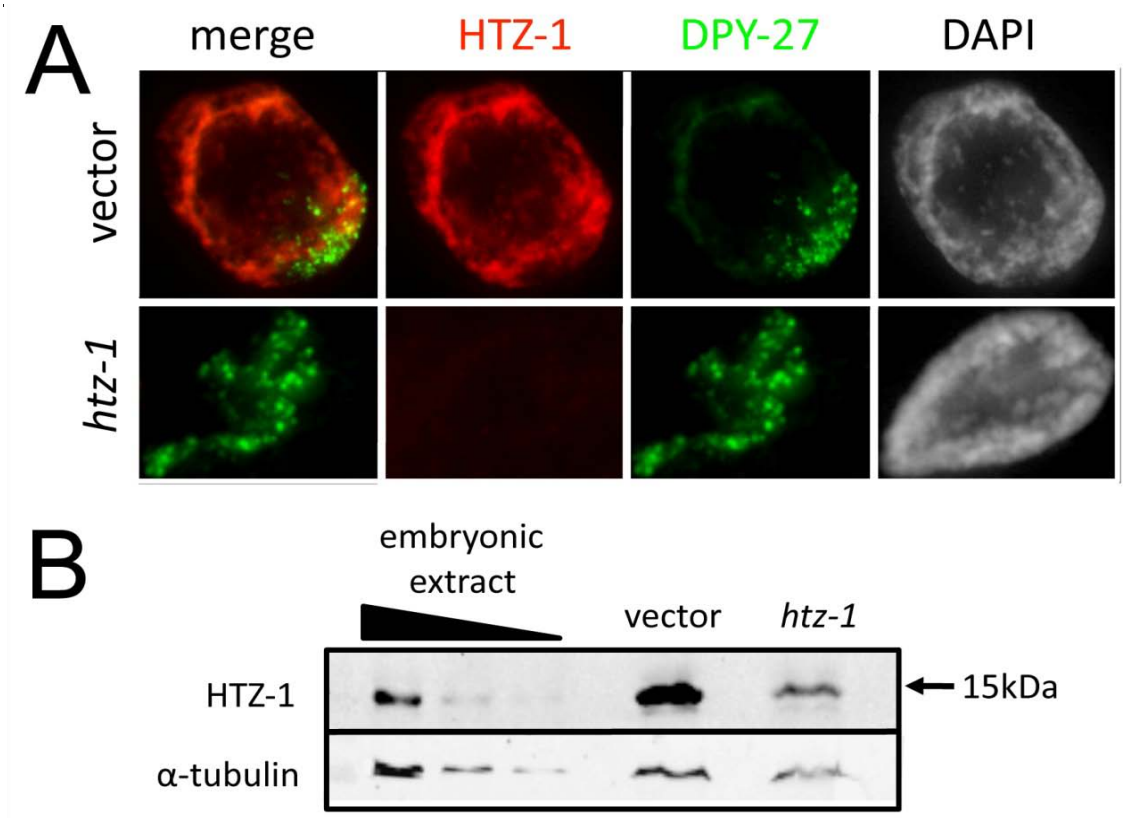

Figure 4.9 α-HTZ-1 antibody is specific. (A) HTZ-1 (red), DPY-27 (green), and DAPI (grayscale) staining of adult intestinal nuclei in vector and *htz-1* RNAi treated hermaphrodites. The HTZ-1 signal is greatly reduced after *htz-1* RNAi. (B) α-HTZ-1 Western blot. α-HTZ-1 recognizes a band of the expected size (~15 kDa) in both embryonic extract and adult protein samples. The α-HTZ-1 signal is reduced in *htz-1* RNAi treated animals as compared to vector treated animals.

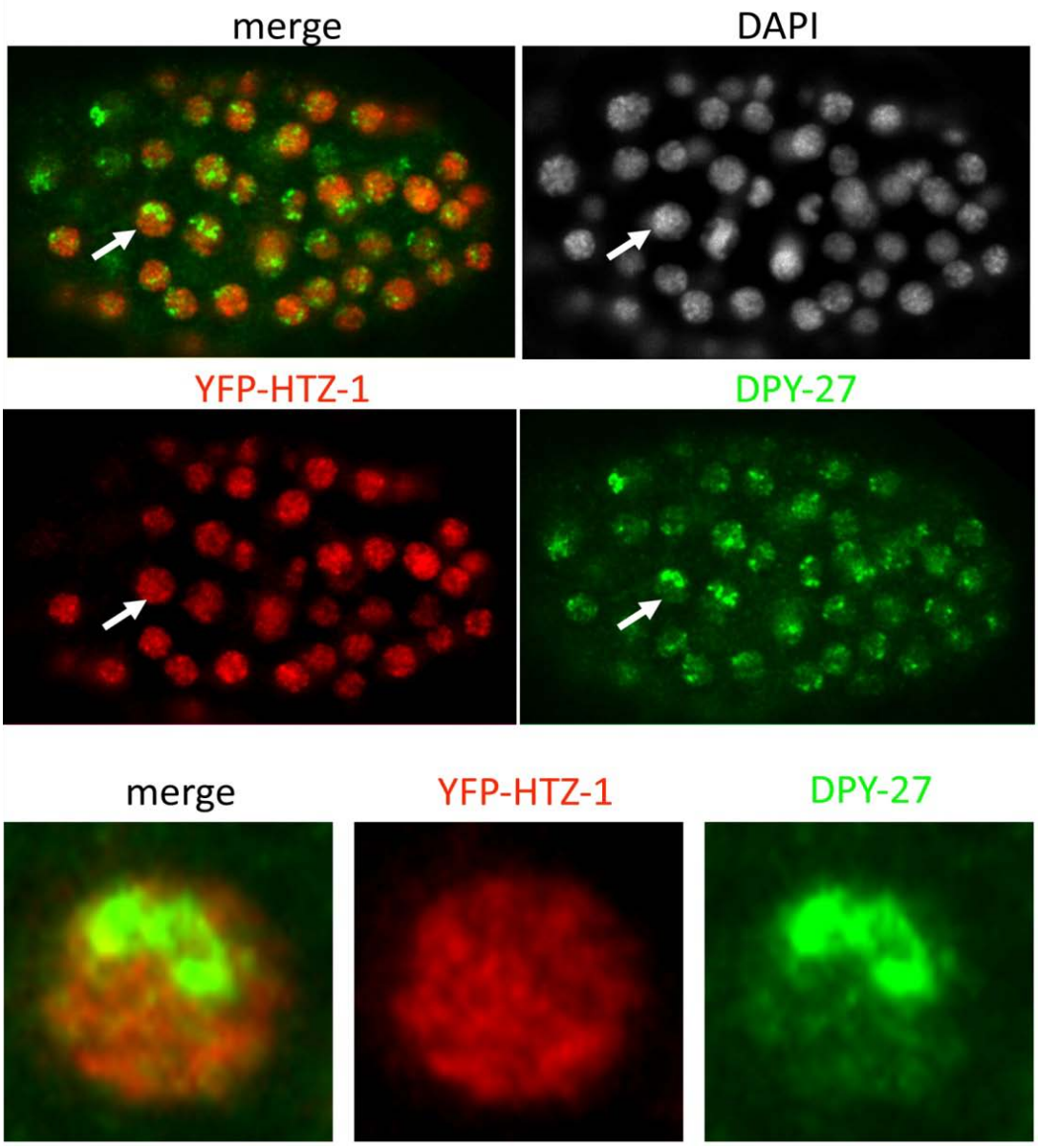

Figure 4.10 Transgenic YFP-HTZ-1 is also under-represented on the dosage compensated X chromosomes. Embryos after the onset of dosage compensation were stained with α-GFP antibodies to observe YFP-HTZ-1 localization (red), α-DPY-27 to mark the X chromosome (green) and DAPI (grayscale). Arrows in the top panels indicate enlarged nucleus shown below. YFP-HTZ-1 levels are reduced in the territory of the dosage compensated X chromosomes.

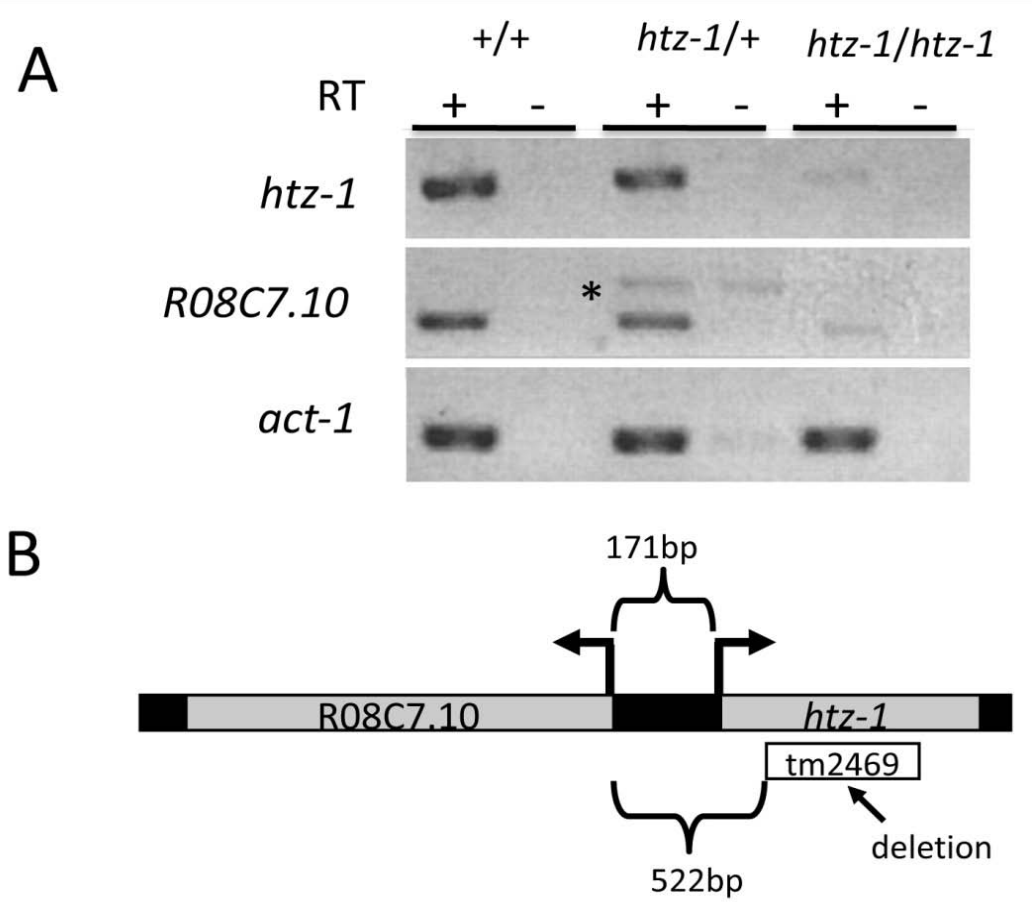

Figure 4.11 tm2469 deletion affects *htz-1* and R08C7.10 expression. (A) Reverse-transcription polymerase chain reaction (RT-PCR) analysis of expression of *htz-1*, R08C7.10 and actin (control) in wild type (+/+), heterozygous (*htz-1(tm2469)/nT1*), or homozygous (*htz-1(tm2469)*) animals. Expression of both *htz-1*and R08C7.10 is affected in homozygous animals. Contaminating amplification product from residual DNA in the RNA sample is indicated by a star. (B) Schematic showing relative positions of *htz-1* and R08C7.10 on chromosome IV (not to scale). The tm2469 deletion removes most of the coding region of*htz-1*. In addition, it likely the affects the promoter or other *cis* control elements of the R08C7.10, a gene located only 522 base pairs away from the deletion.

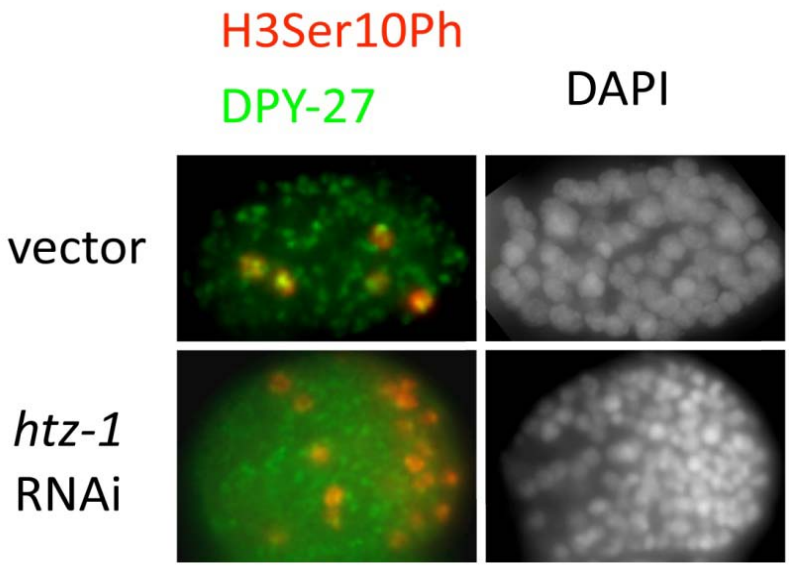

Figure 4.12 *htz-1*-depleted embryos also show compromised DCC localization. Vector and *htz-1* RNAi embryos were stained with α-Phospho-H3 Ser10 (red) (to mark mitotic nuclei) and α-DPY-27 (green). After htz-1 RNAi, 16% of embryos with Phospho-H3 Ser10 staining (>50 cell stage) had diffuse nuclear DPY-27 localization (n = 372), as opposed to 2% in vector embryos (n = 314).

CHAPTER 5

DPY-30 function in *C. elegans* dosage compensation is independent of Set1/MLL

Abstract

Previously, we found that loss of HTZ-1 results in partial disruption of dosage compensation localization to the X chromosomes. We were interested to know whether other chromatin components coordinated with HTZ-1 to properly restrict DCC localization to the X. We chose to focus specifically on the histone H3 methylation complex, SET1C for several reasons. First, HTZ-1 and SET1C/COMPASS coordinate in the restriction of silencing complexes in yeast. Second, similar to HTZ-1, H3K4 trimethylation is found at reduced levels on the X chromosome. Finally, DPY-30 has a known role in *C. elegans* dosage compensation and as a component in H3K4 methylation complexes from yeast to humans. We do not find any evidence of a cooperative role for SET1C complexes in HTZ-1-dependent DCC restriction. Surprisingly, apart from DPY-30, none of the SET1C components tested interact with dosage compensation. Our results suggest that DPY-30 and HTZ-1 use different mechanisms to

regulate chromosomal targeting of the DCC, and both of these mechanisms are independent of H3K4 methylation.

Introduction

The intricate regulation of gene expression that occurs in all organisms is the result of coordinate activity of multiple machineries (RNA Polymerases, transcription factors, histone modifiers, chromatin modifiers, etc.). In order for this to be achieved, these machineries all need to be targeted to very specific sites of action within the vast expanse of the genome. How these various proteins and complexes find their proper targets is an important question to answer to further our understanding of how gene regulation, ultimately, is achieved.

Here, we discuss the targeting of a specialized gene regulatory complex in *C. elegans* called the dosage compensation complex or DCC. In organisms such as *C. elegans*, the difference in sex chromosome makeup in the sexes, left uncorrected, would result in an imbalance of X-linked gene expression in the affected sex. To correct the imbalance, in *C. elegans* hermaphrodites, the DCC is recruited to the two X chromosomes and dosage compensated genes are down-regulated an average of two-fold to match expression levels observed in the XO male. Without DCC function, hermaphrodites die very early in development.

The DCC is comprised of a regulatory subcomplex composed of SDC-1, SDC-2, SDC-3, DPY-30, and DPY-21, and an enzymatic condensin complex comprised of DPY-27, MIX-1, CAPG-1, DPY-28, and DPY-26 (Condensin I^{DC}) [1, 2]. SDC-2 and SDC-3 can bind to chromatin independent of the condensin

complex but the reverse is not true [3, 4]. Based on descriptions of condensin function in chromosome compaction and segregation in mitosis and meiosis the current model is as follows: Loading of Condensin I^{DC} by the regulatory subcomplex results in partial condensation of the X chromosomes which reduces transcription rates two-fold to match expression from the single male X [5].

Hermaphrodite-specific expression of *sdc-2* triggers loading of the complex onto the X chromosomes in an unequal fashion. Chromosome-wide analyses of DCC binding by chromatin immuneprecipitation followed by microarray analysis (ChIP-chip) has revealed that some regions of the X accumulate more/are more stably bound by the DCC than others [6, 7]. Correspondingly, some regions of the X have the capacity to recruit DCC to ectopic sites while others do not [8]. Sites that can attract DCC binding independently are called *rex* sites (for *r*ecruitment *e*lement on *X*) and all other sites of DCC binding are called *dox* sites (for *d*ependent *o*n *X*) [9]. Sequence analyses have revealed a slight enrichment of a specific sequence on the X chromosome, called MEX motif, which may be important for recruiting the DCC on the X chromosome [6, 7]. Repeats of different versions of this sequence as multicopy extrachromosomal arrays are able to bind the DCC *in vivo* [7]. However, the presence of the sequence and even high amounts of DCC binding do not strictly correlate with the ability to recruit the DCC. We have determined at least one other class of DCC binding sites that display very high levels of binding when physically associated with the X but in single copy chromosomal duplications, fail to attract robust complex binding [10]. We refer to such sites as

way-stations and predict that these sites assist in DCC spreading down-stream of the initial recruitment. Combined, these data suggest that DCC localization on the X occurs in a step-wise fashsion. First, the DCC is recruited to specific sites in a manner that is at least partially sequence-driven. Next, the complex spreads to and accumulates at way-stations which assist in local spreading of the complex to nearby *dox* sites, which includes the promoter regions of many genes. Curiously, although the complex is found at promoters of expressed genes and changes in gene expression during development correlate with changes in DCC binding, the actual effect of dosage compensation on expression levels does not correlate with presence of DCC at the promoter [7].

The motifs that have been described are not X specific and are only moderately enriched on the X compared to autosomes [6, 7]. Also, access to such sequences will be determined by how the DNA is packaged in chromatin. Therefore, it is unlikely that sequence is the only factor driving the accumulation of DCC on the X chromosomes, chromatin organization is also likely involved. Indeed, previously we have shown that the H2A.Z variant in *C. elegans* (HTZ-1) plays a role in regulating DCC targeting to the X chromosomes [11]. In *D. melanogaster*, dosage compensation is achieved by up-regulation of the single male X chromosome by the MSL (*m*ale-*s*pecific *l*ethal) complex [12, 13]. Targeting of the MSL complex to the X chromosome occurs at GA-dinucleotide repeats that are also depleted of nucleosomes, so there is both a sequence and chromatin component driving targeting in flies as well [14, 15]. In mammals, dosage compensation is achieved by X chromosome inactivation (XCI) in female

[16]. This system is different in that targeting is achieved by expression of the long, non-coding RNA Xist followed by long-range spreading of Xist RNA from its site of transcription on X to the rest of the chromosome[17-19]. Tethering of Xist RNA to the inactive X requires heterogeneous nuclear ribonuclear protein U (hnRNP U) [20]. Both the DNA-binding and RNA-binding domains are required for hnRNP U function in Xist tethering. It will be interesting to know whether the SAF DNA-binding domain of hnRNP U recognizes specific sequences to result in chromosome-specific tethering of Xist RNA.

H2A.Z is a histone variant conserved in all eukaryotes and is essential in all except yeast [21-23]. It is highly associated with promoter regions, however this is not necessarily associated with active expression [24-29]. Although not fully understood, H2A.Z likely functions in the positive regulation of gene expression [30-36]. H2A.Z displays antagonistic activity with repressive complexes and signatures [11, 37-41]. In yeast, Htz1 is required to restrict the spread of silencing complexes from the silent mating loci and telomeres [40-42]. In Arabidopsis and human cells, H2A.Z specifically antagonizes DNA methylation, a signature of long-term gene silencing [37, 39].

In *C. elegans,* HTZ-1 is found at significantly lower levels on the X chromosomes than autosomes [11, 26]. Depletion of HTZ-1 in hermaphrodites disrupts dosage compensation. Also, *htz-1* depletion and mutant animals exhibit ectopic localization of the DCC on autosomes [11]. Therefore, we hypothesized that HTZ-1 functions to prevent autosomal binding of the DCC in hermaphrodites, similar to the functions described in yeast, Arabidopsis, and humans, in

antagonizing the spread of gene repression activities. In continuation of this work we were interested to know whether other chromatin components cooperate with HTZ-1 in restricting DCC localization.

Cooperation of HTZ-1 with other chromatin factors has been demonstrated in the literature. It has been shown that HTZ-1 cooperates with H3K4methylation to restrict genome-wide spreading of the Sir2 silencing complexes in budding yeast [41]. H3K4 methylation is the result of of Set1/MLL histone methyltransferase complex function . These complexes are made up of a SET-domain containing methyltransferase belonging to either the Set1 family or the Trithorax-related Mixed-Lineage Leukemia (MLL) family and at least four other subunits, WDR5, RbBP5, Ash2L, and DPY-30 [43-50]. *In vitro* studies indicate that Set1 and MLL proteins have relatively weak function on their own compared to other HMTs as they can only monomethylate H3K4 [51]. In budding yeast, Set1 is unstable in mutants lacking Swd3/WDR5 subunit and Set1 levels are significantly reduced in Swd1(RbBP5), so *in vivo*, these three components are required for methylation [44, 51-53]. WDR5 binds to the Set1/MLL subunit, RbBP5 and Ash2L interact through WDR5 and when these components are combined the minimal complex is able to trimethylate H3K4 *in vitro* [45, 53]. Loss of either RbBP5 or Ash2L from an MLL minimal complex results in loss of H3K4me3 and reduced H3K4me2 *in vitro*, but without WDR5, no methyltransferase activity is detected [45]. The Set1 complex-specific subunits SPP1/CFPL1 and WDR82 contribute specifically to trimethylation activity of that complex [54, 55].

Intriguingly, orthologs of the known dosage compensation protein, DPY-30, are found in all Set1/MLL complexes and contribute to methylation activity of the complexes in other organisms [46, 47, 52, 56, 57]. DPY-30 binds ASH2L, a core component of Set1/MLL HTMs, and also forms homodimers, allowing for dimerization of the entire complex [52, 57]. Without DPY-30, global levels of H3K4me3 are significantly reduced in yeast, *C. elegans*, and mammals [52, 56-59]. Slight reductions of dimethylation have also been reported in yeast and *C.elegans* [57, 59]. Loss of DPY-30 has not been shown to affect H3K4 monomethylation. In addition to a global reduction in H3K4 methylation, *dpy-30* mutant hermaphrodites in *C. elegans* exhibit DCC mislocalization and dosage compensation function in gene regulation is impaired [58, 60, 61]. It has also recently been proposed that DPY-30 and H3K4 methylation may assist in DCC spreading to sites of active transcription [62]. We, therefore proposed that HTZ-1 and H3K4methylation (involving DPY-30 function in the *C. elegans* Set1/MLL complexes) cooperate in regulating DCC binding, so that in concert with sequence-driven targeting, the DCC is targeted correctly to the X chromosomes.

Recent data suggest that DPY-30 function is important for DCC recruitment in a similar fashion as the recruitment proteins SDC-2 and SDC-3 [58] . At the restrictive temperature in *dpy-30* temperature sensitive mutant animals, DCC binding to rex sites is almost abolished. DCC binding to *dox* sites is significantly reduced at 20-40% of sites and absent from the remaining sites. Interestingly, the *C. elegans* Ash2L homolog, ASH-2, can also be found at many recognition sites and overlaps DCC binding at some genes. The authors

concluded that DPY-30 binding on X and genome-wide was the result of its association with both DCC and MLL/Set1 complexes. Additionally, there is some physical association by immunoprecipitation between SDC-2 and ASH2L. Overall, current evidence suggests that DPY-30 is a member of multiple complexes, DCC and Set1/MLL complexes. However, it has not been tested whether DPY-30 function in histone methyltransferase complexes contributes to its function in dosage compensation. The overlap of DPY-30, ASH-2 and DCC proteins at promoter regions lends support to the hypothesis that DPY-30 as a part of H3K4 methyltransferase complexes allows the DCC to identify active genes on X. Furthermore, whether H3K4 methylation itself functions in dosage compensation has not yet been addressed.

To address the possibility of an HTZ-1/H3K4methylation cooperation in DCC targeting, we observed DCC localization in Set1C/MLL depleted animals. Depletion of these components led to decreased H3K4me3 as expected from previous analysis in other organisms and in *C. elegans*. There was, however, no correlation between H3K4me3 reduction and affects on DCC localization. Furthermore, the DCC mislocalization phenotype observed in *htz-1* animals was not enhanced in animals with reduced H3K4 methylation. We conclude that H3K4methylation does not contribute to HTZ-1 regulated DCC localization and that the function of DPY-30 in DCC localization is completely independent of its role in Set1/MLL histone methytransferase complexes.

Results

H3K4 is differentially methylated on the dosage compensated X Chromosomes

In order to investigate whether H3K4 methylation cooperates with HTZ-1 in regulating DCC localization we first observed the methylation status of H3K4 on the dosage compensated X chromosomes. To observe methylation levels on the X chromosome at the resolution of a single cell we performed immunofluorescence analysis in adult hermaphrodite intestinal nuclei. We utilized antibodies specific for the mono, di, and trimethylated forms of H3K4 along with antibodies specific for subunits of the dosage compensation complex (DCC) to label the X chromosomes. To compare the levels of the methylated H3K4 species on the X chromosomes to the rest of the nucleus we measured the ratio of the average intensity of the H3K4me signal in the DCC positive region compared to the average intensity of the entire nucleus. We have then compared these results to levels of HTZ-1 on X which is known to be found at lower levels on the X chromosome compared to autosomes.

Interestingly, we found that H3K4me3 is found at lower levels on the X by nearly 20%, nearly identical to the ratio found for HTZ-1. H3K4me2 levels are unchanged on the X, while there is a slight enrichment of the monomethylated form of H3K4 by immunofluorescence. These results are consistent with the recent genome-wide ChIP-chip results in L3 animals, where the greatest difference in H3K4 methylation on X was observed with H3K4me3 [63]. The

slight enrichment of H3K4me1 that we observe was not specifically reported by Liu et al., however the published results comparing levels are limited to analysis of H3K4 methylation localization on a composite gene. It will be interesting to see whether there is also a slight enrichment of total H3K4me1 peaks on X compared to autosomes.

H3K4 differential methylation is not regulated by dosage compensation

We next wanted to investigate whether the differences in methylation levels on the dosage compensated X chromosomes are regulated by dosage compensation. To do this we performed the same analysis as described above in the dosage compensation mutants *sdc-1(y415)* and *dpy-21(e428)*. We chose these specific mutants because although dosage compensation function is disrupted by these mutations, the DCC still localizes to the X chromosome [64]. This allows us to again utilize DCC specific antibodies to label the X. The alternative method of labeling the X chromosome by X Paint fluorescent *in situ* hybridization (FISH) was not possible as the H3K4 methylation antibodies fail when combined with FISH.

For the most part, the differential methylation and differential HTZ-1 levels on the X were unchanged in dosage compensation mutants. The only exception was in *sdc-1* where the slight enrichment of H3K4 monomethylation is lost. These results indicate that differential H3K4me3 and HTZ-1 levels on the X chromosome are not regulated by dosage compensation. The loss of H3K4me1 enrichment in *sdc-1* indicates that dosage compensation may be responsible for

monomethylation enrichment on the X chromosomes. However, the fact that enrichment is still observed in *dpy-21* mutants indicates that there is no strict correlation between loss of enrichment and loss of dosage compensation function. Alternatively, dosage compensation may regulate the differential methylation of H3K4 downstream of DCC localization on the X chromosomes. That is, because the DCC is still present on the X chromosomes in *sdc-1* and *dpy-21* it is able to perform H3K4 methylation regulation to some extent. Perhaps the fact that *sdc-1* appears to have less DCC binding by IF than *dpy-21* some of this regulation is lost resulting in the change in monomethylation that we observe.

DPY-30 is required for DCC localization and binding to chromatin

Next, we wanted to understand the effect of the Set1C/MLL component DPY-30 on dosage compensation localization at the resolution of a single cell. Previously, DPY-30, a subunit of Set1C/MLL, was described to cause DCC mislocalization [61] and very recently has been shown to be required for DCC localization by ChIP-chip analysis in mixed stage embryo preparations [58]. Whether these changes are due to changes in H3K4Me has not been addressed. We utilized DPY-27 immunofluorescence combined with X-Paint FISH to observe the extent of DCC mislocalization in *dpy-30(y228)* animals at the resolution of a single cell.

In *dpy-30* nuclei, DPY-27 has a completely diffuse, nuclear appearance with inconsistent overlap with the X chromosomes (Figure 5.2A). The signal is so

diffuse that we hypothesized that the DCC was not bound to chromatin, but rather largely nucleoplasmic. To test this we performed a detergent extraction prior to fixing the tissue to remove nucleoplasmic content. What we observed was striking- most of the DPY-27 signal was lost upon detergent extraction. This strongly suggests that DPY-30 is required for the complex to stably bind chromatin. These results are in contrast to what we observe in *htz-1(tm2469).* As reported previously, *htz-1* animals exhibit ectopic DCC localization to autosomes and this ectopic signal is not sensitive to detergent extraction (Fig 5.2A and [11]. Therefore, while both DPY-30 and HTZ-1 affect DCC localization, they both do so in a markedly different manner.

Previously, it has been shown that DCC assembly on the X chromosome requires all subunits such that the absence of one component affects the stability or localization of the rest of the complex [1]. Because of this we hypothesized that the DCC as a whole was mislocalized in *dpy-30* animals, rather than DPY-27 on its own. To address this we observed three other members of the complex, MIX-1, CAPG-1, and DPY-28 by immunofluorescence in *dpy-30* nuclei. All of these components had a diffuse, nuclear pattern in *dpy-30* exactly as we observe for DPY-27 (Figure 2B). This strongly suggests that the DCC as a whole cannot load onto chromatin in *dpy-30* animals.

Set1C/MLL depletion affects H3K4 methylation but not DCC localization

Having an understanding of how *dpy-30* affects DCC localization, we next wanted to test whether loss of other Set1/MLL subunits has a similar effect. We

hypothesized that the role of DPY-30 in dosage compensation was linked with its function in the histone methyltransferase Set1 or MLL compexes and predicted that loss of other Set1C or MLL complex members would also disrupt DCC binding to chromatin. To test this, we depleted individual members of the Set1 and MLL complexes by RNAi and observed DCC localization in the adult animals. Although we tested all homologs by RNAi, we focused on the two SET-domain containing genes *set-2* (homologous to Set1 in yeast, Set1A in humans) and *set-16* (homologous to MLL2 in mammals) as well as *ash-2* (homologous to Bre2 in yeast and Ash2L in humans) and *hcf-1* (homologous to human Hcf1).

We focused on *set-2* and *set-16* as these are the only genes in *C. elegans* homologous to H3K4 methyltransferases in other organisms and have been shown previously to function in H3K4 methylation [59, 65, 66]. We focused on *ash-2* because the homologs in other organisms are known binding partners of DPY-30 in Set1/MLL complexes and this interaction is essential for full methyltranferase activity [52, 56, 57]. Finally, we chose *hcf*-1 because the mammalian homologs, in addition to being a physical component of Set1/ MLL serve as molecular tethers between MLL and other chromatin modifying complexes [50, 67, 68]. To observe the effect of the depletion of each gene on Set1C/MLL complex activity we observed H3K4me3 levels by immunofluorescence and western blotting as loss of individual components in other systems affects this modified form most dramatically [45, 46, 51, 52, 57]. We also observed H3K4me2 and H3K4me1 levels by immunofluorescence and western blotting upon depletion of *set-2, set-16, ash-2, hcf-1,* and *dpy-30*.

We found that depletion of each individual Set1C/MLL subunit homolog led to a reduction in H3K4me3 (Figure 5.3 and Figure 5.8). This is consistent with the fact that full H3K4 methyltransferase activity by Set1/MLL complex requires all subunits in other organisms [52]. By contrast, mono and di-methylation levels were less affected (Fig 5.9). Only depletion of the catalytic subunits *set-2* and *set-16* reduced H3K4me2 and H3K4me1 levels. Depletion of *ash-2* leads to a reduction in di- and trimethylation, consistent with published *in vivo* analysis in other organisms, however we do not observe any change in H3K4 monomethylation levels [51-53, 57]. DPY-30 and HCF-1 depletion animals showed reduced H3K4me3 by IF, but di and monomethylation levels were unchanged (Fig 5.9). As a control, we also analyzed H3K27me3 levels and found that these levels did not change after Set1C/MLL depletion, as expected (Fig 5.10). Western blot analysis confirmed what was observed by IF: *set-2* and *set-16* depletion leads to reductions in all forms of H3K4methylation, *ash-2* affects di- and trimethylation, and *dpy-30* specifically affects H3K4 trimethylation in young adult hermaphrodites (Fig 5.11). Analysis of *set-2(ok952)* and *hcf-1(ok559)* deletion mutants led to similar conclusions (Fig.5.12).

Surprisingly, the only Set1C/MLL component that also affects DCC localization is *dpy-30*. Depletion of *dpy-30* by RNAi leads to the same diffuse, nuclear DCC localization pattern as we observe in the *dpy-30* mutant. In all other Set1/MLL depletion animals, the level of H3K4me3 staining was similar to *dpy-30* depletion animals, but the DCC staining pattern appeared exactly as our empty vector controls (Fig. 5.3, Fig. 5.8).

Although the DCC appears normal in all of the Set1C/MLL depletion animals except *dpy-30*, we wanted to be certain that the DCC was truly localizing to the X chromosomes. Again, we combined DCC immunofluorescence with X-Paint FISH to observe DCC localization on the X chromosomes in Set1C/MLL depletion animals. We found that the DCC signal colocalized with the X-Paint signal in the Set1C/MLL depletion animals similar to the control, further demonstrating that loss of these components does not affect DCC localization (Fig. 5.4).

We next hypothesized that residual Set1C/MLL activity remaining upon depletion of only one component prevented us from observing a change in DCC localization. To address this, we performed RNAi depletion of *set-2, set-16, ash-2,* and *hcf-1* in the *set-2(ok952)* deletion mutant background. We observed further reductions of H3K4me3 (Fig. 5.5), H3K4me2, and H3K4me1 signals (Fig. 5.13) upon depletion of these components in the *set-2* background. We still did not observe any obvious change in DCC localization in these animals. This suggests that Set1C/MLL complexes and H3K4 methylation are not involved in dosage compensation at the level of DCC localization and loading onto chromatin. These data also indicate that DPY-30's role in DCC localization is independent of its function in H3K4 methylation.

Set1C/MLL complexes do not cooperate with *htz-1* to restrict DCC localization

It is clear from our analysis so far that neither Set1C nor MLL on their own play a role in DCC localization or binding to chromatin, however, it is possible that these complexes may function with other chromatin components to affect DCC localization. Previous work in yeast has demonstrated that the Set1C complex cooperates with the histone variant H2A.Z/Htz1 to limit genome-wide mislocalization of the SIR complexes [41]. Our lab has shown that loss of HTZ-1 in *C. elegans* results in partial mislocalization of the DCC to autosomes [11]. We therefore wanted to test whether H3K4 methylation defects will enhance the DCC mislocalization observed in *htz-1* animals. To do this we depleted Set1C/MLL components in the *htz-1(tm2469)m+z-* background. We then used DCC immunofluorescence combined with X-Paint FISH to visualize DCC localization to the X chromosomes at the single cell resolution. To measure the degree of DCC mislocalization we measured the colocalization of the DCC and X-Paint signals using Slidebook software. The result of this analysis is a Pearson's correlation value where 1 represents complete colocalization of the signals and 0 represents no measureable colocalization [11].

Colocalization analysis in the *htz-1* mutant background revealed that the degree of DCC mislocalization is unchanged upon Set1C/MLL depletion (Fig. 5.6). A majority of the colocalization values collected in the wildtype background treated with empty vector RNAi are above 0.5 (16/18) and the average *R* is 0.61. The average *R* value in *htz-1* homozygous animas treated with vector control

RNAi is significantly lower than wildtype (0.47). The average *R* (0.43-0.48) and profiles for Set1C/MLL depletion are very similar to empty vector control RNAi in the *htz-1* homozygous background. We used one-way ANOVA analysis to determine whether there was any statistical difference among the colocalization data collected. When comparing the control and Set1C/MLL RNAi samples in the *htz-1* background, no statistical difference was observed. However, addition of the control RNAi in N2 data indicated a significant difference (F=4.29, F_{Crit}=2.30, P=0.0014). By Tukey's test, the significant differences in colocalization are found between the N2 control and each of the *htz-1* background samples and not between the *htz-1* control and the Set1C/MLL RNAi samples in the *htz-1* background. We conclude that depletion of H3K4 methylation does not enhance the DCC mislocalization defect seen in *htz-1* mutants.

Set1C/MLL homologs do not function in dosage compensation.

To confirm that DPY-30's role in dosage compensation is independent of its histone methylation role, we tested whether Set1/MLL complex subunits contribute genetically to dosage compensation. We utilized a genetic assay to test for Set1C/MLL function in dosage compensation. In this sensitized genetic assay we deplete components of the Set1C/MLL complexes by RNAi in the *him-8 xol-1 sex-1* mutant background [1, 11]. The *him-8* mutation results in an average 38% male progeny however the *xol-1* mutation turns on dosage compensation and all male progeny die as a result [69]. The *sex-1* mutation weakens dosage compensation function, thereby sensitizing the assay[70].

Therefore, RNAi depletion of a gene required for dosage compensation function will rescue some of the males in this background.

Although we observe that the DCC component *capg-1* results in significant male rescue in this assay the only Set1C/MLL component with significant male rescue was *dpy-30* ($p>0.05$ by t-test analysis). This suggests that *dpy-30* is unique among Set1C/MLL components in its contribution to dosage compensation function. Combined with the data outlined above we conclude that the function of DPY-30 in dosage compensation is completely independent of its role in the H3K4 methylation.

Discussion

It has long been hypothesized that chromatin organization plays a substantial role in driving proteins and complexes to their proper targets within the genome. The predicted mechanism is that chromatin organization blocks access to all but a subset of potential binding sites at any given time. In support of this, functional transcription factor binding sites are commonly depleted of nucleosomes in human T-cells [24]. Also,In *C. elegans*, ectopic expression of the pharynx-specific transcription factor, PHA-4 in intestinal cells does not result in binding of PHA-4 to pharynx-specific genes, suggesting that these sites are unavailable for binding in the intestinal nuclei [71]. Targeting of the X-chromosome specific DCC in *C. elegans* also involves both sequence and chromatin organization [6, 7, 11].

Here, we were interested in testing a potential role for H3K4 methylation in DCC targeting. We were interested in this particular chromatin modification for several reasons. First, DPY-30 is a core subunit of H3K4 methyltransferase complexes from the yeast COMPASS up to the Set1 and MLL complexes in humans, yet DPY-30 was first described in *C. elegans* as a gene essential in the process of dosage compensation [43, 46, 60]. DPY-30 is a member of both the DCC and Set1/MLL complexes in *C. elegans*, suggesting a possible functional link between the two complexes [58]. However, whether other Set1/MLL subunits play a role in DCC targeting has not been analyzed. DPY-30 can bind chromatin in concert with either ASH-2 or SDC-2, and ASH-2 is observed at *rex* sites consistent with a functional link between the two complexes [58]. Finally, it has been proposed that DCC localization to active promoters from recruitment sites or way-stations may recognize a marker of active transcription [62]. Set1/MLL and H3K4methylation are good candidates to serve such a role as DPY-30 is already known to affect DCC localization [61].

In this paper we have thoroughly tested the hypothesis that H3K4methylation is involved in DCC localization both on its own, dependent upon DPY-30 activity in H3K4 histone methyltransferase complexes, and in conjunction with histone variant H2A.Z/HTZ-1. We have found that the dosage compensated X chromosomes have reduced levels of H3K4me3, similar to what has been reported for HTZ-1, and slightly higher levels of H3K4me1. Depletion of H3K4me3 and HTZ-1 are both independent of dosage compensation, but

enrichment of monomethylated H3K4 may be subject to regulation by dosage compensation.

Recently, it has become increasingly clear that the X and autosomal chromatin makeup is significantly different both at the population level by high resolution ChIP-chip and single-cell resolution microscopy studies. HTZ-1 was the first reported chromatin component found to be differentially incorporated on the dosage compensated X chromosomes. The enrichment of monomethylated H3K4 follows the recent observations that H4K20me1 and H3K27me1 are also found at higher levels on X and suggests that this may be functionally important for gene regulation on the X chromosomes [63]. The fact that loss of dosage compensation function in *sdc-1* animals abolishes this enrichment also suggests that the transcriptional regulation function of dosage compensation may involve H3K4me1. However, the fact that we do not observe any changes in DCC localization in the Set1/MLL depletion animals with lowest H3K4me1 signal (*set-2* or *set-16(RNAi)* in *set-2* mutant animals, see Figure 5.5), suggests that if there is a role for monomethylation of H3K4, it is clearly downstream of DCC localization. We did not detect any genetic function of either *set-2* or *set-16* in dosage compensation, so the overall contribution of H3K4me1 to chromosome-wide gene regulation by DCC may be minor. This could be tested more closely by looking for expression changes of dosage compensated genes in animals with reduced H3K4me1 in future studies.

Our observation that H3K4me3 is found at lower levels on the X chromosomes than on autosomes in a manner very similar to HTZ-1 is congruent

with our hypothesis that the two cooperate in preventing ectoptic DCC binding to autosomes. Also interesting is the fact that the Set1/MLL component DPY-30 is required for normal levels of H3K4me3, and is required for dosage compensation (see figures 5.3 and 5.9) [59]. The similarities between H3K4me3 and HTZ-1 prompted us to continue testing a role for H3K4me3 in DCC localization.

We predicted that if DPY-30-dependent H3K4me3 and HTZ-1 coordinately regulated DCC localization, their effects on DCC localization may be similar. As we have reported previously in *htz-1* animals, the DCC ectopically binds autosomes and this binding is able to withstand detergent extraction indicating that the interactions are stable [11]. Loss of *dpy-30*, on the other hand, leads to a diffuse, nucleoplasmic pattern of condensin I^{DC} localization that is sensitive to detergent extraction, suggesting that the DCC is either largely unbound or very loosely associated with chromatin. This substantial difference in DCC mislocalization phenotype between *dpy-30* and *htz-1* provided the first piece of evidence that H3K4 methylation does not function with HTZ-1 in preventing DCC binding to autosomes, however it does not address the possibility that DPY-30's role in dosage compensation is related to its function in H3K4 HMTs.

To test whether the role of DPY-30 in DCC targeting is related to its H3K4 methylation function, or is independent of this function, we observed DCC localization upon depletion of other MLL subunits. RNAi depletion or genetic mutation of these components individually and in a *set-2* mutant background clearly leads to reductions in H3K4methylation. Set1/MLL complexes require all components for full methylation activity *in vitro* and *in vivo* [45, 46, 51, 52, 56,

57]. All Set1/MLL complexes contain a SET-domain containing catalytic subunit (Set1 or MLL-like), along with the core subunits RbBP5, Ash2L, WDR5 and DPY-30 [43, 45-47, 50]. Loss of Set1 in yeast results in global reductions of all H3K4 methylated species [44, 51]. Our results in *set-2* and *set-16* depletion animals are consistent with published observations, as these two were the only components that contributed to all forms of methylation in adults, both by IF and western. The core subunits RbBP5, Ash2L, contribute to di- and trimethylation and WDR5 is required for any methylation of H3K4 by Set1 and MLL complexes both *in vivo* and *in vitro* [45, 51, 52]. We observe reduced trimethylation upon depletion of RbBP5, and WDR5 by IF. Also in agreement is our observation that ASH-2 depletion affects both di- and trimethylation of H3K4 by IF and western analyses. SET-independent monomethylation activity by these core subunits plus DPY-30 has also recently been reported

[72, 73]. The monomethylation activity function has been narrowed down to an Ash2L-RbBP5 heterodimer *in vitro* and this activity likely contributes to the full methyltransferase activity of the entire complex *in vivo* [72]. However, we did not observe a change in monomethylation upon ASH-2 depeletion in our studies. Loss of Set1-specific subunits Spp1 (CFP1 in mammals) and WDR82 specifically affect global levels of H3K4 trimethylation [54, 55] and we indeed observe lower levels of H3K4me3 in animals depleted for the *C. elegans* orthologs. HCF-1 depletion in HeLa cells has been shown to disrupt Set1 and MLL recruitment and H3K4me3 levels at infection initiation genes in herpes simplex viral infection [67]. Similarly, we find that HCF-1 depletion adults have reduced H3K4me3 by IF.

Although DPY-30 has been reported previously to contribute to both di- and trimethylation in *C. elegans* mixed stage samples [59], in adults we only detect reductions in H3K4me3. This difference could be due to the fact that the feeding RNAi utilized in our experiments did not appear to have a significant effect on the accumulation of H3K4methylation in the germline (data not shown), so the germline signal may mask a subtle difference in H3K4me2 in *dpy-30(RNAi)* adult somatic nuclei. Alternatively, the contribution of DPY-30 to dimethylation could be more important at earlier stages in development.

In summary, all of the Set1/MLL homologs in *C. elegans* affected global methylation in a manner consistent with what is known about the complex function in previous work. DPY-30 actually has a less severe effect on overall methylation than does ASH-2 or the catalytic subunits SET-2 and SET-16. In spite of the more severe effect on methylation levels upon depletion of ASH-2, SET-2, and SET-16, we observed no effect on DCC localization. Additionally, the reduced H3K4me3 we observe upon depletion of all other homologs of Set1/MLL complex members does not correlate with an effect on DCC binding to chromatin. Therefore, the role of DPY-30 in DCC targeting is independent of its activity in H3K4 methyltransferase complexes.

We then tested whether reduced global H3K4methylation by Set1/MLL depletion enhances the DCC mislocalization phenotype we have reported in *htz-1* mutant animals. We find no quantifiable difference in DCC localization to X in *htz-1* animals upon global reductions in H3K4methylation. These data provide clear evidence that the function of DPY-30 in dosage compensation is completely

independent of H3K4 methylation. Moreover, H3K4methylation does not assist in targeting the DCC to the X chromosomes. Finally, genetic analysis revealed no evidence for Set1/MLL function in dosage compensation.

How does DPY-30 contribute to dosage compensation if not through the Set1/MLL complexes? Current evidence indicates a physical interaction between DPY-30 and the DCC recruitment protein SDC-2. DPY-30 immunoprecipitation pulls down SDC-2 (although a reciprocal interaction was not reported), and DPY-30 is found at DCC binding sites in an SDC-2 dependent manner. The binding domains that have been mapped by structure function analyses between Ash2L/DPY-30 in mammals and Bre2/Sdc1 in yeast [57] are not found in SDC-2 nor in any of the other known dosage compensation proteins by blast analysis (although the *C. elegans* ASH-2 is identified in these searches). The proposed interaction between SDC-2 and DPY-30, if direct, is likely through a different domain entirely from the ASH-2 domain, or the interaction may be indirect, requiring an as-yet unidentified intermediate. The DPY-30 homolog in yeast, Sdc1, functions in the dimerization of the whole complex through interactions with Bre2 (ASH-2) and in homodimer formation [52, 57, 74]. DPY-30 may play a similar role within the DCC, aiding to the assembly of the DCC onto SDC-2.

The unique DCC mislocalization phenotype of *dpy-30* animals suggests that DPY-30 plays a distinct role in dosage compensation. In *sdc-2* mutant adult nuclei, immunofluorescence experiments reveal loss of the Condensin I^{DC} signal. Although Pferdehirt et al 2011 report that DPY-27 levels are unchanged in *sdc-2* embryos, the loss of signal in adults suggests that over the course of

development, DCC proteins are lost. In *dpy-30* adults, however, the DCC, although grossly mislocalized, is still easily detectable. In *dpy-30* embryos, binding of DCC proteins DPY-27 and SDC-3 is nearly absent at sites involved in recruitment, identical to the effect of *sdc-2* mutation. It would be interesting to test how *dpy-30* affects SDC-2 levels and localization. If SDC-2 is specifically required for the long-term stability of the DCC as well as chromosome specific loading onto the X, perhaps if SDC-2 is not able to bind chromatin, its presence in the nucleus may still be able to perform its DCC stabilizing function. In this case, we would predict that *dpy-30*'s function in dosage compensation is to facilitate SDC-2-specific binding on chromatin such that loss of *dpy-30* results in failure of SDC-2 to "anchor" the stable complex to chromatin. The overall effect on complex localization would be specific loss of DCC at sites where SDC-2 is absolutely required for DCC binding. Alternatively, *sdc-*2 may be required for positively regulating expression of the other dosage compensation genes in addition to directing DCC loading onto the X. All DCC proteins except SDC-2 are maternally loaded into oocytes, which could account for the similarity in DPY-27 levels in *sdc-2* and wildtype embryos. Eventually this maternally provided DCC supply is lost in *sdc-2* animals. Whether *sdc-2* regulates DCC expression at the level of protein stability or transcription could be discerned by observation of mRNA and protein levels in developing *sdc-2* embryos. Understanding the nature of the DPY-30-SDC-2 interaction in dosage compensation will be the crucial first step in understanding how DPY-30 promotes DCC binding and may

also shed light on novel Set1/MLL-independent functions of DPY-30 in other organisms.

Materials and Methods

Strains and alleles

All strains used were maintained as described [75]. Strains include N2 Bristol strain (wild type) TY4403 *him-8(e1489)* IV; *xol-1(y9) sex-1(y263)* X; EKM11 *htz-1(tm2469)*IV /*nT1(qIs51)* IV,V; EKM32 *hcf-1(ok559)IV*; EKM31 *set-2(ok952)III*. *hcf-1(ok559)* and *set-2(ok952)* were back-crossed four times prior to analysis.

RNA interference

E. coli HT115 bacteria expressing double stranded RNA for *capg-1*, *set-2,dpy-30, hcf-1,* F52B11.1 (CFP1 homolog), F21H12.1 (RbBP5 homolog), *wdr-5.1*, *swd-3.2, swd-3.3*, *swd-2.1*, and *swd-2.2* or vector control (polylinker), were used for feeding RNAi using the Ahringer feeding RNAi clones [76]. To generate RNAi vectors for *set-16* and the 3′ *ash-2* the regions were PCR amplified, digested with NotI and XhoI (*set-16*) or XhoI and SpeI (*ash-2*), and cloned into the DT7 vector as described [76]. The following primers were used for amplification:

set-16:

cgcggccgccgagcaacaacagggag and cctcgaggctgagaaggctgtttgc

ash-2:

gactcgaggctacacgttcacctgcaaa and tgactagtgccattccttttctgcttg

RNAi experiments for IF/FISH and to score male rescue in *him-8(e1489) IV*; *xol-1(y9) sex-1(y263) X* were conducted as described [11].

Immunostaining

Adult animals were dissected and stained as described [8]. Millipore Anti-Monomethyl Histone H3 (Lys4) rabbit polyclonal antibody (cat # 07-436) was used at 1:100 dilution. Abcam H3 dimethyl K4 goat polyclonal antibody (ab11946) was used at 1:100. Millipore Anti-Trimethyl Histone H3 (Lys4) clone CMA304 mouse monoclonal antibody (Cat. #05-1339) was used at 1:100. Upstate anti-trimethyl-Histone H3(Lys27) (Cat. #17-622) rabbit polyclonal was used at 1:200 Affinity purified polyclonal rabbit anti-DPY-27 and polyclonal rat anti-CAPG-1 [1] were used at 1:100. Polyclonal rabbit anti-DPY-28 (gift of K. Hagstrom) was used at 1:500 and polyclonal rabbit anti-MIX-1 (gift of R. Chan) was used at 1:100. Mouse monoclonal Anti-α-tubulin by Sigma (T6199) was used at 1:500. Mouse monoclonal antibody [Mab414] to Nuclear Pore Complex Proteins by Abcam (ab24609) was used at 1:1000. Secondary antibodies used are: Fluorescein (FITC) conjugated donkey α-rabbit (Jackson ImmunoResearch) and Cy3 conjugated donkey α-rabbit IgG (Jackson ImmunoResearch) both at a dilution of 1:100. Images were captured with a Hamamatsu ORCA-ERGA CCD camera mounted on an Olympus BX61 motorized X-drive microscope using a 60× oil immersion objective. Captured images were deconvolved using 3i Slidebook imaging software. Projected images were taken at 0.2 µm intervals through samples. Adobe Photoshop was used for assembling images.

Fluorescent *in situ* hybridization

FISH probe templates were generated by degenerate oligonucleotide primed PCR to amplify purified yeast artificial chromosome DNA. The labeled X-paint probe was prepared and used as described [8]. Hybridization was performed on young adult animals (24 hours post-L4) as described [11].

Quantification of colocalization

3i Slidebook imaging software was used to measure colocalization of DPY-27 (FITC) and X-Paint (Cy3) signals on images obtained as described above. The FITC:Cy3 correlation coefficient was recorded and used as an indication of colocalization between DPY-27 and X-Paint as described [11].

Detergent extraction

Detergent extraction of nucleoplasmic protein from dissected nuclei was performed by dissecting animals in 1× sperm salts plus 1% Triton detergent [77]. Dissected animals were then processed for Fluorescent *in situ* hybridization followed by immunofluorescence.

Western blot analysis

100 (2X lanes) and 50 (1X lanes) young adult Set1C-RNAi worms (24 hours post-L4) were picked into 1XM9, washed, and incubated for ten minutes at 95°C in 19 µl SDS-PAGE loading dye (0.1 M Tris-HCl pH 6.8, 75 M Urea, 2% SDS, Bromophenol Blue for color) plus 1 µl β-mercaptoethanol. 10ul of the worm extract in loading buffer was loaded per lane into a 15% polyacrylamide gel.

SDS-PAGE was performed and protein was transferred onto nitrocellulose. The following antibodies and dilutions were used: Millipore Anti-Monomethyl Histone H3 (Lys4) rabbit polyclonal antibody at 1:500, Abcam H3 dimethyl K4 goat polyclonal antibody at 1:1000, Anti-Trimethyl Histone H3 (Lys4) clone CMA304 mouse monoclonal antibody at 1:1000, and mouse monoclonal Anti-α-tubulin at 1:1000. Secondary antibodies used were as follows: anti-mouse-HRP, anti-goat-HRP, and anti-rabbit-HRP (Jackson ImmunoResearch) all at 1:5000.

Acknowledgements

We thank K. Hagstrom and R. Chan for the DPY-28 and MIX-1 antibodies, respectively, the *Caenorhabditis* Genetics Center and the *C. elegans* Gene Knockout Consortium for the *hcf-1* and *set-2* deletion alleles. We would also like to thank Alysse Cohen for initial assistance with backcrossing and antibody testing. We also thank Yali Dou, Ken Cadigan, and Steve Clark for helpful comments and suggestions.

Author Contributions

ELP and GC conceived and designed the experiments. ELP, KSC, and EL performed the experiments. ELP and GC wrote the paper.

References

1. Csankovszki, G., et al., *Three distinct condensin complexes control C. elegans chromosome dynamics.* Current biology : CB, 2009. **19**(1): p. 9-19.
2. Csankovszki, G., E.L. Petty, and K.S. Collette, *The worm solution: a chromosome-full of condensin helps gene expression go down.* Chromosome research : an international journal on the molecular, supramolecular and evolutionary aspects of chromosome biology, 2009. **17**(5): p. 621-35.

3. Davis, T.L. and B.J. Meyer, *SDC-3 coordinates the assembly of a dosage compensation complex on the nematode X chromosome.* Development, 1997. **124**(5): p. 1019-31.
4. Dawes, H.E., et al., *Dosage compensation proteins targeted to X chromosomes by a determinant of hermaphrodite fate.* Science, 1999. **284**(5421): p. 1800-4.
5. Csankovszki, G., *Condensin function in dosage compensation.* Epigenetics : official journal of the DNA Methylation Society, 2009. **4**(4): p. 212-5.
6. Ercan, S., et al., *X chromosome repression by localization of the C. elegans dosage compensation machinery to sites of transcription initiation.* Nature genetics, 2007. **39**(3): p. 403-8.
7. Jans, J., et al., *A condensin-like dosage compensation complex acts at a distance to control expression throughout the genome.* Genes & development, 2009. **23**(5): p. 602-18.
8. Csankovszki, G., P. McDonel, and B.J. Meyer, *Recruitment and spreading of the C. elegans dosage compensation complex along X chromosomes.* Science, 2004. **303**(5661): p. 1182-5.
9. McDonel, P., et al., *Clustered DNA motifs mark X chromosomes for repression by a dosage compensation complex.* Nature, 2006. **444**(7119): p. 614-8.
10. Blauwkamp, T.A. and G. Csankovszki, *Two classes of dosage compensation complex binding elements along Caenorhabditis elegans X chromosomes.* Molecular and cellular biology, 2009. **29**(8): p. 2023-31.
11. Petty, E.L., et al., *Restricting dosage compensation complex binding to the X chromosomes by H2A.Z/HTZ-1.* PLoS genetics, 2009. **5**(10): p. e1000699.
12. Straub, T. and P.B. Becker, *Transcription modulation chromosome-wide: universal features and principles of dosage compensation in worms and flies.* Current opinion in genetics & development, 2011. **21**(2): p. 147-53.
13. Gelbart, M.E. and M.I. Kuroda, *Drosophila dosage compensation: a complex voyage to the X chromosome.* Development, 2009. **136**(9): p. 1399-410.
14. Gorchakov, A.A., et al., *Long-range spreading of dosage compensation in Drosophila captures transcribed autosomal genes inserted on X.* Genes & development, 2009. **23**(19): p. 2266-71.
15. Straub, T., et al., *The chromosomal high-affinity binding sites for the Drosophila dosage compensation complex.* PLoS genetics, 2008. **4**(12): p. e1000302.
16. Lyon, M.F., *Gene action in the X-chromosome of the mouse (Mus musculus L.).* Nature, 1961. **190**: p. 372-3.
17. Brockdorff, N., et al., *Conservation of position and exclusive expression of mouse Xist from the inactive X chromosome.* Nature, 1991. **351**(6324): p. 329-31.
18. Brown, C.J., et al., *A gene from the region of the human X inactivation centre is expressed exclusively from the inactive X chromosome.* Nature, 1991. **349**(6304): p. 38-44.
19. Clemson, C.M., et al., *XIST RNA paints the inactive X chromosome at interphase: evidence for a novel RNA involved in nuclear/chromosome structure.* The Journal of cell biology, 1996. **132**(3): p. 259-75.
20. Hasegawa, Y., et al., *The matrix protein hnRNP U is required for chromosomal localization of Xist RNA.* Developmental cell, 2010. **19**(3): p. 469-76.
21. Liu, X., B. Li, and GorovskyMa, *Essential and nonessential histone H2A variants in Tetrahymena thermophila.* Molecular and cellular biology, 1996. **16**(8): p. 4305-11.
22. Clarkson, M.J., et al., *Regions of variant histone His2AvD required for Drosophila development.* Nature, 1999. **399**(6737): p. 694-7.

23. Ridgway, P., et al., *Unique residues on the H2A.Z containing nucleosome surface are important for Xenopus laevis development.* The Journal of biological chemistry, 2004. **279**(42): p. 43815-20.
24. Barski, A., et al., *High-resolution profiling of histone methylations in the human genome.* Cell, 2007. **129**(4): p. 823-37.
25. Guillemette, B., et al., *Variant histone H2A.Z is globally localized to the promoters of inactive yeast genes and regulates nucleosome positioning.* PLoS biology, 2005. **3**(12): p. e384.
26. Whittle, C.M., et al., *The genomic distribution and function of histone variant HTZ-1 during C. elegans embryogenesis.* PLoS genetics, 2008. **4**(9): p. e1000187.
27. Weber, C.M., J.G. Henikoff, and S. Henikoff, *H2A.Z nucleosomes enriched over active genes are homotypic.* Nature structural & molecular biology, 2010. **17**(12): p. 1500-7.
28. Raisner, R.M., et al., *Histone variant H2A.Z marks the 5' ends of both active and inactive genes in euchromatin.* Cell, 2005. **123**(2): p. 233-48.
29. Millar, C.B., et al., *Acetylation of H2AZ Lys 14 is associated with genome-wide gene activity in yeast.* Genes & development, 2006. **20**(6): p. 711-22.
30. Allis, C.D., et al., *hv1 is an evolutionarily conserved H2A variant that is preferentially associated with active genes.* The Journal of biological chemistry, 1986. **261**(4): p. 1941-8.
31. Santisteban, M.S., T. Kalashnikova, and M.M. Smith, *Histone H2A.Z regulats transcription and is partially redundant with nucleosome remodeling complexes.* Cell, 2000. **103**(3): p. 411-22.
32. Adam, M., et al., *H2A.Z is required for global chromatin integrity and for recruitment of RNA polymerase II under specific conditions.* Molecular and cellular biology, 2001. **21**(18): p. 6270-9.
33. Larochelle, M. and L. Gaudreau, *H2A.Z has a function reminiscent of an activator required for preferential binding to intergenic DNA.* The EMBO journal, 2003. **22**(17): p. 4512-22.
34. Zhang, H., D.N. Roberts, and B.R. Cairns, *Genome-wide dynamics of Htz1, a histone H2A variant that poises repressed/basal promoters for activation through histone loss.* Cell, 2005. **123**(2): p. 219-31.
35. Dhillon, N., et al., *H2A.Z functions to regulate progression through the cell cycle.* Molecular and cellular biology, 2006. **26**(2): p. 489-501.
36. Brickner, D.G., et al., *H2A.Z-mediated localization of genes at the nuclear periphery confers epigenetic memory of previous transcriptional state.* PLoS biology, 2007. **5**(4): p. e81.
37. Conerly, M.L., et al., *Changes in H2A.Z occupancy and DNA methylation during B-cell lymphomagenesis.* Genome research, 2010. **20**(10): p. 1383-90.
38. Hardy, S., et al., *The euchromatic and heterochromatic landscapes are shaped by antagonizing effects of transcription on H2A.Z deposition.* PLoS genetics, 2009. **5**(10): p. e1000687.
39. Zilberman, D., et al., *Histone H2A.Z and DNA methylation are mutually antagonistic chromatin marks.* Nature, 2008. **456**(7218): p. 125-9.
40. Meneghini, M.D., M. Wu, and H.D. Madhani, *Conserved histone variant H2A.Z protects euchromatin from the ectopic spread of silent heterochromatin.* Cell, 2003. **112**(5): p. 725-36.
41. Venkatasubrahmanyam, S., et al., *Genome-wide, as opposed to local, antisilencing is mediated redundantly by the euchromatic factors Set1 and H2A.Z.* Proceedings of the

National Academy of Sciences of the United States of America, 2007. **104**(42): p. 16609-14.
42. Dhillon, N. and R.T. Kamakaka, *A histone variant, Htz1p, and a Sir1p-like protein, Esc2p, mediate silencing at HMR.* Molecular cell, 2000. **6**(4): p. 769-80.
43. Miller, T., et al., *COMPASS: a complex of proteins associated with a trithorax-related SET domain protein.* Proceedings of the National Academy of Sciences of the United States of America, 2001. **98**(23): p. 12902-7.
44. Krogan, N.J., et al., *COMPASS, a histone H3 (Lysine 4) methyltransferase required for telomeric silencing of gene expression.* The Journal of biological chemistry, 2002. **277**(13): p. 10753-5.
45. Dou, Y., et al., *Regulation of MLL1 H3K4 methyltransferase activity by its core components.* Nature structural & molecular biology, 2006. **13**(8): p. 713-9.
46. Nagy, P.L., et al., *A trithorax-group complex purified from Saccharomyces cerevisiae is required for methylation of histone H3.* Proceedings of the National Academy of Sciences of the United States of America, 2002. **99**(1): p. 90-4.
47. Roguev, A., et al., *The Saccharomyces cerevisiae Set1 complex includes an Ash2 homologue and methylates histone 3 lysine 4.* The EMBO journal, 2001. **20**(24): p. 7137-48.
48. Dou, Y., et al., *Physical association and coordinate function of the H3 K4 methyltransferase MLL1 and the H4 K16 acetyltransferase MOF.* Cell, 2005. **121**(6): p. 873-85.
49. Lee, J.H. and D.G. Skalnik, *CpG-binding protein (CXXC finger protein 1) is a component of the mammalian Set1 histone H3-Lys4 methyltransferase complex, the analogue of the yeast Set1/COMPASS complex.* The Journal of biological chemistry, 2005. **280**(50): p. 41725-31.
50. Yokoyama, A., et al., *Leukemia proto-oncoprotein MLL forms a SET1-like histone methyltransferase complex with menin to regulate Hox gene expression.* Molecular and cellular biology, 2004. **24**(13): p. 5639-49.
51. Schneider, J., et al., *Molecular regulation of histone H3 trimethylation by COMPASS and the regulation of gene expression.* Molecular cell, 2005. **19**(6): p. 849-56.
52. Dehe, P.M., et al., *Protein interactions within the Set1 complex and their roles in the regulation of histone 3 lysine 4 methylation.* The Journal of biological chemistry, 2006. **281**(46): p. 35404-12.
53. Steward, M.M., et al., *Molecular regulation of H3K4 trimethylation by ASH2L, a shared subunit of MLL complexes.* Nature structural & molecular biology, 2006. **13**(9): p. 852-4.
54. Wu, M., et al., *Molecular regulation of H3K4 trimethylation by Wdr82, a component of human Set1/COMPASS.* Molecular and cellular biology, 2008. **28**(24): p. 7337-44.
55. Takahashi, Y.H., et al., *Regulation of H3K4 trimethylation via Cps40 (Spp1) of COMPASS is monoubiquitination independent: implication for a Phe/Tyr switch by the catalytic domain of Set1.* Molecular and cellular biology, 2009. **29**(13): p. 3478-86.
56. Jiang, H., et al., *Role for Dpy-30 in ES cell-fate specification by regulation of H3K4 methylation within bivalent domains.* Cell, 2011. **144**(4): p. 513-25.
57. South, P.F., et al., *A conserved interaction between the SDI domain of Bre2 and the Dpy-30 domain of Sdc1 is required for histone methylation and gene expression.* The Journal of biological chemistry, 2010. **285**(1): p. 595-607.
58. Pferdehirt, R.R., W.S. Kruesi, and B.J. Meyer, *An MLL/COMPASS subunit functions in the C. elegans dosage compensation complex to target X chromosomes for transcriptional regulation of gene expression.* Genes & development, 2011. **25**(5): p. 499-515.

59. Simonet, T., et al., *Antagonistic functions of SET-2/SET1 and HPL/HP1 proteins in C. elegans development.* Developmental biology, 2007. **312**(1): p. 367-83.
60. Hsu, D.R. and B.J. Meyer, *The dpy-30 gene encodes an essential component of the Caenorhabditis elegans dosage compensation machinery.* Genetics, 1994. **137**(4): p. 999-1018.
61. Hsu, D.R., P.T. Chuang, and B.J. Meyer, *DPY-30, a nuclear protein essential early in embryogenesis for Caenorhabditis elegans dosage compensation.* Development, 1995. **121**(10): p. 3323-34.
62. Ercan, S. and J.D. Lieb, *C. elegans dosage compensation: a window into mechanisms of domain-scale gene regulation.* Chromosome research : an international journal on the molecular, supramolecular and evolutionary aspects of chromosome biology, 2009. **17**(2): p. 215-27.
63. Liu, T., et al., *Broad chromosomal domains of histone modification patterns in C. elegans.* Genome research, 2011. **21**(2): p. 227-36.
64. Yonker, S.A. and B.J. Meyer, *Recruitment of C. elegans dosage compensation proteins for gene-specific versus chromosome-wide repression.* Development, 2003. **130**(26): p. 6519-32.
65. Greer, E.L., et al., *Members of the H3K4 trimethylation complex regulate lifespan in a germline-dependent manner in C. elegans.* Nature, 2010. **466**(7304): p. 383-7.
66. Fisher, K., et al., *Methylation and demethylation activities of a C. elegans MLL-like complex attenuate RAS signalling.* Developmental biology, 2010. **341**(1): p. 142-53.
67. Narayanan, A., W.T. Ruyechan, and T.M. Kristie, *The coactivator host cell factor-1 mediates Set1 and MLL1 H3K4 trimethylation at herpesvirus immediate early promoters for initiation of infection.* Proceedings of the National Academy of Sciences of the United States of America, 2007. **104**(26): p. 10835-40.
68. Wysocka, J., et al., *Human Sin3 deacetylase and trithorax-related Set1/Ash2 histone H3-K4 methyltransferase are tethered together selectively by the cell-proliferation factor HCF-1.* Genes & development, 2003. **17**(7): p. 896-911.
69. Hodgkin, J., H.R. Horvitz, and S. Brenner, *Nondisjunction Mutants of the Nematode CAENORHABDITIS ELEGANS.* Genetics, 1979. **91**(1): p. 67-94.
70. Gladden, J.M., B. Farboud, and B.J. Meyer, *Revisiting the X:A signal that specifies Caenorhabditis elegans sexual fate.* Genetics, 2007. **177**(3): p. 1639-54.
71. Fakhouri, T.H., et al., *Dynamic chromatin organization during foregut development mediated by the organ selector gene PHA-4/FoxA.* PLoS genetics, 2010. **6**(8).
72. Cao, F., et al., *An Ash2L/RbBP5 heterodimer stimulates the MLL1 methyltransferase activity through coordinated substrate interactions with the MLL1 SET domain.* PloS one, 2010. **5**(11): p. e14102.
73. Patel, A., et al., *A novel non-SET domain multi-subunit methyltransferase required for sequential nucleosomal histone H3 methylation by the mixed lineage leukemia protein-1 (MLL1) core complex.* The Journal of biological chemistry, 2011. **286**(5): p. 3359-69.
74. Wang, X., et al., *Crystal structure of the C-terminal domain of human DPY-30-like protein: A component of the histone methyltransferase complex.* Journal of molecular biology, 2009. **390**(3): p. 530-7.
75. Brenner, S., *The genetics of Caenorhabditis elegans.* Genetics, 1974. **77**(1): p. 71-94.
76. Ahringer, J., *Reverse genetics. .* WormBook : the online review of C. elegans biology, 2005.
77. Chan, R.C., A.F. Severson, and B.J. Meyer, *Condensin restructures chromosomes in preparation for meiotic divisions.* The Journal of cell biology, 2004. **167**(4): p. 613-25.

Table 5.1 Summary of Set1C/MLL RNAi. The Set1C/MLL homologs tested in this study are shown. Names of budding yeast and mammalian homologs are included for reference. Depletion of all subunits led to reduced H3K4me3 by IF or a combination of IF and western. The only subunit to also affect DCC localization is *dpy-30.*

S. cerevisiae	**Human**	***C. elegans***	**H3K4me3**	**DCC**
SET1	*hSET1*	*set-2*	Reduced	WT
	MLL2/3	*set-16*	Reduced	WT
SWD1/Cps50	*RbBP5*	F21H12.1	Reduced	WT
SWD3/Cps30	*WDR5*	*wdr-5.1*	Reduced	WT
		swd-3.2	Reduced	WT
		swd-3.3	Reduced	WT
SWD2/Cps35	*WDR82*	*swd-2.1*	Reduced	WT
		swd-2.2	Reduced	WT
	WDR83	F33G12.2	Reduced	WT
SPP1/Cps40	*CFP1*	F52B11.1	Reduced	WT
BRE2/Cps60	*Ash2L*	*ash-2*	Reduced	WT
SDC1/Cps25	*hDPY30*	*dpy-30*	Reduced	Diffuse
	HCF1/2	*hcf-1*	Reduced	Diffuse

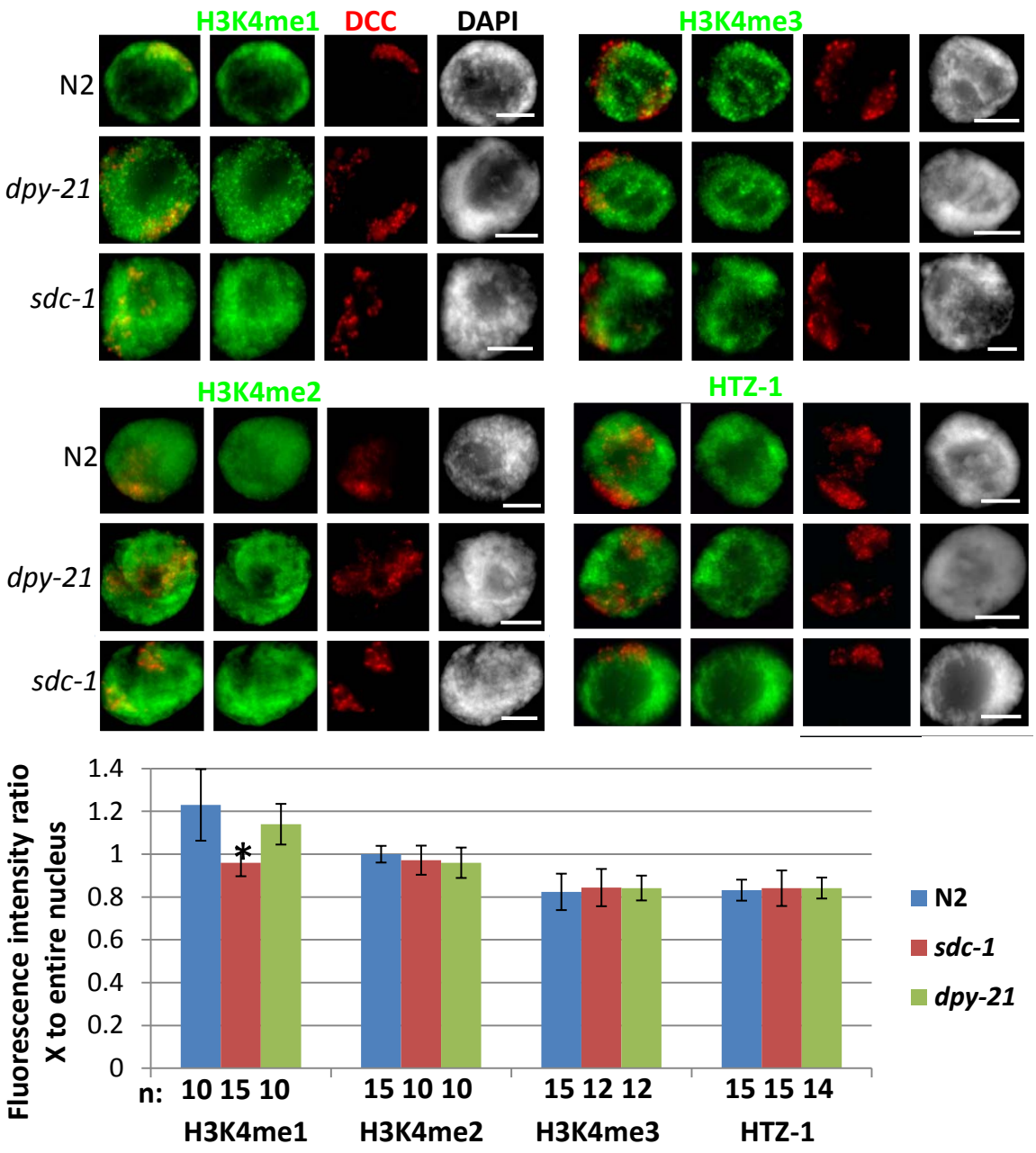

Figure 5.1 H3K4 is differentially methylated on dosage compensated X Chromosomes. **A.** DCC IF(red) and H3K4me1, H3K4me2, H3K4me3 or HTZ-1 (green) in N2 (wildtype), or dosage compensation mutants *sdc-1(y415)* and *dpy-21*(*y428*) shows higher H3K4me1 and lower H3K4me3 and HTZ-1levels on X chromosomes in adult hermaphrodite intestinal nuclei. DCC is marked by α-DPY-27 with H3K4me2, H3K4me3 and HTZ-1. DCC is marked by α-CAPG-1 with H3K4me1. DAPI (grayscale) stains DNA. Scale bar equals 5µm. **B.** Quantification of H3K4 methylation and HTZ-1 levels on the X chromosomes in N2 and dosage compensation mutants. The ratio of average intensity on X versus the average intensity for the entire nucleus was calculated. Error bars indicate standard deviation. Star indicates significant difference from N2 by t-test analysis (p>.05).

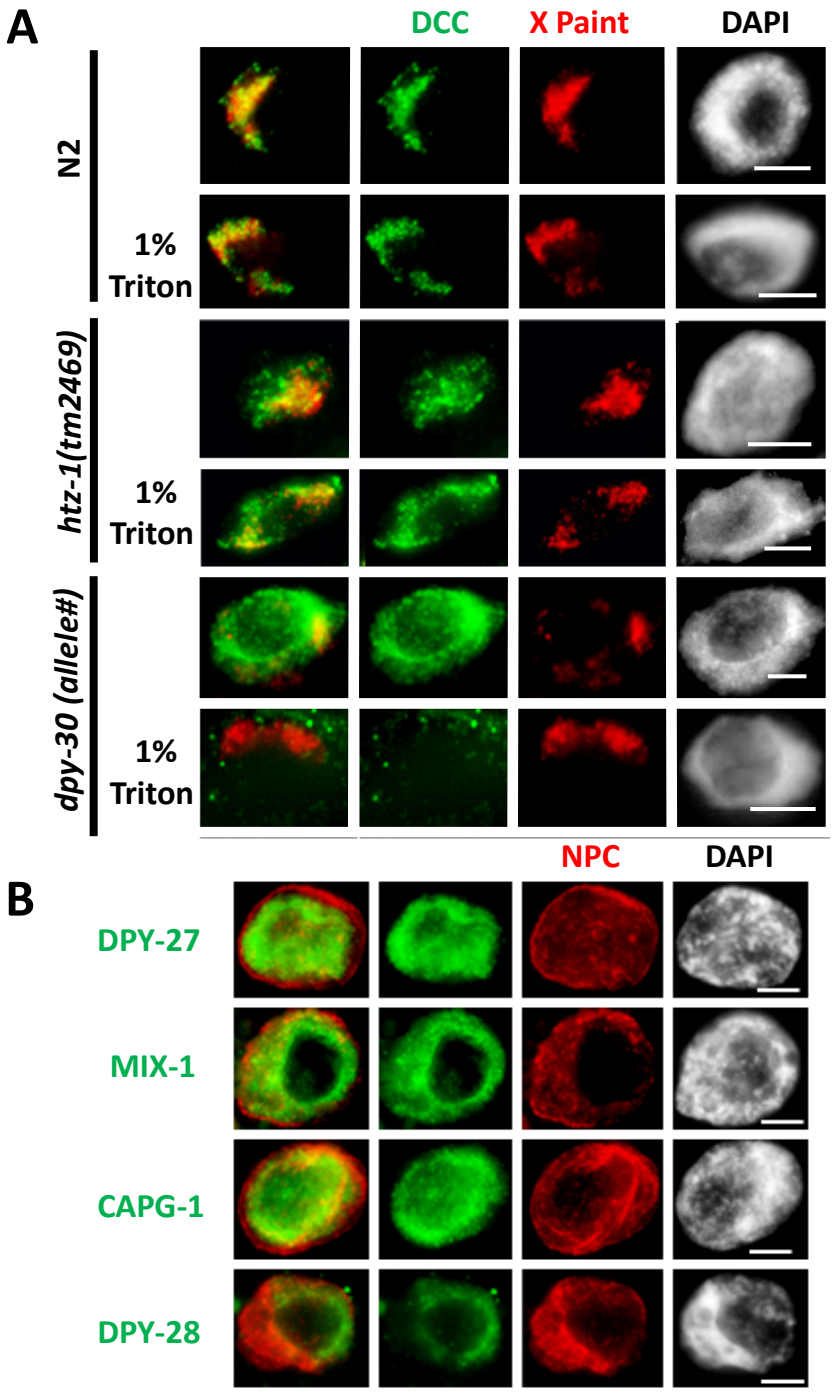

Figure 5.2 DCC binding to or stability on chromatin is compromised in *dpy-30* animals. A. DPY-27 IF (green) and X-paint FISH (red) with and without detergent extraction in N2, *dpy-30 (y228)*, and *htz-1*(*tm2469*) hermaphrodite intestinal nuclei shows that DCC binding in *dpy-30* is sensitive to detergent treatment while DCC in *htz-1* is not. **B.** Condensin I^{DC} mislocalizes in *dpy-30 (y228)* animals. DPY-27, DPY-28, CAPG-1, and MIX-1 (green) are diffusely localized in hermaphrodite adult intestinal nuclei. The nuclear envelope is marked with a nuclear pore complex antibody (red) as a control. DAPI (grayscale) stains DNA and scale bar is 5µm in both panels.

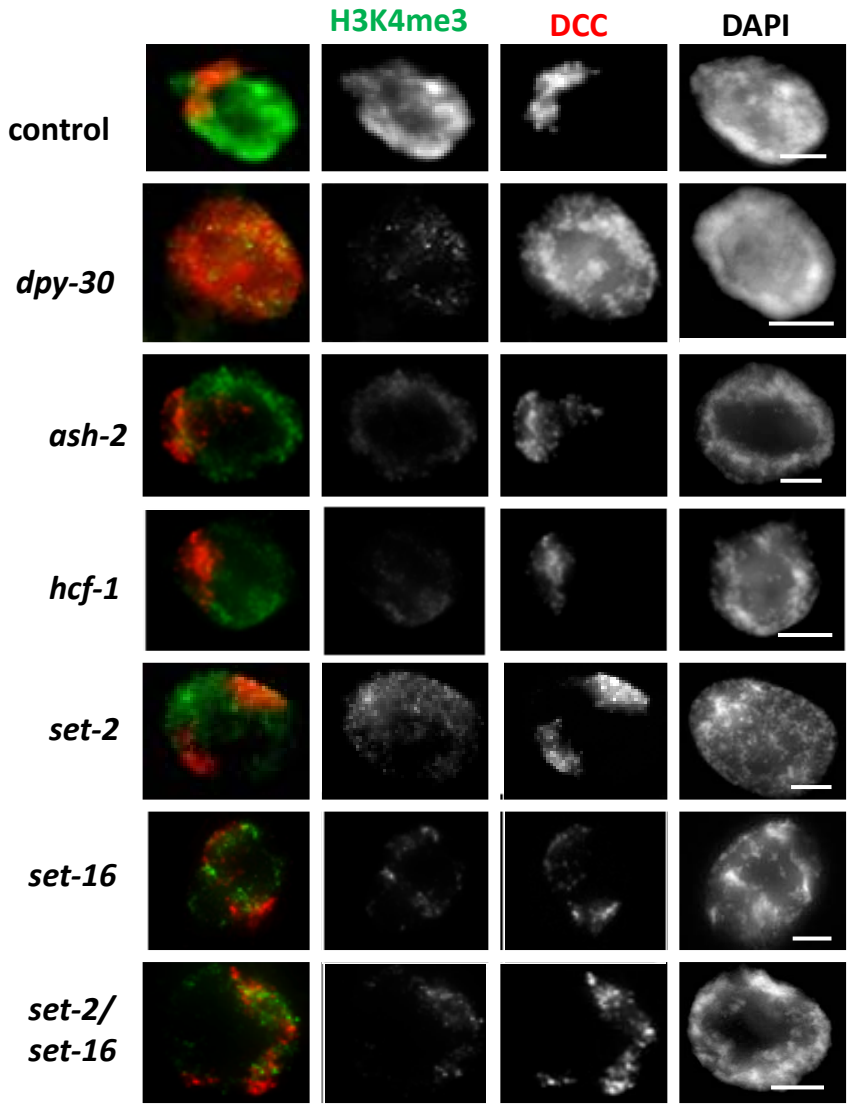

Figure 5.3 Depletion of Set1C/MLL subunits by RNAi affects H3K4me3 levels. H3K4me3 (green) and DPY-27 (red) immunofluorescence in control RNAi and Set1C/MLL depletion animals shows a reduced H3K4me3 signal upon Set1C/MLL RNAi in adult intestinal nuclei. Note that only *dpy-30* depletion leads to a diffuse DCC localization phenotype. In all panels DAPI is shown in grayscale and scale bar equals 5µm.

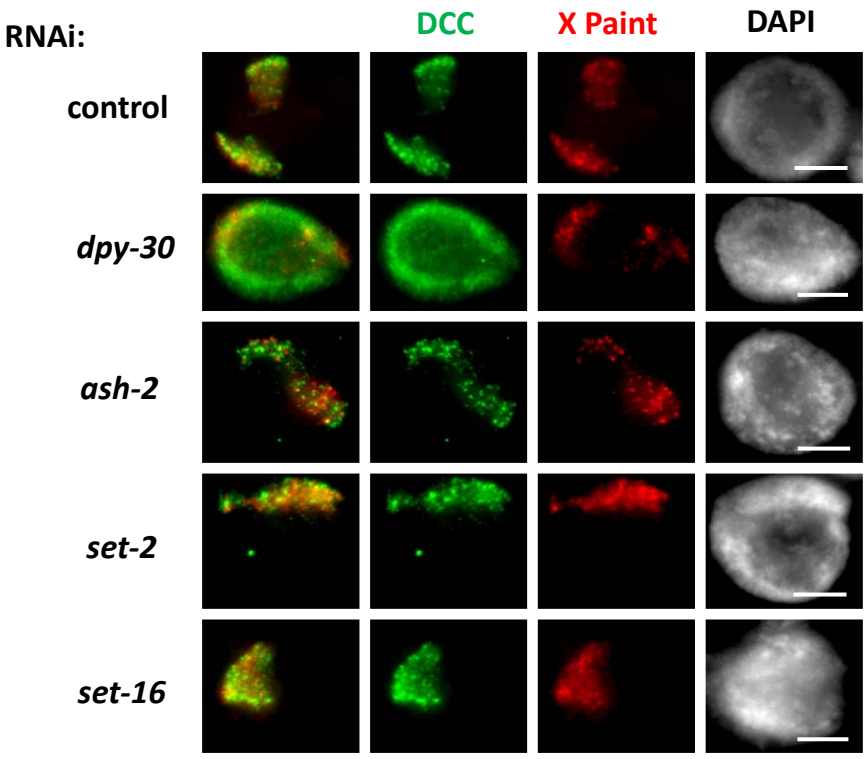

Figure 5.4 DCC mislocaization in N2 occurs only in *dpy-30* depleted animals. DPY-27 (green) and X-Paint FISH (red) in control and Set1C/MLL depletion animals shows proper localization of DPY-27 to the X chromosomes in all adult, hermaphrodite intestinal nuclei except *dpy-30*. DAPI (grayscale) stains DNA and scale bar equals 5µm.

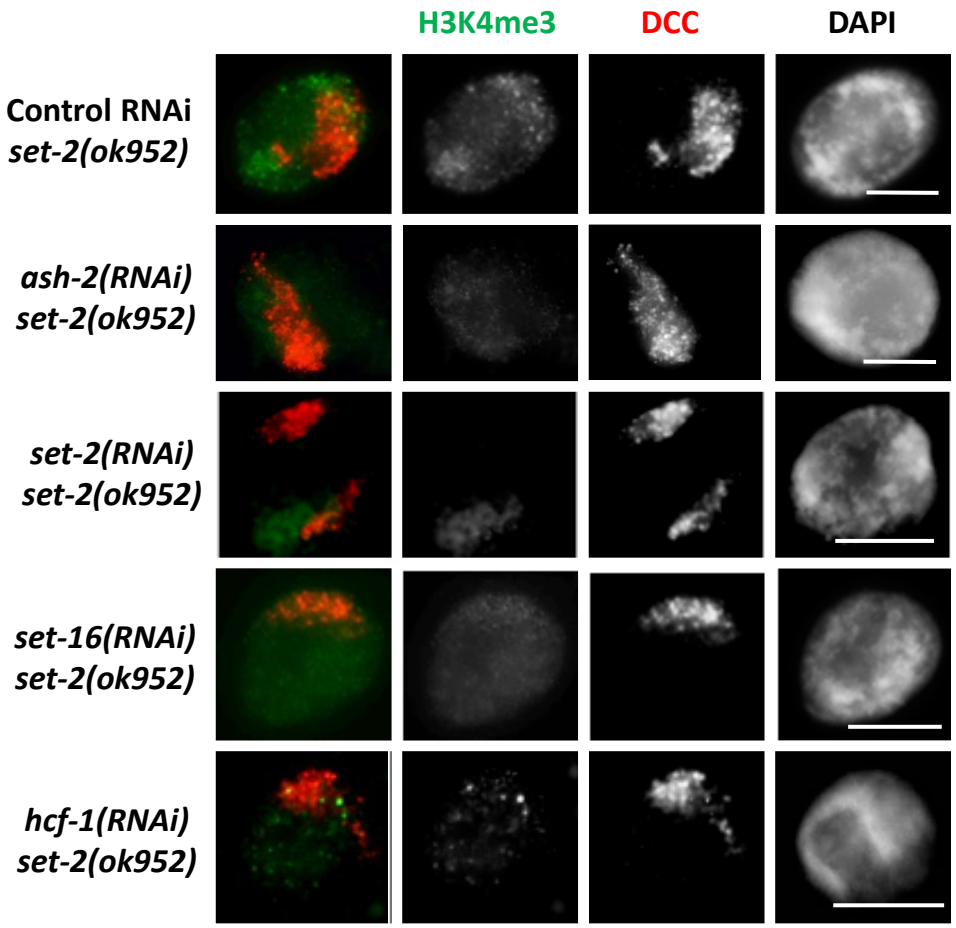

Figure 5.5 Further loss of H3K4 methylation by Set1/MLL depletion in *set-2(ok952)* hermaphrodites . Hermaphrodite intestinal nuclei co-stained for H3K4me3 (green) and DPY-27 (red) in Set1/MLL complex depletion in *set-2* mutant animals demonstrates that increased loss of H3K4 methylation does not correlate with DCC mislocalization. DAPI (grayscale) stains DNA and scale bar equals 5µm.

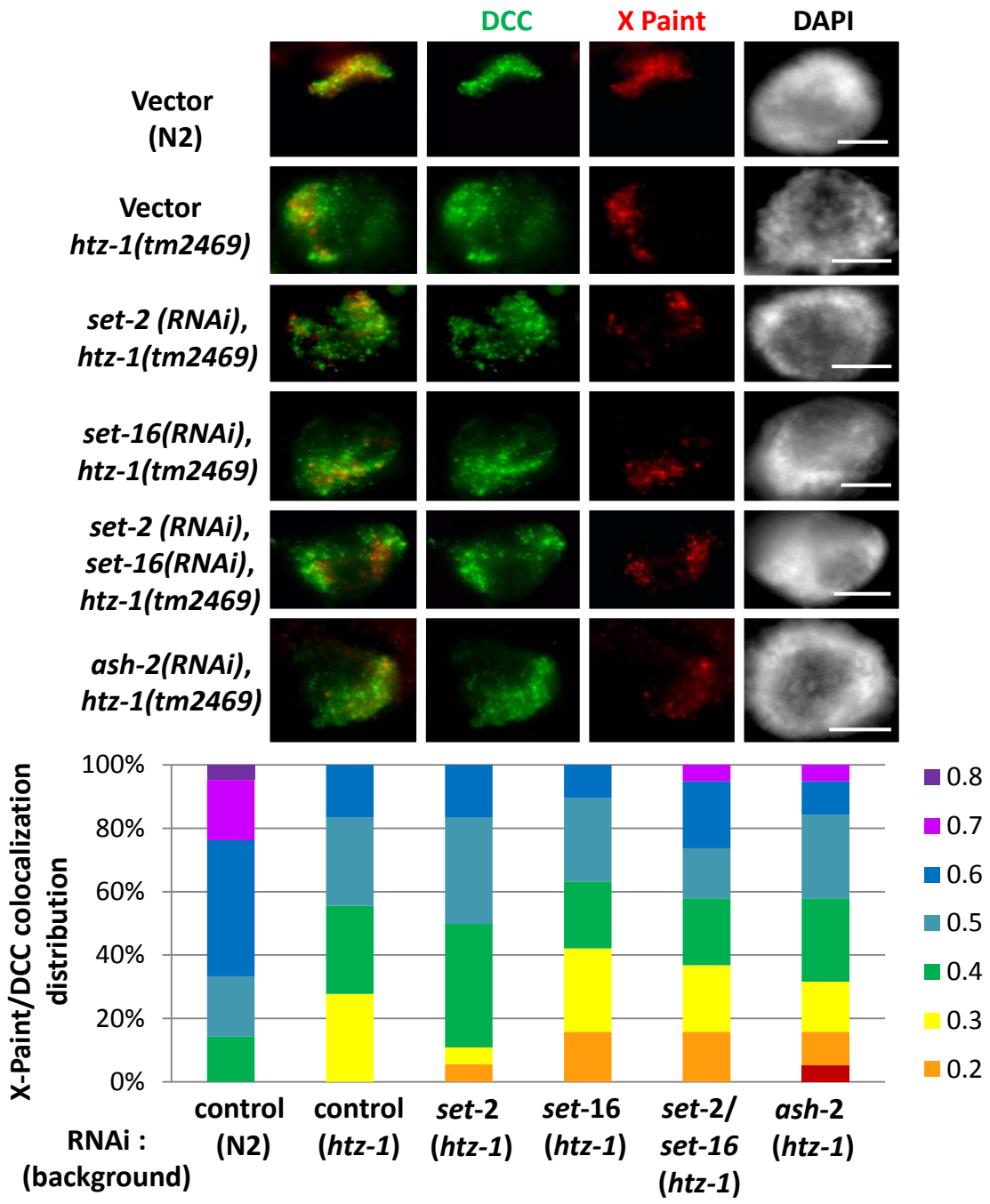

Figure 5.6 Reduced H3K4methylation by Set1C/MLL depletion does not enhance DCC mislocalization in *htz-1(tm2469)*. A. DPY-27 (green) and X-Paint FISH (red) colocalization analysis upon Set1/MLL depletion in *htz-1(tm2469)* mutant animals indicates that reduced H3K4methylation does not further disrupt DCC localization. DAPI is shown in grayscale and scale bar equals 5µm. **B.** Quantification of colocalization by Pearson's correlation coefficient *R* indicating the degree of overlap between the DCC and X-Paint masks. *R* measurements were binned every 0.1 from 0 to 1 (where 0 indicates no detectable overlap and 1 indicates perfect colocalization) and percent of total sample per bin is shown. See Figure 5.12 for statistical analysis.

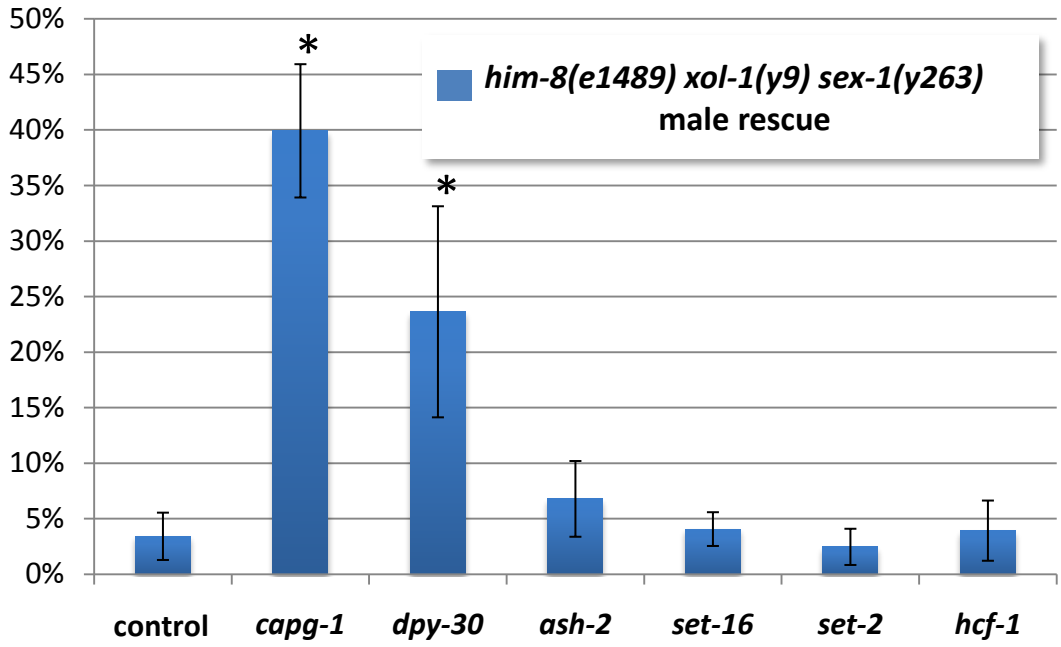

Figure 5.7 H3K4methylation compexes do not function in dosage compensation. Rescue of sensitized male animals in which *xol-1* mutation ectopically turns on dosage compensation is used as a measure of genetic function of dosage compensation. Disruption of DCC subunit gene *capg-1* by RNAi is able to disrupt ectopic dosage compensation, rescuing about 40% of expected male progeny. The only Set1/MLL complex subunit gene that, when depleted by RNAi, results in significant rescue is *dpy-30*. Stars indicate significant difference from control by t-test (p>.05).

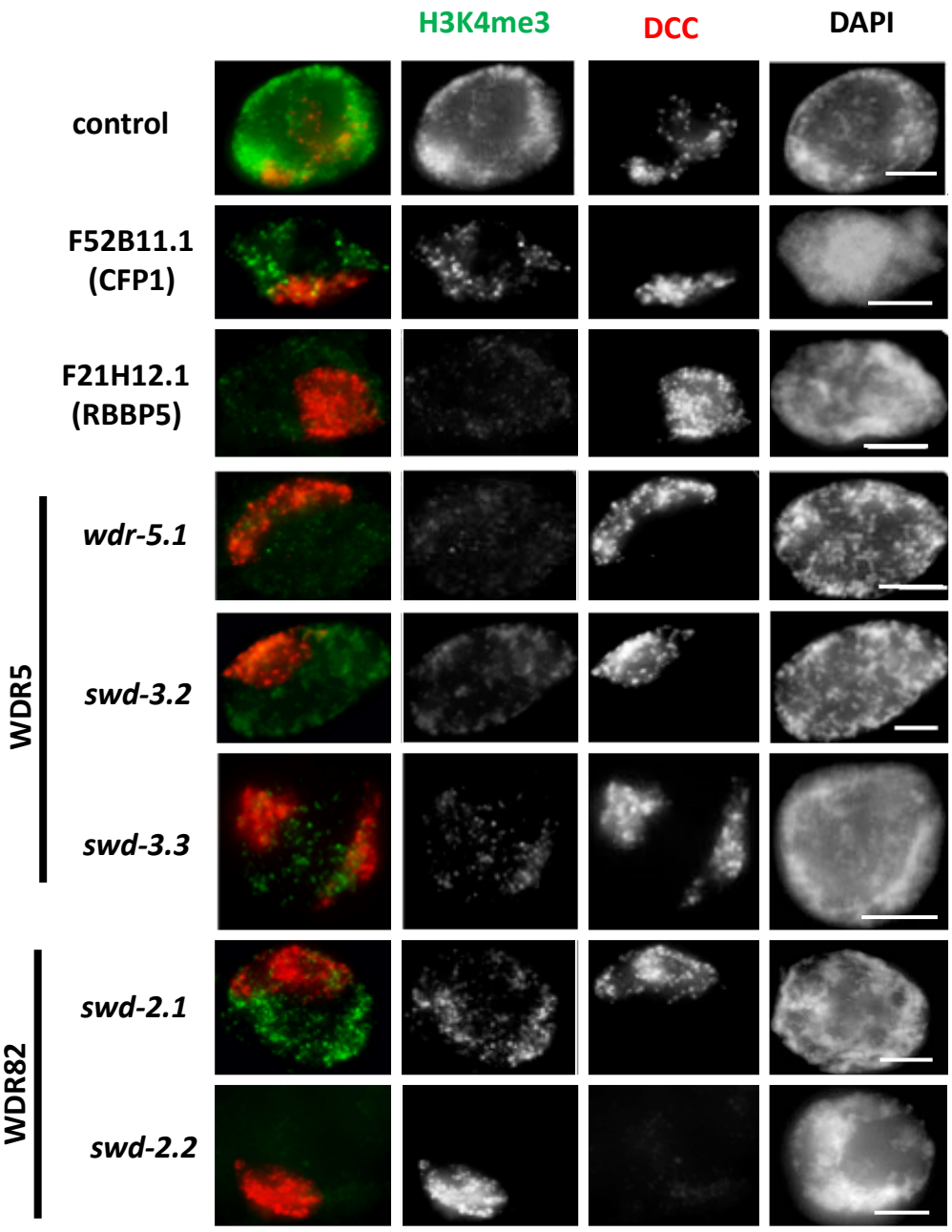

Figure 5.8 Depletion of Set1C/MLL components reduces H3K4me3 but does not affect DCC binding. H3K4me3 (green) and DPY-27 (red) immunofluorescence in control RNAi and Set1C/MLL depletion animals shows a reduced H3K4me3 signal upon Set1C/MLL RNAi in adult, hermaphrodite intestinal nuclei. The names of the mammalian homologs are included for reference. In all panels DAPI is shown in grayscale and scale bar equals 5µm.

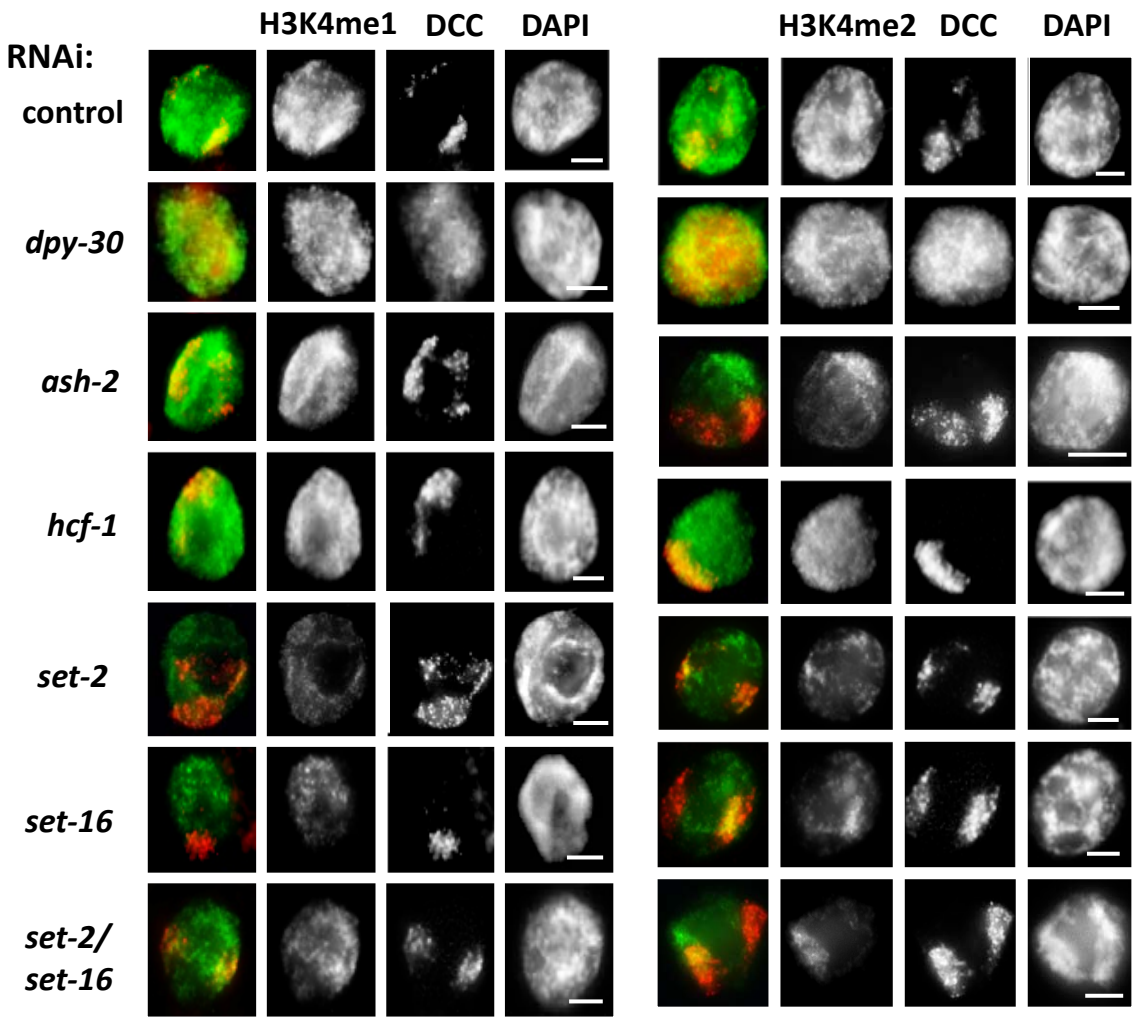

Figure 5.9 H3K4me1 and me2 levels in Set1C/MLL depletion nuclei. A. H3K4me1 (green) and CAPG-1 (red) co-staining in control RNAi and Set1/MLL depletion nuclei (adult intestine). Reduction in H3K4me1 is only observed in *set-2* and *set-16* depletion animals. **B.** H3K4me2 (green) and DPY-27 (red) co-staining slight reductions in signal are observed in all Set1/MLL depletion nuclei except in *dpy-30*. In all panels DAPI is shown in grayscale and scale bar equals 5µm.

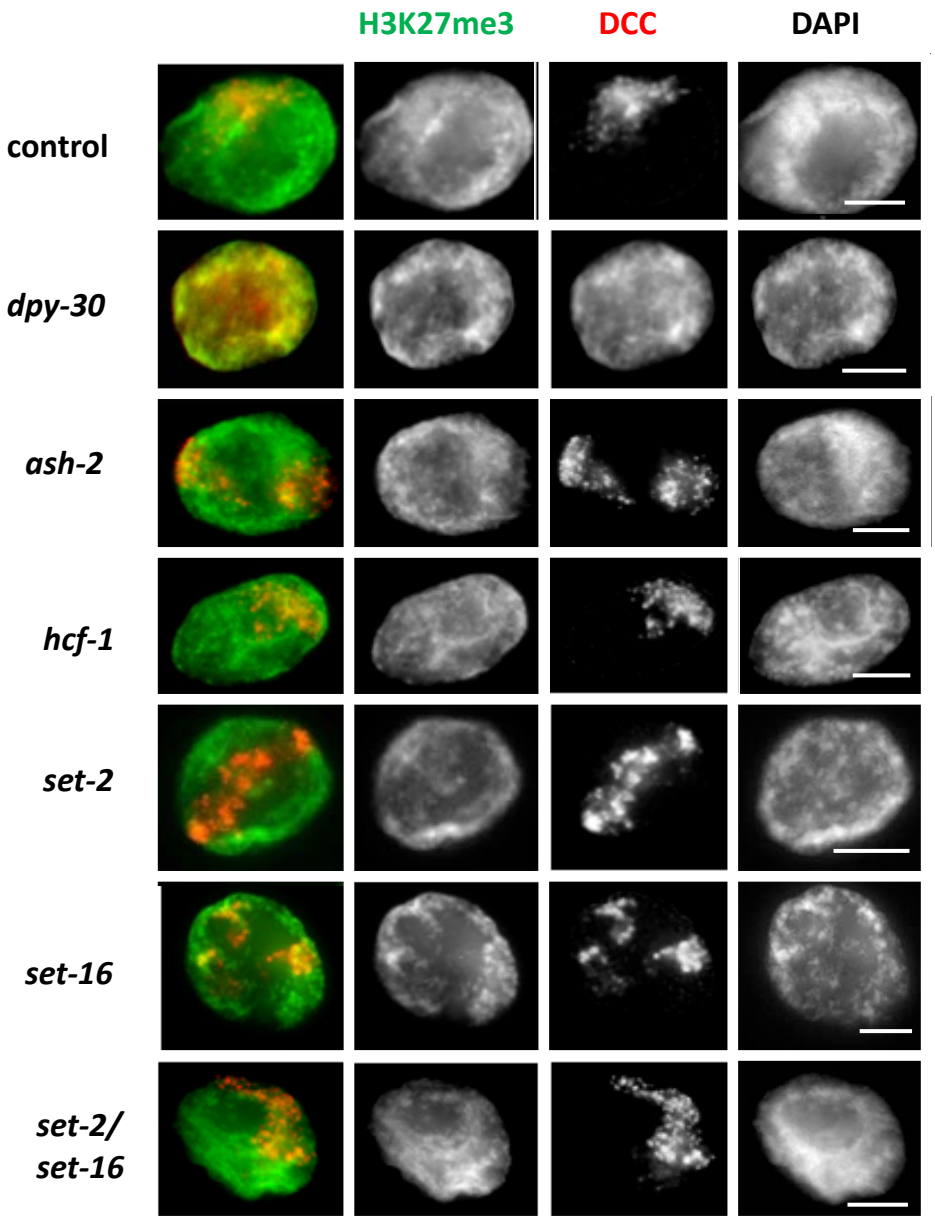

Figure 5.10 H3K27me3 levels unchanged in Set1C/MLL depletion adults. H3K27me3 (green) and DPY-27 (red) co-staining in control and Set1/MLL depletion nuclei reveal no change in H3K27Me3 levels. In all panels DAPI is shown in grayscale and scale bar equals 5µm.

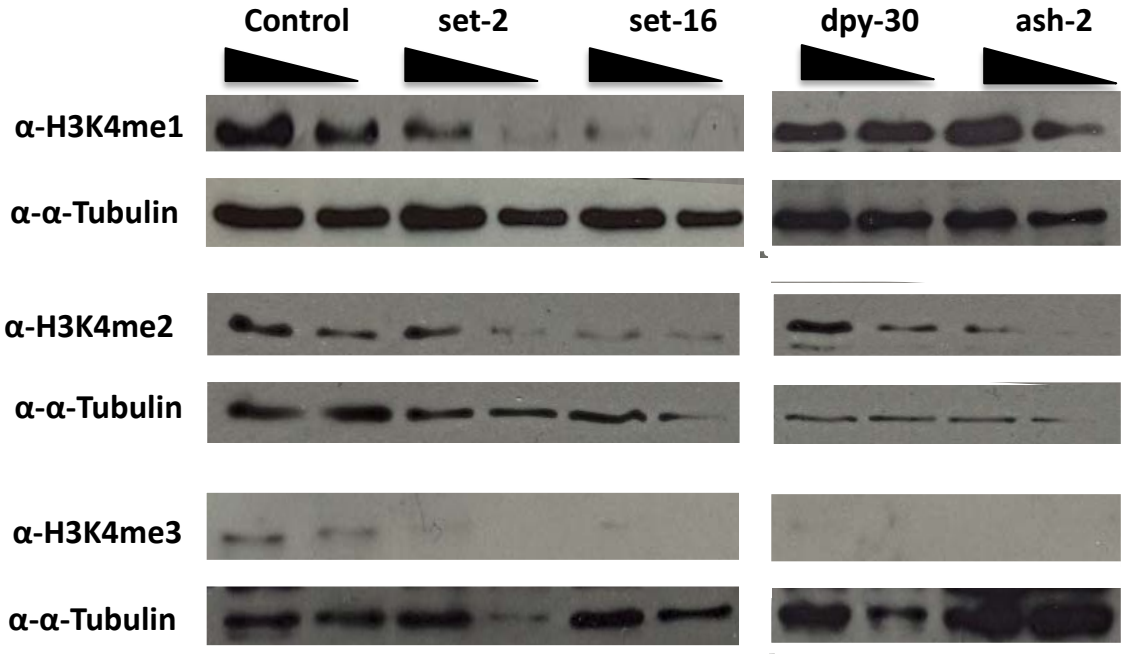

Figure 5.11 H3K4 methylation levels upon Set1C/MLL depletion in wildtype, hermaphrodite adults. Western blot analysis of H3K4 methylated species in young adult hermaphrodites (100 and 50 per lane). H3K4me1 is reduced in *set-2* and *set-16*. H3K4me2 levels are reduced in all except *dpy-30*. H3K4me3 levels are reduced in *set-2, set-16*, *ash-2*, and *dpy-30*. α-Tubulin is used as a loading control.

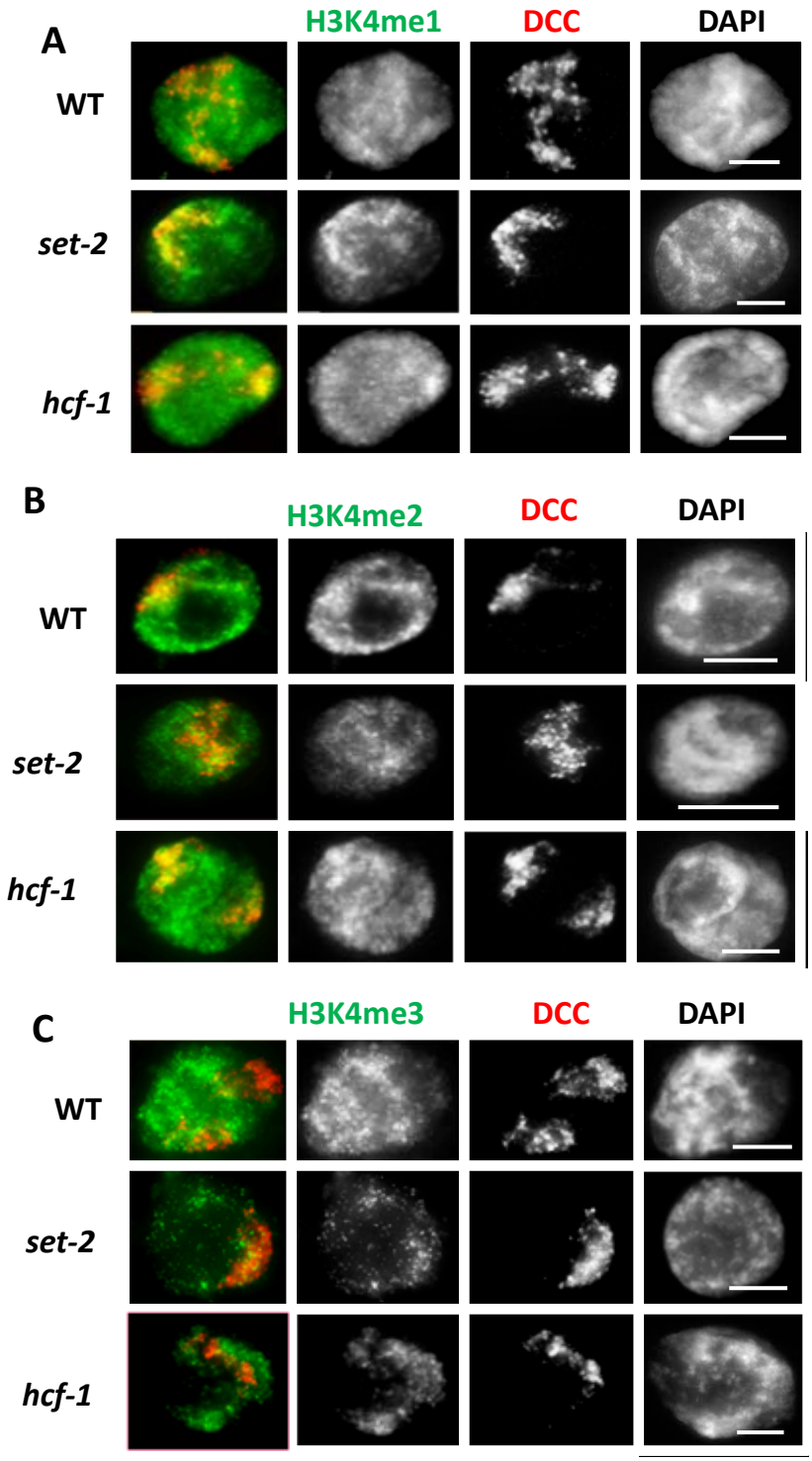

Figure 5.12 H3K4methylation levels in *set-2, hcf-1* deletion mutants. H3K4 methylation staining is in green, DPY-27 is in red with H3K4me2 and me3, H3K4me1 is co-stained with CAPG-1 (red). *hcf-1* adult intestinal nuclei show reduced H3K4me3 staining, while *set-2* shows reductions in all marks to varyring degrees. Neither mutant displays a DCC localization/binding phenotype. In all panels DAPI is shown in grayscale and scale bar equals 5µm.

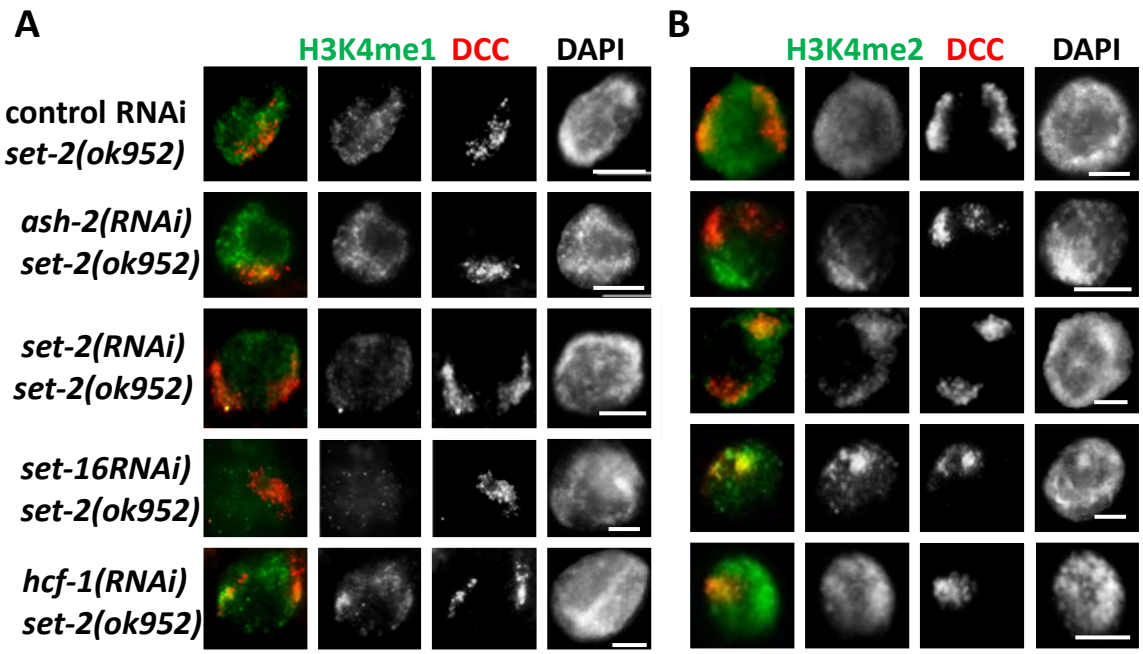

Figure 5.13 H3K4me1 and me2 levels after Set1C/MLL depletion in *set-2(ok952)* adults. A. H3K4me1 (green) and CAPG-1 (red) immunofluorescence and **B.** H3K4me2 (green) and DPY-27 immunofluorescence in adult intestinal nuclei. Although effects on methylation can be detected, there is no effect on DCC localization in the *set-2* mutant and Set1c/MLL depletion animals.

Anova: Single Factor

SUMMARY

Groups	*Count*	*Sum*	*Average*	*Variance*
vector N2	21	13.05	0.621429	0.013882857
vector	18	8.51	0.472778	0.011233007
set-2	18	8.77	0.487222	0.009538889
set-16	19	8.24	0.433684	0.018224561
set-2/16 double	19	8.85	0.465789	0.021325731
ash-2	19	8.54	0.449474	0.023827485

ANOVA

Source of Variation	*SS*	*df*	*MS*	*F*	*P-value*	*F crit*
Between Groups	0.470733	5	0.094147	5.7394160	9.79E-05	2.29
Within Groups	1.771579	108	0.016404			
Total	2.242312	113				

Tukey's test:

Vector N2: Vector *htz-1 p >0.1*
Vector N2: *set-2(RNAi), htz-1 p >0.1*
Vector N2: *set-16(RNAi) htz-1 p >0.1*
Vector N2: *set-2(RNAi), set-16(RNAi) htz-1 p >0.1*
Vector N2: *ash-2(RNAi) htz-1 p >0.1*

No other comparisons statistically significant.

Figure 5.14 Statistical analysis of X-Paint/DCC colocalization study in *htz-1(tm2469)* background. One-way ANOVA of all colocalization data reveals statistically significant differences between samples. When the N2 control data is omitted, the null is accepted. Tukey's test reveals that the significant differences between samples are specifically between the N2 control and each of the *htz-1* (control and Set1/MLL depletion) samples.

CHAPTER 6

Conclusions and Future Directions

Coordinating the dynamic changes in gene expression that occur during the development of an organism involves global changes in how the information driving developmental programs is packaged [1]. Changes in chromosome architecture accompany differentiation in a manner that may directly result in the stable silencing of genes no longer required by the daughter cell and increased expression of cell-specific genes. Current data strongly suggest that chromatin organization gates access to important regulatory sequences such that the chromatin reorganizations that accompany differentiation result in a unique set of regulatory sequences available for recognition [2-5]. Additionally, proper packaging of DNA is essential for its faithful segregation during cell division, which is vital for maintaining the genome integrity [6, 7].

The overall goal of my thesis work has been to determine the requirements for binding and targeting of an important developmental gene regulation complex. I have utilized the system of dosage compensation in *C. elegans* as it involves coordinated gene regulation on the scale of an entire chromosome [8]. Additionally, by studying targeting of the dosage compensation

complex (DCC) in *C. elegans*, we can get a better understanding of condensin targeting to sites of regulation in other organisms and also elucidate how genes are targeted for transcriptional fine-tuning. I have focused my work specifically on understanding how chromatin organization is involved in DCC targeting.

What I found in my initial experiments in the lab is that Condensin I^{DC} requires all members for proper localization on the X chromosome. In our characterization of the newest component of the Condensin I^{DC} complex, CAPG-1, I found that *capg-1* expression was required for the X chromosome localization of all of the other Condensin I^{DC} subunits. This led us to conclude that this complex binds in an all-or-none fashion. During the course of our characterization of CAPG-1 we found that this protein also binds in a very specific pattern to mitotic and meiotic chromosomes. CAPG-1 diffusely coats mitotic chromosomes and localizes to the region between separating meiotic chromosomes of the male and hermaphrodite germline (where dosage compensation does NOT occur). We determined that this population of CAPG-1 is a member of a second Condensin I complex that functions specifically in chromosome segregation. I went on to test whether the characteristic all-or-none chromatin binding was shared between the two Condensin complexes. I tested Condensin I binding to both mitotic and meiotic chromosomes upon loss of one of the subunits either by mutation or RNAi. I confirmed that Condensin I binding to mitotic and meiotic chromosomes requires the presence of all subunits just as Condensin I^{DC} requires the presence of all subunits to bind the dosage compensated X chromosomes.

The discovery and characterization of CAPG-1 has been of great importance to the field of dosage compensation. The biochemical analyses strongly indicated that CAPG-1 is a subunit of condensin in *C. elegans* and my data that condensin assembly on chromatin requires all subunits demonstrate Condensin I^{DC} subunits function as a complex *in vivo*. The fact that dosage compensation in *C. elegans* requires a complete condensin complex to assemble on the chromosome lends more support to the hypothesis that chromosome-wide gene regulation is achieved by changes in higher order chromosome organization. Additionally, the knowledge that the Condensin I^{DC} SMC subunit DPY-27 is the only member of the complex that functions solely in dosage compensation indicates functional studies of this protein will be key to our overall understanding of the process in the future.

This work has also contributed to the wider field of condensin biology. The discovery of Condensin I that functions specifically in mitosis and meiosis has provided a powerful model in which to study the evolutionarily conserved function of this complex. Additionally, the distinct localization patterns of Condensin I and Condensin II indicated that *C. elegans* may be an ideal system to use to discern the specific regulation and function of the two complexes in mitosis and meiosis. The fact that Condensin I subunits are interdependent in assembly onto mitotic and meiotic chromatin may also allow us to draw parallels between Condensin I^{DC} and Condensin I chromatin binding features in the future.

I then wanted to better understand the role of chromatin organization in DCC binding. To do this, we performed a directed screen to test genes encoding

different chromatin modifying enzymes, putative chromatin binding proteins, and histone variants for function in dosage compensation. We found that expression of *htz-1*, which encodes the H2A.Z variant of canonical H2A, is uniquely required for dosage compensation. Upon characterization of the function, I found that loss of H2A.Z/HTZ-1 results in mislocalization of the DCC to autosomes. Previous work has focused exclusively on identifying potential DCC binding sequences, yet my work clearly demonstrates that sequence information is not the only input driving DCC targeting.

We propose that either HTZ-1 or an HTZ-1-regulated autosomal repellent functions to limit where the DCC can bind in the genome. HTZ-1 may directly block access to autosomal occurrences of the widespread MEX motifs by preventing access to the sequences themselves. Consistent with this, the X chromosomes overall have reduced HTZ-1 levels compared to autosomes and *rex* sites are specifically depleted of HTZ-1. If this is the case, it is likely that non-acetylated HTZ-1 is providing DCC blocking function based on the described function for hypoacetylated H2A.Z in forming heterochromatin (Figure 1.7). HTZ-1 nucleosomes on autosomes may also prevent motif clustering from occurring on autosomes through an effect on higher order chromosome organization. In this case, I would predict that acetylated HTZ-1 (as shown in Figure 1.6) functions to prevent MEX clustering based on the data that acetylated HTZ-1 is refractory to the formation of condensed structures (Figure 1.8). I favor the first possibility over the second due to the fact that acetylated HTZ-1 is likely to be important for activities at promoters both on autosomes and on the X

chromosomes. Indeed, the only areas where DCC and HTZ-1 overlap on the X chromosomes occur at promoter regions where HTZ-1 is likely to be acetylated. However, it is also possible that nucleosomes with only HTZ-1 acetylation (and not the other marks associated with promoter activity) have boundary function on autosomes to prevent DCC binding. This would be similar to the function of acetylated H2A.Z at boundary elements at the chicken globin locus [9]. Understanding whether acetylation of HTZ-1 contributes to the dosage compensation function of HTZ-1 will be an important step in testing these proposed functions.

My work on HTZ-1 in dosage compensation has made a significant contribution to the field. The data show for the first time that successful targeting of the DCC to the X chromosomes relies on chromatin organization. More specifically, it appears that dosage compensation targeting may take advantage of pre-existing differences in chromatin organization between the X and autosomes. I have found that depletion of HTZ-1 on the X chromosome occurs very early in development (Figure 5.1 and [10]). HTZ-1 begins to visibly accumulate on chromosomes at the four-cell stage, but accumulation of HTZ-1 is somehow blocked on the X chromosome. An exciting possibility currently being pursued in the lab is that the system responsible for X chromosome silencing in the germline is inherited in the zygote. The *C. elegans* Polycomb-like MES proteins (for Maternal Effect Sterility) are responsible for silencing the X chromosomes in the germline. Interestingly, I also observe depletion of HTZ-1 from the silenced X chromosomes, supporting a possible link between MES

silencing in the germiline and its unique chromatin characteristics in the early embryo.

This work has also contributed to the knowledge of the function of H2A.Z outside of transcription activation. This provides another example that one of the conserved functions of H2A.Z is in setting up boundaries in chromatin to specifically block repressive activities. Continued investigation in HTZ-1 regulation of DCC localization will provide more insight into this less-well characterized function of H2A.Z

In continuation of the previous study I wanted to know whether other chromatin factors assisted in HTZ-1 regulated DCC localization. H3K4 methylation was an attractive candidate as there is a well documented physical and functional relationship between H2A.Z and H3K4 methylation in the literature [11-13]. Additionally, DPY-30 is a member of the DCC but in all other organisms in which it has been studied, it functions in H3K4 methyltransferase complexes (Figure 1.10). Upon extensive testing of Set1/MLL complex subunit homologs in *C. elegans*, however, we were intrigued to find that DPY-30's affect on dosage compensation is unique and independent of H3K4methylation. Loss of several other subunits actually had a more dramatic effect on global H3K4 methylation levels (such as the methyltransferases themselves, SET-2 and SET-16) but did not affect DCC localization. Also, I found that the DCC mislocalization caused by loss of *dpy-30* and loss of *htz-1* are very different. Whereas HTZ-1 depletion leads to ectopic DCC localization on autosomes, DPY-30 depletion significantly affects the stability of chromatin binding in general, suggesting two very different

mechanisms of controlling DCC localization are at work. Finally, we directly tested for coordination between H3K4methylation and HTZ-1 in preventing autosomal DCC binding and found that HTZ-1 function in DCC targeting is also independent of H3K4 methylation.

This study has laid to rest the hypothesis that the role of DPY-30 in dosage compensation is linked to its evolutionarily conserved role in H3K4 methyltransferase complexes. Instead, we have revealed that the function of DPY-30 in dosage compensation is completely independent of Set1/MLL. This provides an exciting avenue to dissect the unique role of DPY-30 outside of H3K4 methylation. The DCC mislocalization phenotype I have observed in *dpy-30* animals is unique even among dosage compensation genes. Loss of *htz-1* expression, as described above results in mislocalization of the complex. Loss of the any one of the Condensin I^{DC} subunits results in failure of the remaining subunits and eventually the signal of the remaining subunits is lost. Similarly, loss of either *sdc-2* or *sdc-3* results in failure of Condensin I^{DC} and the other DCC subunits to load onto X and the signals of these proteins are lost over developmental time [6, 14, 15]. However in *dpy-30*, the DCC proteins are maintained even though their chromatin binding is severely compromised. Therefore, the key to understanding how the DCC is stabilized on the X chromosomes may lie with DPY-30.

Proposed future directions

In the following I will briefly describe an experimental strategy one could follow to address some of the new questions my work has raised. The goal of Aim 1 is to take advantage of ectopic DCC binding in *htz-1* animals to get a better understanding of where DCC prefers to bind and also to understand how changes in DCC occupancy change gene expression locally. In Aim 2 I propose to test whether loss of HTZ-1 leads to expansion of other repressive activities in the genome such as histone deacetylation and H3K9 methylation. To continue research on the role of DPY-30 in dosage compensation, it will be important to determine whether DPY-30 affects SDC-2 binding and whether DPY-30 affects SDC-3 expression as outlined in Aim 3.

Aim 1: Utilize ectopic DCC binding in htz-1 to understand DCC binding preferences and link changes in DCC binding to changes in gene expression. Preliminary analysis by ChIP-qPCR suggests that way-stations, *rex,* and *dox* sites have reduced DCC binding in htz-1 depleted embryos (Figure 6.2). These results need to be confirmed using primer sets that span these sites, rather than just looking at regions that center on the reported ChIP-chip peak. We should also survey the previously reported sites of DCC binding on autosomes for changes in DCC occupancy. I would suggest starting with the few sites that were identified by the Lieb lab as their conservative statistical cut-off utilized to identify peaks of DCC binding increases the likelihood that their autosomal sites are robust [16]. To directly test our hypothesis that HTZ-1

prevents DCC binding at autosomal occurrences of the MEX motif, we should also survey DCC occupancy at autosomal MEX sites by DPY-27 ChIP-qPCR.

To complement the directed survey of DCC binding changes upon *htz-1* depletion, a genome-wide association study by DPY-27 ChIP-chip may be important to reveal any unexpected changes that occur genome-wide. If significant changes are observed, motif searches should be utilized to identify potentially functional binding sites within sites of ectopic DCC binding in *htz-1* animals. To better understand the local chromatin environment at ectopic DCC binding sites, ChIP-qPCR for modified histones should also be utilized. Together, these analyses could provide significant insight into the specific sequence and chromatin characteristics recognized by the DCC.

I have spent a great deal of time trying to understand the role of HTZ-1 in gene expression, both on the X chromosomes and autosomes. I surveyed a panel of genes on the X chromosome for changes in expression upon *htz-1* depletion and found that dosage compensated genes are more likely to have changes in expression than non-dosage compensated genes tested and these all increase in expression when *htz-1* is depleted (Figure 6.3). I have also performed two microarray experiments to understand expression changes throughout the genome in *htz-1* depletion embryos, the first using a scaled-up RNAi protocol and the second using the typical feeding RNAi protocol in the lab (Figures 6.4 and 6.5). I have found that there are changes in expression genome-wide, but that a majority of genes with ≥1.5-fold changes in expression are up-regulated. For the first experiment (Figure 6.4) I recorded the chromosomal locaction of each gene

and analyzed the changes chromosome-by-chromosome. Intriguingly, the majority of genes on X with expression changes are up-regulated and many of these genes have previously been identified as dosage compensated (Table 6.1). This analysis remains to be completed for the second set of data. What will be very interesting is to see if there is a direct correlation between regions that lose DCC on X and expression changes in nearby genes. Furthermore, it would be very exciting if any ectopic DCC binding sites show local down-regulation in *htz-1* depletion animals.

Aim 2: Does loss of htz-1 lead to expanded heterochromatin in C. elegans as it does in yeast, Arabidopsis, and mammals? To address this question we can first use immunofluorescence and Western analysis to detect global changes in modified histones associated with silencing such as H3K9 and H3K27 methylation. If changes are observed, we could utilize ChIP-qPCR to directly test if sites that are normally occupied by HTZ-1 become occupied by heterochromatin signatures in its absence as is reported for H2A.Z and methylation in plants. If expanded heterochomatin is observed, we should also test whether this is functionally coupled with expanded DCC localization in *htz-1* depleted animals. This could be done by testing for suppression of DCC mislocalization in *htz-1* mutant animals by RNAi of heterochromatin-related factors.

Aim 3: Determine the effect of DPY-30 on SDC-2 binding and SDC-3 expresion.

My data indicates that the majority of DCC signal in the nucleus is either not bound or weakly bound to chromatin. The DCC binding pattern in *dpy-30* embryos is the same as when *sdc-2* is lost by ChIP-chip analysis, but is SDC-2 binding to the X compromised in *dpy-30* animals? There is one IF experiment reported in Dawes et al. (1999) [14], where the author states SDC-2 is still present on the X in dpy-30 embryos, however this data is not shown. It will be important to confirm that this is indeed the case by SDC-2 IF combined with X-Paint FISH. If we confirm the previous finding, one possible explanation of DPY-30 function is that it serves as a scaffolding protein through which the rest of the complex stably associates with SDC-2. DPY-30 immunoprecipitation pulls down SDC-2 supporting that there is some form of physical interaction between it and SDC-2 in the cell. DCC tethering function of DPY-30 could be tested by utilizing a *dpy-30* transgenic animal where expression is driven by an inducible promoter in the *dpy-30* mutant background. If SDC-2 is still present on the X but simply requires DPY-30 to tether the rest of the complex, induction of *dpy-30* expression should trigger the re-assembly of the DCC to the X.

We will also need to go back and check the effect of DPY-30 on SDC-3. It was previously reported by IF analysis in embryos that loss of DPY-30 led to the specific loss of SDC-3 [17]. However SDC-3 ChIP-chip was recently performed in *dpy-30* embryos and although the signal on X was reduced, it was still present. It is possible that SDC-3 is indeed present in embryos, but is below the level of

detection by IF [18]. To address this we should determine the degree to which SDC-3 levels are reduced in *dpy-30* by quantitative western analysis. If we find that SDC-3 levels are significantly reduced in *dpy-30* animals we should next attempt to rescue the DCC mislocalization phenotype by over-expressing SDC-3 in *dpy-30* animals. As long as SDC-2 binding is unaffected in *dpy-30*, and if *dpy-30*'s role in dosage compensation is to promote SDC-3 expression, I would predict that over-expression of SDC-3 will rescue DCC localization. If this is in fact what is observed, the next step would be to determine the nature of *dpy-30* regulation of SDC-3. We should first detect levels of *sdc-3* mRNA in *dpy-30* animals by RT-qPCR, followed by DPY-30 ChIP-qPCR at the *sdc-3* promoter to observe whether any changes detected in *sdc-3* expression may be due to direct regulation by DPY-30 at the level of transcription. If there is no evidence for transcriptional regulation of *sdc-3* by DPY-30 we can then go on to explore potential mechanisms of SDC-3 stabilization by DPY-30. This may be difficult to study, however, as DPY-30 can pull down SDC-3 but not the reverse, arguing against a direct interaction between the two proteins. Also, SDC-3 may simply require the binding of the full complex for stability as is the case for Condensin I^{DC}.

References

1. Meister, P., S.E. Mango, and S.M. Gasser, *Locking the genome: nuclear organization and cell fate.* Current opinion in genetics & development, 2011. **21**(2): p. 167-74.
2. Li, X.Y., et al., *The role of chromatin accessibility in directing the widespread, overlapping patterns of Drosophila transcription factor binding.* Genome biology, 2011. **12**(4): p. R34.
3. Fakhouri, T.H., et al., *Dynamic chromatin organization during foregut development mediated by the organ selector gene PHA-4/FoxA.* PLoS genetics, 2010. **6**(8).

4. John, S., et al., *Interaction of the glucocorticoid receptor with the chromatin landscape.* Molecular cell, 2008. **29**(5): p. 611-24.
5. Carr, A. and M.D. Biggin, *Accessibility of transcriptionally inactive genes is specifically reduced at homeoprotein-DNA binding sites in Drosophila.* Nucleic acids research, 2000. **28**(14): p. 2839-46.
6. Csankovszki, G., et al., *Three distinct condensin complexes control C. elegans chromosome dynamics.* Current biology : CB, 2009. **19**(1): p. 9-19.
7. Hudson, D.F., K.M. Marshall, and W.C. Earnshaw, *Condensin: Architect of mitotic chromosomes.* Chromosome research : an international journal on the molecular, supramolecular and evolutionary aspects of chromosome biology, 2009. **17**(2): p. 131-44.
8. Csankovszki, G., E.L. Petty, and K.S. Collette, *The worm solution: a chromosome-full of condensin helps gene expression go down.* Chromosome research : an international journal on the molecular, supramolecular and evolutionary aspects of chromosome biology, 2009. **17**(5): p. 621-35.
9. Bruce, K., et al., *The replacement histone H2A.Z in a hyperacetylated form is a feature of active genes in the chicken.* Nucleic acids research, 2005. **33**(17): p. 5633-9.
10. Whittle, C.M., et al., *The genomic distribution and function of histone variant HTZ-1 during C. elegans embryogenesis.* PLoS genetics, 2008. **4**(9): p. e1000187.
11. Venkatasubrahmanyam, S., et al., *Genome-wide, as opposed to local, antisilencing is mediated redundantly by the euchromatic factors Set1 and H2A.Z.* Proceedings of the National Academy of Sciences of the United States of America, 2007. **104**(42): p. 16609-14.
12. Kelly, T.K., et al., *H2A.Z maintenance during mitosis reveals nucleosome shifting on mitotically silenced genes.* Molecular cell, 2010. **39**(6): p. 901-11.
13. Barski, A., et al., *High-resolution profiling of histone methylations in the human genome.* Cell, 2007. **129**(4): p. 823-37.
14. Dawes, H.E., et al., *Dosage compensation proteins targeted to X chromosomes by a determinant of hermaphrodite fate.* Science, 1999. **284**(5421): p. 1800-4.
15. Yonker, S.A. and B.J. Meyer, *Recruitment of C. elegans dosage compensation proteins for gene-specific versus chromosome-wide repression.* Development, 2003. **130**(26): p. 6519-32.
16. Ercan, S., et al., *X chromosome repression by localization of the C. elegans dosage compensation machinery to sites of transcription initiation.* Nature genetics, 2007. **39**(3): p. 403-8.
17. Davis, T.L. and B.J. Meyer, *SDC-3 coordinates the assembly of a dosage compensation complex on the nematode X chromosome.* Development, 1997. **124**(5): p. 1019-31.
18. Pferdehirt, R.R., W.S. Kruesi, and B.J. Meyer, *An MLL/COMPASS subunit functions in the C. elegans dosage compensation complex to target X chromosomes for transcriptional regulation of gene expression.* Genes & development, 2011. **25**(5): p. 499-515.

Table 6.1 *htz-1* affects expression of dosage compensated genes.

gene name	htz-1 RNAi fold change	sdc-2 fold change	dpy-27 fold change
F41B4.1	0.59	3.5	3
T14E8.4	0.59	2.2	1.8
Y102A11A.3	0.59	3.7	2.4
F08B12.1	0.6	2.4	3.1
pqn-62	0.61	2.9	3
C53C9.2	0.61	2.2	2
tts-1	0.62	10	1.7
F48E3.8	0.64	1.5	2.9
sad-1	0.64	1.8	3
T06F4.1	0.66	3	2.8
T21B6.3	0.69	2.1	1.7
grd-1	0.69	1.5	2
dyc-1	0.69	2.3	2.8
F15A8.6	0.7	1.7	2.8
F29G6.3	0.7	2	1.9
plc-1	0.76	2.1	3.1
lgx-1	0.81	1.5	2.8
B0416.1	0.85	1.6	1.7
clc-1	0.88	3.1	2.4
C45B2.8	0.89	4	1.8
hum-6	1.07	1.7	1

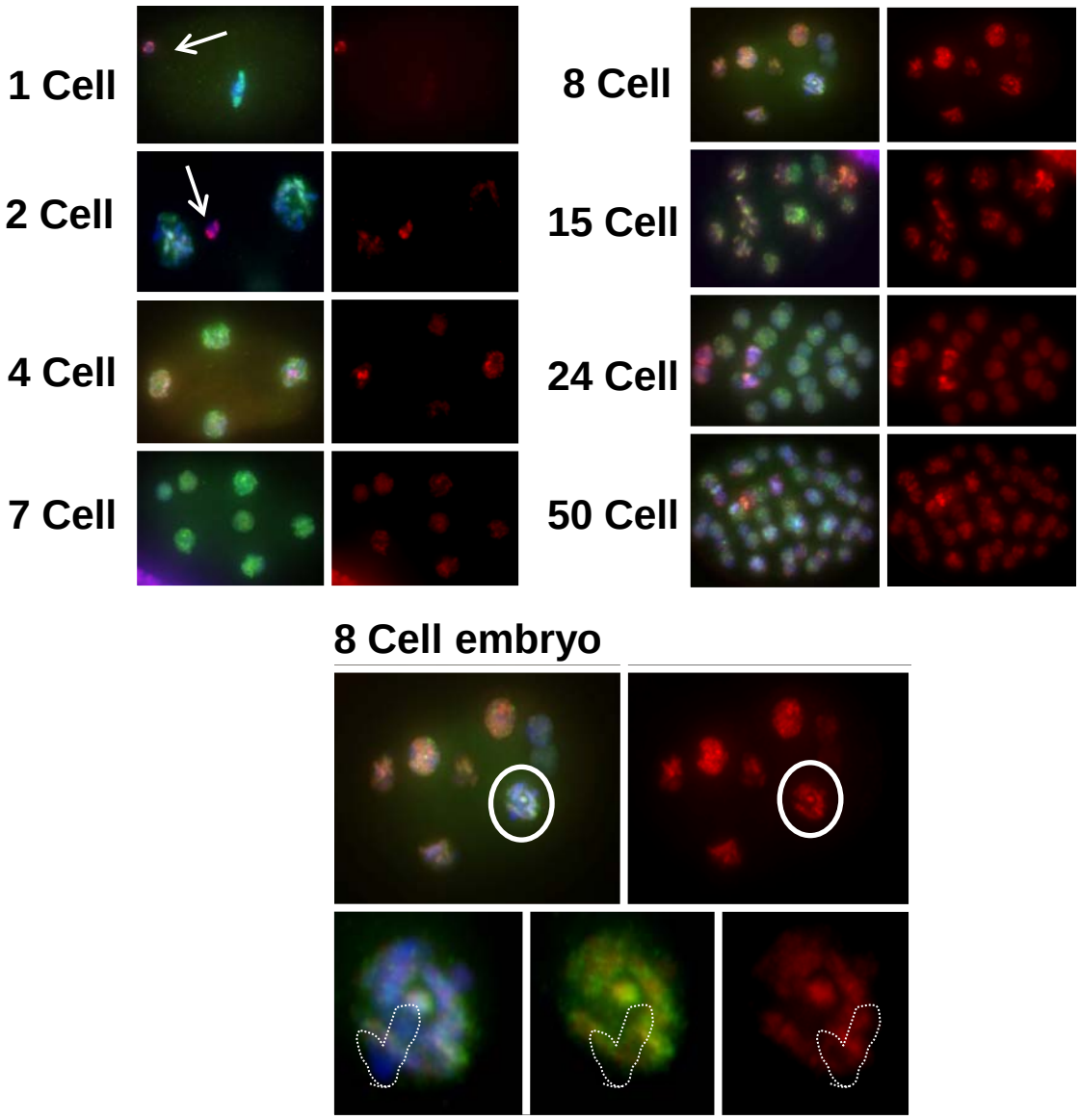

Figure 6.1 HTZ-1 accumulates on autosomes at the four cell stage but does not accumulate on the X chromosomes. MES-4 (green) is an autosomal marker in the early embryo. HTZ-1 (red) is absent on the same chromosomes that are MES-4 negative, indicating that HTZ-1 does not get incorporated into X chromatin. A. IF of embryos in early development before the onset of dosage compensation, which begins at the 50 cell stage. DAPI (blue) stains DNA . Arrows in 1 and 2-cell embryo indicate the polar body, which has intense HTZ-1 staining. B. Individualized chromosomes of a prophase nucleus (circled) is shown. The MES-4 and HTZ-1 negative region is outlined.

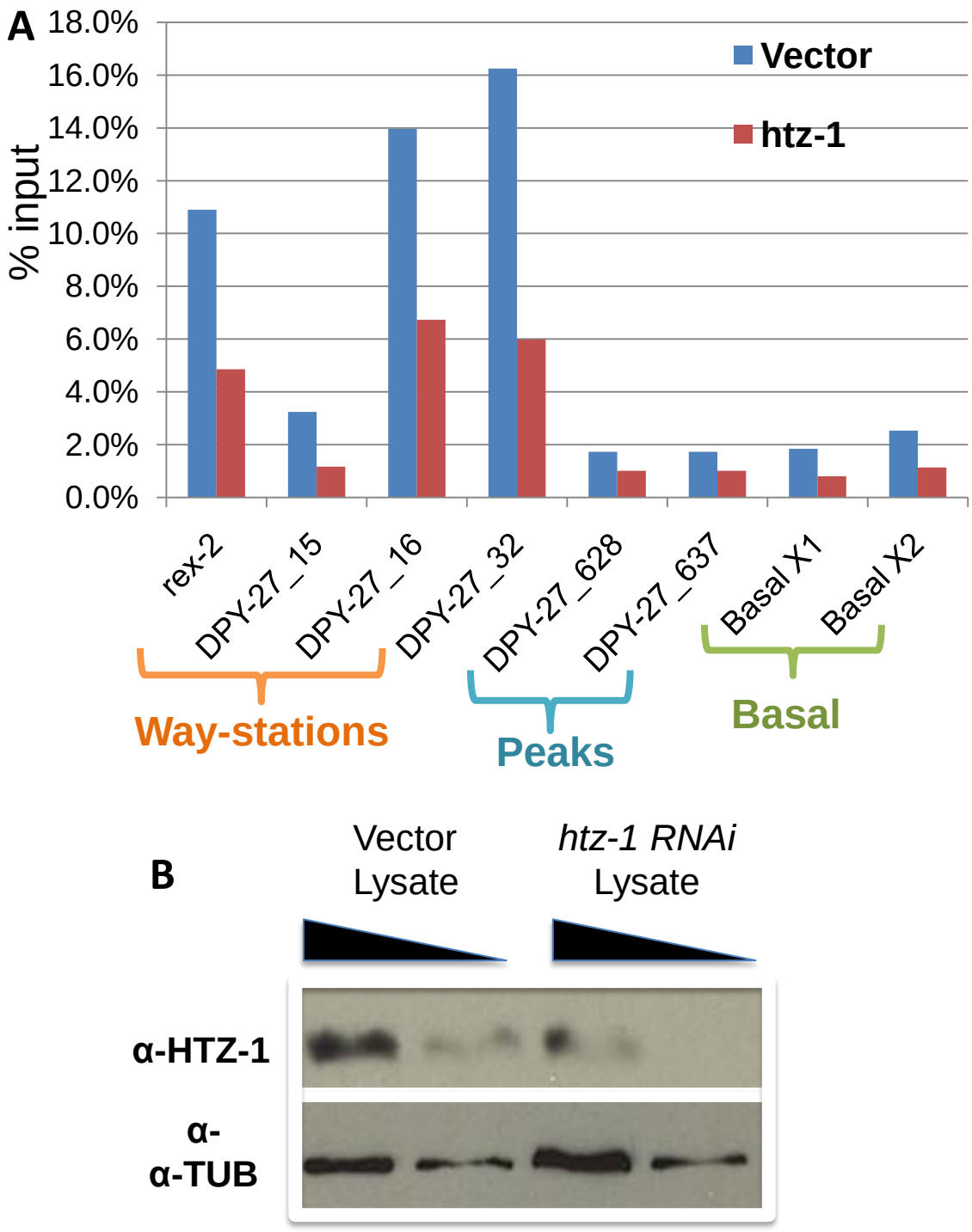

Figure 6.2 Preliminary DPY-27 ChIP-qPCR shows reduced DPY-27 occupancy at all classes of DCC binding sites. A. DPY-27 was performed from embryonic extracts of vector control and *htz-1* RNAi embryos. DPY-27 occupancy at way-stations, peaks (*dox* sites) and basal regions outside of peaks is observed in *htz-1* knock-down embryos. B. Western blot analysis of HTZ-1 levels in the lysate used in this experiment.

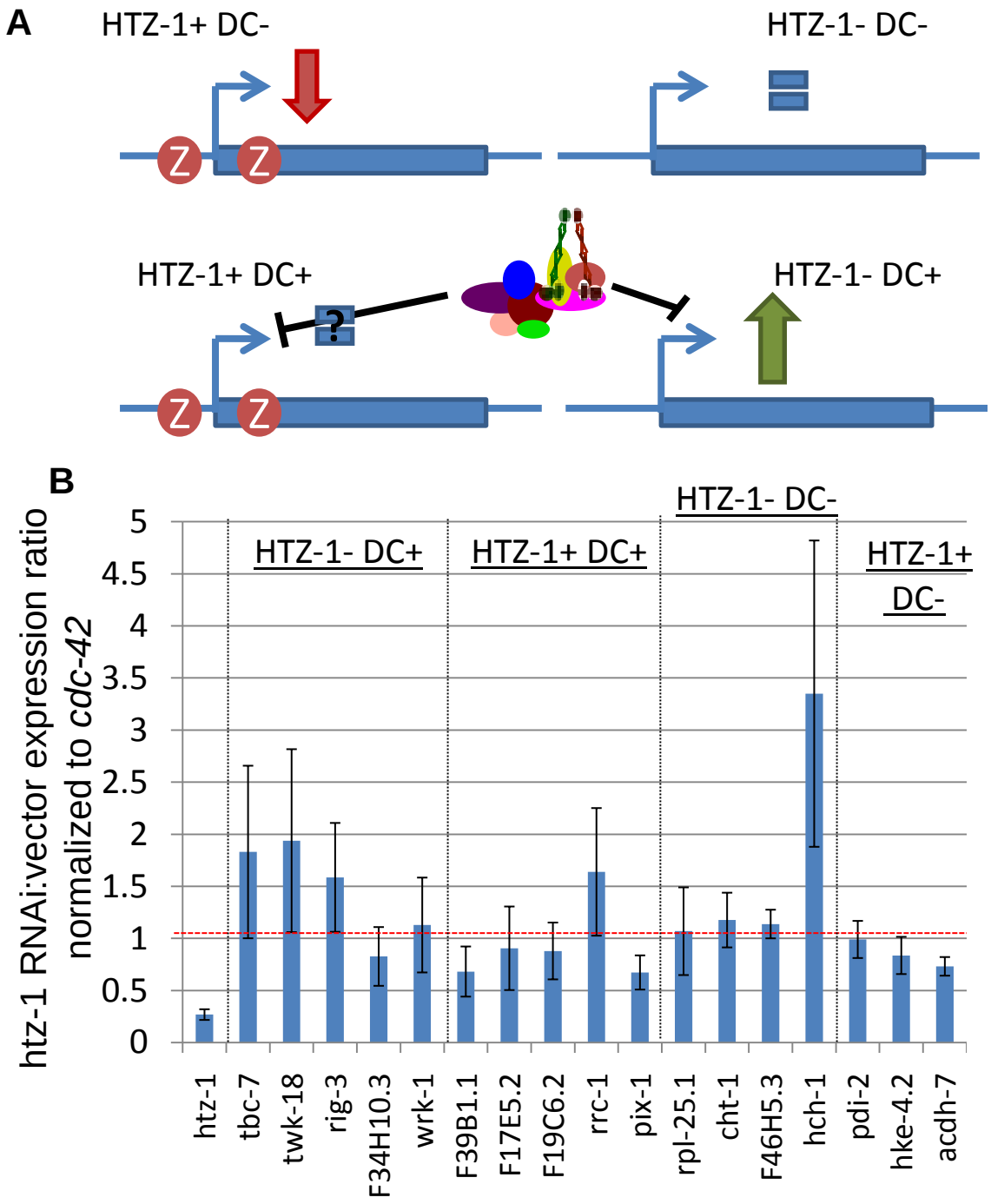

Figure 6.3 Loss of htz-1 results in changes in gene expression of X-linked genes. A. We predicted that loss of *htz-1* would affect X-linked genes in different ways depending on whether or not the gene has HTZ-1 associated with its promoter in wildtype embryos and depending on whether the gene is dosage compensated. B. RT-qPCR analysis of a panel of genes falling into the categories described in A. Several dosage compensated genes show increased expression in *htz-1* embryos, but only one non-compensated gene is upregulated.

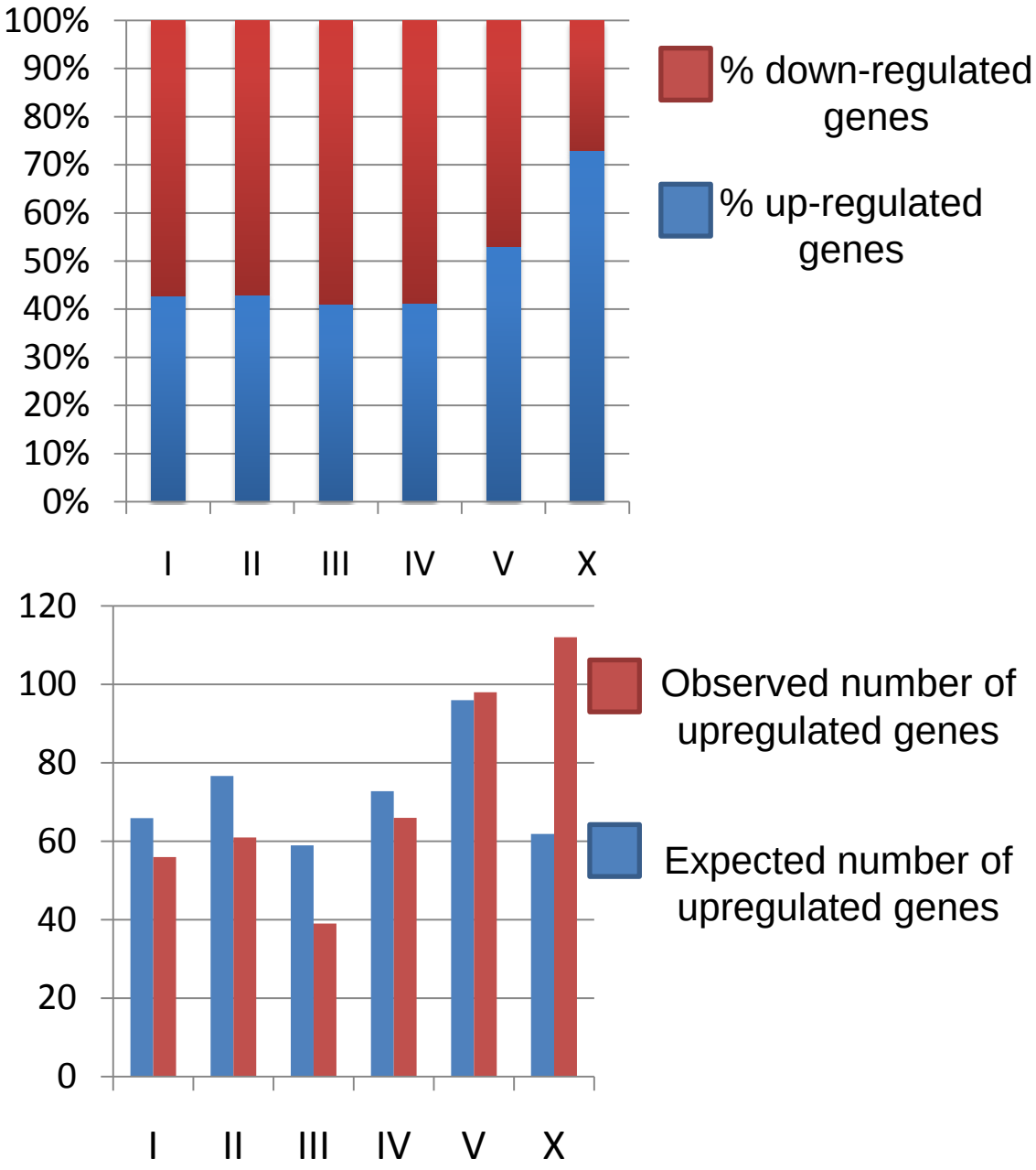

Figure 6.4 Microarray analysis of *htz-1* depleted embryos identified 863 genes with ≥1.5 fold change in gene expression. A. Analysis of expression changes by chromosome. A strong majority of genes with expression changes on X are up-regulated, consistent with disruption in dosage compensation. B. The number of upregulated genes observed on each chromosome versus the expected number (calculated by multiplying the total number of upregulated genes by the percentage of genes in the genome on each chromosome). The number of genes upregulated on the X is nearly twice the expected value. Embryos were collected for this analysis using a scaled-up feeding RNAi protocol.

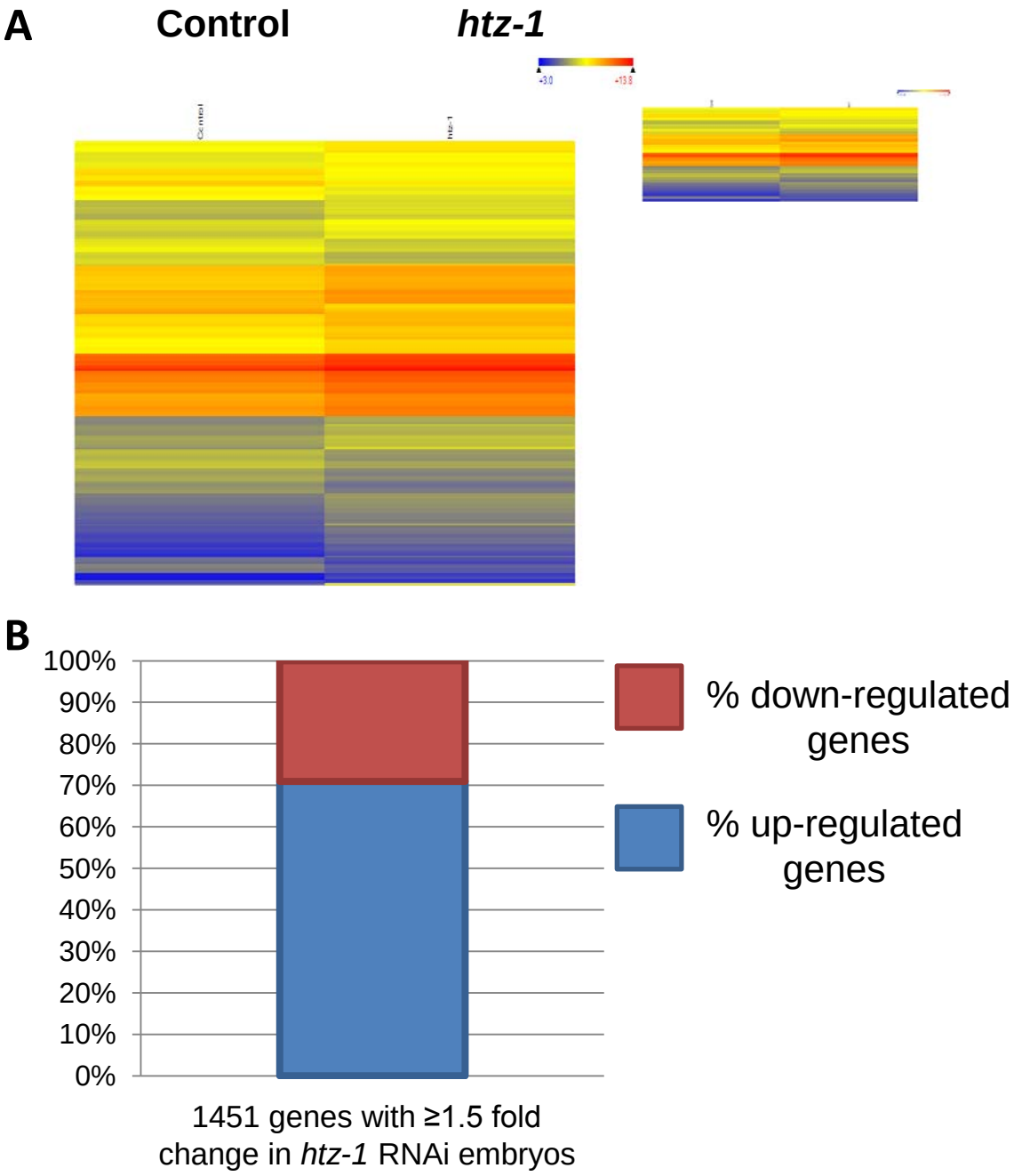

Figure 6.5 Repeat of *htz-1* microarray using a smaller-scale RNAi protocol has identified 1451 genes with ≥1.5 fold change in gene expression. A. Heat map showing the changes in gene expression upon *htz-1* RNAi of the 1451 genes with at least a 1.5-fold change in expression. B. Most genes with changes are up-regulated upon *htz-1* depletion. Mapping of these genes to chromosomal locations has not been completed yet.